ENERGY-CONSCIOUS PRODUCTION OF TITANIA AND TITANIUM POWDERS FROM SLAG

by

Scott C. Middlemas

A dissertation submitted to the faculty of
The University of Utah
in partial fulfillment of the requirements for the degree of

Doctor of Philosophy

Department of Metallurgical Engineering

The University of Utah

December 2014

Copyright © Scott C. Middlemas 2014

All Rights Reserved

The University of Utah Graduate School

STATEMENT OF DISSERTATION APPROVAL

The dissertation of **Scott C. Middlemas**

has been approved by the following supervisory committee members:

Zhigang Zak Fang	, Chair	**8/23/2013** Date Approved
Michael Free	, Member	**8/23/2013** Date Approved
Richard Ernst	, Member	**3/18/2014** Date Approved
Ravi Chandran	, Member	**4/29/2014** Date Approved
Peng Fan	, Member	**8/23/2013** Date Approved

and by **Manoranjan Misra**, Chair of the Department of **Metallurgical Engineering**

and by David B. Kieda, Dean of The Graduate School.

ABSTRACT

Titanium dioxide (TiO_2) is used as a whitening agent in numerous domestic and technological applications and is mainly produced by the high temperature chloride process. A new hydrometallurgical process for making commercially pure TiO_2 pigment is described with the goal of reducing the necessary energy consumption and CO_2 emissions. The process includes alkaline roasting of titania slag with subsequent washing, HCl leaching, solvent extraction, hydrolysis, and calcination stages. The thermodynamics of the roasting reaction were analyzed, and the experimental parameters for each step in the new process were optimized with respect to TiO_2 recovery, final product purity, and total energy requirements. Contacting the leach solution with a tertiary amine extractant resulted in complete Fe extraction in a single stage and proved effective in reducing the concentration of discoloring impurities in the final pigment to commercially acceptable levels.

Additionally, a new method of producing Ti powders from titania slag is proposed as a potentially more energy efficient and lower cost alternative to the traditional Kroll process. Thermodynamic analysis and initial experimental results validate the concept of reducing titanium slag with a metal hydride to produce titanium hydride (TiH_2) powders, which are subsequently purified by leaching and dehydrided to form Ti powders. The effects of reducing agent type, heating time and temperature, ball milling, powder compaction, and eutectic chloride salts on the conversion of slag to TiH2 powders were determined. The purification of reduced powders through NH4Cl, NaOH, and HCl

leaching stages was investigated, and reagent concentration, leaching temperature, and time were varied in order to determine the best conditions for maximum impurity removal and recovery of TiH_2.

A model plant producing 100,000 tons TiO_2 per year was designed that would employ the new method of pigment manufacture. A comparison of the new process and the chloride process indicated a 25% decrease in energy consumption and CO_2 emissions. For the Ti powder making process, a 10,000 tons per year model plant employing the metal hydride reduction was designed and a comparison with the Kroll process indicated potential for over 60% less energy consumption and 50% less CO_2 emission.

TABLE OF CONTENTS

LIST OF TABLES

ACKNOWLEDGMENTS

The US Department of Energy and the Office of Energy Efficiency and Renewable Energy are acknowledged for funding this research (DE-EE003476). Rio Tinto Iron and Titanium is also acknowledged for providing raw materials.

I would like to thank Dr. Zak Fang for his guidance and support throughout my undergraduate and doctoral studies. Thank you also to Prof. Michael Free, Prof. Richard Ernst, Prof. Ravi Chandran, and Dr. Peng Fan for their guidance and willingness to serve on my supervisory committee.

Finally, special thanks to my loving, patient, and supportive wife, Amberly Middlemas.

PREFACE

The purpose of this research was to develop and demonstrate the potential of two new hydrometallurgical process technologies to reduce the energy consumption and CO_2 emissions from the production of titanium dioxide (TiO_2) pigment and titanium (Ti) powders. TiO_2 is one of the most commonly used minerals in the chemical manufacturing industry and has a wide variety of domestic and industrial applications, while Ti and its alloys are highly sought after engineering materials. The current processes for producing both materials rely on high temperature carbo-chlorination of TiO_2 bearing raw materials, hence producing large quantities of CO_2.

The key objectives of this study were to 1) demonstrate the scientific validity of the two concepts, 2) understand the primary chemical reactions of each unit process, 3) characterize the final and intermediate reaction products, 4) optimize the parameters of each process with respect to product purity and energy consumption, and 5) model the energy consumption and CO_2 emissions of the new processes and compare them to existing technologies. The research efforts completed to meet these objectives are detailed in this dissertation, which is divided into two parts, with Part I (Chapters 1–5) describing the development of the new TiO_2 pigment making process and Part II (Chapters 6–8) describing a new Ti metal powder making process.

Chapter 1 provides background information and context for the new TiO_2 making process, including the current applications, global production, and markets of TiO_2

pigment. The process chemistry of the two current commercial pigment making processes, the sulfate and chloride, are also described in detail, as well as the methods of preparing the feed stocks for these processes, namely synthetic rutile and high-titania slag. Several hydrometallurgical processes for refining TiO_2 have been in development in the last decade as alternatives to the chloride and sulfate processes and are reviewed as well. Finally, a brief overview of the new TiO_2 pigment making process is given and the flow sheet is described.

The new process includes alkaline roasting of titania slag followed by leaching, solvent extraction, hydrolysis, and calcination stages, with each step described in detail in the subsequent chapters. Chapter 2 focuses on the roasting of titania slag with molten NaOH to convert titanium dioxide in the slag to acid soluble sodium titanate compounds. The chapter includes a thermodynamic analysis of the reaction and the results of parametric optimization experiments and characterization of slag and intermediate roasted products.

Chapter 3 investigates the separation of Ti compounds from other impurities through leaching with HCl acid in a variety of different experimental conditions, as well as the purification of Ti leach liquor via solvent extraction with a tertiary amine extractant.

Chapter 4 describes the conditions that affect the rate and extent of recovery of Ti from solution through hydrolysis and precipitation of hydrous titanium oxide compounds. The hydrated compounds are calcined at various temperatures to remove the physically and chemically bound water to form crystalline anatase, rutile, or mixed phase products of varying morphology and size distributions.

The purpose of Chapter 5 is to estimate the total energy consumption and CO_2 emissions of a model plant producing 100,000 metric tons per year TiO_2 pigment using the new process. The range of values for the energy consumption and CO_2 emissions of the sulfate and chloride processes are reported and depend on the various feed stocks and system boundaries studied. A cradle-to-gate comparison of the new TiO_2 process with the two conventional processes (using slag as the feed) indicates potential for a 25% reduction in energy consumption and CO_2 emissions compared to the chloride process.

Despite its numerous attractive properties as an engineering material, titanium is not more widely used due to its cost. Chapter 6 discusses the traditional Ti manufacturing processes as well as the numerous alternative processes that have been investigated with the aim of reducing cost, most of which involve the electrochemical or metallothermic reduction of purified TiO_2 or titanium tetrachloride ($TiCl_4$). A new method is proposed to make titanium hydride (TiH_2) or Ti powders by direct reduction of Ti slag (DRTS) using metal hydrides such as MgH_2 followed by separation of the reaction product from MgO and remaining impurities.

Chapter 7 includes a preliminary thermodynamic analysis and initial experimental development of the reduction reaction. The effects of reducing agent type, heating time and temperature, ball milling, powder compaction, and the addition of eutectic chloride salts on the extent of conversion of slag to TiH_2 powders are reported.

Chapter 8 discusses the separation of the resulting TiH_2 powder from impurities in the reduction product and the dehydrogenation of TiH_2 to Ti by heating in vacuum or an inert atmosphere. Chapter 8 also includes an estimation of the energy consumption and CO_2 emissions of a model plant producing 10,000 metric tons per year of Ti powder

using the new process. A comparison of the new process with the traditional Kroll process of Ti manufacture indicates potential for substantial energy savings and reductions in CO_2 emissions.

Finally, the key conclusions of this study are presented in Chapter 9.

CHAPTER 1

A NEW PROCESS FOR MAKING TITANIUM DIOXIDE PIGMENT

1.1 History and Mineralogy

Titanium ranks as the ninth most abundant element found on earth (0.63% of lithosphere). It was first identified by Reverend William Gregor in 1790 in the form of a black rutile sand found in Cornwall, England, and given the name "Titanium" after the Titans from Greek mythology by Klaproth [1]. The pioneer investigations of titanium minerals used beneficiation techniques not too dissimilar from those of modern times. The ore was finely ground and leached with hydrochloric acid to remove iron. The leached residue was fused with sodium carbonate and then dissolved in dilute hydrochloric acid. When the resulting solution was treated with zinc, it became dark purple (indicative of Ti^{3+} ion) and then colorless when exposed to air (Ti^{4+}). When it was heated, it formed a white, turbid suspension resembling milk, which could not be dissolved with the addition of more acid (hydrous titanic oxide.) The hydrous oxide was heated and formed a white oxide, which we now identify as titanium dioxide, TiO_2. Despite these early investigations, TiO_2 pigments were not commercially available on the American market until 1918. Since then, the demand for TiO_2 has steadily increased and has become an essential component in millions of modern consumer products.

Titanium is a frequently occurring constituent in almost all crystalline rock,

occurring in 784 out of 800 igneous rocks analyzed by the USGS [1]. A list of the most common natural and synthetic TiO_2 bearing minerals is shown in Table 1.1 [2]. Of these, only ilmenite ($FeTiO_3$), natural and synthetic rutile (TiO_2), leucoxene ($Fe_2O_3 \cdot n\ TiO_2$), and slag are currently used for the production of Ti pigments and metal. Ilmenite is found in black sand placer deposits, whereas rutile and leucoxene occur in heavy mineral coastal sand deposits [3]. In the US, minor titanium mineral deposits can be found in Wyoming, Montana, and California, although the most significant source of domestic titanium minerals are the black coastal sands of Florida [1].

Table 1.1. The most common titanium minerals and upgraded TiO_2 feed stocks.

Raw Material	% TiO_2 Content	Formula	Process
natural rutile	92–98	TiO_2	Chloride
synthetic rutile	92–96	TiO_2	Chloride
leucoxene	55–65	$Fe_2O_3 \cdot n\ TiO_2$	Chloride
titanium slag	75–85	$Ti_3O_5 \cdot MgTi_2O_5 \cdot FeTi_2O_5$	Chloride or Sulfate
ilmenite	45–65	$FeTiO_3$	Sulfate
anatase	90–95	TiO_2	-
brookite	90–100	TiO_2	-
geikilite	66–75	$MgTiO_3$	-
perovskite	40–60	$CaTiO_3$	-
pseudorutile	60–71	$Fe_2O_3 \cdot n\ TiO_2 \cdot m\ H_2O$	-
sphene	30–42	$CaTiSiO_5$	-
titanomagnetite	2–20	$(Fe \cdot Ti)_2O_3$	-

1.2 Applications

Titanium dioxide (TiO_2) is one of the most commonly used minerals in the chemical manufacturing industry. It has been commercially processed since the early 1900s and has a wide variety of applications. Pigment is used in paints, plastics and paper [4], sunscreen [5], cosmetics, and even as a food additive [6]. TiO_2 has also been used in photovoltaic cells [7], biomedical devices [8], and in air purification [9]. The rutile form of TiO_2 has a refractive index of 2.7, which imparts a high level of opacity (and hence whiteness) to whatever material it is added [10]. It should be noted that even diminutive concentrations of other transition metals such as iron can have a significant impact on the whitening ability of the pigment.

1.3 Production and Markets

The current worldwide titanium mineral reserves (ilmenite and rutile) are estimated to be 690 million metric tons. The current world production of titanium mineral concentrates is 6.3 million metric tons, with 91% coming from ilmenite ores and the remainder coming from rutile and other ores. Approximately 95% of the world's titanium minerals are consumed for titanium dioxide pigment production, with titanium metal and alloys accounting for the remaining 5%. The leading producers of titanium bearing minerals are Australia (29%), South Africa (22%), Canada (16%), and China (10%) [11]. The United States produced only 200 thousand metric tons in 2010 while importing 1.2 million tons and consuming nearly 1.5 million tons of Ti minerals. Ilmenite (54% TiO_2) was purchased for \$75/ton, rutile (95% TiO_2) for \$760/ton, and slag (80–95% TiO_2) for \$450–570/ton. US pigment manufacturers produced 1.32 million tons of TiO_2 in 2010 with a value of 3.0 billion USD, a 7% increase from the previous year. The

current price of TiO_2 pigment is $1.30–1.40/lb. The major markets for pigments include paints (59%), paper (26%), and plastics (9%) [4].

1.4 Feed Material

The two main commercial processes for producing titanium dioxide pigment are the sulfate process [1, 3] and chloride process [2]. The main feed stocks for each of the processes are shown in Figure 1.1. The sulfate process is able to accommodate lower grade stocks such as ilmenite, whereas the chloride process requires high grade stocks such as natural or synthetic rutile. High grade TiO_2 slag has been used for both processes.

1.4.1 High-Titania Slags

High-titania slags are produced by a smelting process which reduces iron oxides to liquid iron in large electric arc furnaces using anthracite as a reductant [12]. The main

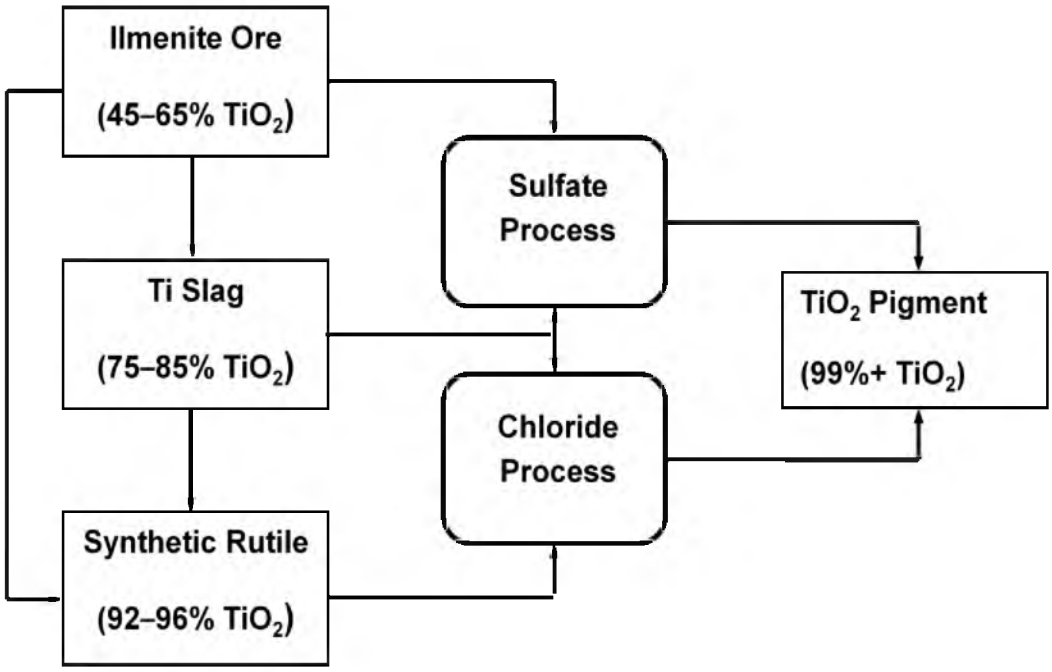

Figure 1.1. Schematic illustration of conventional TiO_2 pigment manufacturing processes from ore to pigment.

product of smelting is titania slag containing approximately 75 to 85% TiO_2. The coproduct of smelting is pig iron, which can be used as raw material for the steel industry. Titanium slags are chiefly produced in Quebec, Canada (Rio Tinto Iron and Titanium), South Africa (Richard Bay Minerals), and in Norway (Tinfos). The slag from these producers comprise about 30% of the total global TiO_2 pigment feed stocks [2].

A comprehensive review of early investigations (early 1900s to late 1960s) of Ti slag making is provided by Barksdale [1]. These investigations involved upgrading a wide variety of Ti bearing feed stocks including ilmenites, titaniferous magnetites and sands, and waste slags from Fe-Ti alloy processing. Most of the smelting tests were performed in small blast furnaces or in crucibles in laboratory furnaces. Industrial-scale smelting of ilmenite ore using electric arc furnaces began in 1952 and soon became the preferred method of slag making due to higher processing efficiency and consistency in high grade slag making. The research was aimed at understanding and optimizing the Ti recovery in the slag phase by varying the time, temperature, types, and amounts of reducing and fluxing agents, etc. It was generally found that the use of alkali carbonate or basic oxide fluxes lowered the slag formation temperature and viscosity of the melts and facilitated separation, but generally led to a slag with higher impurities. It was also found that many slag melts did not require fluxing agents as long as the proportion of reducing agent was carefully controlled.

Generally, only enough carbon to reduce all iron to metal and titanium to monoxides or trioxides is used in order to prevent the formation of carbide phases that made subsequent separation very difficult. Keeping a proper amount of FeO in the slag (~2–5 %) was also necessary to prevent carbide formation and prevent solidification of

the slag melt. It was also found that the solubility of slags in sulfuric acid increased with an increased proportion of lower valence oxides. The cooling rate also proved to have an effect on the solubility of slag. Rapid cooling was found to lead to fine grain sizes and large proportions of the rutile phase, which is refractory to leaching, whereas slow cooling of slag led to larger grain sizes, smaller amounts of insoluble TiO_2, and greater overall leaching efficiency.

An excellent review of the more recent research efforts in Ti slag making is provided by Sahu et al. [13]. The research has aimed at increasing energy efficiency, enriching TiO_2 content, expanding applicability to low grade ores, and improving leachability of titania slags. The effects of feed particle size and the amounts of reducing and fluxing agents on slag grade and total titanium recovery have been studied. Research has also led to the improvement of the DC plasma arc furnace design, lowering of energy and electrode consumption by the use of prereduction techniques, and the lowering of fluidity temperatures by the addition of basic oxides as flux.

1.4.2 Synthetic Rutile

Titania slag can be used to produce synthetic rutile, which is a further upgraded raw material with a TiO_2 content of 92–96%. However, the majority of synthetic rutile production is performed by partial reduction and oxidation of ilmenite with subsequent hydrochloric acid leaching. A comprehensive review of the various HCl leaching methods to upgrade ilmenite to synthetic rutile prior to 1975 is provided by Jackson [14]. He determined that most of these early investigations could be subcategorized into 5 approaches: single-state ambient pressure leaching with no pretreatments, single-stage high pressure leaching at high temperatures with no pretreatments, single-stage ambient

pressure leaching with oxidation/reduction pretreatments, multistage leaching, and complete digestion at low pulp densities with subsequent solvent extraction. Most of these studies aimed to optimize the HCl concentration and consumption, reaction time and temperature, and oxidation/reduction preleach treatments for particular ilmenite deposits. It was generally found that more severe temperature, pressure, and acidic conditions led to shorter reaction times and higher Ti losses; high pulp densities led to the saturation of the solution with Ti leading to titanium dioxide precipitation, whereas low pulp densities favored complete dissolution of both Fe and Ti; and Fe and Ti dissolution kinetics improved with oxidation and reduction pretreatments.

Since 1975, numerous investigators have sought to improve the synthetic rutile making process as well as widen its applicability to various ilmenite ores. Most of these studies have followed the oxidation/reduction pretreatment approach followed by subsequent leaching with hydrochloric or sulfuric acid. One industrial approach, the Becher process, involves four major steps: oxidation, reduction, oxidative precipitation, and H_2SO_4 leaching [15–17]. Ilmenite ($FeTiO_3$) is first oxidized with air in a rotary kiln to convert the iron bound to titanium dioxide to Fe_2O_3. The oxidized Fe product is then reduced to metallic iron with coal and sulfur at temperatures >1200 °C, which is then reoxidized by a 1% NH_4Cl solution to form a fine Fe_2O_3 slime, which is physically separated from coarser synthetic rutile particles. Any remaining Fe_2O_3 is leached away with 0.5 M H_2SO_4.

The Murso process follows a similar sequence; however, it uses a fluidized bed roaster for oxidation at 900–950 °C, H_2 gas for reduction, and 20% HCl to remove the reduced Fe instead of NH_4Cl and H_2SO_4 leaching [18]. The use of HCl allows for greater

ease in recycling of acid. The Laporte process also uses a fluidized bed roaster for oxidation at 950 ºC followed by coal reduction at 900 ºC. The reduced ore is leached with 18% HCl in a bed contactor in order to prevent the formation of very fine TiO_2 precipitate particles, which make liquid-solid separation very difficult [19]. The Benelite process omits the use of an oxidation stage and instead uses carbothermic reduction to convert all ferric ions in ilmenite to ferrous followed by subsequent leaching with 20% HCl [20]. While this one-step pretreatment saves production time and energy, it is limited in the types of ilmenite ores it can process.

The Austpac process uses an oxidative roast pretreatment to magnetize ilmenite, which facilitates the removal of impurities through magnetic separation and obviates the need for a reduction step [21]. The magnetic concentrate is then leached with 25% HCl, filtered, washed, and calcined. A final magnetic separation stage produces a > 97% TiO_2 synthetic rutile product. The omission of a reduction step does lead to lower energy consumption but does require more HCl for subsequent leaching. The Dunn process also uses unconventional separation techniques [22]. The process uses chlorine gas to selectively chlorinate iron in ilmenite to volatile $FeCl_3$ which is separated and oxidized to form Fe_2O_3 and Cl_2 gas that is recycled. Any Ti that chlorinates reacts with iron oxide to form TiO_2.

In the last decade, several investigators have revisited direct HCl leaching of ilmenite without pretreatment with moderate success. Both Mahmoud et al. [23] and El-Hazek et al. [24] were able to significantly increase the total iron dissolution rate of ilmenite in HCl by adding iron powder as a reducing agent. Lasheen [25] directly leached a Rosetta ilmenite concentrate (40–47% TiO_2) with 12 M HCl to produce an 89% TiO_2

product. The use of concentrated HCl and metallic iron as a reductant allowed for efficient removal of iron in the mineral without significant Ti losses, whereas only 55% Fe leaching efficiency was achieved without the addition of metallic iron. The addition of a reducing agent such as metallic iron facilitates the conversion of ferric ions in the ilmenite lattice to the highly soluble ferrous form and results in a purer TiO_2 product.

1.4.3 Environmental Comparison of Slag and Synthetic Rutile

The energy consumed in producing either slag or synthetic rutile is roughly equivalent (35.5 and 35.0 MJ/ton TiO_2, respectively) [26]. However, the upgrading of ilmenite to synthetic rutile produces acidic effluents as well as a considerable amount of solid waste (2 tons/ton TiO_2) [27]. The slag making route produces a saleable Fe product from low grades of ilmenite with minimal waste generation. For this reason, titania slag could be considered a more economical and environmentally friendly upgraded feed material for pigment manufacture. This is a key reason Ti slag was used as the feed material for the current investigation instead of synthetic rutile.

1.5 Chloride Process

1.5.1 Process Description

The chloride process was first developed in the late 1950s by DuPont [28, 29]. A flow sheet of the process is shown in Figure 1.2. The chloride process involves reacting rutile (natural or synthetic) or titania with petroleum coke and chlorine gas at high temperatures, forming a titanium tetrachloride ($TiCl_4$) vapor. The vapor is distilled and then oxidized at 1300–1800 °C with oxygen and $AlCl_3$. The key reactions for this process are shown below.

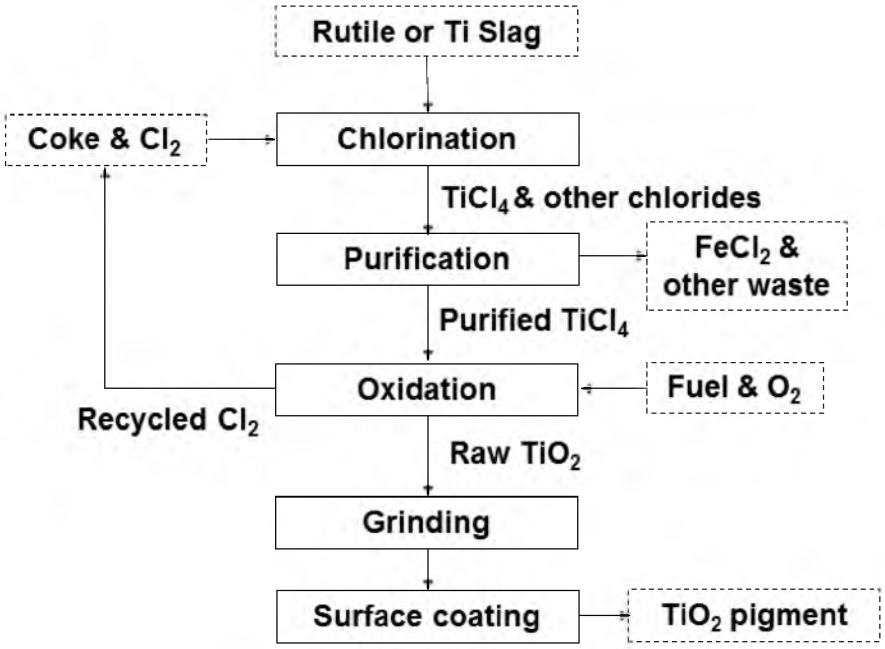

Figure 1.2. Flow sheet of the chloride process.

$$TiO_2 + C + 2Cl_2 \rightarrow TiCl_4 + CO_2 \quad (1.1)$$

$$TiCl_4 + O_2 \rightarrow TiO_2 + 2Cl_2 \quad (1.2)$$

1.5.2 Environmental Issues

The resulting product of these reactions is a highly purified TiO_2 pigment. While the process does not produce the same magnitude of wastes as the sulfate method, it still has several environmental issues of its own. From the stoichiometry of reaction (1.1), we can see that 1 mole of CO_2 is directly generated for every mole of TiO_2 produced, which equates to 550 kg CO_2 per ton TiO_2 produced. The world production capacity of titanium dioxide pigment by the chloride process is an estimated 3.4 million metric tons per year [4], resulting in approximately 1.9 million tons per year of CO_2 emitted from this reaction alone.

1.6 Sulfate Process

1.6.1 Process Description

Titania slag or raw ilmenite is used as the feed material for the sulfate process, which was developed nearly 100 years ago. A flow sheet of the sulfate process is shown in Figure 1.3. The feed material is digested with concentrated sulfuric acid to produce titanium sulfate followed by the bulk removal of iron sulfate ($FeSO_4 \cdot 7H_2O$) through crystallization and filtration steps. The titanium sulfate is hydrolyzed at boiling temperatures, and a hydrous titanium oxide compound is precipitated and removed from solution. This compound is calcined at 650–1000 °C to form either anatase or rutile-type TiO_2. The major reactions of this process are shown in (1.3)–(1.5).

$$FeTiO_3 + 2H_2SO_4 + 5\,H_2O \rightarrow FeSO_4 \cdot 7H_2O + TiOSO_4 \quad (1.3)$$

$$TiOSO_4 + 2H_2SO_4 \rightarrow H_2TiO_3 + H_2SO_4 \quad (1.4)$$

$$H_2TiO_3 \rightarrow TiO_2 + H_2O \quad (1.5)$$

1.6.2 Environmental Issues

The major advantages of this process include low capital costs and flexibility in feed material. The major disadvantages include an abundant generation of acidic and solid waste and a variable quality of product due to batch processing. Sulfate plants can generate as much as 1500 kg acidic waste per metric ton of TiO_2, although full neutralization greatly reduces this amount (<100 kg/ton) [26]. Some plants have managed to employ sulfuric acid regeneration and recycling techniques, but these plants release effluents that are still 5–6 times more acidic than those at full neutralization plants.

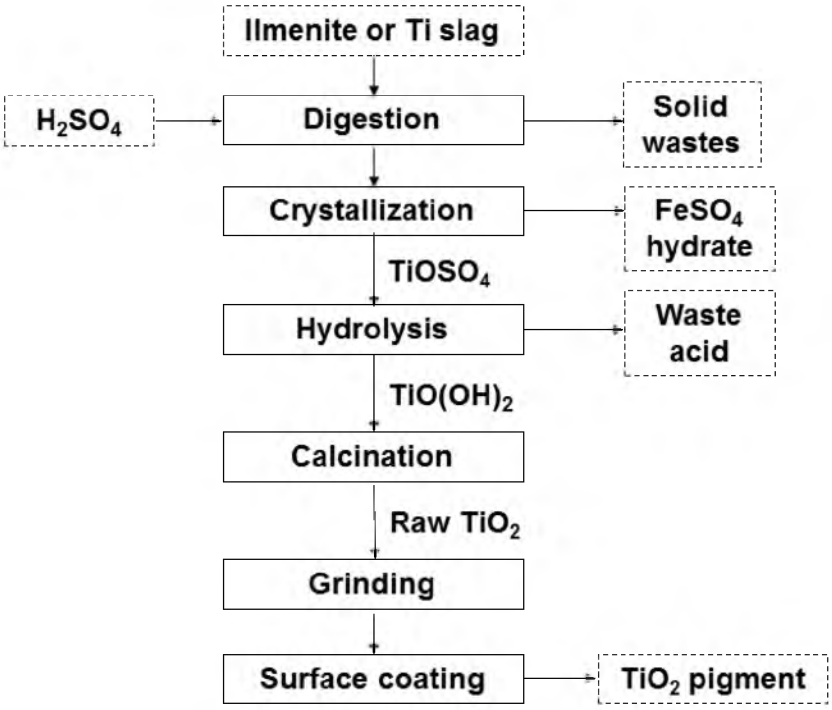

Figure 1.3. Flow sheet of the sulfate process.

The amount of solid waste is proportional to the degree of neutralization of acidic wastes. A sulfate plant with no neutralization generates roughly 0.5 ton solid waste per ton of TiO_2, while a plant employing full neutralization generates more than 5 tons/ton TiO_2. Despite these disadvantages, this process still accounts for 40% of the total TiO_2 pigment produced worldwide [30]. There are currently no sulfate plants in the United States [4].

1.6.3 Research Efforts into Improving Sulfate Process

Hundreds of investigations have been performed in the last century into improving the purity and yield of titanium dioxide pigments from numerous grades of titanium ores and slags using the sulfate process. A comprehensive review of early research of the sulfate processing of titanium ores and slags is found in Barksdale [1].

With few exceptions, most of the research has focused on optimizing the various process steps described above.

1.6.3.1 Benefits of Slag over Ilmenite as Feed

The review also noted that the use of slag in the process had several advantages over using ilmenite. Using slag results in Ti recoveries equal or greater than ilmenite and eliminates the need for several processing steps, including reduction of ferric sulfate to ferrous with the addition of Fe scrap, crystallization and filtration of ferrous sulfate for bulk iron removal, and vacuum evaporation to concentrate the Ti in solution. This leads to significantly less waste generated by the process. Also, using slag as a feed stock generally consumes 2.51 tons of sulfuric acid per ton of TiO_2, whereas ilmenite consumes 3.75 tons of acid. The optimal reaction conditions for the digestion of slag include digesting 40 to 60 micron slag particles with a 2:1 ratio of 92% sulfuric acid to ore (by weight), at an initial temperature of 115 °C and a final temperature of 180 °C. The reaction time is 2 to 3 hours and results in a yield of over 96%.

1.6.3.2 Reduction of Energy Consumption

Much of the research efforts of the past few decades have focused on lowering the energy and acid consumption of the process as well as generating less solid and liquid waste. Particular focus has been on regenerating and/or reusing sulfuric acid in the process and is in fact required in many parts of the world [27]. Roche et al. [31] have developed an improved sulfate process that uses sulfuric acid streams more efficiently by reusing the raffinate from a solvent extraction step as the lixiviant for the initial leaching step, resulting in a reduction in acidic effluents and solid waste neutralization products.

The use of reducing agents during leaching allows for lower H_2SO_4 concentrations and eliminates the need for acid reconcentration through energy intensive evaporation procedures. The process uses solvent extraction to separate Ti from iron and other impurities. It was found that the presence of fine titanyl sulfate particulates in the recycled acid acted as seeds for premature precipitation of Ti in the leaching step, which would carry coprecipitated ferric complexes downstream and lower the final pigment purity [32]. Fine filtration of the recycled acid helped somewhat to ameliorate this issue, and the process is able to produce a pigment with 99% purity and total Fe content of 0.07% (700 ppm).

A patented process by Watanabe and Sei [33] also uses solvent extraction to recover Ti from sulfuric acid solutions. NaCl is added to the solution in order to form an iron chloride anionic complex, which is extracted with oxygen-containing organic solvents and/or alkylamines. An alkylphosphoric acid is then used to extract Ti, which is stripped with a NH_4^+ / HF solution, and the titanium in the liquor is precipitated with NH_3, $NH_4(OH)$, or KOH as titanium hydroxide, $Ti(OH)_4$, which is then converted to a chloride or alkoxide. The addition of a strong base to the liquor eliminates the need for a hydrolysis stage, which lowers energy consumption, although it is unknown if the precipitate is suitable for pigment upon calcination.

1.7 Other Hydrometallurgical Methods

1.7.1 Direct Leaching and Solvent Extraction

Several hydrometallurgical processes for producing pigment grade TiO_2 have been in development in the last decade as alternatives to the chloride and sulfate processes. Most of these processes involve HCl leaching of ilmenite or upgraded feeds. A

direct leaching method of ilmenite using chloride media has been developed by Lakshmanan et al. [34] in which the ore was leached between 65 and 80 °C in 20% HCl and 150–300 g/L $MgCl_2$. Iron impurities were removed from the leach solution by solvent extraction using tributyl phosphate and recovered as iron oxides through pyrohydrolysis. This process produced a pigment with a composition of > 99.0% TiO_2 and < 0.01 % Fe (100 ppm). The Altair process [35] uses concentrated HCl (> 360 g/L) to directly leach ilmenite. The solution is cooled to crystallize $FeCl_2$ for bulk iron removal and fed to a two stage solvent extraction procedure that uses a phosphine oxide to extract titanium and ferrous ions in the first stage and an amine extractant to remove ferric ions in the second. The purified titanium solution is hydrolyzed in a spray dryer and calcined to produce TiO_2 pigment particles. Pigments with iron concentrations of 6 ppm have been achieved. This process also uses pyrolysis to regenerate acid. While these processes reduce the generation of acidic wastes, the pyrolysis procedure can be quite energy intensive (2.5–5.0 MJ/liter solution [36]), and the use of concentrated HCl solutions requires high capital costs for process equipment.

1.7.2 Alkaline Roasting and Leaching

Other investigators have used alkaline roasting to digest titanium feed stocks. Foley and McKinnon [37] roasted ilmenite concentrates with potassium and sodium carbonate salts at 860 °C followed by leaching with HCl or H_2SO_4 acids. Lahiri and Jha [38] studied the kinetics of ilmenite roasting with soda ash in the 600 to 900 °C temperature range. Lasheen [39] roasted titania slag made from Rosetta ilmenite with soda ash at 850 °C followed by a water leach, 20% HCl leach, and a 2 N NaOH leach to produce a synthetic rutile product of 97% purity. Xue et al. [30] have decomposed high

grade titania slag (> 90% TiO_2) in concentrated sodium or potassium hydroxide and washed with water to form a sodium or potassium titanate intermediate. A pigment with a purity as high as 99.3% and a Fe content of 600 ppm was achieved. These methods indicate that alkaline digestion of titanium slag can yield high decomposition rates at medium temperatures and atmospheric pressure. Such conditions will conceivably lead to lower energy consumption for the entire pigment manufacturing process.

1.7.3 Pigment Purity Specifications

In summary, the existing commercial processes for making TiO_2 pigment consume large amounts of energy and/or generate large amounts of carbon emissions and solid waste. Many of the processes in development, however, have similar challenges. Another challenge includes producing a pigment with sufficient purity. For example, although each pigment application has a unique set of purity specifications, most commercial pigments require Fe levels of less than 50 ppm [40], and some manufacturers produce pigment with less than 10 ppm. Therefore, it is imperative that any novel process of pigment manufacture be able to realize certain advantages over current methods, but also be able to meet commercial pigment purity standards.

1.8 A New TiO_2 Pigment Making Process

A new TiO_2 making process has been developed that utilizes a unique combination of alkaline roasting of Ti-slag, leaching in HCl acid, and solvent extraction [41–43]. A flow sheet of the new process is shown in Figure 1.4. Titanium slag is roasted with sodium hydroxide and washed with water to remove soluble impurities and excess NaOH. The products of roasting and washing are leached with HCl acid, and the resulting solution undergoes a solvent extraction stage to produce a titanium rich raffinate. The

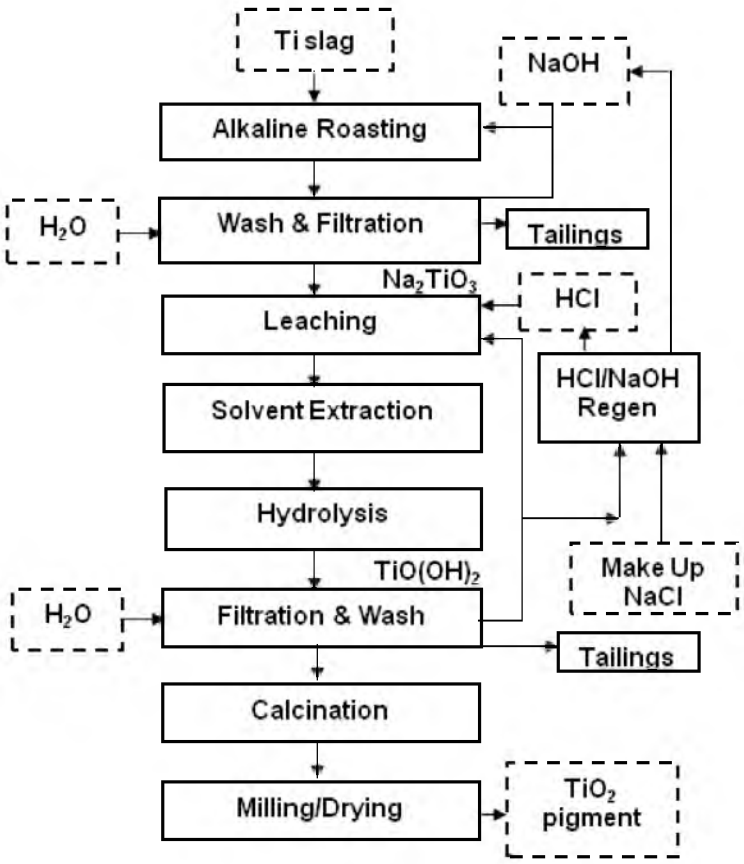

Figure 1.4. Flow sheet of the new TiO_2 pigment process.

raffinate is heated and stirred to precipitate metatitanic acid, $TiO(OH)_2$, which is then calcined to drive off chemically bound water and complete crystalline transformation to TiO_2. In order to minimize waste, the caustic, acid, and organic streams are filtered, regenerated, and recycled in the process. Various techniques are used to utilize the waste heat of roasting and calcination operations for leaching and hydrolysis, which can further reduce the energy consumption of the new process. It was hypothesized that this synergistic combination of established metallurgical processes could produce high-quality TiO_2 pigment while reducing the energy consumption and CO_2 emissions of the current pigment making processes. The specific steps of the new process are described in

detail and the results of optimization experiments using the new process are reported. Additionally, a comparison of the calculated energy consumption and carbon emissions of the new process is made with those of the chloride and sulfate processes.

1.9 References

[1] J. Barksdale, *Titanium: Its Occurrence, Chemistry, and Technology.* New York: Ronald Press Co, 1966, pp. 3–4.

[2] J. Winkler, *Titanium Dioxide*. Hannover, Germany: Vincentz Network, 2003, pp. 30–40.

[3] K.J. Stanaway, "Overview of titanium dioxide feedstocks," *Mining Eng.*, vol. 46, no. 12, pp. 1367–1370, 1994.

[4] J. Gambogi, "USGS mineral commodities summary report," USGS, Washington, DC, 2010.

[5] S. Yuan, W. Chen, and S. Hu, "Fabrication of TiO_2 nanoparticles/surfactant polymer complex film on glassy carbon electrode," *Mater. Sci. Eng., C*, vol. 25, pp. 479–485, 2005.

[6] P.M. Kuznesof, "Titanium dioxide – chemical and technical assessment," JECFA, Rome, Italy, 2006.

[7] M. Gratzel, "Photoelectrochemical cells," *Nature*, vol. 414, pp. 338–344, 2001.

[8] W.E. Yang, M.L. Hsu, and M.C. Lin, "Nano/submicron-scale TiO_2 network on titanium surface for dental implant application," *J. Alloys Compd.*, vol. 479, pp. 642–647, 2009.

[9] M. Hassan, "Life-cycle assessment of titanium dioxide coatings," in *Construction Research Congr.*, Seattle, WA, 2009, pp. 836–845.

[10] T.C. Patton, *Pigment Handbook: Properties and Economics*, 2nd ed. Hoboken, NJ: Wiley and Sons, 1973, p. 3.

[11] J. Gambogi, "USGS mineral commodities summary report," USGS, Washington, DC, 2011.

[12] A.F.S. Schoukens, D.J. Morris, and F.S. McComb, "Production of high titania slag from ilmenite," US Patent No. 6 733 561, May 11, 2004.

[13] K.K. Sahu, T.C. Alex, D. Mishra, and A. Agrawal. "An overview on the production of pigment grade titania from titania-rich slag," *Waste Mgmt. & Res.*, vol. 24, no. 1, pp. 74–79, 2006.

[14] J.S. Jackson, "A kinetic study of the dissolution of Allard Lake iIlmenite in hydrochloric acid." Ph. D. dissertation, Dept. Met. Eng., Univ. of Utah, Salt Lake City, UT, 1975.

[15] B.F. Bracanin, R.J. Clements, and J.M. Davey, "Direct reduction – the Western titanium process for the production of synthetic rutile, ferutil and sponge iron," in *AusIMM Proc.*, Victoria, Australia, 1980, pp. 33–42.

[16] P.W. Cassidy, R.J. Clements, B.A. Ellis, and P.R. Rolfe, "The AMC Narngulu synthetic rutile plant, a world source of ilmenite, rutile, monazite and zircon," in *AusIMM Proc.*, Victoria, Australia, 1986, pp. 61–67.

[17] J.B. Farrow, I.M. Ritchie, and P. Mangono,"The reaction between reduced ilmenite and oxygen in ammonium chloride solution," *Hydromet.*, vol. 18, pp. 21–38, 1987.

[18] H.N. Sinha, "The Murso synthetic rutile process," *Light Metals*, pp. 367–73, 1975.

[19] M. Robinson, F. Clamp, D.B. Mobbs, and R.V. Pearse, "The Laporte high-efficiency ilmenite beneficiation process," *Adv. Extract. Met.*, pp. 89–96, 1977.

[20] G.F. Balderson and C.A. MacDonald, "Method for the production of synthetic rutile," US Patent No. 5 885 324, Mar. 23, 1999.

[21] E.A. Walpole and J.D. Winter, "The Austpac ERMS and EARS processes for the manufacture of high-grade synthetic rutile by the hydrochloride leaching of ilmenite," *Proc. of Chloride Metallurgy*, Montreal, Canada, 2002, pp. 401–415.

[22] W.W. Minkler and E.F. Baroch, "The production of titanium, zirconium, and hafnium," in *Metallurgical Treatises*, J.K. Tien and J.F. Elliott, Ed. Warrendale, PA: AIME, 1981, pp. 171–189.

[23] M.H.H. Mahmoud, A.A.I. Afifi, and I.A. Ibrahim, "Reduction leaching of ilmenite ore in hydrochloric acid for preparation of synthetic rutile," *Hydromet.*, vol. 73, pp. 99–109, 2004.

[24] N. El-Hazek, T.A. Lasheen, R. El-Sheikh, and S.A. Zaki, "Hydrometallurgical criteria for TiO_2 leaching from Rosetta ilmenite by hydrochloric acid," *Hydromet.*, vol. 87, pp. 45–50, 2007.

[25] T. Lasheen, "Chemical benefication of Rosetta ilmenite by direct reduction leaching," *Hydromet.*, vol. 76, no. 1–2, pp. 123–129, 2005.

[26] E. Reck and M. Richards, "Titanium dioxide – manufacture, environment and life cycle analysis: the tioxide experience," *Surface Coatings Inter. Part B: Coatings Inter.*, vol. 80, no. 12, pp. 568–572, 1997.

[27] European Commission, "Integrated pollution prevention and control: best available techniques for the manufacture of large volume inorganic chemicals-solids and other industries," European Commission, Seville, Spain, 2007.

[28] A.H. Reid, "The development and commercialization of the DuPont chloride process for the manufacture of pigments based on titanium dioxide," *Proc. of AIChE Annual Meeting*," Philadelphia, PA, 2008, p. 224.

[29] L.E..Helberg, "The purification of titanium tetrachloride: a history," in *TMS 2011 Annu. Meeting,* San Diego, CA, 2011, pp. 503–509.

[30] T.Y. Xue, L.N. Wang, T. Qi, J.L. Chu, J.K. Qu, and C.H. Liu, "Decomposition kinetics of titanium slag in sodium hydroxide system," *Hydromet.,* vol. 95, no. 1–2, pp. 22–27, 2009.

[31] E.G. Roche, A.D. Stuart, and P.E.Grazier, "Production of titania," US Patent No. 7 429 364, Sept. 30, 2008.

[32] A.D. Stuart, J.A. Lawson, B.B. Ward, and H. Peng, "A sulphate process," WO Patent 2010034083-A1, Sept. 22, 2011.

[33] M. Watanabe and R. Sei, "Method for recovering titanium," European Patent No. 0198763-A2, July 16, 1988.

[34] V.I. Lakshmanan, R. Sridhar, G.B. Harris, and G. Puvvada, "Process for the recovery of titanium in mixed chloride media," US Patent No. 7 803 336, Sept. 28, 2010.

[35] D.Verhulst, B. Sabacky, T. Spitler, and W. Duyvesteyn, "The Altair TiO_2 pigment process and its extension into the field of nanomaterials," *CIM Bulletin*, vol. 95, no. 1065, pp. 89–94, 2002.

[36] A.S. Ferreira and M.B. Mansura, "Statistical analysis of the spray roasting operation for the production of high quality Fe_2O_3 from steel pickling liquors," *Proc. Safety Env. Protect.*, vol. 89, no. 3, pp. 172–178, 2011.

[37] E. Foley and K.P. MacKinnon, "Alkaline roasting of ilmenite," *J. Solid State Chem.*, vol. 1, no. 3–4, pp. 566–575, 1970.

[38] A. Lahiri and A. Jha, "Kinetics and reaction mechanism of soda ash roasting of ilmenite ore for the extraction of titanium dioxide," *Metall. Mater. Trans. B,* vol. 38, no. 6, pp. 939–948, 2007.

[39] T. Lasheen, "Soda ash roasting of titania slag product from Rosetta ilmenite," *Hydromet.*, vol. 93, no. 3–4, pp. 124–128, 2008.

[40] W.P.C. Duyvesteyn, T.M. Spitler, B.J. Sabacky, A. Vince, and J. Prochazka, "Processing aqueous titanium solutions to titanium dioxide pigment," US Patent No. 6 548 039 B1, Apr. 15, 2003.

[41] Z.Z. Fang, S. Middlemas, and P. Fan, "Production of titanium dioxide pigments," US Patent App. No. 2011/067583, 2011.

[42] S. Middlemas, Z.Z. Fang, and P. Fan, "A new method for production of TiO2 pigment-eliminating direct CO2 emissions," in *T.T. Chen Honorary Symp. on Hydrometallurgy, Electometallurgy, and Materials Characterization*, TMS 2012 Conf., Orlando, FL, 2012, pp. 285–294.

[43] S. Middlemas, Z.Z. Fang, and P. Fan, "A new method for production of titanium dioxide pigment," *Hydromet.*, vol. 131–132, pp. 107–113, 2013.

CHAPTER 2

ALKALINE ROASTING OF TITANIA SLAG

2.1 Introduction

2.1.1 Purpose of Roasting

Roasting is one of several commonly used chemical metallurgy techniques for preparing ore concentrates or intermediate products such as slag for leaching or other recovery processes. Alkaline roasting of vanadium slags has been an established upgrading process for several years [1]. The role of the alkaline roasting of Ti slag is twofold: 1) chemically separate titanium dioxide from iron oxides, silica, and other impurities and 2) form water soluble sodium compounds with impurity metals so that they may be removed with water in subsequent steps. Impurity elements such as Al, Mn, and Si form water soluble compounds that can easily be washed away, whereas Fe, Mg, and Ca compounds are insoluble and must be removed in subsequent extraction stages. Various experiments were conducted to characterize and optimize the roasting process and are described in detail.

2.1.2 Feed Material

The slag used in this investigation is a product of the smelting of Allard Lake ilmenite as described in Chapter 1 and was processed by Rio Tinto Iron and Tinto in Quebec, Canada; it is sold under the trade name of Sorelslag®. The slag is a solid-

solution of various titanate compounds with a pseudobrookite structure [2]. The relative proportion of metal titanate compounds within the primary phase is $(FeTi_2O_5)_{0.31}(MgTi_2O_5)_{0.30}(Ti_3O_5)_{0.31}(Al_2TiO_5)_{0.06}$ $(MnTi_2O_5)_{0.008}$. A minor glassy silicate phase ((Ca, Al, Mg, Fe, Ti) SiO_3) is also present as veins or inclusions in the bulk material. A small amount of free rutile TiO_2 is also present as well as metallic Fe. A more detailed description of the mineral characteristics of Sorelslag is provided by Gueguin and Cardarelli [3]. The nominal composition of the slag was provided by Rio Tinto Iron and Titanium and is shown in Table 2.1. In order to properly characterize the roasting reaction, some initial analysis and characterization of the feed material, titania slag, was also performed and is detailed in this chapter.

2.1.3 Advantages of Molten Salts

Molten NaOH has been used extensively in the chemical and metallurgical processing industries as a high-temperature electrolyte or ionized solvent [4]. Molten NaOH is composed of a strong cation (Na^+) and anion (OH^-) and thus has a very high electrical conductivity [5] that is an order of magnitude higher than its aqueous electrolyte. It has a relatively low vapor pressure and viscosity, high heat conductance and capacity, and maintains its molten state over a wide temperature range (> 318 °C) [6]. It dissolves most inorganic and organic substances quite readily and is highly corrosive to

Table 2.1. Composition of Sorelslag® (in wt. %).

Total TiO_2 (equiv)	TiO_2	Ti_2O_3	Total Fe (equiv)	Fe Metal	FeO	Fe_2O_3	Al_2O_3
78.5	64.4	12.7	7.73	0.15	9.75	0	2.36
CaO	MgO	MnO	SiO_2	Cr_2O_3	V_2O_5	Nb_2O_5	ZrO_2
0.66	5.57	0.3	2.75	0.21	0.56	0.01	0.05

most metals, although nickel and its alloys show a fair amount of resistance [7]. It also has a very high solubility for oxides such as TiO_2, Al_2O_3, and SiO_2, which is critical to the present technology.

2.1.4 Thermodynamic Analysis of the Alkaline Roasting of Slag

Prior to experimentation, however, some thermodynamic analysis of the reaction was performed. Thermodynamics is a powerful tool for predicting the products of chemical reactions in a defined closed system, which in this case, is the reaction of TiO_2 slag with molten sodium hydroxide in a reactor of constant volume. This system is fairly complex and involves numerous heterogeneous reactions involving solid, liquid, and gas phases. As previously discussed, TiO_2 slag is a complex mixture of numerous mineral phases in solid solution. Since the composition and properties of slag are highly dependent on the original feed material, additives, and smelting conditions in its synthesis, it is difficult to find standardized thermodynamic data for the material as a whole. However, the composition of the slag in terms of its various metal oxide compounds is known with a fairly high degree of accuracy; therefore, throughout this work, the chemical interactions of slag will be described thermodynamically in terms of its individual components.

The slag decomposition reaction can be assumed to take place at constant temperature and pressure; therefore, the behavior of the reactants and products in the system can be described by the Gibbs standard free energy of a reaction, ΔG°, which at standard conditions is defined in (2.1).

$$\Delta G^\circ = \Delta H^\circ - T\Delta S^\circ \tag{2.1}$$

where ΔH° is the change in enthalpy, or heat adsorbed or evolved by a system at constant pressure, T is the absolute temperature, and ΔS° in the change in entropy, a measure of the randomness or disorder in the system. At standard state, the enthalpy of formation of a chemical compound i at a temperature T can be determined according to (2.2).

$$\Delta H^{\circ}_{i,T} = \Delta H^{\circ}_{i,298} + \int_{298}^{T_1} C_{p,i}\, dT + L_{1,i} + \int_{T_1}^{T_2} C_{p,i}\, dT + L_{2,i} + \ldots \quad (2.2)$$

Where $C_{p,i}$ is the heat capacity expression, and $L_{n,i}$ is the latent heat of a particular phase transformation in the compound. Similarly, the entropy of formation can be determined from (2.3).

$$\Delta S^{\circ}_{i,T} = \Delta S^{\circ}_{i,298} + \int_{298}^{T_1} \frac{C_{p,i}}{T} dT + \frac{L_{1,i}}{T} + \int_{T_1}^{T_2} \frac{C_{p,i}}{T} dT + \frac{L_{2,i}}{T} + \ldots \quad (2.3)$$

The standard free energy of a reaction is also defined as the sum of the standard free energies of formation of products minus the sum of the reactants, as shown in (2.4).

$$\Delta G^{o}_{r} = \Sigma\, \Delta G^{o}_{products} - \Sigma\, \Delta G^{o}_{reactants} \quad (2.4)$$

With these equations, the standard free energies of the reactions between the various slag components and molten NaOH for a wide range of temperatures can be calculated. Normally, these calculations would be quite tedious; however, with the aid of commercial thermodynamic software such as HSC Chemistry 5.11, a tabulation of the change in Gibbs free energy with temperature is performed with relative ease. The results of this tabulation in a temperature range of 300 °C to 700 °C (573–973 K) are represented graphically in Figure 2.1. The reactions shown are not a comprehensive list of all possible reactions, but do represent the most thermodynamically favorable for each particular

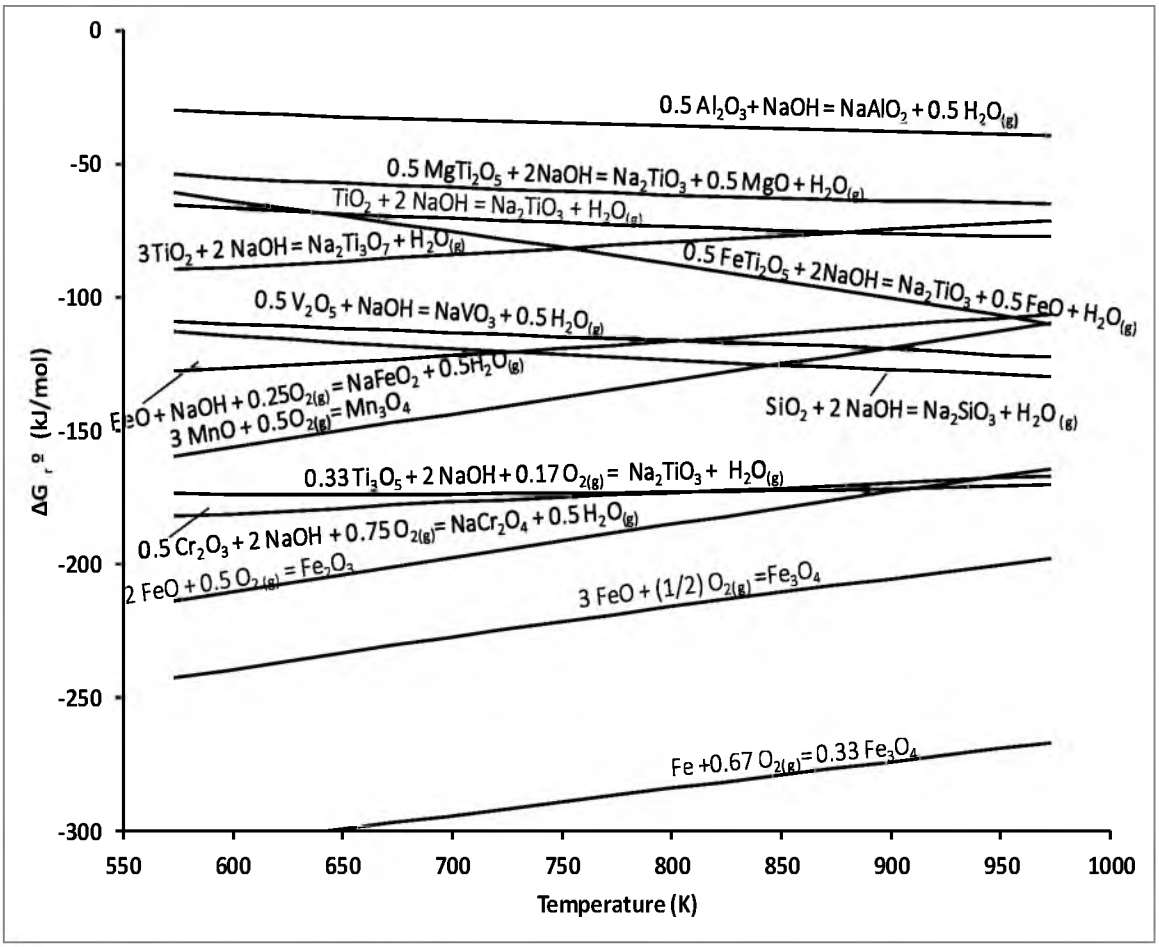

Figure 2.1. The change in standard free energy with temperature for the reactions of Ti slag and molten NaOH.

compound. Fe, FeO, and MnO readily oxidize in air to form higher valent oxides, and their reactions are also shown. The major components of the slag react with the molten NaOH according to reactions (2.5)–(2.8).

$$TiO_2 + 2NaOH = Na_2TiO_3 + H_2O \quad (2.5)$$

$$1/3\ Ti_3O_5 + 2NaOH + 1/6O_2 = Na_2TiO_3 + H_2O \quad (2.6)$$

$$1/2\ FeTi_2O_5 + 2NaOH = Na_2TiO_3 + 1/2\ FeO + H_2O \quad (2.7)$$

$$1/2\ MgTi_2O_5 + 2\ NaOH = Na_2TiO_3 + 1/2\ MgO + H_2O \quad (2.8)$$

TiO_2 and the various titanate phases react with the NaOH to form Na_2TiO_3 and water vapor. By forming Na_2TiO_3, TiO_2 is chemically separated from iron oxides and other impurities. It is clear by the negative ΔG^o_r values that the reaction of molten NaOH with each of the compounds in the slag is thermodynamically favorable and will occur spontaneously. Other sodium titanates such as $Na_3Ti_3O_7$ (which $Na_2O{\cdot}3TiO_2$) can form, depending on the NaOH:TiO_2 ratio. It should be noted that most of the sodium compound forming reactions have a positive entropy term (and hence negative slope) corresponding to the coproduction of water vapor, which has a greater degree of disorder than existed in the slag. Conversely, the compounds that oxidize have a negative entropy term (positive slope) owing to the consumption of oxygen in the system, forming more ordered oxide solids. Although Cr forms a sodium compound, it consumes a half mole more of O_2 than H_2O and thus also has a positive slope.

2.2 Experimental Methods

For initial roasting experiments, several grams of slag were mixed with excess NaOH in a nickel crucible and heated for 4 hours inside a muffle furnace. The molten mixture was removed and washed 3 times with distilled water and filtered to remove excess NaOH and remove soluble impurity compounds. To determine the degree of conversion in the roasting reaction, degree of conversion of the roasted slag samples was determined by dissolving ~ 0.5 g of the washed and dried product in 50 ml of 2 M HCl at 50 °C for 30 minutes. This concentration of acid was determined experimentally and proved to be sufficient to dissolve the washed roast product but not leach out metal values from unreacted slag, with the exception of small amounts of iron. The resulting solution was diluted by a factor of 100 in 5% nitric acid and analyzed using ICP-OES.

The degree of conversion X of metal i can be calculated using (2.9) and represents the amount of each metal in the slag that becomes acid soluble during the roasting process.

$$X_i = 100 \times \frac{C_i \times V}{F_i \times m_{rps} \times \frac{m_s}{m_{tot}} \times \frac{m_{wps}}{m_{wp}}} \quad (2.9)$$

Where C_i is the measured concentration adjusted for dilution (g/L), V is the volume of acid solution (L), and m_{rp}, m_s, m_{tot}, m_{wps}, and m_{wp} is the mass of roast product sample taken from the reactor, original mass of slag put into the reactor, total mass of slag and NaOH put into reactor, mass of wash product sample, and total mass of roast product after washing (in g), respectively. F_i is the weight fraction of the metal i per gram of slag as determined in the original slag assay. The factor of 100 is to convert the value to a percent. The composition of the wash water was also analyzed using ICP-OES. Roasted slag samples both before and after washing were analyzed using X-ray diffraction and SEM.

For subsequent roasting experiments, a cylindrical reaction vessel was fabricated from ¼ inch thick Inconel 200 pipe. A nickel based alloy was necessary due to the highly corrosive environment of molten sodium hydroxide. The vessel was 6" high and 4" in diameter with an internal volume of 600 ml. The vessel had ports for an agitator and a thermocouple as well as a sampling port in which the slag and NaOH were poured and sampled during the experiment. The agitator was fabricated from nickel rod. Each experiment was agitated at a speed of 100 rpm. The temperature was monitored with an Omega K-type thermocouple with the tip 1 mm above the bottom of the vessel. The vessel was placed inside a Xin Yoo XY1200 top loading crucible furnace, and the

periphery of the vessel was filled in with insulating wool. The furnace was equipped with a self-regulating temperature control unit that allowed for a constant temperature with +/- 1 °C precision to be maintained within the reaction vessel. A diagram of the vessel and furnace setup is shown in Figure 2.2. The sodium hydroxide, acids, and other reagents used were analytical grade and supplied by Cole-Parmer. Dissolved metal concentrations of solutions were determined using an ICP Agilent 7500ce quadrupole mass-spectrometer or a Spectro ICP-OES. X-ray diffraction of slag, intermediate, and final products was performed with a Philips 1140 diffractometer (Cu Kα) and the patterns were analyzed using X'Pert High Score Plus software. Intermediate and final products were examined with SEM microscopy using a Topcon SM100 microscope with an EDAX EDS detector operating at 20 kV tension.

2.3 Characterization of Slag Feed

2.3.1 Size Distribution of Slag

The size distribution of the slag was determined by splitting a ~200 g sample of slag from a 5 kg sample by a cone and quartering method and sizing it in a series of 3 inch sieves ranging from 400 to 10 mesh. The sieves were vibrated in a rotary tap for at least 15 minutes. The mass of slag in each of the sieves was weighed, and the cumulative percent passing for each size class was determined after averaging four trials. The size distribution of the slag is shown in a semilog plot in Figure 2.3. The error bars shown are one standard deviation, calculated using Excel 2010 statistical tools. The P_{50} and P_{80} were determined to be 108 and 610 μm, respectively. The mass retained on the +20/-10# screen showed the highest degree of error. A regression line shows a strong linear fit characteristic of a well behaved sample distribution.

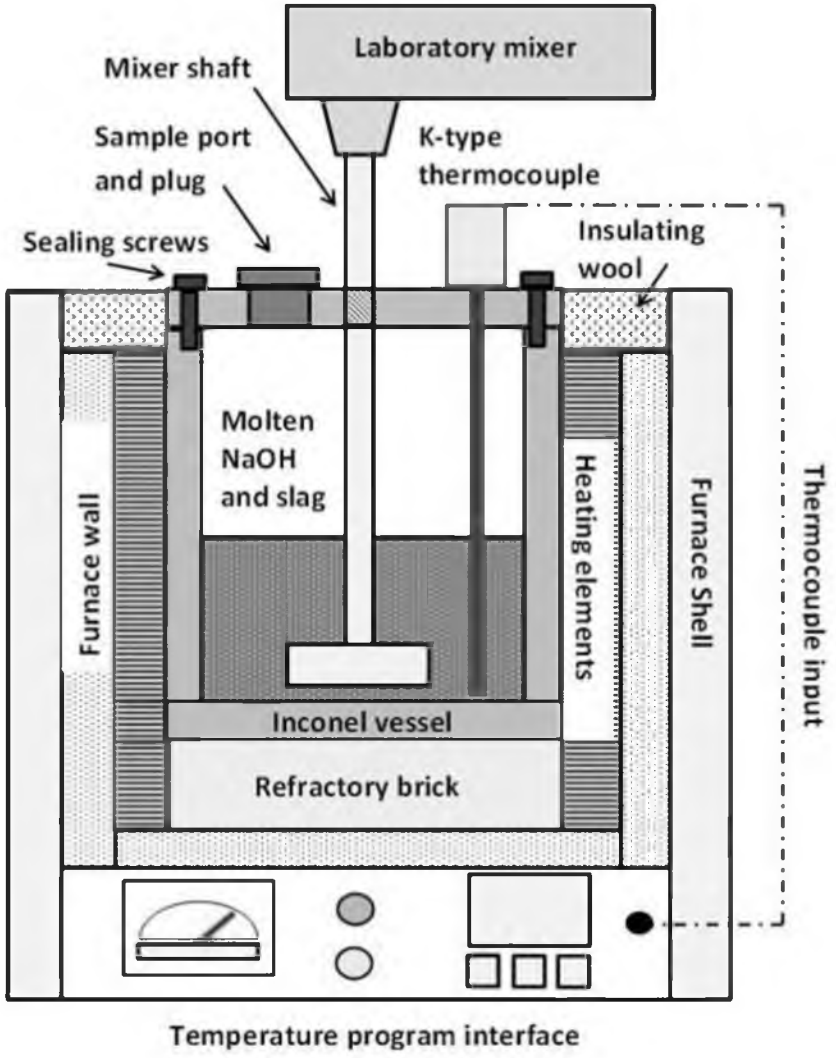

Figure 2.2. Experimental setup for the alkaline roasting of titania slag.

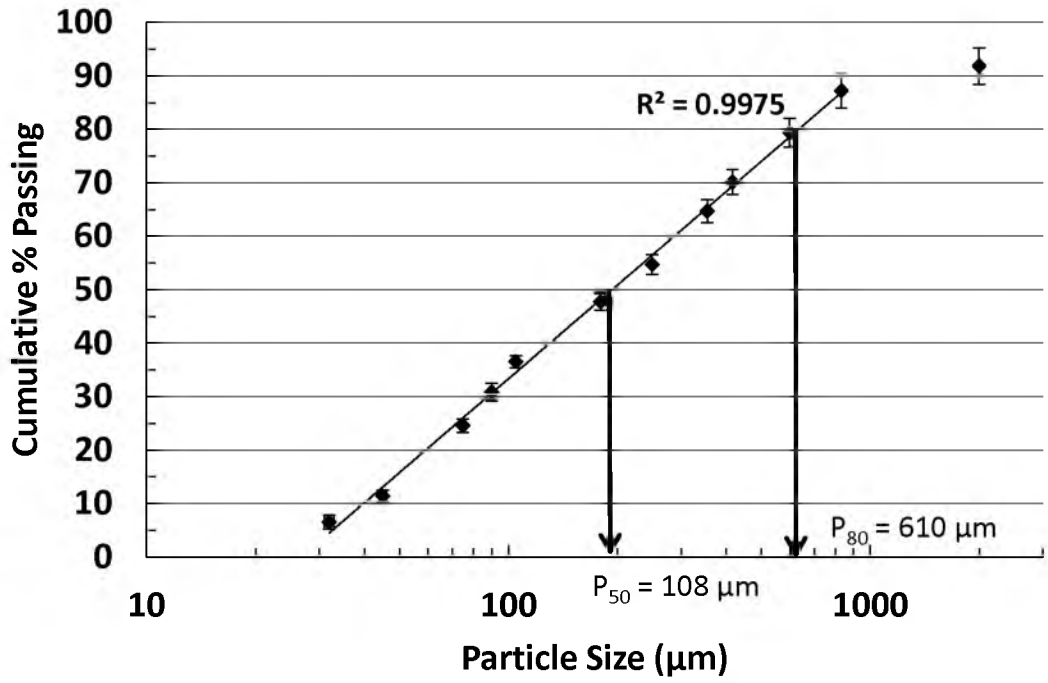

Figure 2.3. Cumulative % passing vs. particle size for as-received Sorelslag®. Error bars shown as one standard deviation.

2.3.2 Phase Distribution and Morphology of Slag

The composition and phases of the slag were characterized by various methods. The presence of titanate phases as well as rutile TiO_2 was confirmed by using XRD as shown in Figure 2.4. Optical microscopy and SEM confirmed the presence of three distinct phases, as shown in Figure 2.5. The silicate phase appears as dark grey veins in the optical and SEM images. The bright white inclusion in the silicate phase is metallic iron and appears commonly in other micrographs of Ti slag [3]. The optical microscope image also indicates that the morphology of the slag particles is fairly heterogeneous and angular in shape as a result of the crushing of large blocks of cooled slag. Elemental mapping performed using an EDS detector can give information about the elemental distribution within the different slag phases. In Figure 2.6, an EDS elemental map of a

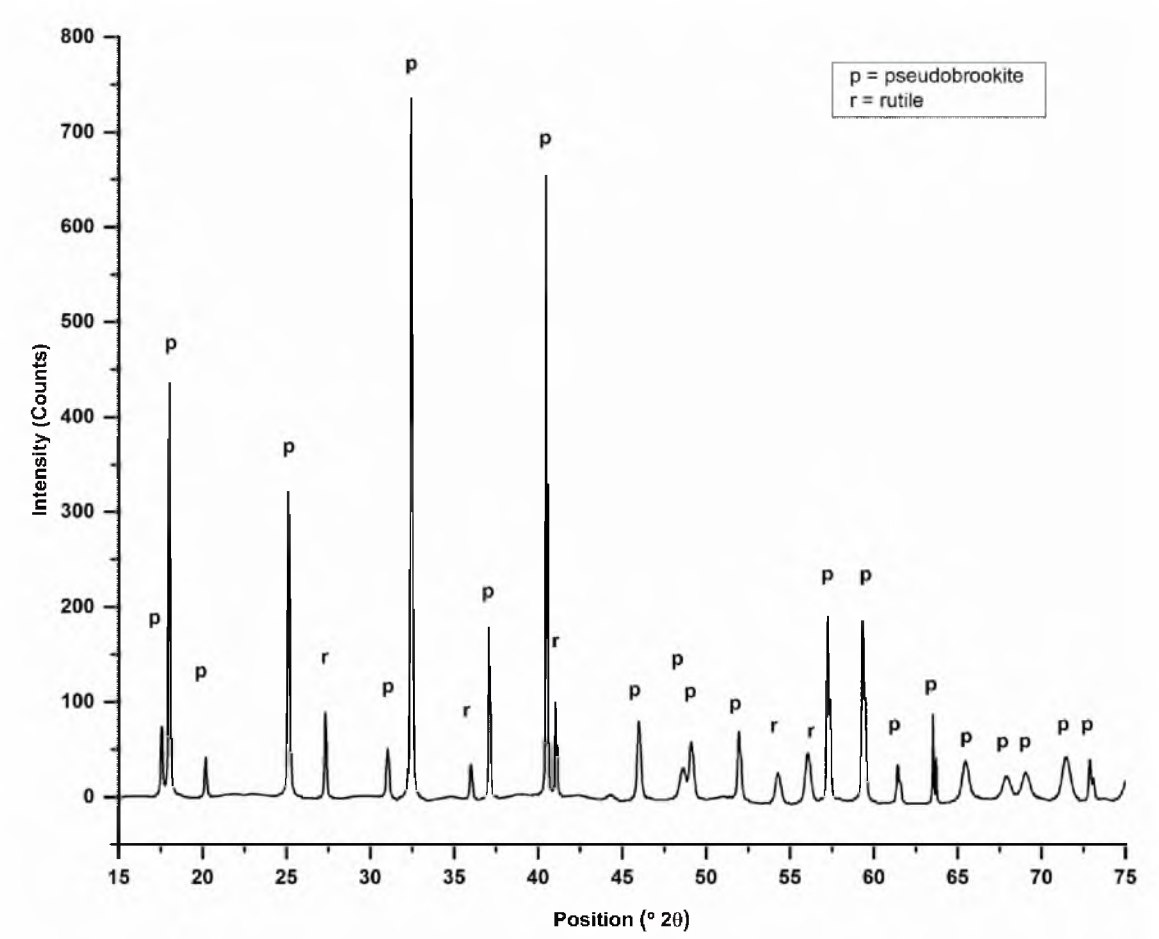

Figure 2.4. XRD pattern of as-received Sorelslag®.

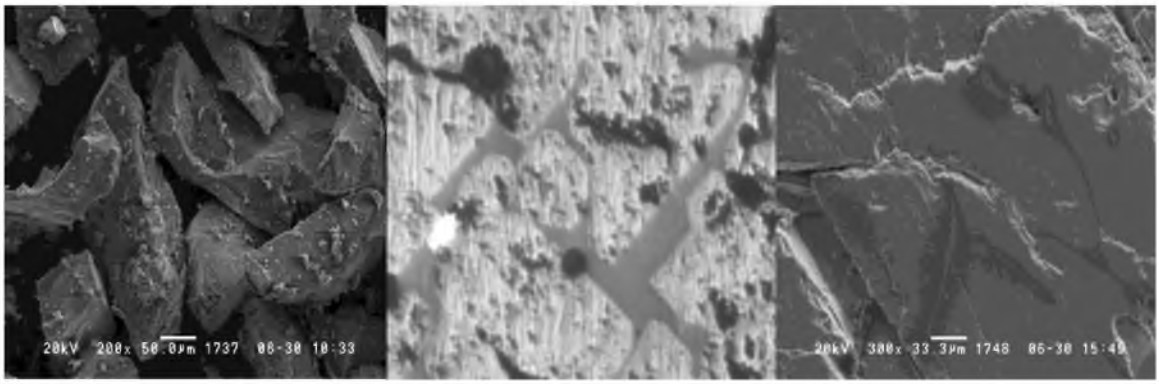

Figure 2.5. SEM and optical microscope images of as-received Sorelslag. (a) SEM image of 130 µm fraction, 200x (b) optical image of bulk Sorelslag, 200x (c) SEM image of bulk Sorelslag, 300x.

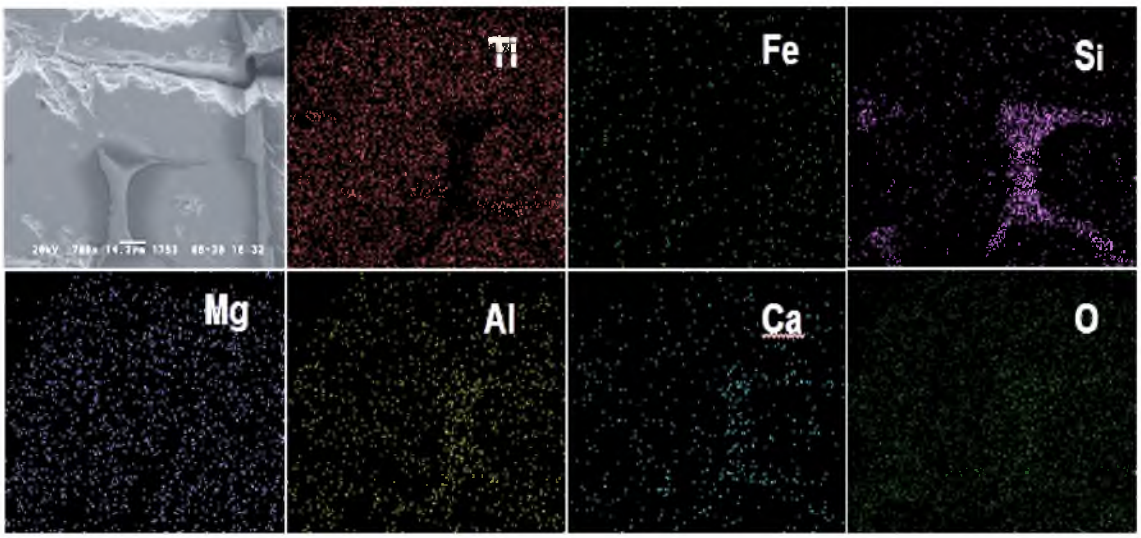

Figure 2.6. EDS Elemental maps of polished Sorelslag sample, 700x.

polished slag surface is shown with the SEM image of a silicate vein surrounded by a pseudobrookite matrix. The map confirms that the majority of Ti and Fe are present in the pseudobrookite phase as shown by a dark exclusion zone in the respective maps. Mg and Al appear to be evenly distributed between both phases. The majority of Si and Ca appear in the silicate phase. EDS can also be used to quantify the elemental composition. The bulk composition of titanium was measured as 45.5 wt. %, or 77.2 % in terms of TiO_2, which is in fair agreement with the TiO_2 composition reported by QIT of 78.5 %. Iron is also confirmed as the impurity of highest concentration.

2.4 Characterization and Optimization of Roasting Reaction

A series of experiments was conducted to characterize and optimize the various parameters of the roasting process with the objective of maximizing the conversion of Ti values in the slag to acid soluble sodium titanates. The parameters that were determined to have the greatest effect on the degree of conversion include slag particle size, NaOH to slag ratio, temperature, and time. The effects of each of these parameters on the roasting

reaction are described.

2.4.1 Effect of Particle Size

To determine the effect of particle size on the roasting reaction, four size classes of slag particles were used: +400/-325#, +325/-200#, +200/-170#, and +170/-140#, which correspond to median particle sizes of 38, 58, 82, and 97 microns, respectively. A 40 g sample of slag from each size class was reacted with 60 g of NaOH for 60 minutes at 500 °C. The degree of conversion was determined as stated previously. The degree of conversion versus median slag particle size is shown in Figure 2.7. It is clear that the extent of the reaction increases with decreasing particle size, and +400/-325# slag particles were determined to be the best size class for subsequent experiments.

2.4.2 Effect of NaOH to Slag Ratio

The proper amount of NaOH molten salt to react with the slag was determined by varying the ratio at a constant time, temperature, and particle size. For each experiment, 40 grams of +400/-325# slag particles were reacted with an amount of NaOH reagent corresponding to a NaOH/slag ratio of 1, 1.25, 1.5, 1.75, and 2. Each sample was roasted for 60 minutes at 500 °C. The degree of conversion versus NaOH/slag ratio is shown in Figure 2.8. It is apparent that the degree of metal conversion increases with an increase in NaOH to slag ratio. Doubling the ratio from 1 to 2 led to an increase of Ti conversion from 68% to 79%, respectively. A ratio of 1.5 led to a Ti conversion of 76% after one hour. The reaction mixtures with ratios of 1 and 1.25 proved to be quite viscous and restricted diffusion of reactants during the reaction. The reaction mixtures with higher ratios were quite fluid and led to more favorable reaction conditions. However, while a

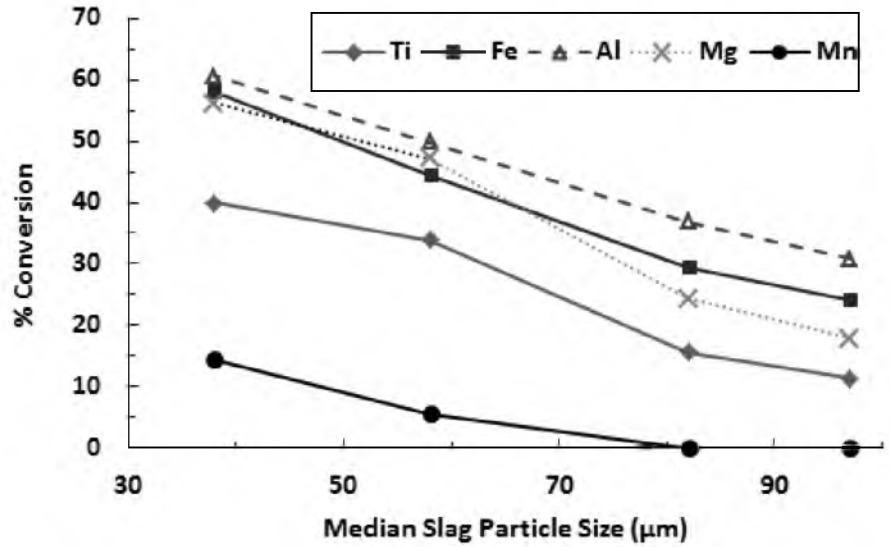

Figure 2.7. The effect of median particle size on degree of conversion for the roasting of slag with molten NaOH. NaOH/slag ratio: 1.5; Time: 90 minutes; Temperature: 500 ºC.

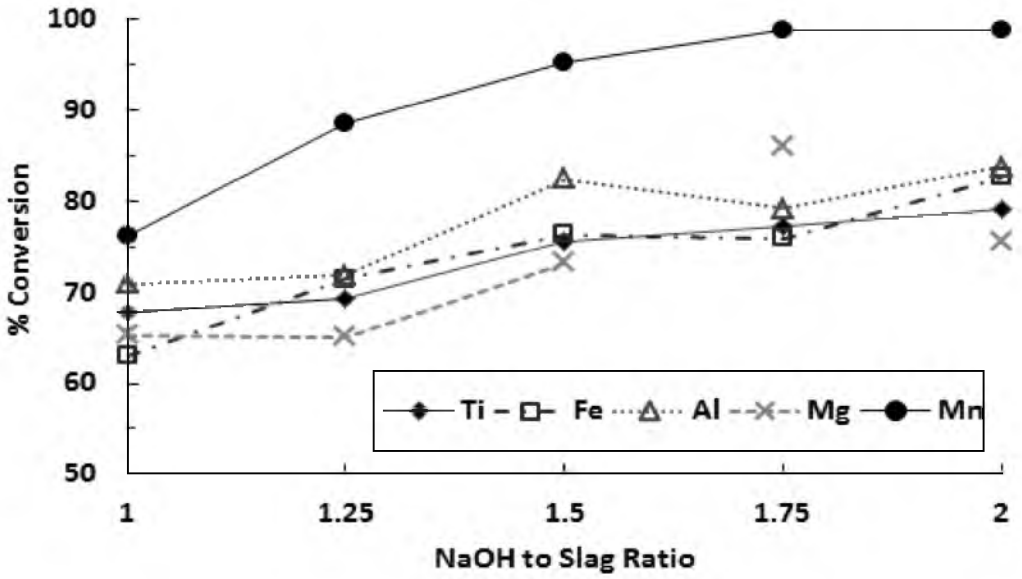

Figure 2.8. The effect of NaOH/slag ratio on the degree of conversion for the roasting of slag with molten NaOH. Size: +400/-325 mesh particles; Time: 60 minutes; Temperature: 500 ºC.

the mixture would likely be too fluid for a rotary kiln or multiple hearth roaster; therefore, a NaOH to slag ratio of 1.5 was considered to be the best ratio for subsequent reactions.

A sample from each experiment was analyzed using XRD, and the peaks in each of the patterns were identified, as shown in Figure 2.9. The intensity of slag peaks generally diminish as the NaOH to slag ratio increased, indicating a greater extent of reaction, supporting the solution analysis data. At lower ratios, the cubic Na_2TiO_3 appears to be the dominate titanate phase, which is consistent with the $Na_2O \cdot TiO_2$ binary phase diagram for this composition and temperature [8]. However, as the NaOH/slag ratio increases, the monoclinic titanate phases (Na_2TiO_3 and $Na_2Ti_3O_7$) become more prominent, and the peaks of the cubic phase become slightly less intense. The presence of Na_2O is also more prominent at higher NaOH ratios, which is also consistent with the $Na_2O \cdot TiO_2$ phase diagram.

2.4.3 Effect of Reaction Time and Temperature

The roasting reaction was carried out at a series of increasing temperatures in order to study the effects of temperature on the kinetics of the reaction. The reactions were performed at 400, 450, 500, 550, and 600 °C. For each test, 40 grams of +400/-325# slag particles were reacted with 60 grams of NaOH. An approximately 2 gram sample of roast product was removed from the reactor at fixed time intervals of 5, 15, 30, 60, 90, and 120 minutes. The samples were washed, digested, and analyzed as described previously, and the degree of conversion was calculated for the various metals in the slag. The conversion rates of Ti and Fe with time are shown in Figure 2.10. It is apparent that increasing the reaction temperature dramatically increases the rate of reaction. The

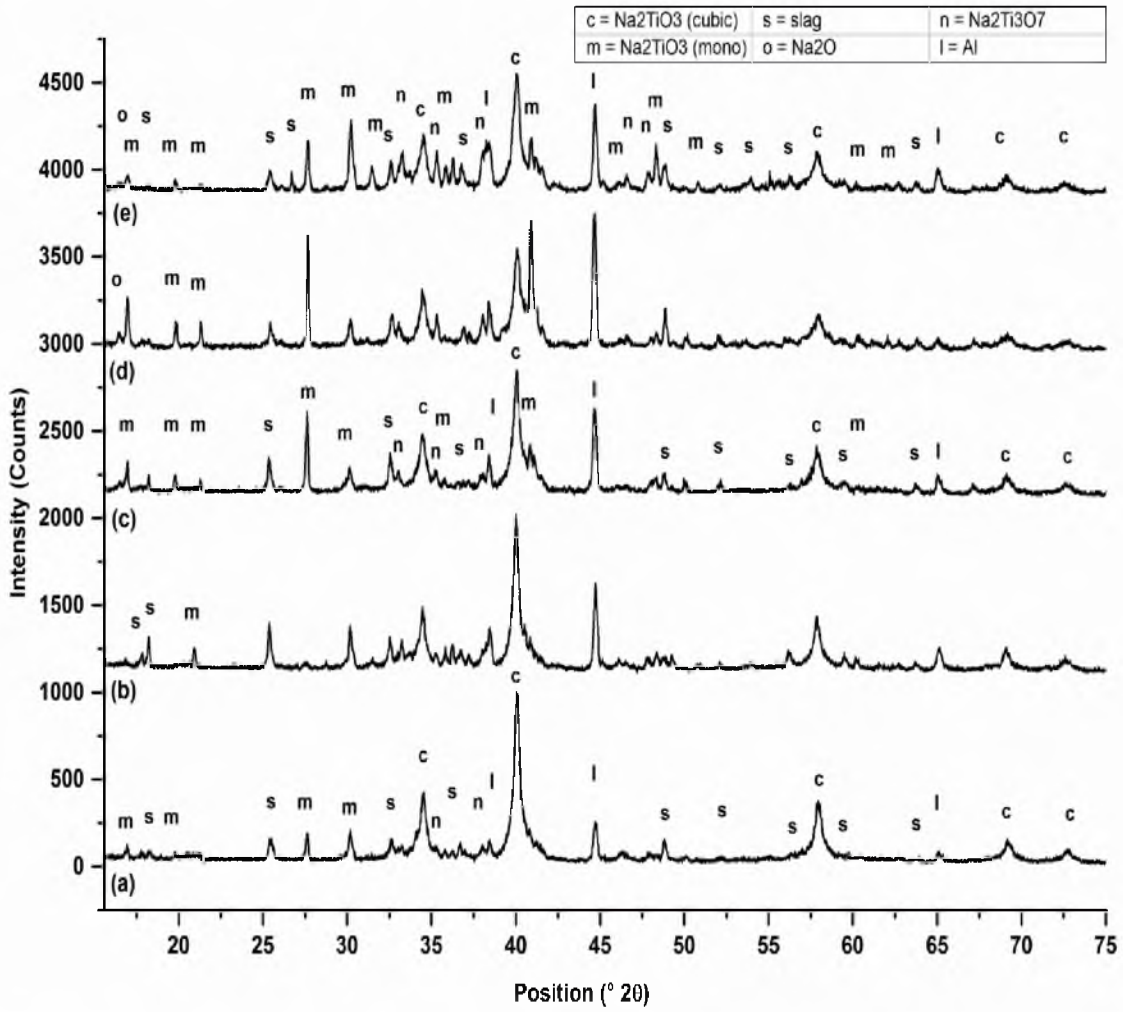

Figure 2.9. XRD graphs of the products of slag roasting at NaOH/slag ratios of a) 1.00, b) 1.25, c) 1.50, d) 1.75, and e) 2.00. Size: +400/-325 mesh particles; Temperature: 500 ºC; Time: 90 minutes.

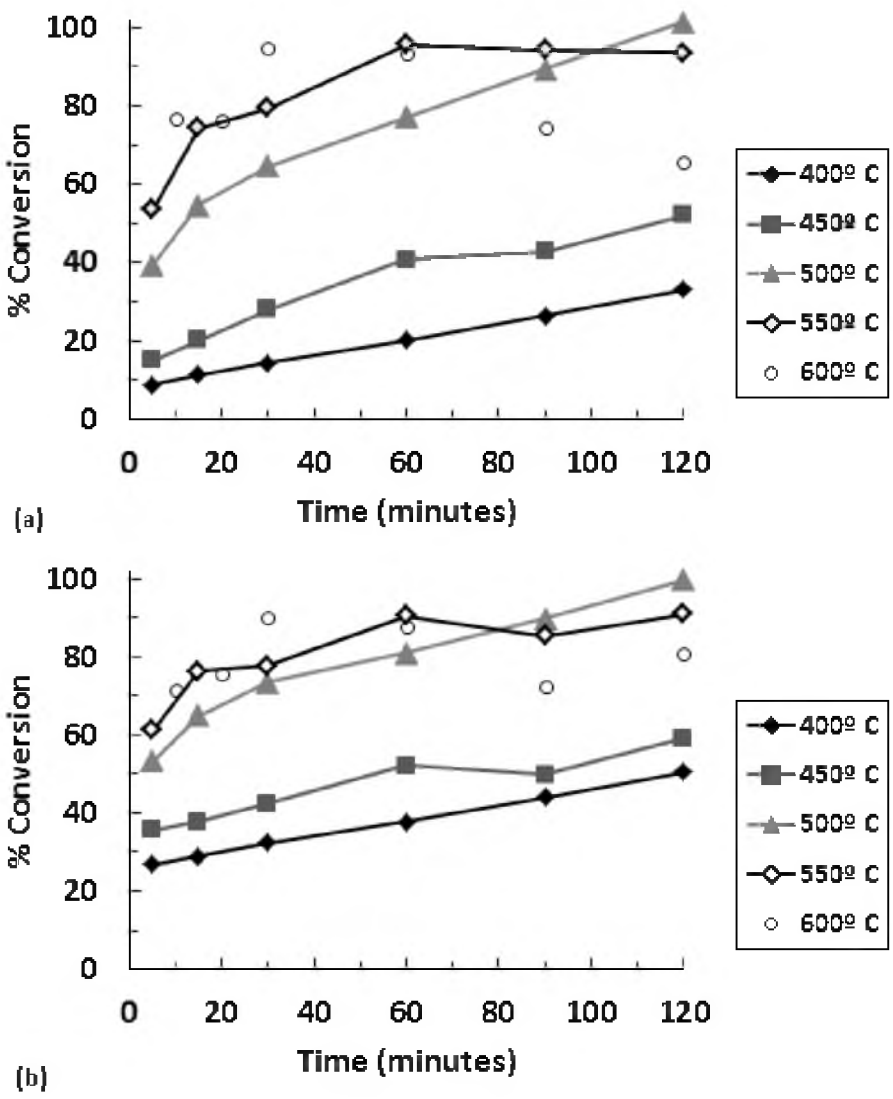

Figure 2.10. Metal conversion in slag vs. time at different reaction temperatures for a) Ti and b) Fe. Size: +400/-325 mesh particles; NaOH/slag ratio: 1.5.

conversion of Fe generally follows the same trends as Ti, although it is slightly overestimated due to the leaching of Fe from unreacted slag. At a temperature of 400 ºC, only 20% of the Ti was recovered after 1 hour, which only increased to 33% after 2 hours. Increasing the reaction temperature to 500 ºC dramatically increased the rate of conversion to 77% after 1 hour and increasing to nearly 100% after 2 hours. The reaction rates at 550 and 600 ºC were quite rapid, reaching over 95% conversion after 60 minutes

and 30 minutes, respectively, although after a certain time the roast product began to sinter and became difficult to leach, which accounts for the decreasing of the reported conversion for both Ti and Fe. Due to the difficulty in scooping the sintered roast product from the reactor at 600 ºC, a sample was taken at 10 and 20 minutes instead of 5 and 15 minutes. Based on these results, it was determined that the optimal reaction temperature and time was 550 ºC for 1 hour, leading to a Ti conversion of 96%.

The effect of temperature on the development of different product phases was also observed by XRD. A sample of roast product taken at 90 minutes from each temperature was analyzed in a 2θ range of 15–75°. The patterns are shown in Figure 2.11. At lower temperatures, peaks corresponding to the pseudobrookite phase of slag dominate the diffraction pattern, although weak peaks corresponding to cubic Na_2TiO_3 and monoclinic $Na_2Ti_3O_7$ are apparent. As the temperature increases, the slag peaks diminish and eventually disappear from the pattern. At 500 ºC, cubic Na_2TiO_3 peaks dominate, although some monoclinic Na_2TiO_3 peaks begin to intensify. Above 500 ºC, the cubic Na_2TiO_3 peaks begin to decrease in intensity and are dominated by monoclinic Na_2TiO_3 peaks, which are more stable at higher temperature. This is particularly apparent at the 40.0 and 40.6º positions, corresponding to the most intense cubic and monoclinic Na_2TiO_3 peaks, respectively. An Al peak at 44.6º was observed in most of the patterns, although this was determined to be an artefact from the sample holder.

The change in morphology of the reaction products as a function of time was also observed with the SEM. Images taken of the 15, 30, 60, and 90 minutes samples from each reaction temperature are shown in Figure 2.12. Each image was taken at 500x magnification. At 400 ºC, the majority of the slag particles remain close to their original

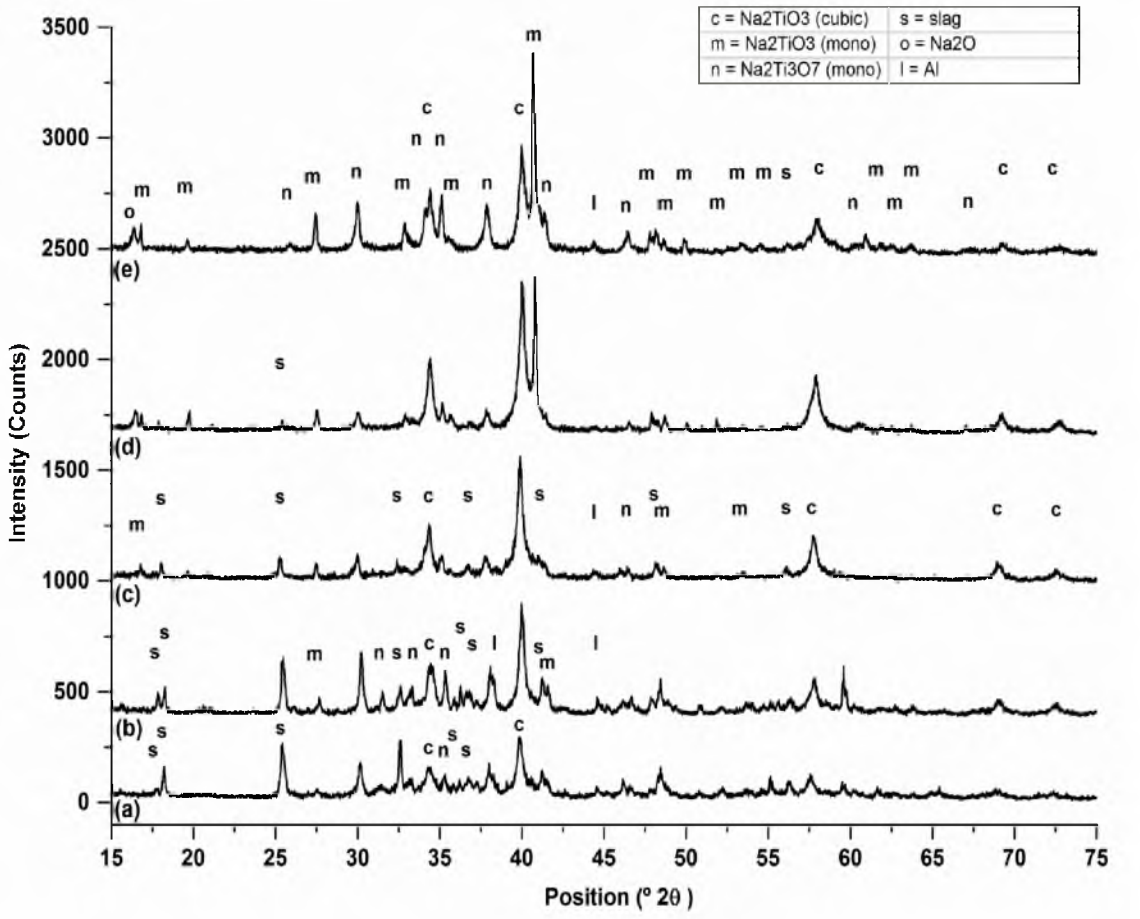

Figure 2.11. X-ray diffraction patterns of roasted slag products reacted at different temperatures: a) 400 ºC, b) 450 ºC, c) 500 ºC, d) 550 ºC, e) 600 ºC; Size: +400/-325 mesh particles; NaOH/slag ratio: 1.5; Time: 90 minutes.

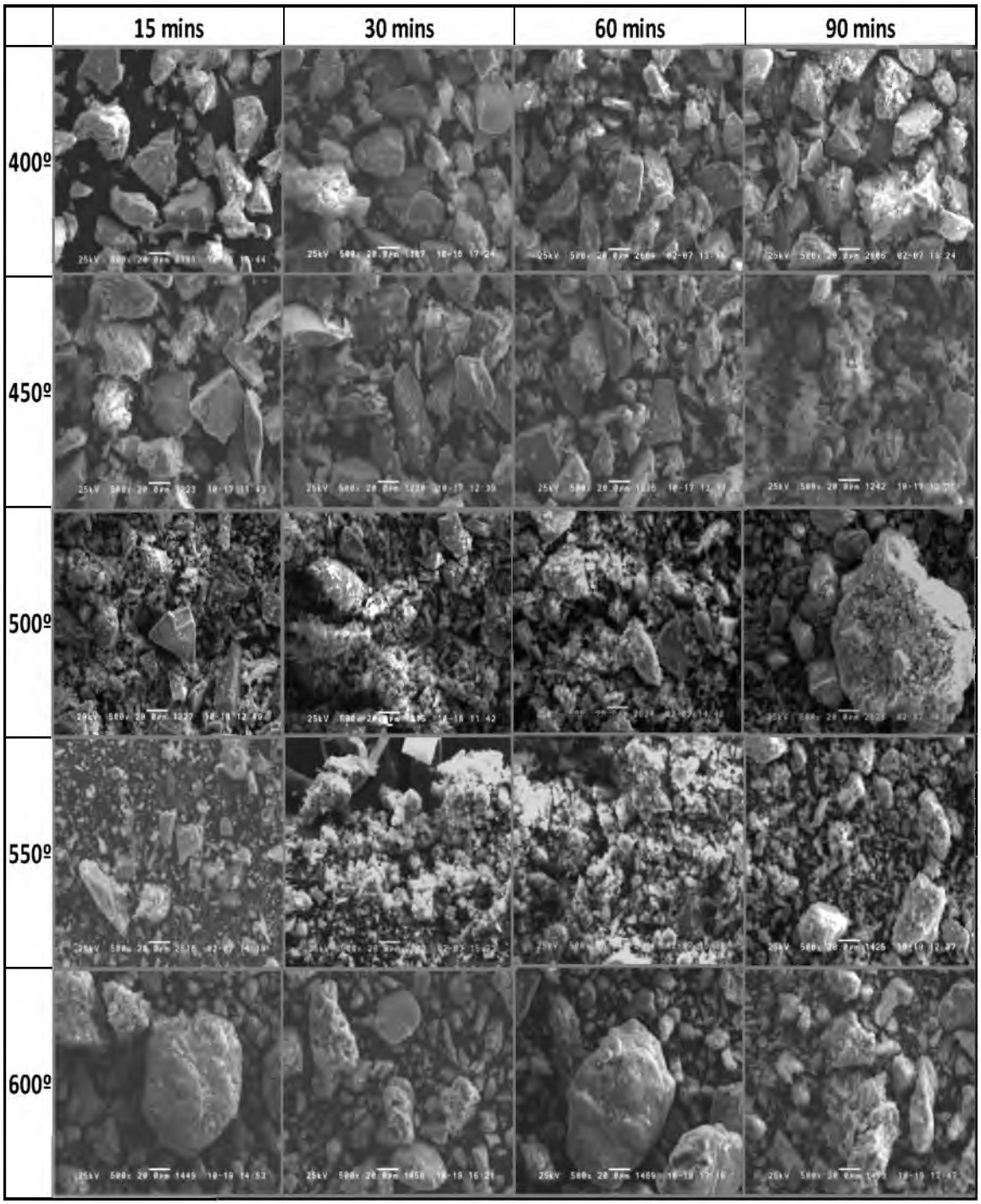

Figure 2.12. SEM (500x magnification) images of roasted and washed slag products at different temperatures and times during the roasting reaction. The scale bar is 20 µm.

90 minutes, although most particles appear to have undergone some reaction. The particles at 450 ºC have mostly begun to react after 15 minutes, and between 30 and 60 minutes, semireacted primary particles have begun to form secondary particles. After 90 minutes, very few if any slag surfaces remain unreacted, and the reacted slag particles have formed loose, fibrous clusters of submicron sodium titanate particles.

At 500 ºC, most of the particles have reacted and formed secondary reacted particles after 15 and 30 minutes. Any unreacted slag surfaces are likely those that stuck to the walls of the reactor and were not suspended in the molten NaOH during the reaction. At 90 minutes, nearly all of the particles have reacted and formed loose fine sodium titanate particles, although some form loosely bound sponge-like aggregates. At 550 ºC, most of the particles have reacted after 30 minutes. After 60 and 90 minutes, the reacted particles have begun to form hard sintered aggregates. Finally, at 600 ºC, it appears that the reacted slag particles form hard sintered aggregates after 15 minutes that get denser as the times goes on. As mentioned previously, these hard, sintered aggregates become resistant to leaching and are generally an unfavorable product.

2.5 Conclusion

The alkaline roasting of titania slag using molten NaOH has been investigated for the purpose of converting titanium dioxide in the slag to acid soluble sodium titanate and certain oxide impurities to water soluble sodium compounds. The experimental parameters for this reaction were optimized with respect to conversion of Ti in the slag to a sodium titanate product. The parameters that were determined to have the greatest effect on the degree of conversion include slag particle size, NaOH/slag ratio, temperature, and time. Ti conversion increased with decreasing particle size, increasing

NaOH/slag ratio, increasing time and increasing temperature. An examination of the morphology of the roast products indicated that higher temperatures and long reaction times led to a sintered reaction product which was difficult to leach. The optimal reaction conditions were determined to be the following: particle size: +400/-325#; NaOH/slag ratio: 1.5; temperature: 550 °C; time: 60 minutes. These conditions led to a Ti recovery of 96%.

2.6 References

[1] G. Bauer, "Vanadium and vanadium compounds" in *Ullmann's Encyclopedia of Industrial Chemistry*. Weinheim, Germany: Wiley-VCH, 1996, pp. 371–374.

[2] K. Borowiec, A.E. Grau, M. Gueguin, and J.F. Turgeon, "Method to upgrade titania slag and resulting product," US Patent No. 5 830 420A, Nov. 3, 1998.

[3] M. Gueguin and F. Cardarelli, "Chemistry and mineralogy of titania-rich slags. Part 1–Hemo-ilmenite, sulphate, and upgraded titania slags," *Min. Proc. Extract. Met. Rev.*, vol. 28, no. 1, pp. 1–58, 2007.

[4] J. Divisek, P. Malinowski, and J. Mergel, "Hydrogen as an energy carrier," in *Hydrogen as an Energy Carrier*, G. Imarisio and A.S. Strub, eds. Brussels, Belgium: Springer, 1983.

[5] G. Mamantov and R. Marassi, *Molten Salt Chemistry: An Introduction and Selected Applications*. NATO Advanced Science Institute Series, New York: Springer, 1987, p. 525.

[6] G.J. Janz, *Molten Salts Handbook*. New York: Academic Press Inc, 1967.

[7] D.D. Williams, J.A. Grand, and R.R. Miller, "The reactions of molten sodium hydroxide with various metals," *J. Am. Chem. Soc.*, vol. 78, no. 20, pp. 5150–5155, 1956.

[8] A. Lahiri and A. Jha, "Kinetics and reaction mechanism of soda ash roasting of ilmenite ore for the extraction of titanium dioxide," *Metall. Mater. Trans. B,* vol. 38, no. 6, pp. 939–948, 2007.

CHAPTER 3

LEACHING AND PURIFICATION OF ROASTED SLAG

3.1 Introduction

After slag is roasted with molten NaOH, Ti can be separated from other impurities in the slag through a series of leaching and purification steps with the goal of preparing a Ti rich solution for subsequent recovery. As noted in the previous chapter, impurity elements in the roasted slag such as Al, Mn, and Si form water soluble compounds that are washed away, whereas Fe, Mg, Ca, and other metal compounds are insoluble and must be separated from Ti by other means. Leaching of the roasted and washed products is necessary to dissolve Ti into solution. Sodium titanate is insoluble in water but is readily soluble in mineral acids such as HCl. Na_2TiO_3 reacts with HCl to form $TiOCl_2$ solution as shown in the dissolution reaction in (3.1).

$$Na_2TiO_{3(s)} + 4H^+_{(aq)} = TiO^{2+}_{(aq)} + 2\,Na^+_{(aq)} + 2\,H_2O \qquad (3.1)$$

Iron oxide and other remaining impurities in the roast product are also leached into solution, following similar dissolution reactions. A series of experiments was conducted to determine the critical variables that affect the recovery of Ti and other metals during the leaching of the roasted slag, with the goal of maximizing the recovery of Ti in solution. It was determined that the critical processing parameters included pulp density, acid concentration, chloride concentration, leaching temperature, and leaching

time. The effects of each of these parameters on final Ti recovery are discussed.

After initial chemical purity evaluation of the TiO_2 product made from the leach solutions, it became clear that presence of entrained impurities (particularly Fe) from the leaching stage had a serious detrimental effect on the whiteness of final product. After rigorous washing treatment of the precalcined metatitanic acid proved insufficient, a method of impurity removal through solvent extraction was developed. As will be shown, this proved to be highly successful in meeting the purity objectives of the final TiO_2 pigment product. Several experiments were performed to determine the optimal parameters for the removal of Fe through solvent extraction including acid concentration, extractant concentration, phase ratio, and time.

3.2 Experimental Methods

The leach solutions were heated in a 1 liter capacity, 3-necked round bottomed glass reactor submersed in a temperature controlled oil-bath. The leach solution was stirred by a polypropylene paddle attached to a Janke and Kunkel laboratory mixer mounted above the oil bath. The leaching temperature was monitored by a standard laboratory thermometer, and a reflux condenser with flowing chilled water was also used to minimize solution loss by evaporation. A diagram of the leaching apparatus is shown in Figure 3.1. Samples of leach liquor were diluted in 5% nitric acid and analyzed using ICP-OES or ICP-MS. Filtration was performed using a Büchner Funnel and Whatman filters or by centrifugation and decantation. Solvent extraction experiments were performed using a glass separatory funnel.

The leach solution used in the solvent extraction experiments was prepared by leaching the washed after-roast product with various concentrations of hydrochloric acid.

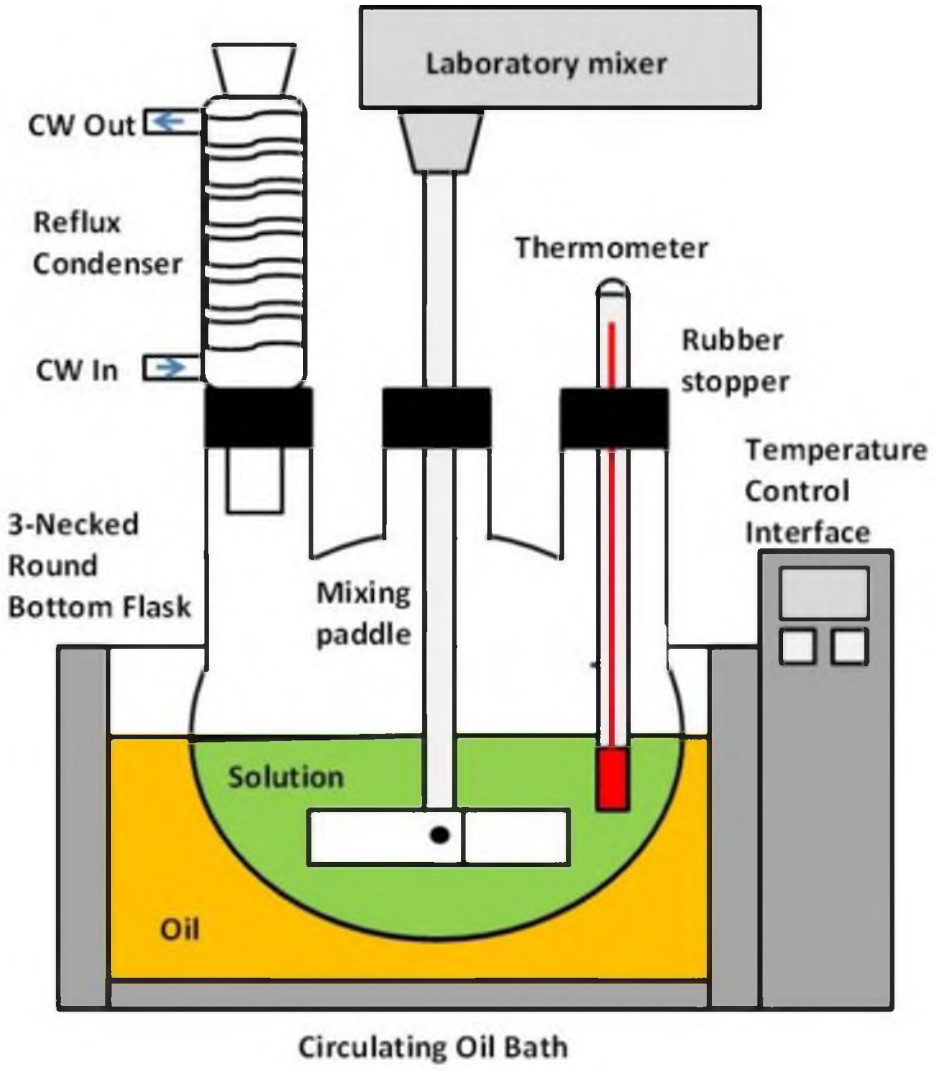

Figure 3.1. Experimental setup for the acid leaching of roasted slag.

The organic solvent was comprised of various volume fractions of Alamine 336 extractant diluted in Orfom SX11 kerosene with 10 volume % dodecanol added as a modifier to prevent third phase formation. The solvent mixtures were protonated before use in the experiments by mixing them with 1 M HCl in a 1:2 organic to aqueous ratio and then disengaging the phases in a 500 mL separatory funnel and repeated once again. Washing of metatitanic acid pulp was performed in 15 ml centrifuge tubes that were repulped using a Fischer Scientific Mini-rotor vortexer. Dissolved metal concentrations

of washing and leach solutions were determined using an ICP Agilent 7500ce quadrupole mass-spectrometer or a Spectro ICP-OES. X-ray diffraction of leached products was also performed with a Philips 1140 diffractometer (Cu Kα), and the patterns were analyzed using X'Pert High Score Plus software.

3.3. Leaching at Low Pulp Densities

3.3.1 Effect of HCl Concentration

The extent of leaching has strong dependence on the concentration of HCl solution. A series of leach tests were performed on washed and dried roasted slag using HCl solutions varying from 0.75 M to 2.0 M at a pulp density of 2% solids by weight. The leaching was conducted at 50 °C for 1 hour. After each leaching experiment, the leach solution and undissolved solids were separated by vacuum filtration, and the solution was diluted for solution analysis by ICP. Recovery was here defined as the concentration of each metal in solution divided by the total amount originally present in the solid (determined separately by complete digestion with HCl/HF and ICP-MS measurement). The changes in recoveries of the metals with HCl concentration are shown in Figure 3.2.

It is apparent that Ti recovery significantly improves with an increase in HCl concentration, whereas the recovery of Na remains relatively unchanged. At lower concentrations, the solution was quite turbid and difficult to filter. Once the HCl concentration exceeded 1.5 M, the filtered solution became clearer and had less fine suspended particles, although precipitation occurred in the filtered solution after a few days. It appears that lower concentrations of acid are sufficient to dissolve Ti but not to keep it in solution, resulting in low temperature hydrolysis. The product of low

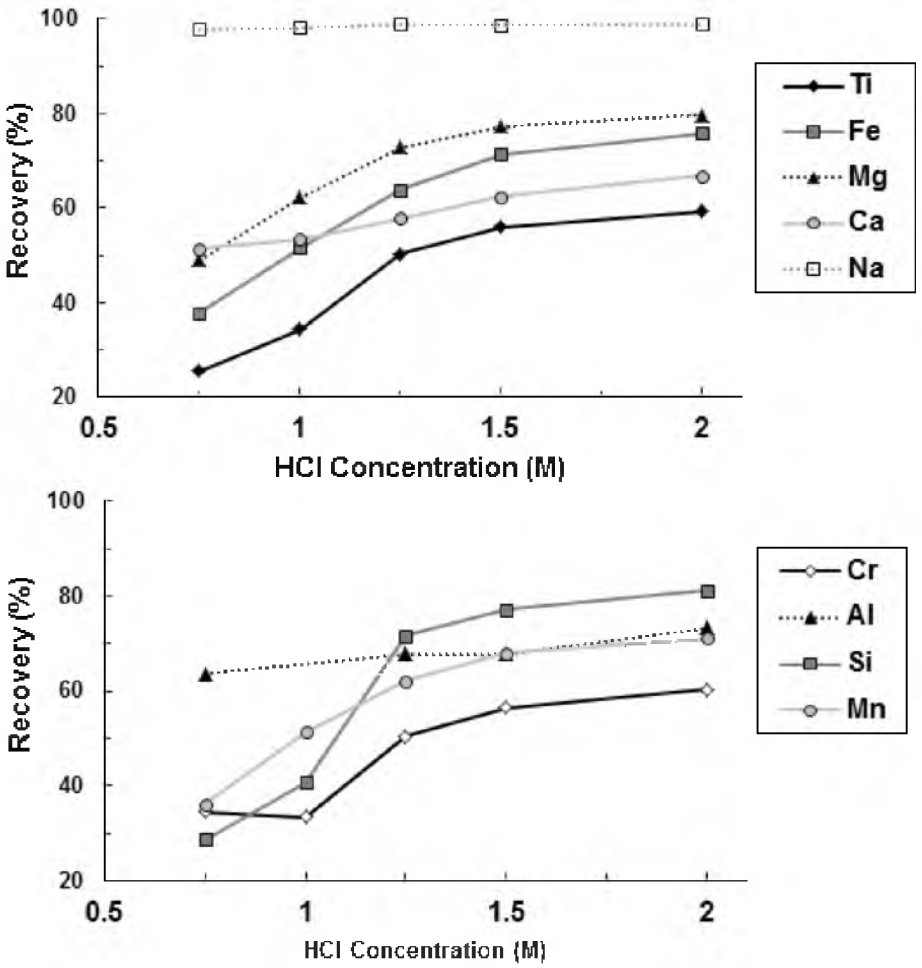

Figure 3.2. Leaching recovery of Ti and impurity metals as a function of HCl concentration. Leaching conditions: Time: 1 hour; Temperature: 50 ºC; Pulp Density: 2% solids by weight.

temperature hydrolysis is a hydrated titanium oxide compound known as orthotitanic acid, $Ti(OH)_4$ ($TiO_2 \cdot 2H_2O$) [1].

3.3.2 Analysis of Leach Residue

The residue of each leaching experiment was rinsed, filtered, dried, and weighed. A sample of residue from each acid concentration was fully digested with a mixture of HCl/HF in a microwave digester, diluted, and measured using ICP-MS. The composition of each residue as well as the original roast product is shown in Table 3.1. The concentration of Ti in the residue did not vary much from sample to sample, although the amount of undissolved residue decreased with increasing acidity. The structure of each of the residue samples was analyzed using XRD. Each pattern was characteristic of amorphous material and did not vary with acid concentration, although some weak anatase peaks were detectable. To confirm whether the residues contained orthotitanic acid, each sample was calcined in a muffle furnace for 2 hours at 650 ºC and analyzed again with XRD. The XRD graphs of the precalcined and calcined residues resulting from 0.75 M and 2.0 M HCl leaching treatments are shown in Figure 3.3, and are

Table 3.1. Composition (in wt. %) of washed and dried roast product before leaching (AW) and after leaching with 0.75–2.0 M HCl. Time: 1 hour; Temperature: 50 ºC; Pulp Density: 2% solids by weight.

Sample	Ti	Na	Fe	Mg	Ca	Mn	Si	Al	Cr	% Undiss
AW	35.7	11.5	6.0	2.7	0.4	0.2	0.2	0.1	0.1	-
0.75 M	46.6	0.4	6.5	2.4	0.4	0.2	0.2	0.1	0.1	57.1
1.00 M	45.7	0.4	5.7	2.0	0.4	0.2	0.2	0.2	0.1	51.2
1.25 M	45.6	0.3	5.6	1.8	0.5	0.2	0.1	0.1	0.1	38.9
1.50 M	48.2	0.5	5.3	1.8	0.5	0.2	0.1	0.1	0.1	32.6
2.00 M	48.3	0.4	4.8	1.8	0.5	0.2	0.1	0.1	0.1	30.1

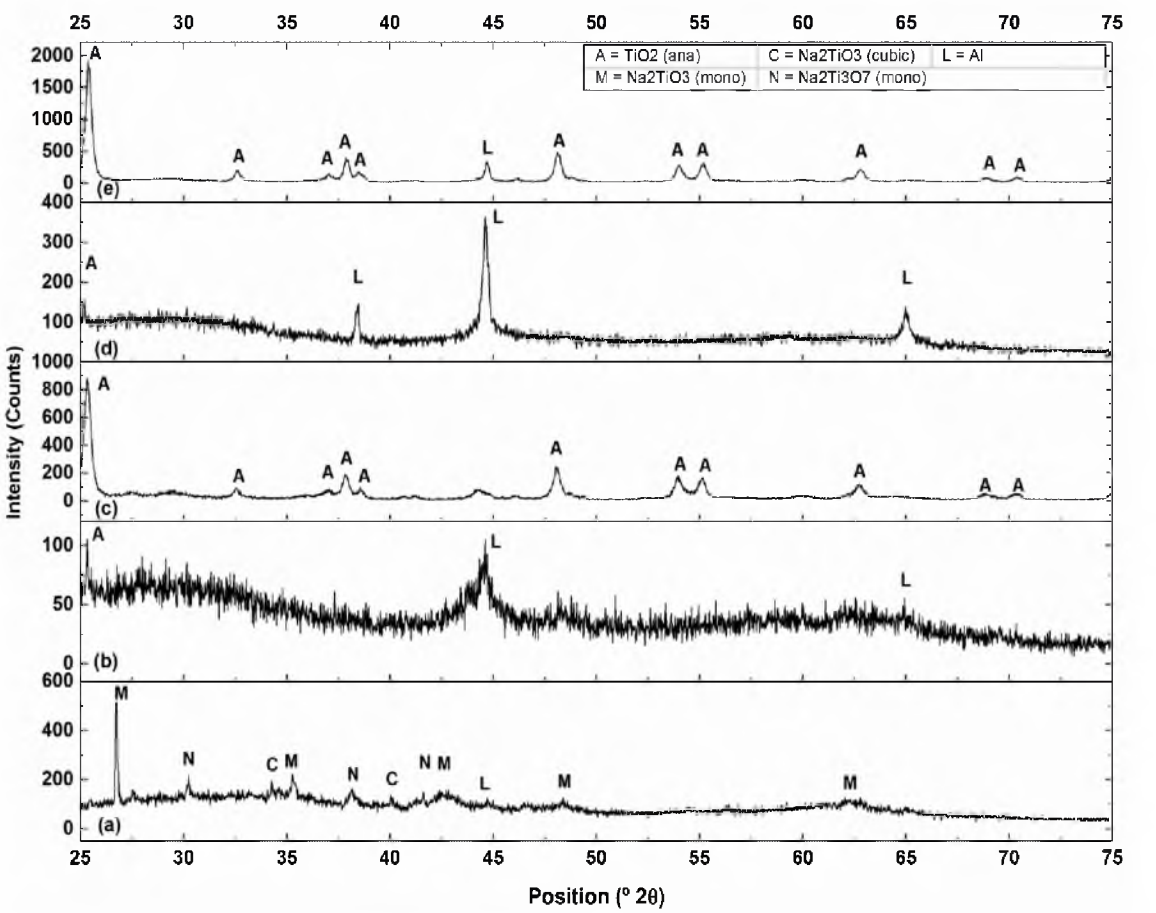

Figure 3.3. X-ray diffraction of washed and dried roast after a) no leaching, b) leaching with 0.75 M HCl and dried, c) leaching with 0.75 M HCl and calcined at 650 °C for 2 hours, d) leaching with 2.00 M HCl and dried, and e) leaching with 2.00 M HCl and calcined at 650 °C for 2 hours. Leaching conditions: Time: 1 hour; Temperature: 50 °C; Pulp Density: 2% solids by weight.

representative of all the samples. Each sample showed sharp anatase peaks, confirming that the residues contained hydrated titanium oxide compounds. The aluminum peaks are artefacts from the sample holder.

3.3.3 Effect of Added Chloride Salts

Several investigators have shown that the activity of the HCl solutions can be increased by increasing the total chloride content of the solution by adding various chloride salts [2, 3]. An attempt was made to increase the activity of HCl leaching

solutions in this study in order to achieve the maximum possible leaching recovery of Ti from the roasted product with using the minimum amount of HCl acid. HCl solutions of the same acid concentration (1.0 and 1.5 M HCl) and total chloride concentration (4.0 M Cl^-) but with different chloride salts (NaCl, $MgCl_2$, and $CaCl_2$) were prepared in order to study their effect on the recovery of Ti in solution. These solutions were also compared with HCl solution of the same acid concentration but with no added salts (1.0, 1.5, and 4.0 M HCl). Approximately 2 g of roast product from the same batch were leached for 1 hour at 50 ºC at a 2% pulp density. The leach solutions were filtered, diluted, and measured using ICP-OES and compared with the solution of a digested sample as described previously.

The recovery of titanium from the various leach solutions is shown in Table 3.2. It is apparent that the addition of chloride salts did indeed enhance the activity of the HCl leaching solution as shown by the increased recovery of Ti in the HCl solutions as compared to equivalent HCl solutions without added salts. The greater than 100% recovery of the 1.5 M HCl + 1.25 M $CaCl_2$ test is attributed to a dilution error. The solutions with no salts were much more turbid after filtration than those with salt, indicating that low temperature hydrolysis had occurred, consistent with previous tests. It appeared that the divalent chloride salts led to a higher recovery at each concentration and that the difference in activity enhancement lessened with higher HCl concentrations. Repeated tests with different roast product batches at higher acid concentrations also showed less difference in recovery between the various salts. These findings are consistent with those reported by Demopolous [3], who found that divalent chloride salts such as $FeCl_2$, $MgCl_2$, and $CaCl_2$ enhance the H^+ activity of 0.5 M HCl solutions

Table 3.2. Recovery of Ti from the leaching of roasted and washed slag with HCl solutions containing various concentrations of added chloride salts.

Leach System	% Ti Recovery
1.0 M HCl + No Salt	31.7
1.0 M HCl + 3.0 M NaCl	48.7
1.0 M HCl + 1.5 M $CaCl_2$	75.3
1.0 M HCl + 1.5 M $MgCl_2$	71.3
1.5 M HCl + No Salt	83.6
1.5 M HCl + 2.5 M NaCl	96.2
1.5 M HCl + 1.25 M $CaCl_2$	108.7
1.5 M HCl + 1.25 M $MgCl_2$	97.6
4.0 M HCl + No Salt	99.9

significantly more than the equivalent amount of added NaCl, although for 4.0 M HCl solutions, the differences in activity became less pronounced.

While the initial leaching tests with low pulp densities yielded acceptable recoveries, it was determined that the volume of solution required would be exorbitant and impractical on an industrially significant scale and would dramatically increase the energy and expense of the process; therefore, leaching of roasted slag at higher pulp densities was investigated.

3.4 Leaching at Higher Pulp Densities

3.4.1 Effects of Acid Concentration

The leaching of roasted slag was also tested using higher concentrations of acid and higher pulp densities. The effect of acid concentration on the amount of Ti and other metals recovered during leaching was investigated by leaching roasted slag from the same batch for the same time, temperature, and pulp density, but at different concentrations of HCl acid solution. Initial leaching experiments were conducted at 50 °C

for 3 hours with a 9% pulp density. The acid concentration was varied from 1.5 M HCl to 12 M HCl. The concentration of dissolved metals in the filtered and diluted leach solutions as measured by ICP-MS are shown in Table 3.3. It is apparent that the recovery of Ti increased with the increase in HCl concentration, although the higher concentrations of HCl (8.4 M and 12 M) appeared to increase recovery of other metals only marginally beyond the 5 M solution. The filtered solution of the 1.5 M HCl test was very turbid, and it was evident that hydrolysis had occurred, leading to a poor recovery of Ti and other metals. The 8.4 and 12 M solutions were also somewhat difficult to filter due to the high viscosity of the solution. Although 12 M HCl solution led to a slightly higher recovery of Ti, the exorbitant reagent expense and complications in filtering and handling make it difficult to justify its use. Subsequent tests with HCl solutions of concentrations lower than 5 M were able to dissolve most of the roast product but soon precipitated Ti upon standing. Based on these considerations, 5 M HCl was determined to be the best concentration for subsequent leaching experiments.

3.4.2 Effects of Time and Temperature

Leaching experiments using higher concentrations of acid and higher pulp densities were also conducted. The effect of temperature was studied by leaching with 5

Table 3.3. Concentration of dissolved metals in HCl leaching solutions (in ppm) of various concentrations after leaching roasted slag. Leaching conditions: Time: 3 hours; Temperature: 50 °C; Pulp Density: 9% solids.

[HCl] (M)	Ti	Fe	Al	Mg	Mn	Ca	Si	Cr
1.6	4710	3117	174	1964	127	360	<30	94
5.0	29070	4290	268	2194	79	476	<30	126
8.4	29887	4464	215	2370	228	476	<30	129
12.0	32552	4388	291	2241	198	423	<30	127

M HCl at a pulp density of 10% at temperatures of 35, 50, 65, and 80 ºC. The solutions were sampled after 5, 15, 30, 60, 120, and 180 minutes. The results for Ti and Fe are shown in Figure 3.4. The rate of dissolution of Ti and Fe increased with increasing temperature, with Fe reaching maximum dissolution after 15 minutes for 50–80 ºC and after 30 minutes at 35 ºC. However, above 50 ºC, the solubility of Ti in the solution decreases and Ti begins to precipitate due to hydrolysis, resulting in low recovery of Ti. This was also evident by the turbidity of the filtered solution and a significant increase in the weight of the leach residue. At 80 ºC, hydrolysis is evident after only 5 minutes and is nearly complete after 60 minutes. At 50 ºC, the maximum concentration is reached after 2 hours, but begins to decrease afterwards, likely due to a small degree of hydrolysis. Therefore, the best leaching conditions for the dissolution of roast product with 5 M HCl were determined to be 120 minutes at 50 ºC.

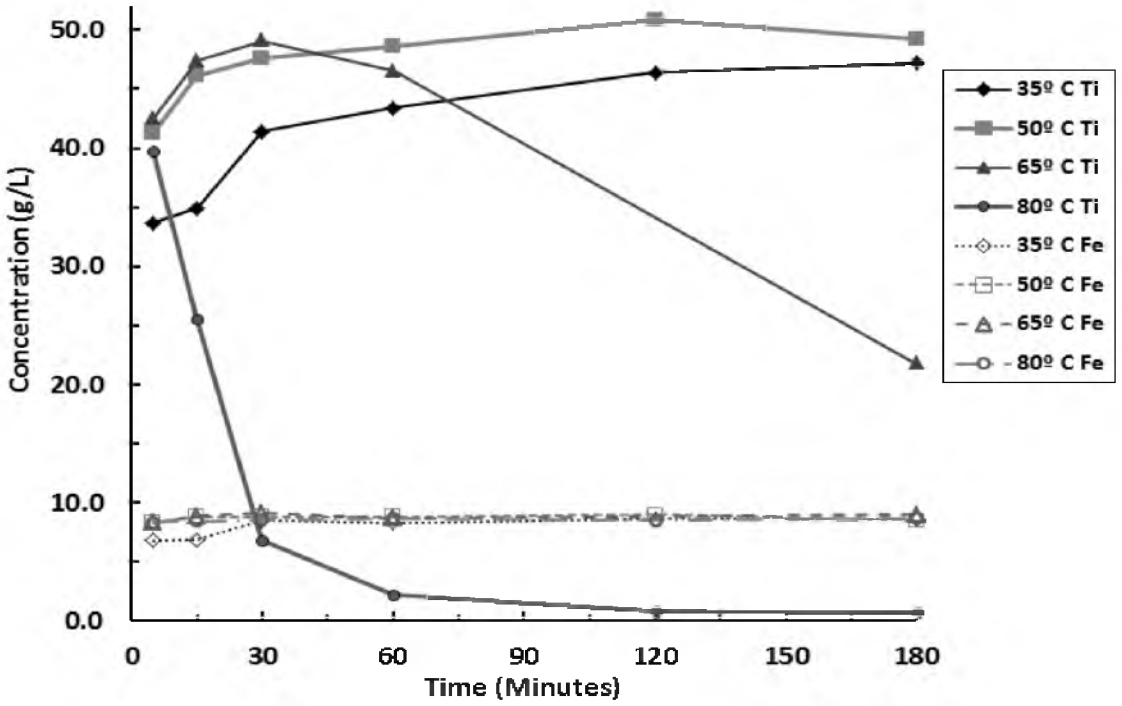

Figure 3.4. Concentration of Ti and Fe in 5 M HCl leaching solutions vs. leaching time. Leaching conditions: Acid Concentration: 5 M HCl; Pulp Density: 10% solids by weight.

3.5 Metatitanic Acid Pulp Washing and Salt Treatment

Following leaching and filtration, Ti was recovered from solution by thermal hydrolysis in the form of metatitanic acid pulp, $TiO(OH)_2$, as described in greater detail in Chapter 4. This pulp was lightly rinsed, filtered, and calcined to produce crystalline anatase or rutile TiO_2. TiO_2 pigment produced in these preliminary tests had a red tint, which was attributed to the presence of transition metals such as iron and chromium, which even in very small concentrations can act as chromophores that significantly reduce the whiteness of the pigment. The surface of metatitanic acid particles is very porous and has a tendency to adsorb impurities from the solution undergoing hydrolysis [1]. Therefore, it became necessary to wash the precipitate "pulp" in order to remove as far as possible adsorbed impurities that discolor the TiO_2 pigment upon calcination. An effort was made to find the optimal washing conditions that would lead to an acceptably pure TiO_2 product.

3.5.1 Titanous Sulfate Bleaching Treatment

The wash solution must be sufficiently acidic and sufficiently reducing in order to prevent impurities such as iron from oxidizing to higher valence states (Fe^{2+} to Fe^{3+}) that tend to hydrolyze and form insoluble compounds. Initially, a 3.7% HCl acid solution with a pH of 1.0 was used as the wash solution. Additionally, the pulp was rinsed with a strong reducing agent, such as $Ti_2(SO_4)_3$, or titanous sulfate solution. This method has been used extensively by sulfate process pigment manufacturers and is commonly referred to as "bleaching" [4]. A solution with 1.25x the stoichiometric amount of trivalent titanium solution needed to keep the impurity metals in their lower valence states was prepared. The solution was prepared by reducing $TiOSO_4$ solution with aluminum powder.

Following hydrolysis, the metatitanic acid pulp was filtered and washed with the HCl solution and then the $Ti_2(SO_4)_3$ solution. This was repeated twice more. Although this method reduced the impurity levels of the final pigment, the lowest concentration of Fe that could be achieved was 962 ppm, which was considered much too high.

3.5.2 Effect of Salt Treatment

Another purification step commonly used in the sulfate process to enhance whiteness is known as "salt treatment" [4]. After an initial washing, metatitanic acid is repulped in a solution containing doping amounts of potassium salts (such as K_2CO_3 or K_2SO_4) and H_3PO_4 or other phosphate sources. Potassium can lower the necessary calcination temperature and prevent sintering while phosphate ions react with any residual iron to form $Fe_3(PO_4)_2$, a compound with a light yellow tint as opposed to the red tint of Fe_2O_3. A sample of thoroughly washed pulp was mixed with a solution containing a small amount of K_2CO_3 and H_3PO_4 (5 mg/g TiO_2 equivalent of K_2O and P_2O_5, respectively) three times. The sample was filtered and calcined at 650 ºC for 1 hour. A noticeable improvement in whiteness was observed, although the treatment did not significantly decrease the concentration of impurities in the final pigment, as shown in Table 3.4.

Table 3.4. Composition of pigment with and without salt treatment.

Sample	**Fe**	**Mg**	**Al**	**Ca**	**Mn**	**Si**	**Cr**	**Na**
W/ Salt Treatment	1128	426	637	166	<17	1233	<21	80
W/O Salt Treatment	1165	498	581	42	<17	2670	<21	76

3.5.3 Zinc/Acid Rinsing Treatment

An alternate washing procedure involved a hot acid rinse in the presence of a small amount of reducing metal powder such as zinc in order to dissolve adsorbed impurities, as reported by Lasheen [5]. This approach was investigated using various concentrations of sulfuric acid and hydrochloric acid. Pulp from the same batch was used in each experiment. The pulp was placed in a centrifuge tube, and acid solution (90 °C) was poured in as well as a small amount of zinc powder (37 mg/g pulp). The tube was agitated for 10 minutes, and centrifuged, and the solution decanted. The pulp was then rinsed with 3.7% HCl acid solution, centrifuged, and decanted. The hot acid/zinc wash and HCl wash steps were repeated, and the washed pulp was calcined at 650 °C for 1 hour. The resulting pigments were digested and analyzed using ICP-MS. The results are shown in Table 3.5. It appears that the sulfuric acid washes were more successful in solubilizing iron and most of the other impurities and that increasing the concentration of HCl did not lower the concentration of impurity metals in the final pigment. A combination of the $Ti_2(SO_4)_3$ washing and zinc/acid treatment produced a pigment with an Fe concentration of 621 ppm. However, since the initial target for Fe in the final pigment was < 100 pm, this method proved to be unsuccessful in that respect.

Table 3.5. Composition of impurities in the final pigment washed by various acid/Zn solutions.

Treatment	Fe	Mg	Al	Ca	Si	Mn	Cr	Na
1.5 M H_2SO_4	1133	394	19	<15	302	<29	<14	62
3 M H_2SO_4	995	394	73	<15	353	<29	<14	388
2M HCl	1815	431	8	<15	393	<29	<14	38
4M HCl	2610	448	512	105	734	<29	87	154
6M HCl	2404	449	208	145	1637	<29	57	170

3.6 Initial Solvent Extraction Experiments

Rigorous washing of the precalcined hydrate with reducing solutions proved to be insufficient in their removal of Fe and other metal impurities. Therefore, the use of solvent extraction to purify the leach solution prior to hydrolysis was investigated. A wide variety of extractants to purify Ti bearing chloride and/or sulfate solutions [6]. Two approaches are generally used: preferential extraction of Ti into the organic phase, leaving the impurities in the raffinate, or preferential extraction of Fe or other impurities into the organic phase, leaving Ti in the raffinate. Two common classes of organic extractants, phosphine oxides and ternary amine extractants, were investigated for the purification of the leach solution produced in this study.

3.6.1 Extraction with Phosphine Oxides

Initial SX experiments were performed with the goal of selectively extracting titanium into the organic phase, leaving iron and other impurities in the raffinate. The first extractant investigated was Cyanex 923 (made by Cytec), a mixture of organic phosphine oxides, namely tri-(n-hexyl) phosphine oxide and tri-(n-octyl) phosphine oxide, diluted in Kerosol, an SX grade kerosene. Dodecanol was also added as a modifier in order to prevent 3rd phase formation. A 20 vol. % Cyanex 923 mixture was contacted with the leach solutions previously described with an organic to aqueous ratio (O:A) of 4. The organic and aqueous phases were separated, and the organic phase was stripped with a 1 M HCl solution with an O:A ratio of 0.25. The Cyanex 923 mixture showed a very strong affinity for Ti; however, it had an even stronger affinity for Fe, which was almost completely extracted from the leach solution after one contact. These results are consistent with Remya and Reddy [7], who also found that Cyanex 923 had a higher

selectivity for Fe over Ti, and both have extractions of over 80% in 4 M HCl solutions. Coextraction of Al, Ca, Mg, Mn, and Na was observed as well. Stripping solutions also contained dilute concentration of every metal in the leach solution. Thus, Cyanex 923 proved to be a poor extractant candidate for creating a purified Ti solution.

3.6.2 Extraction with Ternary Amines

Amine extractants have been used for decades in various solution concentration and purification applications. Alamine 336 is a ternary amine (R_3N) extractant that has been used to recover a wide variety of dissolved metals including cadmium, cobalt, iron, hafnium, tungsten, uranium, and vanadium [8]. Alamine 336 is an insoluble tri-octyl/decyl amine that forms soluble salts of anionic species at low pH in organic diluents such as kerosene. It contains a basic nitrogen atom that can react with a variety of inorganic acids to form amine salts that undergo ion exchange with other anionic species. The general reaction in chloride media occurs in two steps, protonation and exchange, as shown in (3.2) and (3.3) [9].

$$\text{Protonation:} \quad [R_3N]_{org} + [HCl]_{aq} \Leftrightarrow [R_3NH^+Cl^-]_{org} \tag{3.2}$$

$$\text{Exchange:} \quad [R_3NH^+Cl^-]_{org} + [M^-]_{aq} \Leftrightarrow [R_3NH^+M^-]_{org} + [Cl^-]_{aq} \tag{3.3}$$

The extent to which an anionic metal complex, M^-, exchanges for Cl^- is dependent on the affinity of the two anions for the cation and the energy of solvation by the aqueous phase. The formation and extraction of the anionic complexes depends upon the concentration of the anion forming the anionic complex, such as chloride in iron chloro-complexes. Iron forms an anionic chloro-complex, $(FeCl_4)^-$ [10], which exchanges with Cl^- ions in the amine salt, as shown in the following reaction.

$$[R_3NH^+Cl^-]_{org} + [FeCl_4^-]_{aq} \Leftrightarrow [R_3NH^+FeCl_4^-]_{org} + [Cl^-]_{aq} \quad (3.4)$$

3.6.3 Initial Experiments with Alamine 336

For initial experiments, solutions prepared by leaching washed after-roast product with various concentrations of hydrochloric acid were used. A solvent mixture was prepared with 20 vol. % Alamine 336, 10% dodecanol, and the remainder SX 11 kerosene. The solvent and solution were heated to 40–45 ºC and mixed in a 4:3 O:A ratio for at least 10 minutes and separated in a separatory funnel. The raffinate was sampled and diluted for ICP-MS analysis. The compositions of the leach solution prepared with 5.0, 8.4, and 12.0 M HCl and the raffinate after one contact with the Alamine 336 extractant are shown in Table 3.6. The leach solution prepared with 1.6 M HCl was also mixed with the solvent; however, a precipitate formed upon contact; therefore, it was omitted from the table. It is apparent that in every solution, nearly all of the Fe in the leach solution was removed after a single contact, with some coextraction of other metals at higher acid concentrations. Repeated contacts of the raffinate with fresh solvent led to even further removal of Fe. The detectable limit of metals is in the parts per billion range,

Table 3.6. Compositions and extraction coefficients of leach solutions and raffinate after one contact with 20 vol. % Alamine 336 extractant.

[HCl] (M)	*Solution*	Ti	Fe	Al	Mg	Mn	Ca	Cr
5.0	*Feed*	29070	4290	268	2194	79	476	126
	Raffinate	32355	<1	300	2422	100	514	121
	E_c	-	>3200	-	-	-	-	0.03
8.4	*Feed*	29887	4464	215	2370	228	476	129
	Raffinate	25143	9	144	2008	172	370	110
	E_c	0.14	390	0.37	0.14	0.24	0.21	0.13
12.0	*Feed*	32552	4388	291	2241	198	423	127
	Raffinate	28901	18	268	2220	116	369	125
	E_c	0.09	185	0.06	0.01	0.54	0.11	0.01

which when correcting for dilution of the 5 M HCl sample, the concentration of Fe was still measured as less than 1 ppm after one contact. The net concentration of Ti and other metals in the raffinate of the 5 M HCl solution increased slightly due to the removal of Fe.

The extraction efficiency of a particular extractant for a metal is given by the extraction coefficient, E_C. This coefficient is determined by dividing the equilibrium concentration of metal in the organic phase by the concentration in the aqueous phase. The concentration of metal within the organic phase was determined by mass balance. The extraction coefficients of each metal after a single contact of the solvent with each solution are shown in Table 3.6. The 5 M HCl solution exhibited the highest extraction coefficient for Fe, which then decreased with higher concentrations of acid. The coefficients for the other metals are all well below 1, which indicates a preference to remain partitioned in the aqueous phase rather than the organic. It is apparent that moderately high chloride concentrations are needed for significant Fe extraction; however, excessively high concentrations can limit Fe extraction and increase Ti coextraction.

The difference in the Ti extraction behavior can be explained by its speciation in different acid and/or chloride concentrations. Filiz and Sayar [9] reported that the extraction of Ti(IV) in 40 vol. % Alamine 336 in n-xylene increased from 65% in 1 M solutions to 90% in in 10 M HCl. Kislik and Eyal [11] reported the supposed species of Ti(IV) at various HCl acid concentrations. From 4–8 M HCl, Ti can supposedly exist as various cationic complexes with the form $(TiCl_n)^{(4-n)+}$. From 8–11 M Ti forms a neutral $(TiCl_4 \cdot 2HCl)^0$ species, and at >11 M forms anionic chlorocomplex species $(TiCl_5 \cdot 3HCl)$

and $(TiCl_6 \cdot 2HCl)^{2-}$. Cservenyak et al. [12] calculated the speciation of 0.1 M Ti in a 1 M HCl solution at 298 K and reported that from 3–10 M Cl- concentration the neutral species $TiOCl_2$ had the highest activity. In this same range, the activity of $(TiOCl_4)^{2-}$ steadily increases and becomes the dominant species at >10 M Cl- concentrations. From these reports, we can infer that the increase in Ti extraction with an increase in HCl concentration is due to the formation of anionic chlorocomplexes, which can easily be extracted with an amine extractant in a similar manner as the anionic iron chlorocomplex.

3.6.4 Effect on Final Pigment Purity

The raffinate of the 5 M HCl was hydrolyzed, and the resulting precipitate was washed with dilute HCl and calcined at 650 ℃ for 2 hours. The composition of the pigment was analyzed by digestion and ICP-MS and compared to a previous sample that had received bleaching treatment. Two commercial pigments (one anatase and one rutile) were also digested and analyzed for a comparison, and the compositions are shown in Table 3.7. The effect of using a ternary amine extractant is readily noticeable in the final product as the level of Fe decreased from nearly 1000 ppm without the treatment to 20 ppm, which is well below the initial target of 100 ppm, as well as the 50 ppm target mentioned previously. The levels of impurities in the pigment with the treatment nearly meet or are below those of the two commercial pigments. These results demonstrate that sufficiently pure TiO_2 pigment can indeed be produced by the new pigment making process.

Table 3.7 Compositions of TiO_2 produced with and without a solvent extraction step and two commercial TiO_2 pigments.

Sample	**Fe**	**Cr**	**Mg**	**Mn**	**Ca**	**Si**	**Na**
Pigment W/O SX	962	63	492	16	290	19732	68
Pigment W/ SX	20	13	267	4	46	467	204
Company A- Anatase	<11	<63	458	<16	147	855	57
Company B- Rutile	12	<13	300	<7	112	386	110

3.7 Optimization of Solvent Extraction Conditions

Although the initial solvent extraction experiments with ternary amine provedsuccessful in dramatically improving the purity of the final TiO_2 product, further efforts were made to optimize the process conditions. Most industrial processes that use solvent extraction conduct a series of laboratory "shake out" tests in order to investigate the effect of changing various parameters in the SX process. A series of shakeout tests were performed using the leach solution from this process and Alamine 336 extractant in order to study and optimize the effects of extractant concentration, phase ratio, and time on the removal of iron. A large batch of roast product was prepared and leached with 5 M HCl for 3 hours at 50 ºC to prepare a stock solution for the experiments.

3.7.1 Effect of Extractant Concentration

The first tests involved varying the volume percent of Alamine 336 while keeping the organic to aqueous phase ratio constant at a value of 1. Solvent mixtures containing 5, 10, 15, 20, and 30 volume % Alamine 336 were prepared, each diluted in SX 11 kerosene and 10 volume % dodecanol. The stock leach solution contained 43.5 g/L Ti and 9.1 g/L Fe. Equal volumes of stock leach solution and organic solvent were heated to 45 ºC and then mixed vigorously by hand in a separatory funnel and then allowed to disengage for at least 5 minutes. This was repeated twice more, resulting in three trials for each

concentration. The raffinate of each sample was diluted and analyzed using ICP-OES. The average concentrations of dissolved Ti and Fe in the raffinate solutions from each test are shown in Figure 3.5, with the error bars shown as one standard deviation.

The very strong and selective affinity of amine extractant is readily observable from these results. At 5% concentration, 64% of the Fe has been extracted in a single contact, with nearly 98% extraction at 10% concentration. The Fe in the raffinate of 15, 20, and 30% tests was below the detectable limit. It is also apparent that the concentration of Ti concurrently increased with the increase in Fe extraction, confirming the increase observed in initial experiments. At a phase ratio of 1, it appears that the 15% Alamine mixture is the optimal concentration that is able to effectively remove all Fe values from the leach solution in a single contact.

3.7.2 Effect of Phase Ratio

The effect of phase ratio was determined by varying the volume of organic solvent relative to the volume of the aqueous phases while keeping the concentration of both phases constant. For the 5 and 10% solvent mixtures, the O:A ratios tested were 1:5, 1:2, 3:4, 1:1, 4:3, 2:1, and 5:1. For the 15% mixture, the O:A ratios tested were 1:10, 1:5, 1:2, 3:4, and 1:1, with the higher ratio being neglected since full extraction had already been observed at or above 1:1. The tests were conducted as previously described, although only one trial was conducted for each ratio. The concentration of Fe in the organic phase was determined by mass balance. The concentration of Fe in the organic phase can be plotted versus the concentration in the aqueous phase, and the Fe loading profile of each solvent mixture can be observed. The Fe loading profile after one contact of the 5, 10, and 15 % Alamine 336 solvent mixtures with the stock leaching solution is

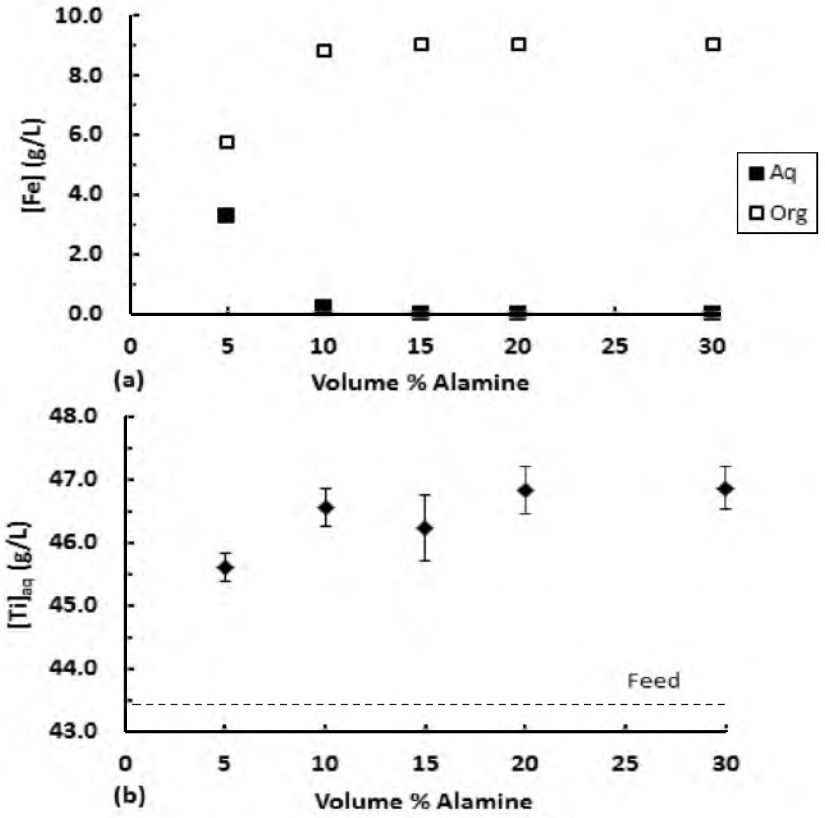

Figure 3.5. The average concentrations of a)Fe and b)Ti in the raffinate resulting from one contact of leach solution (43.5 g/L Ti, 9.1 g/L Fe) with solvent mixtures of different concentrations of Alamine 336 with 10 vol. % dodecanol and remainder kerosene. O:A ratio: 1; Temperature: 45 °C. The error bars shown are one standard deviation.

shown in Figure 3.6.

For the 5% mixture, complete Fe extraction was only observed at an O:A ratio of 5, with the concentration of Fe in the organic phase steadily increasing as the ratio decreased, reaching a maximum of 17.2 g/L at a ratio of 1/5. For the 10% mixture, complete Fe extraction was observed at O:A ratio of 5, 2, and 4/3, with the concentration of Fe in the organic phase steadily increasing as the ratio decreased, reaching a maximum of 20.2 g/L at a ratio of 1/5. Complete Fe extraction was once again observed at an O:A ratio of 1 for the 15% mixture, although the Fe concentration in the organic phase sharply increased to a maximum of 34.1 g/L at a ratio of 1/10. Based on these

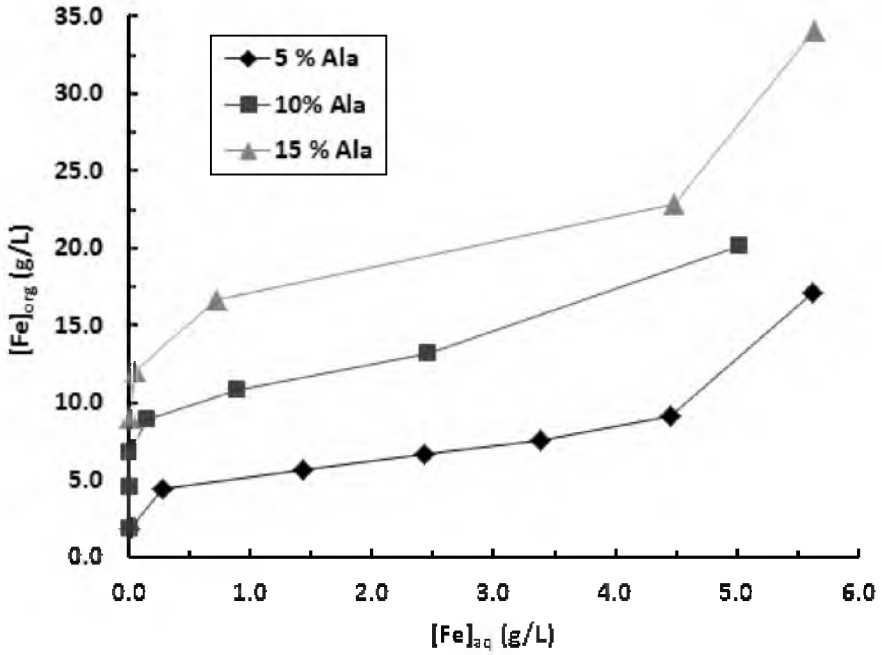

Figure 3.6. The Fe loading curves for 5, 10, and 15 vol. % Alamine 336 obtained by varying the phase ratio of organic solvent mixtures and aqueous leach solution.

observations, however, it was determined that single-stage loading with 15% Alamine 336 at a phase ratio of 1:1 would be the optimal conditions for producing a nearly Fe free raffinate for subsequent hydrolysis treatment.

3.7.3 Effect of Contact Time

The mixing and disengagement times of aqueous/organic phases in a solvent extraction circuit have a large impact on the design of industrial mixer settler units. Several extractant systems such as D_2EHPA have yielded high extraction of Ti and other metals but have proved to be economically unfeasible due to the unreasonably long settling times requires for full phase disengagement [13–15]. While a detailed kinetic study of the extraction of Fe from our leach solution with Alamine 336 is beyond the scope of this project, an idea of the relative time scale of loading and disengagement was determined through some timed tests. Samples of stock leach solution containing 9,060

ppm Fe and 15 % solvent mixture were heated to 45 ºC and shaken at an O:A ratio of 1 for a predetermined amount of time and then allowed to settle for 3 minutes before the aqueous solution was evacuated from the separatory funnel. The solvent mixture was poured into the funnel first, and a stop watch was started at the first instant the aqueous solution was poured in. Shaking began at 5 seconds and ceased after the determined amount of time had passed. Separate tests were conducted for shaking times of 10, 20, 30, 60, and 120 seconds.

The extraction appeared to commence almost instantaneously as the mixture rapidly changed from the dark orange color of the stock solution to a dark red and then to a dark yellow, indicating that Fe was being extracted into the organic phase. After 10 seconds of shaking, only 123 ppm of Fe remained in the aqueous solution (98.6% extraction), and at 20 seconds and longer, complete extraction had occurred. After shaking was stopped, a preliminary phase break was observed after about 5 seconds, with the immiscible phases continuously coalescing, and after 2 minutes, the phases were almost completely disengaged, although 3 minutes was allowed as a safety factor. While this method is rather crude for quantitative kinetic purposes, the results do qualitatively indicate that equilibrium is reached at a relatively rapid pace and that phase disengagement also occurs in a reasonable time scale for a scaled up solvent extraction operation.

3.7.4 Stripping of Loaded Organic

Stripping is an essential part of any solvent extraction operation. When a metal of value is extracted from the pregnant leach solution into the organic phase, aqueous stripping solution is mixed with the loaded organic to reverse the loading reaction and

drive the metal into the aqueous phase, creating a concentrated solution. In this instance, the extracted Fe is an impurity metal and therefore must be adequately removed from the organic phase so that the solvent may be reused for subsequent loading operations and the iron solution properly treated. Critical factors in stripping operations include the stripping reagent and its concentration, phase ratio of loaded organic and stripping solution, mixing and settling times, and the number of stages. Some initial stripping experiments were performed with Fe loaded Alamine 336 solvent mixture from the loading tests in order to determine the best stripping reagent.

As previously mentioned, stripping is a reverse of the loading reaction, and therefore requires the use of a reagent that drives the equilibrium of the reaction the opposite direction, in accordance with LeChatelier's Principle (see (3.4)). Since the ternary amine was loaded in a Cl^- rich solution, contacting the loaded organic in a chloride deficient solution will favor the release of the anionic Fe chlorocomplex ($FeCl_4^-$) back into the aqueous phase. Weak basic solutions such as Na_2CO_3 have also been used as stripping reagents for Alamine 336 [8]. For this initial investigation, DI water and HCl and NaCl solutions of 0.01, 0.1, and 1 M concentrations were used as stripping reagents at an O:A ratio of 1:1. Loaded 15% Alamine 336 mixture containing 17.1 g/L was heated to 45 ºC and shaken for 3 minutes with an equal volume of stripping solution and allowed to settle for at least 5 minutes before the aqueous phase was completely evacuated from the separatory funnel. The volume of the organic was remeasured and contacted with fresh stripping solution for a second stage of stripping. The stripping efficiency of Fe for each solution is shown in Figure 3.7.

The stripping efficiency of DI water was only slightly less than that of 0.01 and

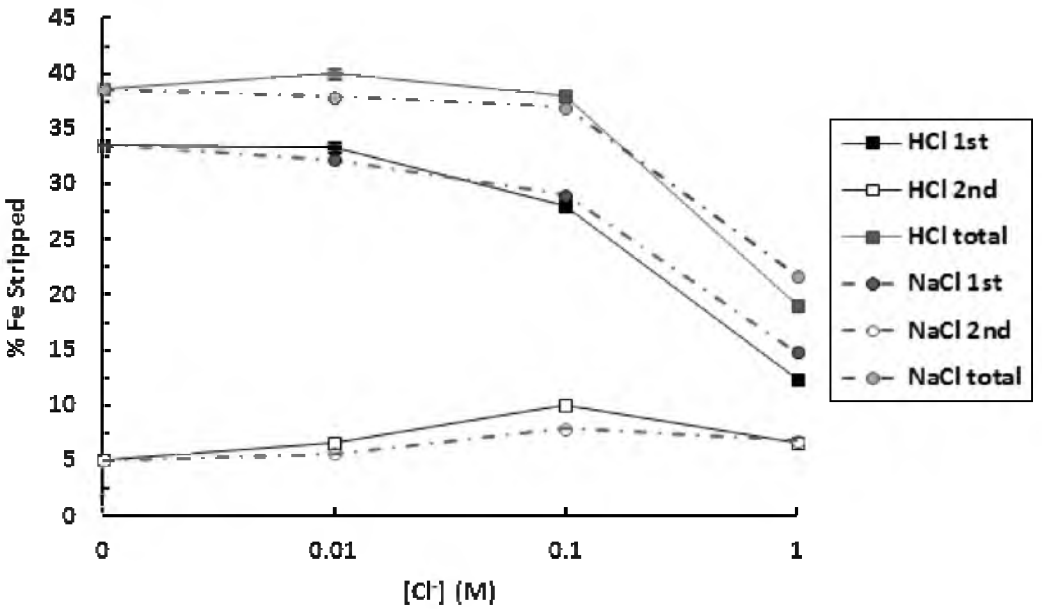

Figure 3.7. The percentage of Fe stripped from loaded organic after the first and second stage of stripping with various concentrations of NaCl and HCl solutions.

0.1 M HCl and NaCl solutions, and that stripping efficiency decreases with an increase in Cl^- concentration. NaCl and HCl solutions appeared to perform also identically at every concentration and at each stage, implying that shift in equilibrium is indeed more dependent on the concentration of Cl^- than on pH, although 0.01 M HCl solutions performed slightly better than 0.01 M NaCl in total extraction efficiency. Further stripping tests with dilute HCl at different phase ratios are warranted in order to make a stripping profile and determine the appropriate number of stripping stages. An investigation using weak bases such as Na_2CO_3 may also yield better stripping efficiencies.

3.8 Conclusion

Leaching and solvent extraction techniques have proven successful in recovering Ti from the alkaline roasted slag and producing a nearly Fe-free $TiOCl_2$ solution ready

for subsequent hydrolysis treatment. Although leaching with low pulp densities resulted in acceptable Ti recovery with more dilute HCl concentrations, it was determined that leaching at higher pulp densities with higher concentrations of HCl was more technically and economically favorable for subsequent purification and acid recovery operations. The best Ti recovery was obtained when leaching was performed for with 5 M HCl for 2 hours at 50 ºC and at a 10% pulp density. The mixing of this solution with Alamine 336 extractant diluted in SX11 kerosene led to complete extraction of Fe in a single stage. The best response for solvent extraction was shown using 15 vol. % Alamine 336 (with 10% dodecanol) at an O:A phase ratio of 1. The organic and aqueous phases reached equilibrium in less than 20 seconds and fully disengaged in 2–3 minutes, indicating that the system is favorable for scaled-up applications. The best stripping solution for the loaded organic phase was determined to be 0.01 M HCl, although further experiments are needed to determine the best phase ratio and numbers of stages.

3.9 References

[1] J. Barksdale, *Titanium: Its Occurrence, Chemistry, and Technology*. New York: Ronald Press Co, 1966, pp. 213.

[2] V.I. Lakshmanan, R. Sridhar, G.B. Harris, and G. Puvvada, "Process for the recovery of titanium in mixed chloride media," US Patent No. 7 803 336, Sept. 28, 2010.

[3] G. Demopolous, "New technologies for HCl regeneration in chloride hydrometallurgy," *World of Metall.*, vol. 61, no. 2, pp. 89–98, 2008.

[4] J. Winkler, *Titanium Dioxide*. Hannover, Germany: Vincentz Network, 2003, pp. 30–40.

[5] T.A. Lasheen, "Sulfate digestion process for high purity TiO_2 from titania slag," *Front. Chem. Eng. China*, vol. 3, no. 2, pp. 155–160, 2009.

[6] Z. Zhu, W. Zhang, and C.Y. Cheng, "A literature review of titanium solvent extraction in chloride media," *Hydromet.*, vol. 105, no. 3–4, pp. 304–313, 2011.

[7] P.N. Remya and M.L.P. Reddy, "Solvent extraction separation of titanium(IV), vanadium(V) and iron(III) from simulated waste chloride liquors of titanium minerals processing industry by the trialkylphosphine oxide Cyanex 923," *J. Chem. Technol. Biotechnol.*, vol. 79, pp. 734–741, 2004.

[8] M. Mackenzie, *The Solvent Extraction of Some Major Metals*. Monheim, Germany: Cognis GmbH, 2008.

[9] M. Filiz and A.A. Sayar, "Extraction of Titanium(IV) from aqueous hydrochloric acid solutions into Alamine 336-m-xylene mixtures," *Chem. Eng. Comm.*, vol. 193, no. 9, pp. 1127–1141, 2006.

[10] K. Saji John, J. Saji, M.L.P. Reddy, T.R. Ramamohan, and T.P. Rao, "Solvent extraction of titanium(IV) from acidic chloride solutions by Cyanex 923," *Hydromet.*, vol. 51, no. 1, pp. 9–18, 1999.

[11] V. Kislik and A. Eyal, "Acidity dependence of Ti(IV) extraction: a critical analysis," *Solvent Extr. Ion Exch.*, vol. 11, no. 2, pp. 259–283, 1993.

[12] I. Cservenyak, G.H. Kelsall, and W. Wang, "Reduction of Ti(IV) species in aqueous sulfuric and hydrochloric acid I: Titanium speciation," *Electrochim. Acta*, vol. 41, no. 4, pp. 563–572, 1996.

[13] K.C. Sole, "Recovery of titanium from the leach liquors of titaniferous magnetites by solvent extraction: Part 1. Review of the literature and aqueous thermodynamics," *Hydromet.*, vol. 51, no. 2, pp. 239–253, 1999.

[14] K.C. Sole, "Recovery of titanium from the leach liquors of titaniferous magnetites by solvent extraction. Part 2. Laboratory-scale studies," *Hydromet.*, vol. 51, no. 3, pp. 263–274, 1999.

[15] K.C. Sole, A. Feather, and J.P. O'Connell, "Recovery of titanium from the leach liquors of titaniferous magnetites by solvent extraction, Part 3. Continuous mini-plant trials," *Hydromet.*, vol. 51, no. 3, pp. 275–284, 1999.

CHAPTER 4

HYDROLYSIS AND CALCINATION OF TiO_2

4.1 Introduction

In many hydrometallurgical operations the desired metal is often recovered from a pregnant solution in the form of a precipitated metal or metal compound. In the case of the hydrometallurgical recovery of Ti, it is recovered from solution through hydrolysis and precipitation of a hydrous titanium oxide compound. This hydrated compound can then be heated to remove the physically and chemically bound water and form a crystalline product, as shown in (4.1).

$$TiO(OH)_2 \xrightarrow{Heat} TiO_2 + H_2O \qquad (4.1)$$

Tight control of the two processes is critical in forming a high quality product with the desired optical properties, as well as obtaining a favorable total recovery. The optical properties are highly dependent on the size, purity, and structure of pigment particles [1].

4.1.1 Formation of Rutile and Anatase

As mentioned previously, one key advantage of the sulfate method is that both rutile and anatase pigments can be produced. The heating of sulfate based solutions yields anatase TiO_2 directly, while halide and nitrate solutions typically produce rutile particles [2]. Under certain conditions, however, these results may be reversed. Adding separately produced rutile nuclei seeds to sulfate solutions will result in the precipitation of rutile

TiO_2 particles, while dissolved $TiCl_4$ solutions may be hydrolyzed in the presence of phosphoric or sulfuric acid to yield anatase. All products from both sulfate and chloride solutions are finally converted to rutile if calcined at 700 to 920 ºC. The quality of pigment particles is dependent on the formation of high quality nuclei during hydrolysis. Two methods of nuclei formation are typically employed: the Mecklenburg or Blumenfeld [1]. The Mecklenburg method involves preparing rutile nuclei (called seeds) by neutralization of $TiOCl_2$ solution with sodium hydroxide and then adding them into the Ti solution to initiate precipitation. The use of added nuclei generally allows for tighter control of particle size and hastens the rate of hydrolysis. Alternatively, the Blumenfeld method involves forming the nuclei autogenously in the Ti solution by progressively adding the Ti solution to heated water. While there are currently no commercial pigment operations that utilize the hydrolysis of chloride solutions, numerous investigators have used the hydrolysis of chloride solutions to produce TiO_2 nanoparticles [3–8].

It was hypothesized that the $TiOCl_2$ solution synthesized from the leaching and purification of roasted slag described in this study could be hydrolyzed and calcined to produce high specific surface area TiO_2 particles suitable for use as pigment or other applications. Several experiments have been conducted to determine the effects of the various hydrolysis and calcination parameters on the recovery and quality of TiO_2 from the purified Ti leach solution. The resulting products have been characterized with respect to their size, morphology, surface area, and crystal structure.

4.2 Experimental Methods

Leach solutions were hydrolyzed in a glass round bottom flasks in a temperature controlled oil bath, using the same experimental setup as was used for leaching. Dissolved metal concentrations of the hydrolyzed leach liquor were measured by diluting samples in 5% nitric acid and analyzing with a Spectro ICP-OES unit. The pH of solutions was measured using an Oakton 2100 series pH meter. Washing of metatitanic acid pulp was performed in 15 ml centrifuge tubes that were repulped using a Fischer Scientific Mini-rotor vortexer. Calcination was conducted by placing the washed pulp in alumina crucibles and heating in an MTI KSL1100X box furnace. DSC-TGA was performed using a TA Instruments SDT Q600 analyzer. X-ray diffraction of the TiO_2 products was performed with a Philips 1140 diffractometer (Cu Kα), and the patterns were analyzed using X'Pert High Score Plus software. BET surface area measurements were made with a Micromeritics Tristar II 3020 calibrated with 20 m^2/g carbon black. SEM microscopy was performed using a Topcon SM100 microscope with an EDAX EDS detector operating at 20 kV tension.

The purified leach solution from the solvent extraction experiments was diluted with different amounts of water to determine the effect of changing acidity on the rate of hydrolysis as well as the size, morphology, and structure of the resulting precipitates. The undiluted leach solution (0.61 M Ti^{4+}, 2.1 M HCl) was compared to solution that was diluted with 10% added water by volume (90% original solution, 10% added water), as well as 25 and 50% dilution, although the total volume was kept constant. The seeding procedure used was similar to the Blumenfeld method of autogenous seeding. The water and the solution were heated separately to 90 °C from room temperature in about 10

minutes, after which the solution was slowly poured into the water as a trickle with no stirring while the bath temperature was increased to 103 °C. The solution was completely poured in after about 3 minutes, and the stirring and timer began when the solution temperature reached 100 °C, which generally took about 10 minutes after the solution was first added. Only the solution was heated from 90 to 100 °C for the no dilution sample. A 3 ml aliquot of solution was taken after 20, 40, 60, 120, 180, and 240 minutes had elapsed. The samples were filtered, measured for pH, diluted, and analyzed using ICP-OES.

The precipitated pulp of each hydrolyzed solution was centrifuged and repeatedly rinsed with diluted HCl instead of DI water to avoid peptization and dried at 90 °C overnight. The size distribution of the metatitanic acid particles from each solution were measured using a Horiba particle size analyzer with a magnetic stir bar and ultrasonication unit to keep the particles in suspension. Samples of the precipitated particles were calcined in a box furnace for 1 hour at 270, 450, and 650 °C. The samples for BET surface area measurement were vacuum-degassed at 90 °C for an hour, weighed, and charged into a glass measuring bulb. The phases of the precipitated and calcined metatitanic acid were quantified by Rietveld refinement [9] using the commercial program X'Pert HighScore Plus. The peak profiles were fitted using the pseudo-Voigt function. The structure data for anatase and rutile were supplied by the JCPDS cards in the software data base (00-21-1272 and 01-070-7347, respectively). Combined TGA-DSC analysis was performed on dried metatitanic acid from each dilution by heating a ~30 mg of each from room temperature to 950 °C at a rate of 20 °C/min and holding for an hour.

4.3 Hydrolysis and Calcination Experiments

4.3.1 Hydrolysis Reactions

Dissolved metals can react with water molecules to form insoluble hydrates in a process known as hydrolysis. Titanium tends to undergo either low temperature or high temperature hydrolysis reactions. The product of low temperatures hydrolysis (25–80 °C) is known as orthotitanic acid ($Ti(OH)_4$ or $TiO_2 \cdot 2H_2O$, as shown in (4.2).

$$TiO^{2+} + 3H_2O \rightarrow Ti(OH)_4 + 2H^+ \quad (4.2)$$

Solutions with low acidity favor this reaction. This reaction is also observed when an alkali hydroxide or carbonate is added to neutralize an acidic Ti solution, such as in the preparation of rutile nuclei in the Mecklenburg process [1]. This reaction was already observed in the leaching of the roasted slag, with more precipitate forming at lower concentrations of HCl leaching solution or at higher leaching temperatures. At higher temperatures (80–110 °C), the solubility of Ti greatly decreases and a less hydrated compound known as metatitanic acid ($TiO(OH)_2$ or $TiO_2 \cdot H_2O$) forms according to (4.3).

$$TiO^{2+} + 2H_2O \rightarrow TiO(OH)_2 + 2H^+ \quad (4.3)$$

It has been well established that precipitating Ti in the less hydrated form leads to higher quality pigment; thus, thermal hydrolysis initiated by dilution and boiling of titanium rich solution has been the established industrial procedure for many decades [2].

Although there has been abundance of reports on the methods and of processing Ti solutions, the exact mechanism of the thermal hydrolysis of of Ti solution is unclear. Most researchers have concluded that it involves the transfer of H^+ ions from the hydration shell of Ti ions into solution with subsequent coordination with OH^- and the

aggregation of 10–20 nm colloidal particles [2, 10, 11]. The hydrolysis process can be roughly divided into 3 stages: nuclei formation, growth and precipitation, and equilibrium. In the first step, very small crystal nuclei form as colloidal aggregates from the solution. The amount and composition of the nuclei will vary under different reaction conditions (temperature, concentration, etc.) and will determine the overall composition and properties of the precipitate. The crystal nuclei will continue to grow if the same hydrolysis conditions continue. After the nuclei reach a critical size they will precipitate from the solution. Once precipitation has commenced, the crystals continue to coarsen while the concentration of TiO_2 gradually (or quickly, depending on conditions) decreases, while the concentration of H^+ continually increases. As the concentration of acid increases, some precipitates may dissolve, resulting in a continual change in Ti and acid concentrations. Eventually, an equilibrium concentration of Ti and acid in the solution is reached resulting is a Ti depleted and acid enriched solution.

Atanasiu et al. [2] found that the rate of hydrolysis of $TiOCl_2$ solutions increased with increasing temperature and dilution and found that adding alcohol diminished the reaction by reducing the amount of water available for hydrolysis. Hydrolysis of the chloride solutions yielded rutile upon calcination; however, anatase also formed when sulfate or phosphate ions were added. Kim et al. [4] found that the phase of the precipitates and extent of hydrolysis was affected by the hydrolysis temperature and amount of added water, but not heating rate. In this study, the purified $TiOCl_2$ solution from leaching will be diluted by various amounts of water in order to study the effect on the rate of hydrolysis as well as the properties of the resulting metatitanic acid precipitates.

The level of dilution also has a significant effect on the energy consumption of the overall process in many respects. First, a greater solution volume will require larger and more expensive and energy intensive processing equipment such as agitators, pumps, etc. Second, a greater solution volume will require significantly more energy to heat to the appropriate reaction temperature. Finally, the level of dilution will affect the final acid concentration of the barren hydrolyzed solution which will be recycled to the leaching stage. The energy analysis of the process (described in Chapter 5) showed that the amount of HCl that had to be regenerated through the chlor-alkali process significantly increased with increased dilution of the hydrolysis solution, resulting in significantly higher energy consumption. Hence, a lower level of dilution is desirable, provided the reaction can still occur at a reasonable rate and yield a product with acceptable properties.

4.3.2 Effect of Water Dilution on Hydrolysis Rate

The change in the relative concentration of Ti for each solution is showed in Figure 4.1. It is readily apparent that the rate of hydrolysis increases with an increase in the level of dilution, or in other words, at higher pH. After 20 minutes, the hydrolysis of undiluted solution was 33% complete while the 25 and 50% diluted samples were at 92% completion, and after one hour the 0, 10, 25, and 50% samples had reached 94, 95, and 99% completion, respectively. After 2 hours, all of the samples had reached their equilibrium concentrations and no further precipitation occurred. The rate of hydrolysis appeared to be the same for the 25 and 50% diluted solutions. It is also apparent that the rate of hydrolysis is the most rapid at the beginning of the reaction since the pH is the highest and becomes more inhibited as the pH decreases due to the release of H^+ ions during the hydrolysis reaction. Measurements of the solution confirmed that the pH

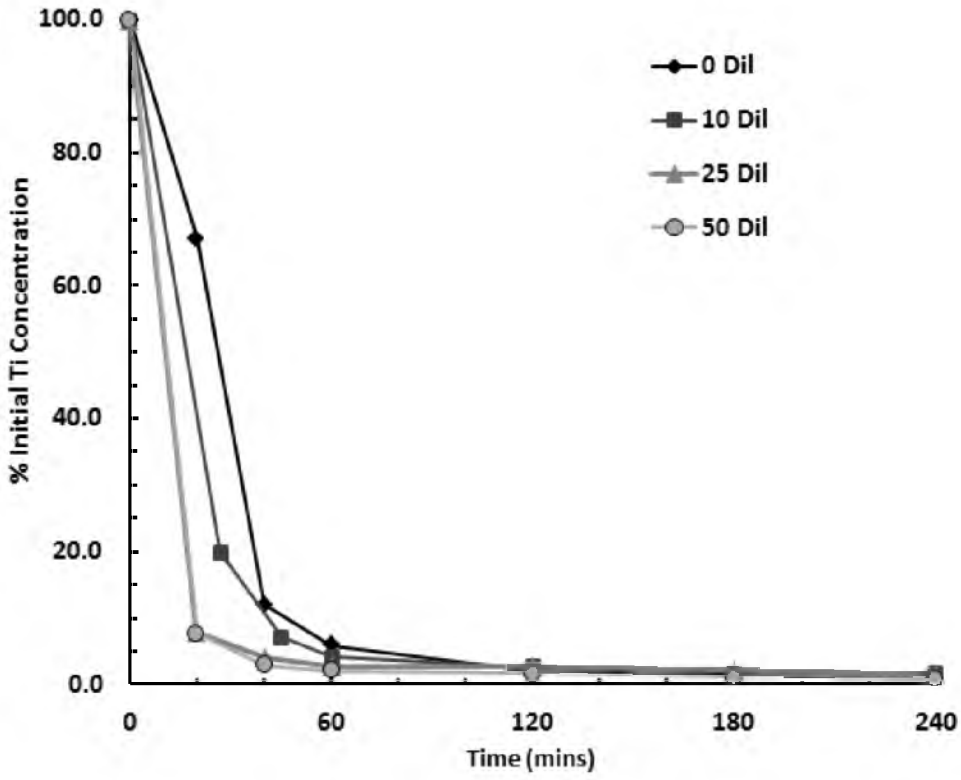

Figure 4.1. The change in relative concentration of dissolved Ti as a function of time during hydrolysis. Conditions: temperature: 100 °C; stirring speed: 300 rpm.

decreased as the reaction proceeded.

4.3.3 Effect of Dilution on Morphology of TiO_2 Particles

The level of dilution in the solution also affects the morphology of the metatitanic acid particles. The particles heat treated at each temperature were observed with SEM, and are shown in Figure 4.2. The metatitanic acid particles from the undiluted solution appear to form clusters of uniform, spherical particles with a diameter of 0.4–0.8 μm. The standard particle size for commercial pigments is 0.2–0.3 μm [12], which is usually obtained after jet-milling. As the calcination temperature increases, the individual particles appear to slightly coarsen and start to fuse with adjacent particles and form larger agglomerates. The particles from the 10% diluted solution also appear to be spherical but less smooth and uniform and slightly smaller in diameter. These particles also appear to fuse and agglomerate with an increase in calcination temperature. The metatitanic acid particles of the the 25 and 50% diluted solutions have a much different morphology than the first two samples. The particles are much finer and appear to form large porous aggregates with a wide size distribution. These particles also appear to coarsen and form denser crust-like aggregate particles as the calcination temperature increased.

4.3.4 Effect of Calcination Temperature on Morphology

The coarsening effect of calcination can also be observed from the measurement of the size distribution of the precipitate. The average particle size distribution of the 0, 25, and 50% dilution particles after drying at 90 °C and 1 hour heat treatment at 650 °C is shown in Figure 4.3. It is apparent that the volume fraction of fine particles (0.4 μm and below) is greater in the 25% diluted solution than that of the undiluted, confirming the

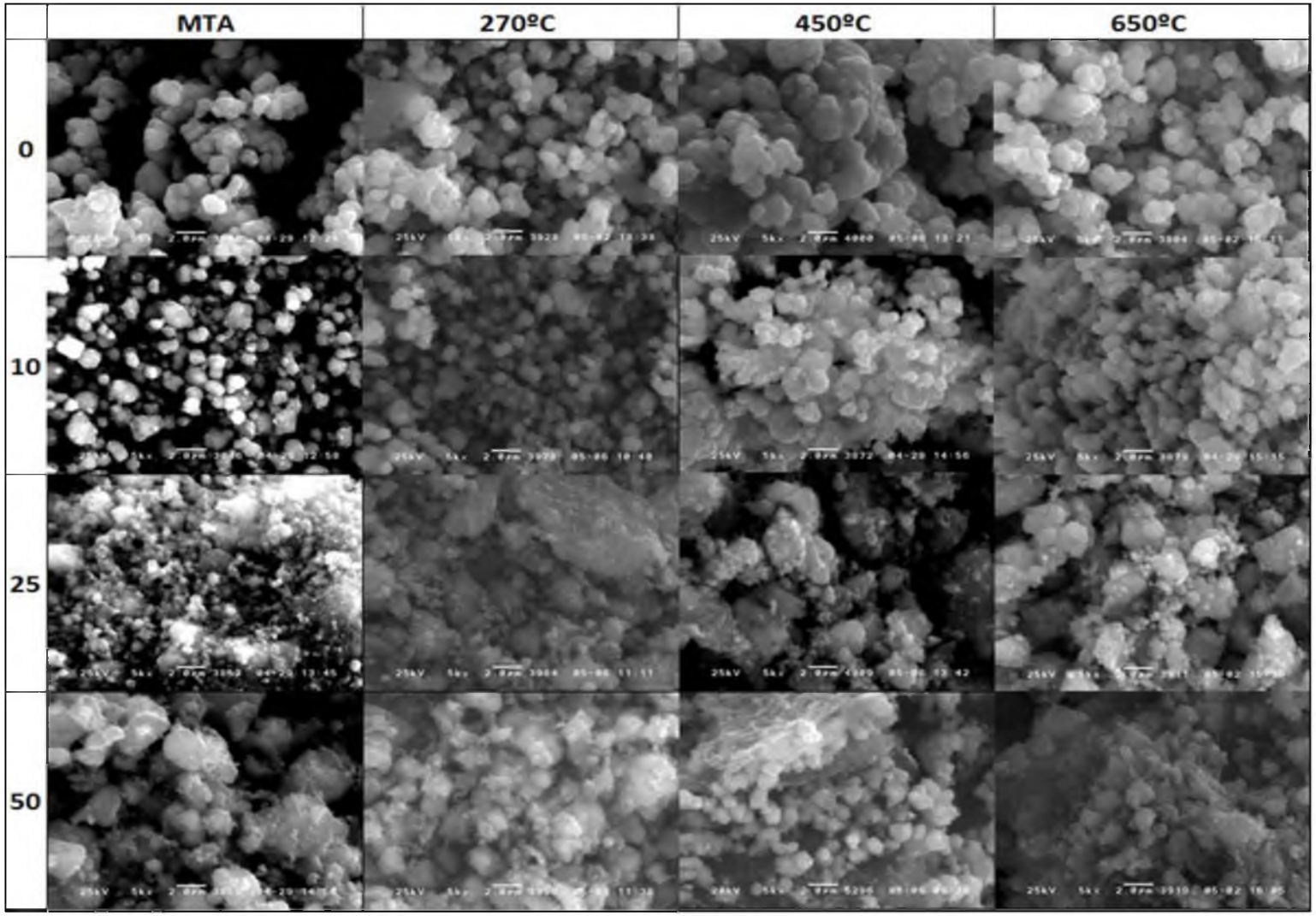

Figure 4.2. SEM images (5000x magnification) of metatitanic acid particles hydrolyzed from solution with 0, 10, 25, and 50 vol % dilution after heating at 90, 270, 450, and 650 ºC for 1 hour. The scale bar is 2 µm.

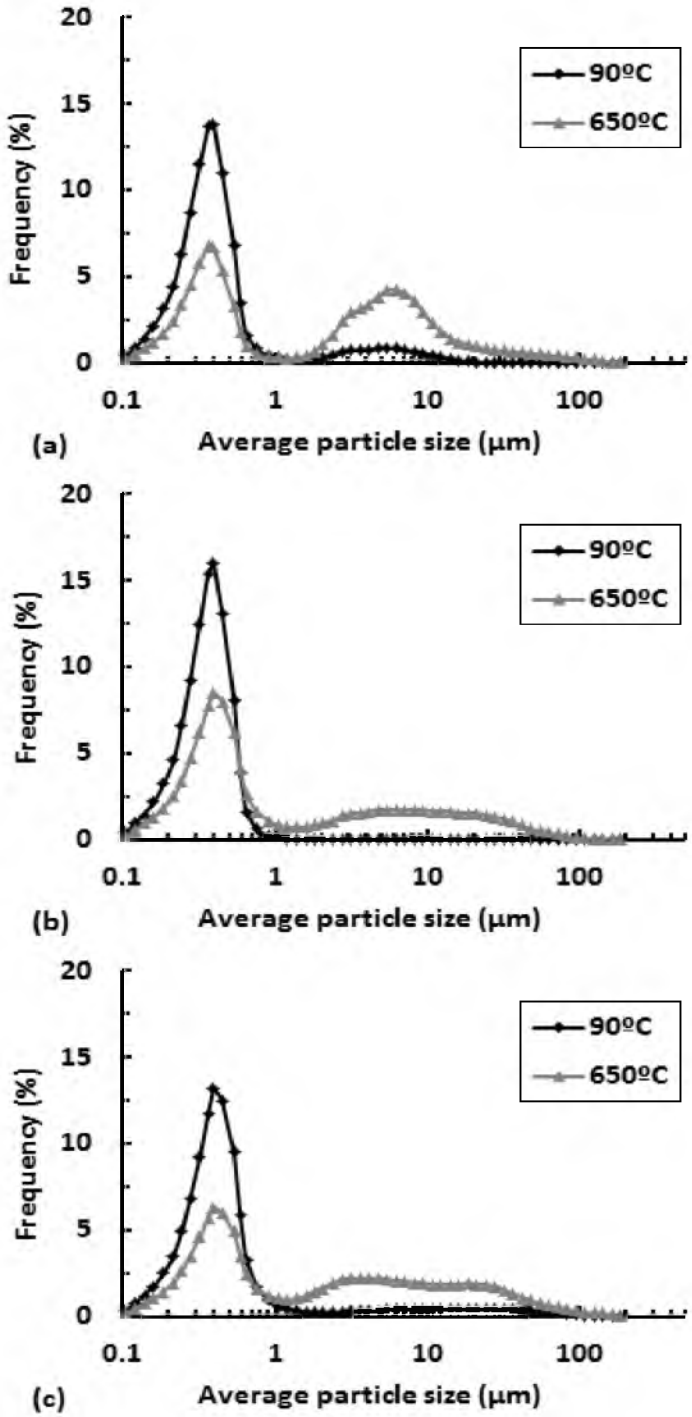

Figure 4.3. Particle size distribution of metatitanic acid particles hydrolyzed from solution with a) 0, b) 25, and c) 50 vol. % dilution after drying at 90 ºC and heating at 650 ºC for 1 hour.

observations from the SEM images. Upon calcination, the percentage of fine particles significantly decreases while the percentage of coarser particles increases. Based on the SEM images, it does not appear that the primary particles have coarsened by the magnitude indicated by the distribution analysis. The increase in the measured average particle size can likely be attributed to the agglomeration of primary particles as previously discussed. The precipitates from the more diluted solutions appeared to have formed slightly larger aggregates as indicated by a larger percentage of particles above 10 μm.

The difference in the morphology and size of precipitates can most plausibly be explained by the nucleation rate in the different dilutions of acid Ti solution. With the undiluted solution, the starting pH was the lowest and least favorable for hydrolysis, likely resulting in a slower nucleation rate of metatitanic acid particles. Under these conditions, precipitate particles can also redissolve, allowing only stable nuclei to continue to grow throughout the reaction. As the pH of the solution increased with higher levels of dilution, the conditions for hydrolysis were more favorable, leading to a more rapid nucleation rate and less dissolution and hence finer and finer particles were observed. Also, the denser appearance of the particles at lower dilutions is likely due to a lower degree of hydration in the precipitates, while the porous appearance of the aggregates of the particles in the more diluted solution is likely due to a higher degree of hydration. The particles at these dilutions become denser with an increase in calcination temperature as the removal of water leads to the collapse of pores and the increased thermal energy results in the consolidation and growth of the particle aggregates.

4.3.5 Effect of Dilution on Phase Composition

The level of dilution appears to not only affect the size and morphology of the precipitates, but also the phase composition as well. X-ray diffraction was used to characterize the structure of the precipitates from each of the dilution samples calcined at different temperatures. The X-ray diffraction patterns of metatitanic acid particles from the 0, 10, 25, and 50% diluted samples dried at 90 ºC are shown in Figure 4.4. At 0% dilution, rutile is the most dominant phase in the precipitates, although some weak anatase peaks are observed as well. It is observed that as the level of dilution increases, the rutile peaks decrease in intensity while the anatase peaks significantly increase. It seems that the formation of rutile is more energetically favorable at lower pH and hence a

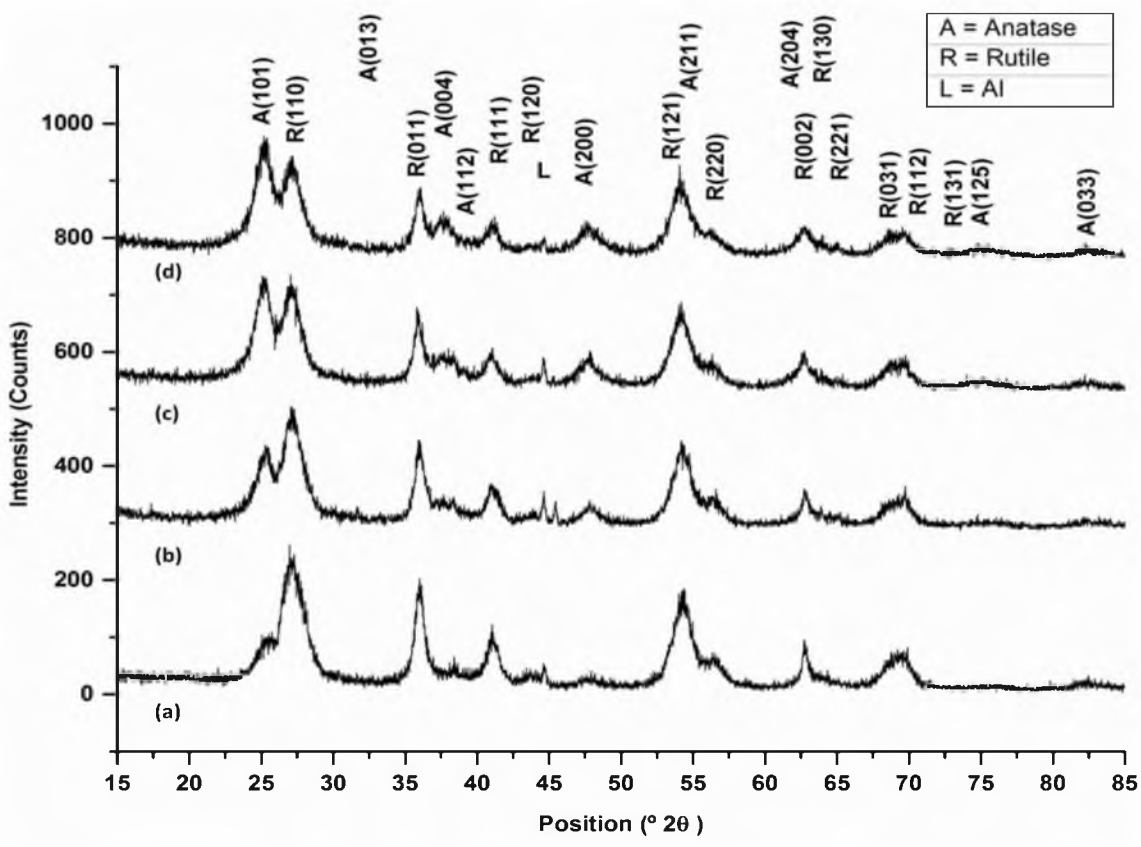

Figure 4.4. X-ray diffraction patterns of metatitanic acid particles hydrolyzed from solution with a) 0, b) 10, c) 25, and d) 50 vol % dilution after heating at 90 ºC for 1 hour.

slower rate of hydrolysis. As the pH and hence hydrolysis rate increases, the formation of anatase becomes increasingly favored. Initial experiments with leach solution diluted by a factor of 4 showed only anatase peaks, even after calcination at 650 ºC for 2 hours.

Cheng et al. [13] have offered an explanation for the favorability of the formation of different TiO_2 phases in titanium chloride solutions. Using ligand field theory, they explained that the Ti(IV) complex $[Ti(OH)_nCl_m]^{2-}$ forms anatase particles when pH is high because of the increased probability of edge-shared bonding and a higher OH^- concentration. At lower pH values, edge-shared bonding is inhibited by the decrease in OH^- concentration, and corner-shared bonding is more favorable, resulting in the formation of the rutile phase.

4.3.6 Effect of Calcination on Phase Composition

The effect of calcination on the phase composition of the precipitates was also observed through X-ray diffraction. The XRD patterns of particles from the undiluted solution after drying at 90 ºC and calcining for 1 hour at 270, 450, and 650 ºC are shown in Figure 4.5. At 90 ºC, broad, weak peaks of both anatase and rutile phases are observed. As the calcination temperature increases, the peaks sharpen, corresponding to an increase in the size of the crystallites. After 270 ºC, the intensity of the anatase peaks remains about the same; however, the intensity and sharpness of the rutile peaks dramatically increases with each raise in temperature. Calcination of the particles at temperatures greater than 650 ºC would eventually convert all of the anatase to rutile phase, which is the thermodynamically favored phase above 400 ºC [2].

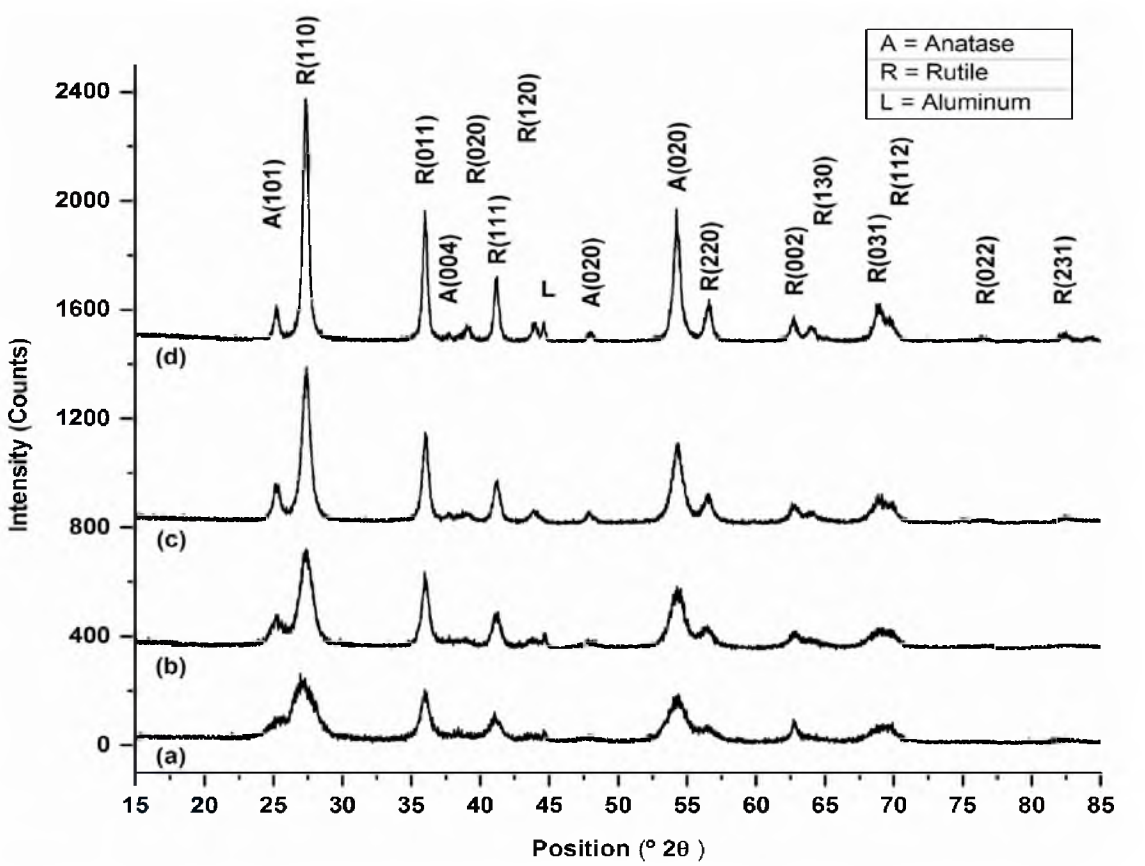

Figure 4.5. X-ray diffraction patterns of metatitanic acid particles hydrolyzed from solution with 0 vol % dilution after heating at a) 90, b) 270, c) 450, and d) 650 ºC for 1 hour.

4.3.7 Rietveld Quantitative Analysis

The effects of dilution and calcination temperature on the structure of themetatitanic acid precipitates can be described quantitatively as well. The proportion of rutile and anatase in each precipitate sample were calculated using Rietveld quantification analysis [9]. The percentage of each phase is shown in Table 4.1. The particles resulting from the hydrolysis of the undiluted leach solution had nearly 20% more rutile than those of the 10% diluted solution and more than 41% more than the 50% diluted solution. At 270 ºC, the proportion of anatase slightly increases as the amorphous component of the metatitanic acid converts at about 260 ºC. At 450 ºC, rutile phase has

Table 4.1. Phase compositions of metatitanic acid particles hydrolyzed from solution with 0, 10, 25, and 50 vol. % dilution after heating at 90, 270, 450, and 650 ºC for 1 hour. Values determined from Rietveld quantification tool of X'Pert High Score Plus.

	Temperature (ºC)							
	90		270		450		650	
Dilution %	%Rut	%Ana	%Rut	%Ana	%Rut	%Ana	%Rut	%Ana
0	87.1	12.9	85.4	14.6	89.7	10.3	97.3	2.7
10	68.4	31.6	68.9	31.1	71.8	28.2	76.9	23.1
25	52.0	48.0	48.7	51.3	53.0	47.0	61.8	31.2
50	45.9	54.1	43.9	56.1	63.3	36.7	54.8	45.2

started to form and continues to do so with an increase in temperature. At 650 ºC, the precipitates from the undiluted solution are more than 97% rutile, while the 50% diluted samples are only 55% rutile, with an 8–10% increase in rutile content for each level of dilution. Since rutile is generally the preferred phase for pigments, hydrolyzing with no dilution appears to be the most favorable process option. The particle size and shape are characteristic of most other commercial pigments as well. However, for most nanoparticle applications, anatase is preferred due to its high photocatalytic activity. Therefore, for the production of extremely fine TiO_2 anatase particles, hydrolysis at even greater dilution of the leach solution is recommended.

4.3.8 Thermal and Gravimetric Analysis

Thermal and gravimetric characterizations of the metatitanic acid particles further confirm the previous observations. The profiles of the samples from each dilution are shown in Figure 4.6. Weight loss is observed for each sample as the chemically bound water is removed through evaporation, with the greatest loss observed for the more dilute samples. The rate of loss is highest for each sample from 25–300 ºC as loosely bound

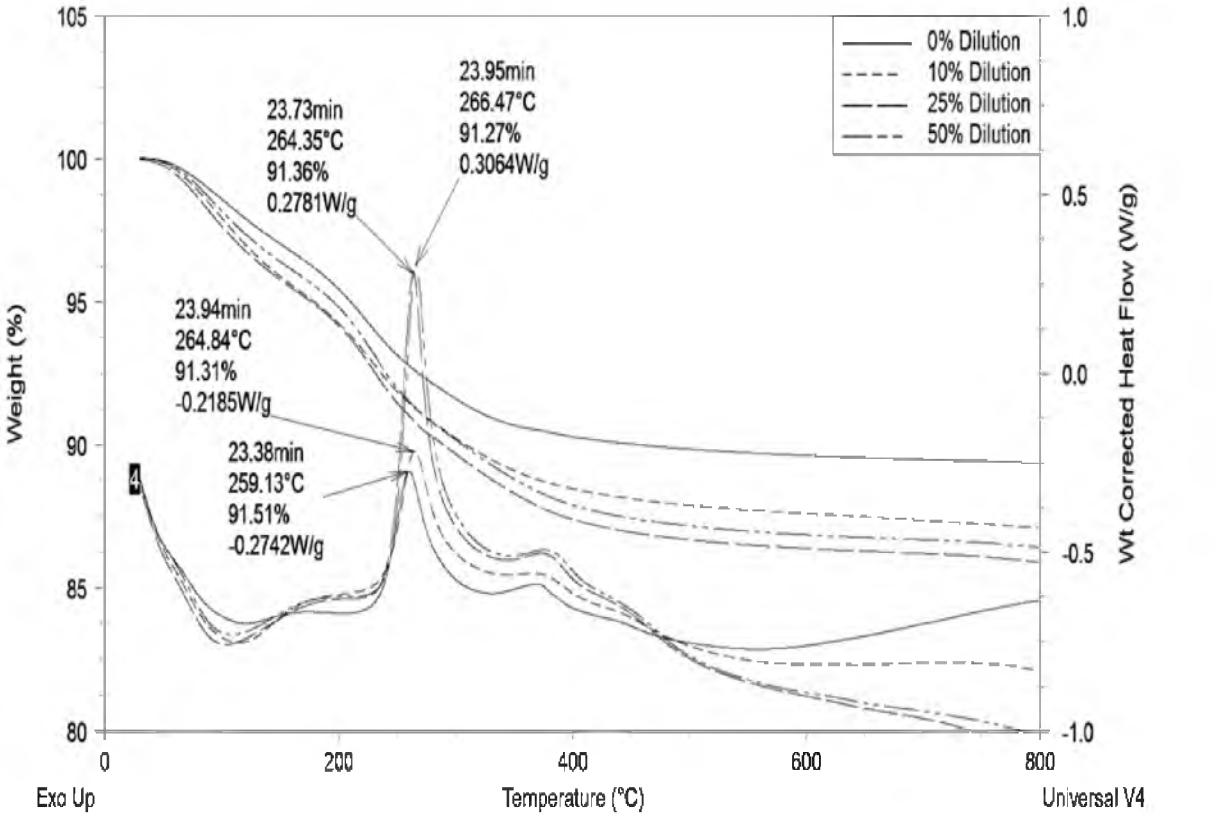

Figure 4.6. TGA-DSC curves of metatitanic acid hydrolyzed from purified leach solution at 0, 10, 25, and 50 volume % dilution.

water molecules evaporate, but the rate begins to taper off after 300 °C and changes minimally after 800 °C. The sample with 0% dilution had a water content of about 10%, while the 25 and 50% diluted samples had about 14% water content by weight. The predicted weight % of water for a TiO_2 molecule with one water of hydration is 18.5 %; therefore, the samples varied from 0.54 to 0.75 water molecules of hydration.

An endothermic peak is observed at about 100 °C, corresponding to the vaporization temperature of water, increasing in intensity with higher dilutions. The exothermic peak observed at about 260 °C is attributed to the phase transformation of amorphous metatitanic acid particles to anatase. An increase in dilution led to a more intense exothermic peak, indicating a larger amount of amorphous material in the original

sample as well as a slight increase in the anatase transformation temperature. The endothermic peak observed at about 380 °C is attributed to the rutile phase transformation. This is corroborated by an increase in the proportion of rutile in the samples as measured by X-ray diffraction. The exothermic heat flow value increases with a lower initial proportion of rutile phase, although the peak heights appear about the same magnitude for samples with an equal change in rutile content (4.3% change for 0 and 25% dilution samples) while the 10% peak height is the smallest, corresponding to the least change in rutile content (2.9%). A shift to higher rutile transformation temperatures was also observed with an increase in dilution.

4.3.9 Surface Area Measurements

The surface area of the precipitate particles was measured using a BET surface area analyzer. The single-point BET surface area of each sample is shown in Figure 4.7. The surface area of the metatitanic acid particles increases significantly with an increase in dilution, with the dried precipitates of the undiluted leach solution having the smallest surface area of 57.2 m^2/g, increasing by nearly a factor of three to 138.6 m^2/g for the 50% diluted solution. These values corroborate the finer and more porous particles initially observed through SEM imaging. Upon calcination at 270 °C, the diluted samples show a 10 to 17% decrease in surface area as the pores begins to collapse. The particles continue to decrease in surface area at a calcination temperature of 450 °C, likely due to an increase in crystallinity and structural ordering. The particles continue to coarsen and agglomerate as the temperature increases to 650 °C, resulting in a 61% surface area reduction for the undiluted sample and a nearly 75% reduction for the 10% diluted sample.

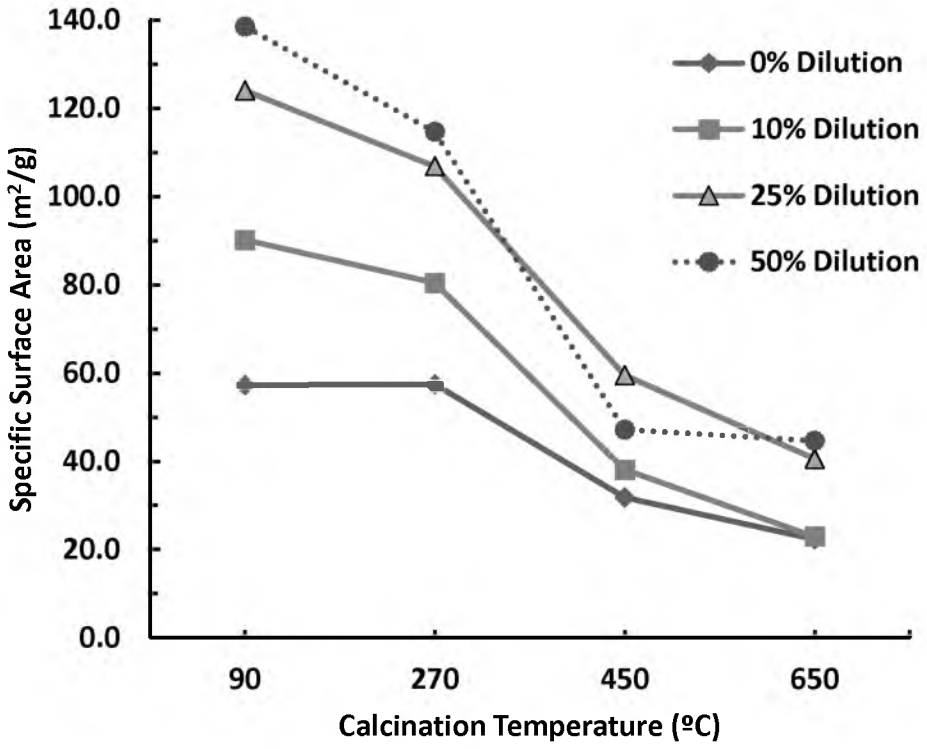

Figure 4.7. Single-point BET specific surface area values for metatitanic acid particles hydrolyzed from purified leach solution at 0, 10, 25, and 50 volume % dilution after calcination at 90, 270, 450, and 650 ºC.

4.4 Conclusion

The effects of hydrolysis and calcination on the size, shape, phase, and surface area of metatitanic acid particles precipitated from titanium chloride leach solutions has been studied. It was determined that increasing the amount of diluting water significantly increased the rate of hydrolysis but not the final TiO_2 recovery. Greater dilution also favored finer and more porous precipitates with a higher degree of hydration in the dried particles. The surface area of the uncalcined particles was highly sensitive to both the initial acid concentration and hydrolysis rate, with a dramatic increase in surface areas for higher pH (more diluted) solutions. The surface areas of the particles from diluted solutions were more sensitive to calcination temperature as seen by the significant decrease in surface area with an increase in calcination temperature. For the purpose of making TiO_2 pigment, the preferred conditions include hydrolyzing leach solution without adding water for 2 hours and calcining for an hour at a temperature of 650 ºC or more. Hydrolyzing at even higher dilutions than used in this study could potentially produce high surface area anatase nanoparticles suitable for photocatalytic applications.

4.5 References

[1] J. Winkler, *Titanium Dioxide*. Hannover, Germany: Vincentz Network, 2003, pp. 30–40.

[2] J. Barksdale, *Titanium: Its Occurrence, Chemistry, and Technology.* New York: Ronald Press Co, 1966, p. 302.

[3] M. Inada, K. Mizue, N. Enomoto, and J. Hojo, "Thermal stability of rutile TiO_2 with high specific surface area synthesized by self-hydrolysis process," *Sci. Adv. Mater.*, vol. 2, pp. 102–106, 2010.

[4] S.J. Kim, S.D. Park, Y.H. Jeong, and S. Park, "Homogeneous precipitation of TiO_2 ultrafine powders from aqueous $TiOCl_2$ solution," *J. Am. Ceram. Soc.*, vol. 82, no. 4, pp. 927–932, 1999.

[5] A. Pottier, S. Cassaignon, C. Chanéac, F. Villain, E. Tronc, and J.P. Jolivet, "Size tailoring of TiO_2 anatase nanoparticles in aqueous medium and synthesis of nanocomposites, *J. Mater. Chem.*, vol. 13, no. 4, pp. 877–882, 2003.

[6] V. Samuel, P. Muthukumara, S.P. Gaikwadb, S.R. Dhageb, and V. Ravi, "Synthesis of mesoporous rutile TiO_2," *Mater. Lett.*, vol. 58, no. 20, pp. 2514–2517, 2004.

[7] M. Ocana, V. Fornes, J.V.G. Ramos, and C.J. Serna, "Factors affecting the infrared and raman spectra of rutile powders," *J. Solid State Chem.*, vol. 75, pp. 364–372, 1988.

[8] E. Matijevic, M. Budnik, and L. Meites, "Preparation and mechanism of formation of titanium dioxide hydrosols of narrow size distributions," *J. Colloid Interface Sci.*, vol. 61, no. 2, pp. 302–311, 1977.

[9] R.A. Young, *The Rietveld Method*. IUCr Monographs on Crystallography, Oxford: Oxford University Press, 1993, pp. 292.

[10] E. Santacesaria, M. Tonello, and G. Storti, "Kinetics of titanium dioxide precipitation by thermal hydrolysis," *J. Colloid Interface Sci*, vol. 111, no. 1, pp. 44–53, 1986.

[11] J.F. Duncan and R.G. Richards, "Hydrolysis of titanium (IV) sulphate solutions: 1. Precipitation of hydrous titanium dioxide," *New Zealand J. Sci.*, vol. 19, pp. 171–178, 1976.

[12] W.A. Kampfer, *Pigment Handbook: Properties and Economics*, T.C. Patton, ed. New York: Wiley, 1973, pp. 1–32.

[13] H. Cheng, J. Ma, Z. Zhao, and L. Qi, "Hydrothermal preparation of uniform nanosize rutile and anatase particles," *Chem. Mater.*, vol. 7, pp. 663–671, 1995.

CHAPTER 5

ENERGY AND EMISSIONS ANALYSIS OF TIO_2 MAKING PROCESSES

5.1 Introduction

The purpose of this analysis is to estimate the total energy consumption and CO_2 emissions of the new method of manufacturing TiO_2 pigment and Ti powder. This estimation will be compared to the current methods to determine if the new processes do indeed have potential for energy savings and reduction in CO_2 emissions at an industrially significant scale.

5.1.1 Evaluating Environmental Impact

In order to improve the efficiency of any industrial process, the current levels of performance must be evaluated. Assessing the environmental impact of any industrial process can be a daunting task considering the numerous metrics and methodologies that can be used. Two common metrics that are frequently examined are the total energy consumed and CO_2 emitted [1]. Reporting values for the total energy consumption and carbon emissions of a particular chemical can be complicated if the end product can be synthesized by a number of processes using a variety of starting materials. This proves to be the case for titanium dioxide pigment.

5.1.2 Choosing System Boundaries

Another complexity occurs when different energy reports consider different system boundaries in their energy accounting. Some reports consider the process from the entry of the feed material to the production of the final pigment product. This boundary is referred to as "feed-to-gate." A more comprehensive consideration includes the energy requirements for mining, transporting and preparing the raw minerals for use as a feed stock in the particular unit processes (often referred to as beneficiation). This method will be referred to as "cradle-to-gate." The treatment and disposal of gaseous and liquid waste streams (referred to as emissions and effluents, respectively) is also considered in some analyses but not in others. A life-cycle assessment accounts for all of the material and energy inputs and outputs of a manufacturing process, including the treatment and/or disposal of its wastes. Table 5.1 summarizes the reported energy and emissions of the sulfate and chloride methods considering different starting materials as well as different system boundaries and effluent treatments.

5.1.3 Feed-to-Gate Data

Several feed-to-gate values of energy consumption and carbon emissions from TiO_2 manufacturing have been reported. Brown et al. [2] reported a complete material and energy balance for each step of pigment manufacture (excluding waste treatment) for the chloride and sulfate processes, using rutile and ilmenite feeds, respectively. A summation of the inputs for each step indicates the chloride method and sulfate method consume 11.58 and 57.95 GJ/ton TiO_2, respectively. Using the EPA Greenhouse Calculator [3], the carbon footprint resulting from the electricity and natural gas consumed in these processes was calculated as 0.606 and 3.048 tons CO_2/ ton TiO_2,

Table 5.1. Summary of the reported energy and emissions of the sulfate and chloride methods considering different system boundaries.

Chloride Process	**Energy (GJ/ton)**			**Emissions (Ton CO_2/ton)**			
Boundary / Feed stock	**Nat Gas**	**Elec**	**Total**	**Nat Gas**	**Elec**	**Total**	**Source**
Feed to Gate- No treatment							
Rutile	11.2	0.4	11.6	0.53*	0.08*	0.61*	[2]
Feed to Gate- W/ treatment							
Rutile			19.0			4	[4,5]
Rutile			17.4-28.7				[13]
Cradle to Gate- No treatment							
Rutile			66.29				[9]
Rutile	57.5	48.1	106	2.73*	3.06*	5.79*	[10]
Leucoxene	63.0	55.8	119	2.80*	3.50*	6.30*	[10]
Slag	67.0*	78.3*	145*	4.07*	4.79*	8.87*	[10]
Cradle to Gate- W/ treatment							
Natural Rutile			79.0			4	[12]
Synthetic Rutile			101				[11]
Slag			109				[11]

Sulfate Process	**Energy (GJ/ton)**			**Emissions (Ton CO_2/ton)**			
Boundary / Feed stock	**Nat Gas**	**Elec**	**Total**	**Nat Gas**	**Elec**	**Total**	**Source**
Feed to Gate- No treatment							
Ilmenite	56.7	1.3	58.0	2.69*	0.36*	3.05*	[2]
Feed to Gate- W/ treatment							
Rutile			27.2-52.2			5	[4,5]
Cradle to Gate- No treatment							
Ilmenite			67.22				[9]
Ilmenite	69.2	10.2	79.4	3.25*	0.64*	3.89*	[10]
Slag	72.7	36.7	109	4.68*	2.14*	6.82*	[10]
Cradle to Gate- W/ treatment							
Ilmenite (ENG)			79				[11]
Ilmenite (ENG)			75				[11]
Ilmenite (ENG)			75				[11]
Slag (ENG)			103				[11]
Ilmenite (DEU)			80			4.7	[12]
Ilmenite (FRA)			90			5.9	[12]
Ilmenite (FIN)			75			5.0	[12]

* Calculated from source data

respectively. The German Federal Environmental Agency has reported [4] the energy consumption and emissions data for TiO_2 manufacture in Germany, including the disposal of and recycling of process waste streams. Energy values of 19.0 and 27.2–52.2 GJ/ton TiO_2 and 4 and 5 ton CO_2/ton TiO_2 were given for chloride and sulfate plants, respectively. These values were also reported by Osterwalder et al. in their comparison of wet and dry synthesis methods of TiO_2 nanoparticles [5]. The variability in the sulfate energy data is a result of the variable level of recycling and/or neutralization of spent sulfuric acid streams employed by individual plants.

5.1.4 Cradle-to-Gate Data

The values reported in the feed-to-gate analyses underestimate the total energy and emissions of each process. Based on these analyses, the chloride process seems significantly more energy efficient than the sulfate process. Indeed, if the available supply of natural rutile were such that it could be used as the sole feed material for the chloride process, this might be the case. However, natural rutile only accounts for 10% of the total titanium feed stocks in the world [6]; hence, the chloride process heavily relies on the use of upgraded feed stocks such as synthetic rutile or titania slag, with each having an associated energy cost not included in these values. Titania slag is produced by smelting ilmenite in large electric arc furnaces [7]. Synthetic rutile is produced by a series of reduction, oxidation, and acid leaching steps [8]. Thus, feed-to-gate analysis can only give a limited scope of the actual energy requirements and environmental impact of different processing routes.

Cradle-to-gate analyses provide a more comprehensive process comparison. Sittig et al. reported nearly equivalent energy values for the chloride method and sulfate method

of 66.29 and 67.22 GJ/ton TiO_2, respectively [9]. It is unknown if these values includes effluent treatment. A US Bureau of Mines industrial energy research report produced by Battelle laboratories [10] includes a line-itemed list of the material and energy (electricity, petroleum, and natural gas) required for each processing step, including mining, transport, and upgrading of raw ore as well as pigment manufacture; however, waste disposal was not included. The chloride route consumed 145.3 and 118.8 GJ/ton TiO_2 using rutile and leucoxene as the feed materials, respectively, resulting in 7.79 and 6.30 tons CO_2/ton TiO_2, also calculated using the EPA Greenhouse Gas Equivalency calculator [3]. The sulfate route consumed 79.4 and 109.4 GJ/ton TiO_2 using ilmenite and slag as feed, respectively, resulting in 3.89 and 5.58 tons CO_2/ton TiO_2. These analyses indicate that when considering a larger system boundary, the chloride route appears to consume as much if not more energy than the sulfate route.

Tioxide Industries conducted a life-cycle assessment study of 6 different TiO_2 manufacturing plants in England employing different process options, including different feed material, method of pigment manufacture and method of waste disposal [11]. The LCA examined all key inputs and outputs in TiO_2 manufacture, including raw materials, products, utilities, and wastes. The LCA report concluded that no single processing option was best, but that the local policies and ore supply considerations would determine the best processing option for each particular plant. The sulfate method consumed 75–79 and 103 GJ/ton TiO_2 when ilmenite and slag were used as feeds, respectively. The chloride method consumed 101 and 109 GJ/ton TiO_2 when synthetic rutile and slag were consumed, respectively. Several trends from this report should be noted. It appears that the chloride process is more energy intensive than the sulfate process in every case.

While the feed-to-gate processing energy (referred to as black end) is comparable, the energy penalty from using upgraded feed material, as well as an increased finishing energy, makes it more energy intensive overall. As the level of neutralization of acidic effluents increases, the amount of energy required slightly increases, but the amount of solid wastes also dramatically increased. It should also be noted that slag production generates considerably less waste than upgrading ilmenite to synthetic rutile.

The values from the Tioxide LCA were also reported in a VTT Coatings environmental impact report [12], although they also reported that sulfate plants in Finland, Germany, and France using ilmenite consumed 75, 80, and 90 GJ/ton TiO_2 and produced 5.0, 4.7, and 5.9 tons CO_2/ton TiO_2, respectively. A chloride plant in Germany using natural rutile consumed 79 GJ/ton TiO_2 and emitted 4.1 tons CO_2/ton TiO_2. It is likely that the variability of data from the plants in each country is due to differences in the mineralogy of the ilmenite feed stocks, electricity mixes, and waste disposal requirements.

5.1.5 Feed Preparation Data

Another source of variability in the reported energy consumption of TiO_2 manufacture results from the variety of feed materials available. As mentioned previously, the individual starting materials require a widely variable amount of energy input to produce. The energy required to prepare various feed stocks is shown in Table 5.2.

Raw ilmenite requires the least preparation to use as a feedstock, but requires the most intense treatment of its liquid and solid byproducts. The energy requirement is 5–8.4 GJ/ton TiO_2 [10, 13]. Natural rutile also requires very little prefeed preparation with

Table 5.2. Reported energy requirements (in MJ/ton TiO_2) of preparing various TiO_2 manufacturing feed stocks.

Feed Material	Mining + Benefic.	Transport	Drying + Grinding	Smelting	Total	Source
Rutile	5.5	3.0	2.3	-	10.7	[10]
Rutile					6.0	[13]
Ilmenite	5.3	0.9	2.2	-	8.4	[10]
Ilmenite					5.0	[13]
Slag	0.7	1.7	1.9	39.0	43.2	[10]
Slag					35.5	[13]
Leucoxene	8.3	0.9	3.1	-	12.3	[10]
Synth Rut					35.0	[13]

6 –10.7 GJ/ton [10, 13], but as mentioned previously, it is limited in supply. Leucoxene can also be used as a feed material in the chloride process, although it requires more preparation than rutile at 12.3 GJ/ton [10]. The upgrading of ilmenite to synthetic rutile requires 35.0 GJ/ton TiO_2 [13]. Similarly, producing slag also requires a considerable amount of energy. Slag production (mining included) has been reported to consume 35.5 and 43.2 GJ/ton TiO_2 [10,13]. It is evident that the energy requirements for producing synthetic rutile and slag are comparable.

5.2 Features of the New Process

5.2.1 Recycling and Regeneration of HCl and NaOH

Recycling and regeneration of HCl and NaOH are critical components of the new process. In general, acid and/or alkaline waste solutions from metallurgical industries are often neutralized with lime or acid [11]. For economic and environmental reasons, however, it is beneficial to recycle and regenerate process reagents as much as possible. Several methods have been developed to regenerate or reconcentrate dilute HCl solutions. The steel industry has developed a method of regenerating HCl from spent pickling

solution via the spray roasting of ferrous chloride acidic solution. This, however, is an extremely expensive and energy intensive process (2.5–5.0 MJ/liter) [14–16]. The generation of HCl and NaOH is possible through electrolytic means, albeit at a significant energy cost. Most of the caustic and chlorine used in the chemicals industry is produced by the chlor-alkali process and few, if any, more efficient methods of obtaining NaOH and HCl are available. The energy requirements for the chlor-alkali process are reported by the European Commission [17]. This includes the energy to run the membrane technology chlor-alkali cells and the concentration of NaOH solution by evaporation. According to this Best Available Techniques report, producing 1 ton of Cl_2 gas via membrane technology requires 2,790 kWhr of electricity.

The residual solutions from TiO_2 production in the new process may contain low concentrations of salts (NaCl) from acid leaching and NaOH from washing of the alkaline roast product. A portion of the NaOH solution can be concentrated and reused in the roasting process using multiple effect evaporators. Another portion can be used to neutralize residual acid streams, forming a residual NaCl brine solution that can be used as the feed solution for the chlor-alkali process. Most of the impurities in the residual solution can also be precipitated and removed as precipitates prior to its feed in to the chlor-alkali cells.

The electrochemical reactions in the chlor-alkali process are shown in (5.1) and (5.2) [17]. Sodium chloride is oxidized at the anode to produce chlorine gas and sodium ions while water is reduced to form hydrogen gas and hydroxyl ions at the cathode. H_2 gas generated at the cathode of the membrane cell can be collected and reacted with Cl_2 gas in an HCl burner to produce HCl vapor as shown in (5.3).

Anode half-cell reaction: $2\ NaCl \rightarrow Cl_2 + 2Na^+ + 2\ e^-$ (5.1)

Cathode half-cell reaction: $2\ H_2O + 2\ e^- \rightarrow H_2 + 2OH^-$ (5.2)

HCl production reaction: $H_2 + Cl_2 \rightarrow 2HCl$ (5.3)

This reaction is highly exothermic; therefore, it will require minimal energy input to operate the burner at steady state. The HCl vapor can be adsorbed by water to produce industrial grade hydrochloric acid or sparged directly into the leaching reactor to increase the HCl concentration. In the aqueous phase, Na^+ and OH^- combine to form NaOH, which can be concentrated with steam in multiple effect evaporators and be used in the roasting step. Thus, the residual acidic or alkaline solutions from the process can be utilized to generate more process reagents, resulting overall in reduced waste streams.

5.2.2 Utilizing Waste Heat

Energy consumption can also be reduced by utilizing waste heat in the new process. The high temperature steps produce a significant amount of so-called medium-temperature (230–650 ºC) or high-temperature (>650 ºC) waste heat, which can be economically utilized for the low temperature steps, thus reducing the energy consumptions of the overall process. For either of the two high temperature steps, i.e., NaOH roasting of titania slag and calcination of H_2TiO_3, one part of the waste heat is contained in the high temperature flue gas consisting of a large amount of water vapor released from the reaction; the other part of waste heat is released during the cooling of the reaction product discharge, i.e., Na_2TiO_3 or TiO_2. The waste heat from both the hot flue gas and the product discharge in the high temperature steps can be recovered by using a waste heat boiler [18]. The waste heat of hot flue gas can be directly fed into the

boiler, while the waste heat of product discharge needs to be transferred first to air passing through a heat wheel then inputted into the boiler. Heat transfer efficiencies of up to 85% have been achieved through this technology [19]. Although experimental data for process heat recovery is beyond the scope of our analysis, the amount of recoverable heat from higher temperature reactions can be approximated using HSC Chemistry 5.11 software.

5.3 Energy Analysis Procedure

5.3.1 Model Plant Using New TiO_2 Process

A cradle-to-gate energy audit was conducted to compare the new TiO_2 manufacturing process to the two conventional processes. To calculate the energy and emissions of the new process, a processing plant producing 100,000 metric tons per year TiO_2 pigment using the new technology was modeled by our group. A flow sheet was developed and process equipment was selected and sized according to data from mineral and chemical engineering equipment handbooks. The material balance for the plant operating on an 11.9 tph TiO_2 basis is shown in Figure 5.1. The energy required for roasting and calcination as well as the recoverable energy from the hot discharge products was calculated using HSC Chemistry 5.11 thermodynamic calculations software available from Outokumpu Technologies. The energy requirements for producing titania slag and of regenerating and recycling process reagents were found in government reports and were also included [10,13]. To make a fair comparison of the different processes, slag was chosen as the common feed material. The CO_2 emissions were calculated using the EPA carbon emission calculator by entering the total kilowatt-hours and therms of natural gas consumed for each step, based on geographically averaged utility values in

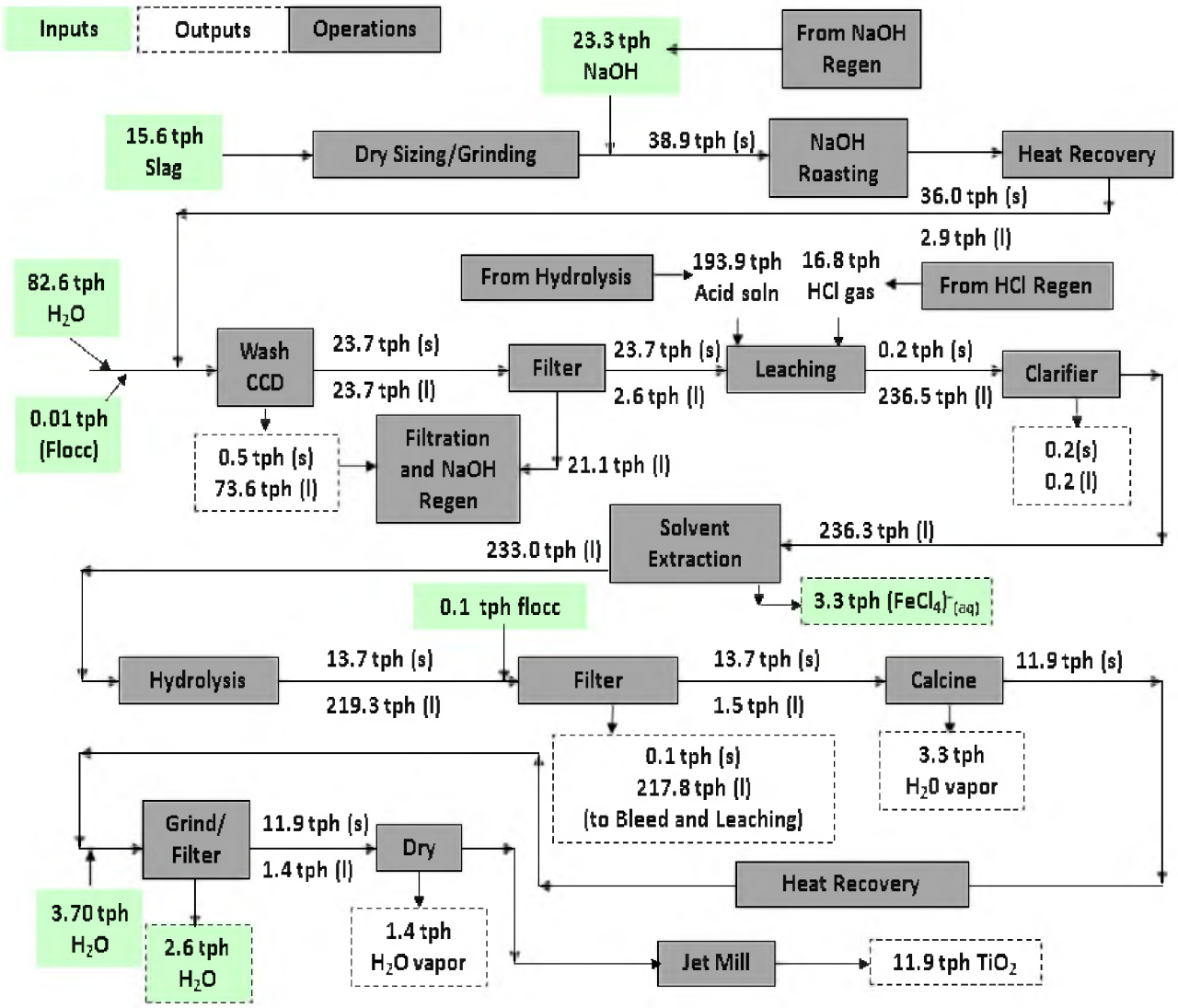

Figure 5.1. Material balance for new TiO_2 process operating on 11.9 tph TiO_2 basis.

the US [3].

5.4 Unit Process Energy Calculations

5.4.1 Slag Making

The feed material for the new process is titania slag produced by Rio Tinto Iron and Titanium in Quebec, Canada. A value of 39.6 GJ/ton TiO_2 for the production of titania slag from ilmenite is used for each of the three pigment making processes [10], which includes mining, beneficiation, and smelting of the ilmenite, but not milling, which is calculated separately.

5.4.2 Slag Milling and Sizing

In order to produce 100,000 tons per year, the plant was designed for a TiO_2 pigment production of 11.9 tph. This requires 15.4 tons of slag be fed into the rotary kiln each hour. In order to enhance reaction kinetics and improve the overall recovery of the roasting reaction, the as-received slag is ball milled to reduce the particle size. The optimum median particle size of slag was determined experimentally to be 38 microns (+450/-325#). The particle size of the ball mill product is determined by an air classifier used in closed circuit with the mill in order to limit overgrinding. The energy required to mill the slag to the desired particle size can be determined using Bond's law [20], which states that the required specific energy input, E (kWhr/ton), is proportional to the size reduction ratio to be achieved, according to (5.4).

$$E = 10 * W_i * \left[\frac{1}{\sqrt{P_{80}}} - \frac{1}{\sqrt{F_{80}}} \right] * 1.3 \tag{5.4}$$

F_{80} and P_{80} are the particle sizes (80% passing) of the feed and product, respectively, and W_i is the Bond work index, which is a material specific index of "grindability." A factor of 1.3 is applied for dry milling calculations [21]. Titania slag has a Bond work index of 17.6 kWhr/ton [22]. The size distribution of the slag from RTIT was experimentally determined using a series of sizing sieves, and the F_{80} and P_{80} were determined to be 610 μm and 50 μm, respectively. Grinding slag thus requires 22.7 kWh/tonne, which for 15.4 tph equals 350 kWhr. Based on this calculation, a 9'D x 10'L ball mill driven by a 470 hp motor and a 10'x 17' air classifier using a 40 hp (29.8 kW) air compressor were selected [23].

5.4.3 Roasting

The slag is roasted with NaOH at a ratio of 1:1.5; therefore, 23.3 tonnes of anhydrous NaOH are added into the rotary kiln with the 15.6 tons of slag per hour. The temperature of the roasting kiln is maintained at 550 °C. The calculations to size a rotary kiln depend on the mean residence time (MRT), the angle of repose of the material (θ), the rotation speed (n), and the inclination angle of the kiln (β) [24], according to (5.5).

$$MRT = 1.77 * \frac{L}{D} * \frac{\sqrt{\Theta}}{n * \beta} \tag{5.5}$$

With a mean residence time of 60 minutes, an angle of repose of 35^0, a rotation speed of 1 rpm, and a typical inclination angle of 3^0, the L/D ratio was 17.2. Rotary kilns generally operate at about 10–15 volume percent. Based on these two factors, a 7' x 120' rotary kiln requiring a 80 hp motor was selected [23].

The energy required for the roasting operations was calculated using HSC

Chemistry 5.11 software. The inputs for the slag are shown in Table 5.3. The slag was treated as a mixture of its metal oxide compounds, with the mass of each component determined from the assay provided from RTIT. All of the input compounds are assumed to be at room temperature and atmospheric pressure. Oxides of Ti, Al, Si, Cr, and V react with the NaOH to form sodium compounds, assuming a 99% conversion factor for this calculation. The air flow in the rotary kiln can be adjusted to maintain the heat balance, although the amount chosen for this calculation was 486 Nm^3/hour. Oxygen is consumed by some of the metals to produce higher valent oxides such as Fe_3O_4 and Mn_3O_4. The unreacted oxide compounds are included as outputs in the "Σ other" entry.

The solid, liquid, and gaseous products leave the reactor at 550 °C. The main

Table 5.3. Material and energy balance for roasting reaction.

INPUT						OUTPUT					
Temp (K)	Compound	kg	kmol	H_L (MJ)	H_{tot} (MJ)	Temp (K)	Compound	kg	kmol	H_L (MJ)	H_{tot} (MJ)
298	TiO_2	12203	153	0	-144290	823	Na_2TiO_3	21454	151	11772	-222858
298	Fe	23	0	0	0	823	$Na_2Al_2O_4$	510	3	303	-6741
298	FeO	1515	21	0	-5637	823	Na_2SiO_3	825	7	503	-10053
298	Al_2O_3	320	3	0	-5262	823	Na_2CrO_4	69	0	45	-526
298	CaO	103	2	0	-1161	823	$NaVO_3$	117	1	60	-1038
298	MgO	803	20	0	-11993	823	Fe_3O_4	1644	7	769	-7170
298	MnO	47	1	0	-253	823	Mn_3O_4	50	0	19	-282
298	SiO_2	410	7	0	-6220	823	Σ other	1052	24	591	-14190
298	Cr_2O_3	33	0	0	-244						
298	V_2O_5	87	0	0	-742	823	NaOH(l)	10357	259	11717	-96295
298	NaOH	23314	583	0	-248196						
						823	H_2O(g)	2913	162	3060	-36044
298	O_2(g)	145	5	0	0	823	O_2(g)	13	0	7	7
298	N_2(g)	477	17	0	0	823	N_2(g)	477	17	268	268

TOTAL		kg	kmol	H_L (MJ)	H_{tot} (MJ)
	Input	39480	812	0	-423998
	Output	39480	631	29115	-394921
BALANCE		0	-178	28821	29077
With 18% loss					**35460**

product is 21.4 tons of sodium titanate with significantly smaller amounts of other sodium compounds and unreacted oxides. Over 10.4 tons of unreacted molten NaOH is also discharged, which contains a considerable portion of the latent heat of the products. Water vapor is a major byproduct of the roasting reaction with 2.9 tons released per hour and also contains a significant portion of latent heat. The heat recovery of the discharge products is calculated in section 5.4.9. Theoretically, the roasting operation will require 29,077 MJ/hr of energy; however, due to inevitable heat loss through the kiln walls, more energy will need to be supplied. Palmer and Howes [25] reported an 18% loss of the total input heat through radiation and conduction in a rotary kiln of similar size. Assuming a loss of 18% of total input heat, the reaction will require 35460 MJ/hr, or over 4.7 MBTU of natural gas per hour.

5.4.4 Counter-current Washing

After cooling, 36.0 tph of solid discharge is washed with 88.5 tph water in order to remove soluble impurity compounds such as $Na_2Al_2O_4$ and Na_2SiO_3, as well as excess NaOH that will consume acid in the subsequent leaching step. The washing operation is to be carried out using 3 high-capacity thickeners arranged in a counter-current-decantation (CCD) configuration, allowing the solid and liquid streams to move in opposite directions, with the solids becoming cleaner by being washed with progressively cleaner water. This significantly decreases the amount of water needed to remove the soluble impurities from the reaction product. The rakes of the 3 thickeners are driven by a 7.5 hp motor [23]. After washing, 23.7 tph of solids leave the final thickener. The discharge of the thickeners is generally 50% solids; therefore, 23.7 tph of solution also exit with the solid. The discharge is filtered to 90% solids with 2 drum filters each driven

by a 45 hp motor [23]. 2.6 tph of dilute NaOH solution is entrained in the filter cake, which will consume some acid in the leaching step; however, it is a relatively small amount compared to the acid consumed by the solids.

5.4.5 HCl Leaching

The leaching is performed with 5 M HCl (16.9% HCl) at pulp density of 10%, which requires 213 tph of solution containing 35.9 tph of HCl (solid equivalent). The temperature of the solution is kept above 50 ºC, which is easily maintained by the recirculation of hot solution from the hydrolysis stage (90–100 ºC) and the exothermic reaction of gaseous HCl being sparged into the solution. The solution will be agitated in six 18,000 gallon tanks in parallel each with a 7.5' diameter agitator. The power P (in hp) required for an agitator in a continuously stirred reactor at a medium speed (20–60 rpm) can be approximated using the following empirical relation in (5.6) [26].

$$P = 1.70 * N^3 * \frac{D^5}{550} \tag{5.6}$$

N is the number of revolutions per second, and D is the diameter (in feet) of the agitator blade. For a speed of 60 rpm (1 rev/sec), each agitator requires a 75 hp motor. After leaching, the solution is passed through a drum filter driven by a 45 hp motor to remove the bulk of undissolved solids. The solution needs to be clarified to remove virtually all dissolved solids, which will form crud and pose other serious problems in the solvent extraction circuit if not removed. The solution is fed through a 100'D x 12'H clarifying thickener with a 7.5 hp motor [23].

5.4.6 Solvent Extraction

The clarified leach solution (53,900 gph) is mixed with the organic extractant phase (53,900 gph) to selectively remove iron. The organic phase contains 15 vol. % tertiary amine diluted in kerosene. The loading step will require 4 mixer-settler units each with a 5 hp motor [27]. The loaded organic phase is then mixed with a dilute HCl solution (53,900 gph) to reverse the loading reaction and strip the iron into the aqueous phase. The stripping is performed in 3 stages and will require 18 mixer-settler units each driven by a 5 hp motor. The stripped organic is sent back to the loading stage while the purified leach solution is sent to the hydrolysis step. In total, the solvent extraction operation will require 60 kW.

5.4.7 Hydrolysis

Following solvent extraction, 236 tph of purified leach solution is hydrolyzed to precipitate metatitanic acid, $TiO(OH)_2$. For a 98% conversion of the titanium in the slag, the reaction will require a 2 hour residence time; therefore, the solution will be fed to six 15'D x 15'H, 20,000 gallon capacity hydrolysis reactors, which are essentially heated continuously stirred tanks. The vessels will have a closed top and a refluxer to minimize evaporative losses. Each tank will be stirred with a 7.5' diameter agitator blade operating at 60 rpm. Using (5.6) as shown above, each agitator will require a 75 hp motor.

For an efficient hydrolysis reaction, the solution needs to be heated from 35 ºC (308 K) to 100 ºC (373 K), which is just below the boiling point of the solution. The heat, q, required to raise the temperature of m kg of solution from 308 K to 373 K ($\Delta T = 65$ K) can be calculated using (5.7).

$$q = m * C_p * \Delta T \tag{5.7}$$

The heat capacity, C_p, of 5% HCl solution is 3.9 kJ/kg-K at 308 K and changes only minimally at 373 K; therefore, the expression above can be used, and a value of 253.9 kJ/kg of solution is obtained [28]. Since the tanks are closed, any vapor that leaves the surface of the liquid will recondense; therefore, at steady state, the heat of vaporization can be neglected. Heating 233,000 kg of solution per hour will require 7.35 x 10^7 kJ of energy. Although the tank will be well insulated, the heat loss in the reactors is estimated to be about 20%; therefore, the hydrolysis step will require 91.9 GJ (7.7 GJ/ton TiO_2) for heating, or 87.1 MBTU of natural gas per hour.

The reaction will produce 13.7 tph metatitanic acid pulp, which will require filtering. The pulp and solution are fed to a 100' dia. high-capacity thickener driven by a 7.5 hp motor where the pulp density is increased from 5.9% to 50%; 40 kg per hour of flocculant is added to aid in the coagulation of the precipitate particles. The underflow of the thickener is then fed to a 10'D x 20'L drum filter driven by a 30 hp motor. The filtered solids are then rinsed with water and filtered in an additional drum filter of the same specifications. The metatitanic acid is discharged from the filters at 90% solids, with approximately 1.5 tph of entrained water. About 0.1 tph of fine metatitanic particles are lost to the filtrate solution, with 217.8 tph total solution leaving the thickener and filter.

In the hydrolysis reaction, H_2O molecules react with the titanyl ion (TiO^{2+}) to form metatitanic acid, $TiO(OH)_2$, releasing H^+ ions into solution. The hydrolysis reaction increases the free acid concentration of the solution. During the reaction, 143.3 kmoles of TiO^{2+} react with 286.6 kmoles of H_2O to produce 286.6 kmol of H^+, which is equivalent

to 10.4 tons of HCl. 193.9 tph of the stream (~89%) leaving the hydrolysis stage will be directly sent back as hot acid solution to the leaching stage. This recycled stream contains 19.1 tons HCl, which provides 53.2% of the HCl needed in the leaching stage, with the remainder HCl to be provided from the chlor-alkali process. The remainder of the posthydrolysis solution will be used as make-up leach solution, solution for the stripping of Fe from the loaded organic phase, or be combined with solution from the CCD circuit to produce brine for the chlor-alkali electrolysis process.

5.4.8 Calcination

After being discharged from the filter, 15.0 tph of metatitanic acid and water are fed to an 8'D x 160'L rotary kiln for calcination. The kiln is driven by a 100 hp motor. The size of the calciner was determined in a similar procedure as the roasting kiln. The heat required to remove the chemically bound water and transform the metatitanic acid to rutile-phase TiO_2 was determined using HSC Chemistry software. The database did not have a record for metatitanic acid (TiO_2–H_2O); therefore, anatase TiO_2 and an equivalent amount of water was included in the input stream. Calcination requires a large amount of air, 3.4×10^5 Nm^3 per hour, to assist in the removal of the chemically bound water in the hydrate. This is the same flow rate of air use in the calcination of metatitanic acid by Brown et al. [2].

The temperature, mass, volume, latent heat, and total enthalpy of input and output streams of the calciner are shown in Table 5.4. The metatitanic acid is assumed to have cooled to 50 ºC as it enters the kiln, and the air is blown in at ambient temperature. The calcination reactor is held at 900 ºC; therefore, the rutile TiO_2 product is discharged at this same temperature. The enthalpy of phase transformation from anatase to rutile TiO_2

Table 5.4. Material and energy balance for the calcination reaction.

INPUT						OUTPUT					
Temp(K)	Compound	kg	kmol	H_L (MJ)	H_{tot} (MJ)	Temp(K)	Compound	kg	kmol	H_L (MJ)	H_{tot} (MJ)
323	TiO_2(Ana)	11903	149	211	-139636	1173	TiO_2(Rut)	11903	149	9181	-131563
323	H_2O(l)	3223	179	337	-50795						
						588	H_2O(g)	3223	179	1806	-41454
298	O_2(g)	99267	3102	0	0	588	O_2(g)	99267	3102	27552	27552
298	N_2(g)	326922	11670	0	0	588	N_2(g)	326922	11670	99813	99813

TOTAL		kg	kmol	H_L (MJ)	H_{tot} (MJ)
	Input	441315	15100	548	-190430
	Output	441315	15100	138351	-45653
BALANCE		0	0	137803	144778
	With 18% loss				176558
	Per ton TiO_2				**14837**

is accounted for in the balance. The volume of the TiO_2 decreases slightly as rutile is a denser phase, while the volume of water increases significantly in the vapor phase. The calcination flue gas, consisting primarily of nitrogen, oxygen, and water vapor, exits the reactor at 315 °C [2] and is captured for heat recovery. The energy required for the calcination process is 1.45 x 10^5 MJ. The heat loss due to radiation and conduction through the kiln walls is similar to that of the roasting kiln and is estimated to be 18%. Accounting for heat loss, the total energy required for calcination is 176.6 GJ. With a production rate of 11.9 tph TiO_2, this equates to 14.8 GJ/ton TiO_2, similar to the value of 15.0 GJ/ ton TiO_2 for calcination reported by Reck and Richards [11].

After cooling, the raw TiO_2 discharge is too coarse to be used as pigment and requires further milling to meet the size specifications of most pigment applications (0.2–0.3 μm). The TiO_2 is fed to a ball mill using ceramic media and liners to avoid contamination from iron. The energy for milling rutile (W_i = 14) [29] was calculated using Bond's law as before and will require a 9'D x 9'L ball mill driven by a 480 hp

motor. Following grinding, the pulp is dewatered via three drum filters with a total filter area of 250 m^2 each driven by 45 hp motors. The resulting filter cake is dried in a rotary drier sized according to the same procedure as the rotary kilns in the process and by using the angle of repose and bulk density of rutile. The drier will be 5'D x 40'L and driven by a 40 hp motor, and will consume 15.6 MBTU of natural gas per hour (16.5 GJ/hr). The dried product is stockpiled and fed to the final pulverization step.

The final size reduction is performed by jet milling, a technique fairly common in the pigment industry. To process 13.7 tph TiO_2, four 42-inch jet mills will be necessary to ensure that a sufficiently fine product is produced. Each of these mills requires 2900 SCFM of compressed air generated by a 900 hp compressor for each mill [30]. The milled pigment is ready for further optional inorganic or organic surface treatments to enhance durability, dispersion, gloss, or other properties [31]. These treatments can be performed in a 300 gallon stainlesss steel tank with an agitator driven by a 2 hp motor [23].

5.4.9 Heat Recovery

As mentioned previously, the energy consumption of the overall process can be reduced by utilizing waste heat from the higher temperature operations to provide heat for lower temperature operations. The amount of recoverable heat from the discharge products of the roasting kiln was calculated using HSC Chemistry 5.11 in a similar fashion as before. The inputs for the calculation are the hot solid discharge as well as flue gas at the conditions they leave the kiln. The outputs of the calculation are the same products at the conditions after heat recovery via the waste heat boiler as described previously. The temperature, mass, latent heat, and total enthalpy of roasting discharge

products before and after heat recovery are shown in Table 5.5.

Full recovery of the sensible and latent heat of the products above room temperature would require exorbitant time and cost, so the final temperature of the solid products after heat recovery will be 50 °C and the temperature of the air and condensate water after passage through the waste heat boiler will be 90 °C. Also, it is unreasonable to assume that the waste heat boiler will perfectly exchange heat without any losses; therefore, a typical value of 15% loss of total recoverable heat was chosen [32]. It is evident that the majority of the heat in the roast products is contained within the sodium titanate product as well as the excess NaOH, which has a relatively large latent heat of melting. The total amount of recoverable heat from the products of roasting is 31, 293 MJ per hour. The amount of recoverable heat from the hot calcination discharge and flue gas was also calculated using HSC Chemistry 5.11. The rutile and the flue gas leave the kiln at a temperature of 900 °C and 315 °C, respectively.

The heat and energy balance of the discharge products before and after heat recovery is shown in Table 5.5. In this instance, most of the sensible heat is contained in the flue gas with rutile accounting for less than 10% of the recoverable heat. Assuming again a 15% heat loss in the waste heat boiler, the total recoverable heat from the calcination discharge products is 99,310 MJ per hour. Between the two high temperature processes, it is estimated 130,300 MJ (10.9 GJ/ton) of heat per hour can be recovered.

5.4.10 Recycling and Regeneration of HCl and NaOH

For economic and environmental reasons, it is beneficial to recycle and regenerate the HCl and NaOH process reagents as much as possible. One method of regenerating acidic solution is inherent in the process and is accomplished through the hydrolysis

Table 5.5. Material and energy balance for the heat recovery of roasting and calcination products.

Roasting Heat Recovery

INPUT						**OUTPUT**					
Temp (K)	Compound	kg	kmol	H_L (MJ)	H_{tot} (MJ)	Temp (K)	Compound	kg	kmol	H_L (MJ)	H_{tot} (MJ)
823	Na_2TiO_3	21454	151	11772	-222858	323	Na_2TiO_3	21454	151	479	-234151
823	$\Sigma Na_xM_yO_z$	1520	11	911	-18357	323	$\Sigma Na_xM_yO_z$	1520	11	35	-19234
823	ΣM_xO_y	2746	31	1379	-21642	323	ΣM_xO_y	2746	31	52	-22969
823	NaOH(l)	10357	259	11717	-96295	323	NaOH(s)	10357	259	393	-109866
823	H_2O(g)	2913	162	3060	-36044	323	H_2O(l)	2913	162	671	-45549
823	O_2(g)	13	0	7	7	323	O_2(g)	13	0	1	1
823	N_2(g)	477	17	268	268	323	N_2(g)	477	17	32	32

TOTAL		kg	kmol	H_L (MJ)	H_{tot} (MJ)
	Input	39480	631	29115	-394920
	Output	39480	631	1662	-431736
BALANCE		0	0	-27453	-36815
	With 15% loss				**-31293**

Calcination Heat Recovery

INPUT						**OUTPUT**					
Temp(K)	Compound	kg	kmol	H_L (MJ)	H_{tot} (MJ)	Temp(K)	Compound	kg	kmol	H_L (MJ)	H_{tot} (MJ)
1173	TiO_2(Rut)	11903	149	9181	-131563	323	TiO_2(Rut)	11903	149	210	-140535
588	H_2O(g)	3223	179	1806	-41454	363	H_2O(l)	3223	179	878	-50254
588	O_2(g)	99267	3102	27552	27552	363	O_2(g)	99267	3102	5961	5961
588	N_2(g)	326922	11670	99813	99813	363	N_2(g)	326922	11670	22112	22112

TOTAL		kg	kmol	H_L (MJ)	H_{tot} (MJ)
	Input	441315	15100	138123	-45881
	Output	441315	15100	29160	-162716
BALANCE		0	0	-108963	-116835
	With 15% loss				**-99310**

reaction, as discussed previously. The titanium depleted acidic solution leaving the hydrolysis filter is directed back to the leaching stage, which is able to provide 52% of the necessary acid to maintain a 16.9 wt % HCl concentration in the leach solution. However, the leaching operation still requires 16.8 tph of fresh HCl, which will require 16.3 tph of Cl_2 and consume 45,500 kWhr of electrical energy.

The coproduct of the electrolysis reaction is 1,128 kg of NaOH/ton Cl_2 (often referred to as an electrochemical unit) produced at the anode of the cell in the form of 33% NaOH solution, which is concentrated to 50% with 180 kWhr of steam [17]. The given production rate of chlorine will generate 18.4 tph NaOH (solid equivalent). The concentration of solution from 33% to 50% will require 10,580 MJ/hr. The 50% NaOH solution can be concentrated to anhydrous NaOH by a series of multiple effect evaporators. The energy required to concentrate 50% NaOH to anhydrous NaOH has been reported to be 3.1 GJ/ton NaOH [33], which for 18.4 tph NaOH requires 57,080 MJ.

The roasting operation will require a total of 23.3 tph of anhydrous NaOH. Most of the NaOH will be generated by the chlor-alkali process as a coproduct of Cl_2, with the remainder of the NaOH generated through the evaporation of after wash solution (12% NaOH) using multiple effect evaporators. The energy required to concentrate 12% NaOH to 50% NaOH has been reported to be 1.95 GJ/ton NaOH [17]; therefore, each ton of NaOH recycled from the after wash solution consumes 5.05 GJ of energy; 4.9 tph of NaOH produced by this method will require 24.7 GJ of energy. In total, the production of 16.8 tph of fresh HCl will consume 500.5 GJ (42.1 GJ/ton TiO_2), and the production of 23.3 tph of NaOH will consume 92.4 GJ (7.76 GJ/ton TiO_2).

5.5 Energy and Emissions Comparison

5.5.1 Energy Total for New TiO_2 Process

The primary sources of energy in the production of TiO_2 include natural gas and electricity. Based on the foregoing process calculations, the total natural gas and electricity requirements of the operation can be tallied and are shown in Table 5.6. The heat recovered in the higher temperature processes is used as a credit and will reduce the need for natural gas in the hydrolysis and NaOH concentration stages. The amount of electrical power needed for pumping and material transport is accounted for by adding an additional 20% to the total power needs of each unit process and represents a neglible portion of the total power. It should also be noted that it was assumed that the electricity would be provided by a coal power plant with 1 kWhr requiring 10,500 BTU equivalent of coal (an efficiency of ~33%). This is consistent with the electrical energy calculations in the Battelle Labs report [10].

Table 5.6. Energy consumption of each step in the new pigment making process.

Energy (GJ/ton TiO_2)				
	Nat Gas	Elec	Total	% Total
Slag Making	9.5	30.1	39.6	33.2
Roasting	3.0	0.5	3.5	2.9
Leaching	0.0	0.5	0.5	0.4
Solvent Extraction	0.0	0.1	0.1	0.1
Hydrolysis	6.2	0.4	6.6	5.6
Calcination/Milling	15.4	3.6	19.0	16.0
NaOH/HCl Regen	7.8	42.1	49.8	41.8
Total	41.9	77.4	119.2	100.0
Heat Recovered	11.0	-	11.0	9.2
Grand Total	**30.9**	**77.4**	**108.2**	

The estimated energy required for processing titania slag process to pigment grade TiO_2 is 29.8 GJ/ton of TiO_2. This value includes the energy consumptions of roasting, leaching, solvent extraction, hydrolysis, calcinations, and milling. This value, however, only accounts for roughly one-quarter of the total energy required when considering slag preparation and reagent regeneration, which account for 41.8 and 33.2% of the total energy, respectively. As mentioned previously, although the chlor-alkali process is an energy intensive process, few alternatives exist for producing industrial amounts of HCl and NaOH reagents. The total energy consumption of the new process is calculated to be 108.2 GJ/ton of TiO_2.

5.5.2 Energy Comparison Between Different TiO_2 Processes

The cradle-to-gate energy consumption for the sulfate process and the chloride process using slag as a feed material are reported by the Battelle Labs report [10]. For purposes of a fair comparison with the new process, the sulfate process energy tally will also include 13.8 GJ/ton TiO_2 to account for the recycle and reconcentration of spent sulfuric acid in the digestion process, which is becoming more common as environmental regulations tighten [13]. Thus, the energy values of 123.2 and 145.3 GJ/ton of TiO_2 were used for comparison.

A comparison of the energy consumptions of the new pigment manufacturing process and the traditional processes is shown in Figure 5.2. The new process would consume 25% less energy than the chloride method and 12% less energy than the sulfate method on a per ton basis. Considering an annual production of 1.4 million metric tons of TiO_2 (entirely by the chloride process) in the US, the new process would potentially result in an annual energy savings of 51.8 million GJ. The annual world production capacity of

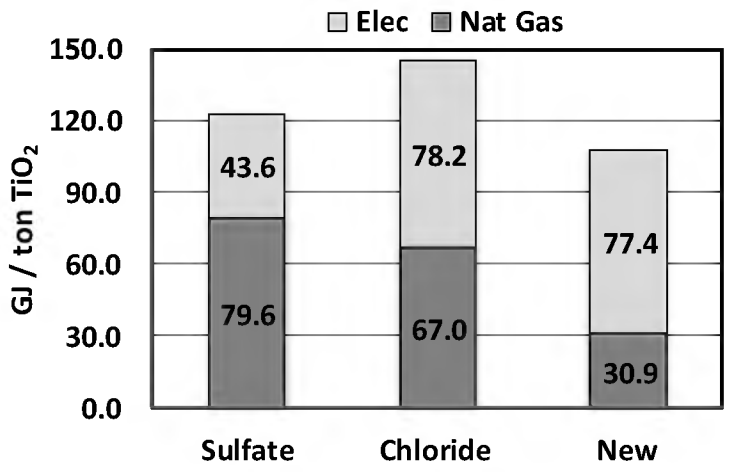

Figure 5.2. Energy consumption of the sulfate, chloride, and new methods of pigment manufacture, divided into contributions from electricity and natural gas.

TiO_2 is approximately 6.5 million tons per year [6] with 60% of that made by the chloride process and the other 40% by the sulfate process. The total energy consumption is thus approximately 320 million GJ per year for the sulfate process and 566 million GJ per year for the chloride process, totaling 886 million GJ per year. If the two processes were replaced by the new process, a total of 183 million GJ would be saved, assuming of course that slag was the only feedstock used.

5.5.3 CO_2 Emissions of New TiO_2 Process

CO_2 emission of any manufacturing processes consists of two parts: a) direct emission of CO_2 as a reaction product of the process and b) indirect emission of CO_2 from the consumed energy of the process because producing energy will emit CO_2. While both the sulfate process and the new process have no direct CO_2 emissions, the chloride process releases a significant amount of CO_2 in the first stage of the process, i.e., carbo-chlorination step, when TiO_2 in the titania slag is converted into $TiCl_4$. The reaction stoichiometry suggests that there will be 1 mol CO_2 released for every 1 mol TiO_2

produced by the chloride process, that is, approximately 550 kg of CO_2 per ton of TiO_2. Based on the electricity and natural gas requirements reported above, the CO_2 emissions from each step in the new process were calculated. The CO_2 emitted from the reduction of slag is included as part of the natural gas value for slag preparation. The emissions are reported as tons of CO_2 emitted per ton TiO_2 produced. The results of this analysis are shown in Table 5.7. The total CO_2 emissions value of the new process is 7.11 GJ/ton TiO_2, with nearly 40.1% of the emission resulting from reagent regeneration and 40.3% from slag preparation.

5.5.4 CO_2 Emission Comparison Between Different TiO_2 Processes

The CO_2 emissions associated with the sulfate process and the chloride process have also been calculated based on the energy consumptions reported in the previous section. The total CO_2 emissions (direct and indirect) of each process are shown in Figure 5.3. The total CO_2 emissions of the sulfate process and the chloride process are 7.26 and

Table 5.7. CO_2 emissions of each step in the new pigment making process.

Emissions (ton CO_2/ton TiO_2)

	Nat Gas	Elec	Total	%Total
Slag Prep	1.35	1.73	3.08	40.3
Roasting	0.14	0.03	0.17	2.3
Leaching	0.00	0.03	0.03	0.4
Solvent Extraction	0.00	0.00	0.00	0.1
Hydrolysis	0.29	0.03	0.32	4.2
Calcination/Milling	0.73	0.23	0.96	12.6
NaOH/HCl Regen	0.38	2.68	3.06	40.1
Total	2.89	4.74	7.63	100.0
Heat Recovered	0.52		0.52	6.8
Grand Total	**2.37**	**4.74**	**7.11**	

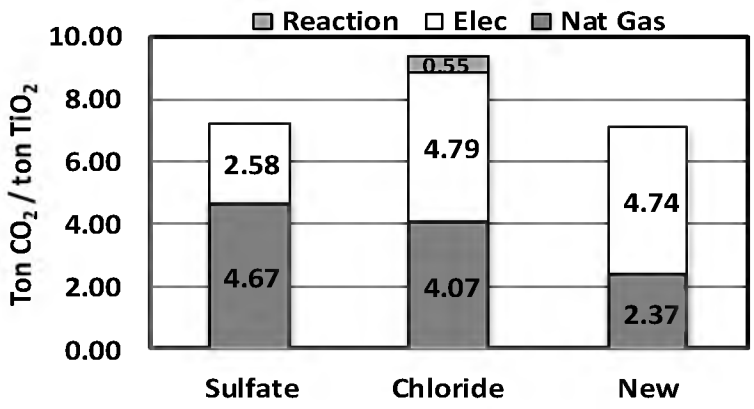

Figure 5.3. CO_2 emissions of the sulfate, chloride, and new methods of pigment manufacture, divided into contributions from electricity, natural gas, and direct emissions.

9.42 tons/ton TiO_2, respectively. Implementation of the new process would potentially result in a 2% decrease in comparison to the sulfate process and a 25% decrease in comparison to the chloride process. Based on the annual US production of 1.4 million metric tons of TiO_2, this means an annual reduction of 3.23 million tons of CO_2. Using the world production values from the previous section, the total carbon footprint is approximately 18.9 million tons per year for the sulfate process and 36.7 million tons per year for the chloride process, totaling 55.6 million tons per year. The new process would reduce CO_2 emissions by 9.4 million tons, assuming once again that slag was the only feedstock used. It should be noted that this comparison of the new process and the current methods is with only one set of reported data.

However, when a comparison is made with the values of the Tioxide LCA [11], the new process consumes more energy than the sulfate method using slag (103 GJ/ton) but slightly less than the chloride method (109 GJ/ton). The new process would thus be considered at least comparable with current methods when considering similar feed

stocks and system boundaries. 108.2 GJ/ton of TiO_2, The largest portion of the energy is consumed in recycling and regeneration process reagents with the second largest being the preparation of the slag feed. The calculated total CO_2 emission of the new process is 7.11 tons/ton TiO_2, which is 25% less than the chloride process and 2% less than the sulfate process, when slag is used as the feed material.

5.6 Conclusion

A wide range of values for the energy consumption and carbon emissions resulting from the production of TiO_2 pigment has been reported and depend on a number of factors, including the processing chemistry used, the system boundaries considered, the feed stocks chosen, and the treatment of effluents. The process flow sheet, material balance, and energy requirement calculations for each step of the new TiO_2 making process have been described in detail. A cradle-to-gate analysis of the energy consumption of the new process indicates that it would consume 108.2 GJ/ton of TiO_2, which is 12 and 25% less than the sulfate and chloride processes, respectively, considering the same feed stock and system boundaries. The largest portion of the energy is consumed in recycling and regenerating NaOH and HCl reagents with the second largest being the preparation of the slag feed. The total CO_2 emission of the new process is 7.11 tons/ton TiO_2, which is 2 and 25% less than the sulfate and chloride processes. Additional testing of the process on a larger scale would be necessary to further refine these conclusions.

5.7 References

[1] M. F. Ashby, *Materials and the Environment.* Oxford, UK: Butterworth-Heinemann-Elsevier, 2009, pp. 42–56.

[2] H.L. Brown, B.B. Hamel, and B.A. Hedman, "Sulfate Method Energy Balance" in *Energy Analysis of 108 Industrial Processes*. New York: Fairmont Press, 1985, pp. 119–121.

[3] U.S. Environmental Protection Agency. (Jan. 10, 2013) *Greenhouse Gas Equivalencies Calculator* [Online]. Available: http://www.epa.gov/cleanenergy/energy-resources/calculator.html.

[4] Federal Environmental Agency, "Large volume solid inorganic chemicals, titanium dioxide, final report," Berlin, DE: Institute for Environmental Technique and Management, 2001.

[5] N. Osterwalder, C. Capello, K. Hungerbühler, and W.J. Stark, "Energy consumption during nanoparticle production: how economic is dry synthesis?," *J. Nanopart. Res.*, vol. 8, no. 1, pp. 1–9, 2006.

[6] J. Gambogi, "USGS Mineral Commodities Summary Report," USGS, Washington, DC, 2012.

[7] K.K. Sahu, T.C. Alex, D. Mishra, and A. Agrawal, "An overview on the production of pigment grade titania from titania-rich slag," *Waste Mgmt. Res.*, vol. 24, no. 1, pp. 74–79, 2006.

[8] G.F. Balderson and C.A. MacDonald, "Method for the production of synthetic rutile," U.S. Patent No. 5 885 324, Mar. 23, 1999.

[9] M. Sittig, *Practical Techniques For Saving Energy in the Chemical, Petroleum and Metals Industries*, Park Ridge, NJ: Noyes Data Corp, 1977.

[10] R.W. Hale, "Energy use patterns in metallurgical and nonmetallic mineral processing-Phase 5 – Energy data and flowsheets, intermediate priority commodities," Columbus, OH, Battelle Laboratories, US Bureau of Mines Report, 1975.

[11] E. Reck and M. Richards, "Titanium dioxide – manufacture, environment and life cycle analysis: The tioxide experience," *Surface Coatings Int. Part B: Coatings Int.*, vol. 80, no. 12, pp. 568–572, 1997.

[12] T. Hakkinen, P. Ahola, L. Vanhatalo, and A. Merra, "Environmental impact of coated exterior wooden cladding," VTT, Finland: VTT Building Technology Report, 1999.

[13] European Commission, "Integrated Pollution Prevention and Control, Best Available Techniques for the Manufacture of Large Volume Inorganic Chemicals-Solids and Other Industries," Seville, Spain: Integrated Pollution Prevention and Control, 2007.

[14] A.S. Ferreira and M.B. Mansura, "Statistical analysis of the spray roasting operation

for the production of high quality Fe_2O_3 from steel pickling liquors," *Proc. Safety Enviro. Protect.*, vol. 89, no. 3, pp. 172–178, 2011.
[15] G. Demopolous, "New technologies for HCl regeneration in chloride hydrometallurgy," *World of Metall.*, vol. 61, no. 2, pp. 89–98, 2008.

[16] W. Karner and W. Hofkirchner, "Modern pickling and acid regeneration technology," *Metall. Plant Tech. Int.*, vol. 19, no. 2, pp. 92–100, 1996.

[17] European Commission, "Best available techniques in the chlor-alkali manufacturing industry," Seville, Spain: Integrated Pollution Prevention and Control, 2001.

[18] A. Martin and J. Mozzo, "Waste Heat Recovery" in *Encylopedia of Energy Engineering and Technology*, B.L. Capehart, ed. Boca Raton, FL: CRC Press, 2007, pp. 1536–1540.

[19] C.J. Simonson, "Heat and Energy Wheels," in *Encylopedia of Energy Engineering and Technology*, B.L. Capehart, ed. Boca Raton, FL: CRC Press, 2007, pp. 794–800.

[20] B.A. Wills and T. Napier-Munn, *Will's Mineral Processing Technology Handbook*, 7th ed, Oxford, U.K.: Butterworth-Heinemann, 2006, p. 111.

[21] N.L.Weiss, *SME Mineral Processing Handbook*. New York: Kingsport Press, 1985, pp. 1053.

[22] W.R. Penney and J.R. Fair, *Chemical Process Equipment: Selection and Design*. Oxford, UK: Butterworth-Heinemann; 2012.

[23] *Mine and Mill Equipment Costs Estimators Guide: Capital and Operating Costs*, 2012 Ed., Infomine, Vancouver, BC, 2012.

[24] X.Y. Liu and E.Specht, "Mean residence time and hold-up of solids in rotary kilns," *Chem. Eng. Sci.*, vol. 61, no. 15, pp. 5176–5181, 2006.

[25] G. Palmer and T. Howes, "Heat transfer in rotary kilns," in *IEEE/PCA Cement Ind. Tech. Conf*, Rapid City, SD, 1998, pp. 1-6.

[26] W.D. Baasel, *Preliminary Chemical Engineering Plant Design. 2nd ed.* New York City: Van Nostrand Reinhold; 1990.

[27] Quinn Process Equipment, "Quinn mixer-settler SX units for pilot plant and commercial solvent extraction applications," Denver, CO: Quinn Process Equipment, 2012.

[28] Solvay Chemicals International, "Specific Heat of Hydrochloric Acid," Brussels, Belgium: Solvay Chemicals International, 2005.
[29] M.C. Fuerstenau and K.N. Han, *Principles of Mineral Processing*, Denver, CO:

SME, 2003, p. 573.

[30] Jet Pulverizer Company. "Micron-Master™ Performance Guidelines," Moorestown, NJ: Jet Pulverizer Company, 2011.

[31] J. Barksdale, *Titanium: Its Occurrence, Chemistry, and Technology*. New York: Ronald Press Co, 1966, pp. 555.

[32] H. Kimura, "Material and energy flow simulation and economic analysis for a novel suspension ironmaking technology," M.S. Thesis, Met. Eng., University of Utah, Salt Lake City, UT: 2010.

[33] E. Worrell, D. Phylipsen, D. Einstein, and N. Martin, "Energy use and energy intensity of the U.S. chemical industry," Berkeley, CA, Lawrence Berkeley National Laboratory Report, 2000.

CHAPTER 6

NEW PROCESS FOR MAKING TITANIUM POWDER

6.1 Properties, Applications, and Cost

Titanium is one of the most sought after engineering materials in the world due to its numerous attractive features, including high strength, light weight, and excellent corrosion resistance. The range of strength for titanium and its alloys is between 205 MPa to 1585 MPa. It has a density that is 60% of stainless steel and nearly half of copper and aluminum [1]. Ti readily forms a passivating oxide layer that makes it an excellent material for resisting corrosion in both acidic and caustic environments. It also exhibits good ductility, low thermal and electrical conductivity, excellent fracture resistance, and biocompatibility (nontoxic). This unique combination of properties makes it a material well suited for numerous potential commercial applications.

Titanium has been commercially manufactured since 1948 and has historically been limited to applications requiring high performance or that were relatively insensitive to cost, such as in the SR-71 Blackbird reconnaissance aircraft, which had over 90% of its structure made from Ti alloys [2]. Even today, it is primarily used in the aerospace, medical, and military defense industries. The main hindrance to the wider use of titanium in many applications is the cost. A comparison of the cost versus specific strength (yield strength/density) of materials that have at least 600 MPa yield strength is shown in Figure 6.1 [3]. It is readily apparent that Ti alloys have the highest specific strength among

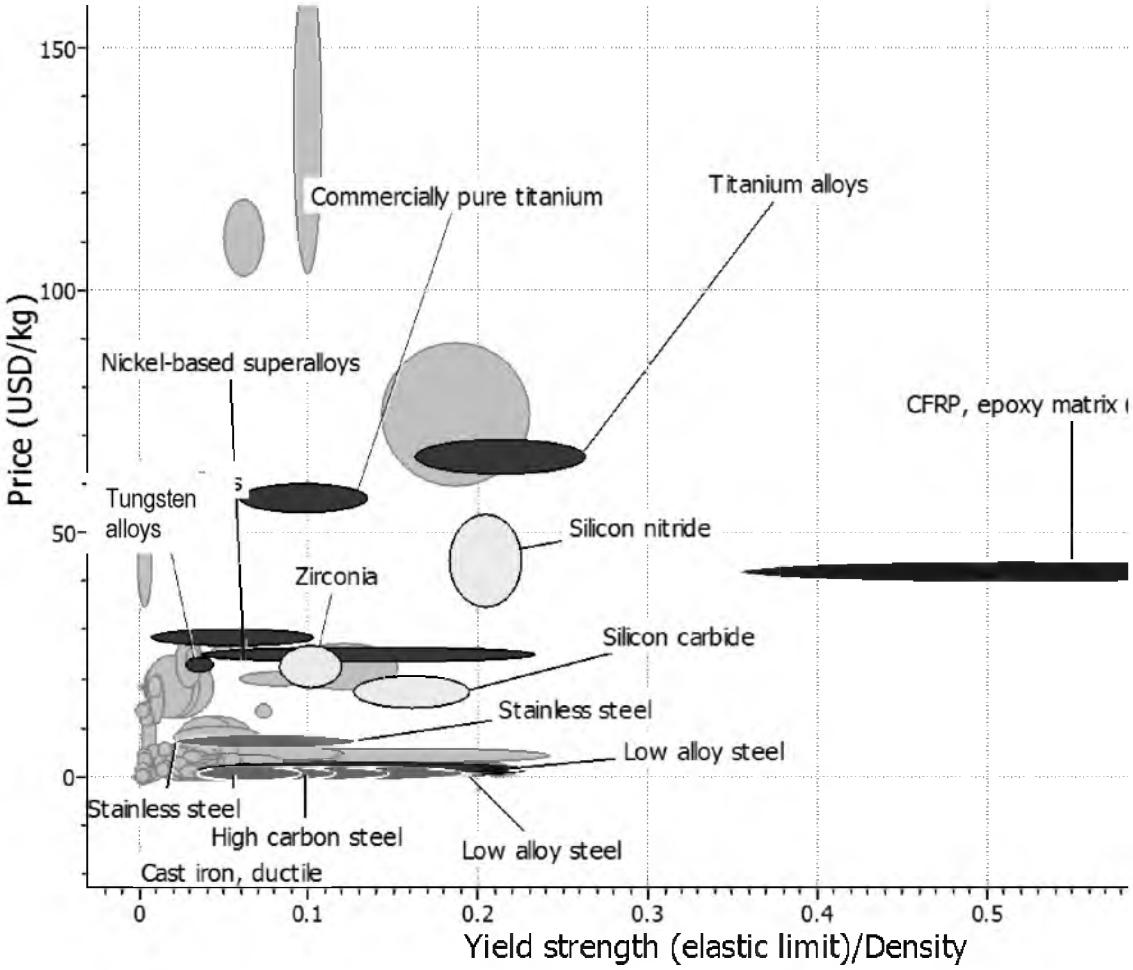

Figure 6.1. Price and specific strength comparison (Yield strength/density) of materials that have at least 600 MPa yield strength. Generated using EduPak 2010 Software.

metals and ceramics, but also have the highest cost. Although titanium is the fourth most abundant metal in the earth's crust, it is very difficult to extract, process, and fabricate into mill products. The relative cost of extraction, refining, ingot, and sheet forming of steel, aluminum, and titanium are shown in Table 6.1 [1]. It is apparent that the extraction and refining of Ti requires 3 times the cost of aluminum and 15 times the cost of steel and on an equivalent weight basis. Additionally, the forging of titanium ingot costs 6 times more than aluminum and 30 times more than steel on a per pound basis.

Table 6.1. The relative cost of extraction, refining, ingot, and sheet forming of steel, aluminum, and titanium (adapted from [1]).

Production step	**Steel**	**Aluminum**		**Titanium**		
	$/lb ($/in^3)	$/lb ($/in^3)	Factor to Steel	$/lb ($/in^3)	Factor to Steel	Factor to Al
Ore extraction	0.02	0.1	5	0.3	15	3
Metal refining	0.1 (0.028)	0.68 (0.066)	6.8 (2.3)	2 (0.33)	20 (11.8)	2.9 (5.1)
Ingot forming	0.015 (0.043)	0.7 (0.068)	4.7 (1.6)	4.5 (0.73)	30 (17)	6.4 (10.6)
Sheet forming	.30–0.60 (.085–0.17)	1–5 (0.098–0.49)	3.3–8.3 (1.2–2.9)	15–50 (2.44–8.14)	50–83 (29–48)	10–15 (17–25)

6.2 Traditional Ti Manufacturing Processes

A contributing factor to the high cost of Ti is the manufacturing of raw Ti sponge. Ti sponge is the raw material for making mill products, which are then used to fabricate final products. Figure 6.2 illustrates the major steps of producing Ti sponge from ilmenite ore by the established and developing processes. Ilmenite is reduced to a titanium rich slag (TiO_2–slag), which is then upgraded to synthetic rutile via thermochemical and leaching treatments as described previously. Synthetic rutile is carbo-chlorinated under high temperature (1000 °C) to form titanium tetrachloride ($TiCl_4$). Two well established commercial processes use $TiCl_4$ as a feed material: the Kroll and Hunter.

In the Kroll process [4, 5], $TiCl_4$ is fed into a sealed reaction vessel where it is combined with molten Mg and reduced to metallic Ti. The solid reaction product is termed a "sponge," a highly porous mixture of Ti and $MgCl_2$. The Ti sponge must be chiseled out of the reactor and the $MgCl_2$ must be removed using another distillation

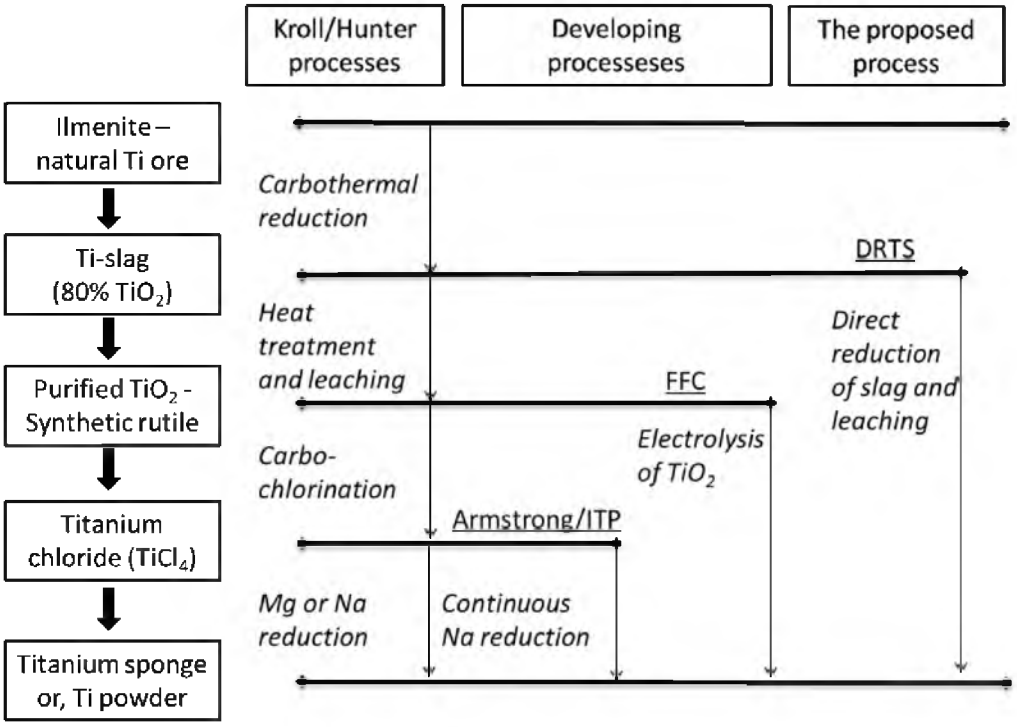

Figure 6.2. Schematic comparison of conventional, developing, and proposed processes for production of Ti sponge or powder.

method, typically with an Ar carrier gas or vacuum or leached in with water and dilute HCl acid. The recovered $MgCl_2$ is then electrolyzed to form Mg and Cl_2, which can be recovered and fed back into the reaction cycle. The sponge is crushed and sized to prepare it for use as feedstock for powder production or for melting in the production process for ingot metallurgy and wrought Ti products. The Hunter process [6], as originally developed by metallurgist and professor Matthew Hunter, involves reducing $TiCl_4$ with elemental sodium in a sealed steel pot under high temperature (900 ^{o}C) and pressure to form titanium sponge and molten sodium chloride. After the sealed pot cools, the excess salt is washed away with hydrochloric acid solution, and the powder is dried. While the Hunter process results in high purity titanium metal, it is inefficient, time consuming, and costly, and therefore not commonly used.

6.3 Alternative Ti Manufacturing Processes

Alternatives to the traditional thermochemical processing of Ti have long been sought after. Even after the commercialization of the Kroll process in the 1950's, Dr. Kroll himself predicted that "titanium will be made competitively by fusion electrolysis within the next 5 to 10 years" [5]. His prediction has yet to be realized, and the Hunter and Kroll processes are still the only commercially viable methods today. In more recent history, particularly the past 20 years, research has continued in attempts to identify more economical methods of producing titanium and can be categorized into two main approaches: electrochemical and thermochemical reduction.

6.3.1 Electrolysis of TiO_2

Several methods of titanium production seek to electrochemically reduce TiO_2 to titanium powder or sponge. The most promising electrochemical extraction method is known as the FFC Cambridge process [7]. The FFC process involves the electrochemical reduction of solid TiO_2 cathodes to titanium sponge inside a molten calcium chloride electrolyte. Although TiO_2 is an electrical insulator, the slight removal of oxygen from TiO_2 via electrolysis results in conductive Magnelli phases, allowing the electrolysis to go to completion. The potential benefits of the FFC process include replacement of $TiCl_4$ as a feed material, the potential for continuous production, and ability to make alloys by mixing oxides of various metals. Despite these promising features, the FFC process has encountered numerous difficulties, including costly feed preparation, redox cycling from multivalent Ti, low current efficiency, entrapment of chloride electrolyte in Ti crystals, and handling of extremely reactive dendritic products.

The Ono Suzuki [8] process involves the reduction of TiO_2 in a $Ca/CaO/CaCl_2$

molten bath contained within a carbon anode bowl. TiO_2 powder is contained within a Ti basket submerged in the bath. At the cathode, Ca^{2+} is reduced to Ca and the TiO_2 converts to a Ti "lump," with O_2 and CO/CO_2 generated at the carbon anode. Ti powder with 2000 ppm oxygen was achieved after 3 hours and decreased to 420 ppm after 24 hours. The separation of the Ti product from the baskets, heavy evaporative loss of Ca, and high levels of Cl in the product remain as unresolved challenges for these processes. The EMR/MSE [9] process also involves the reduction of TiO_2 in a Ti cathodic basket submerged in a $Ca/CaO/CaCl_2$ molten bath. During the reduction, the conductive holder and a calcium alloy slab form an electrochemical couple; no external current is provided during this reaction. After the reduction, the calcium slab is cathodically regenerated, driven by oxidation of the consumable carbon anode. A relatively pure Ti powder compact product has been reported, although the process is still in early stages of development.

Another electrolytic process being developed by the MER Corporation [10] involves blending purified TiO_2 with carbonaceous material, pressing into an electrode, and subsequent heat treating to make an oxycarbide (TixOy–C) anode. Ti^{3+} ions migrate from the anode into the molten chloride electrolyte and subsequently reduce at the cathode as a powder, flake, or solid. While the reported impurities of the Ti powder produced by this method are low (500 ppm O), consistency in the composition and morphology of the powders as well as any economic benefits are yet to be demonstrated.

6.3.2 Electrolysis of slag

Efforts have also been made to electrolytically produce Ti from Ti bearing slag. Quebec Iron and Titanium has patented a process to convert Ti slag to Ti liquid metal that

may be cast into various conventional mill product shapes (ingot, billet, etc.) [11]. A molten cathode is formed by pouring molten slag into a bath containing molten CaF_2 electrolyte and a consumable carbon anode. Despite initial promising results, further research was halted due to technical difficulties. Mohanty electrolytically reduced an iron rich Ti in molten $CaCl_2$ to produce a ferrotitanium alloy [12]. Martinez et al. [13] recently reported an electrolytic process for reducing titania slag to Ti powder via an sintered TiO_xC_y consumable anode in a molten chloride electrolyte. The anode formation requires multiple steps, including ball milling with carbon for 24 hours, carbothermal reduction at 1600 ºC, three washing stages, drying, powder compaction, and finally sintering for 5 hours. The dissolution of the TiO_xC_y anode releases Ti^{3+} ions, which deposit as extremely reactive Ti particle fines on the cathode via a complicated two-step disproportionation reaction. While the use of slag avoids the necessity of using a purified TiO_2 or $TiCl_4$ precursor, the complex process of anode formation, the low current efficiency, and the difficulty in handling a very small reactive product appear to make this technology far from commercial viability.

6.3.3 Electrolysis of $TiCl_4$

The Ginatta process [14–16] involves the electrolytic reduction of $TiCl_4$ by injecting it into a molten halide electrolyte, which forms a layered interphase containing various oxidation states of Ti. Molten Ti falls to the bottom layer and is tapped or solidified with the help of a water cooled Cu hearth. A pilot plant producing 250 mm ingot is under operation, although the process complexity and use of $TiCl_4$ limits its cost reduction over the current metallothermic processes.

Despite considerable promise, electrolytic techniques still face several key

technical and economic challenges including but not limited to: an incomplete fundamental understanding of molten salts in electrochemistry, insufficient experimentation with nondiaphragm cells, low current efficiencies, redox cycling, and extremely fine and/or reactive products. Very few of these processes have demonstrated product quality or economic superiority over current production methods beyond mere projections. Nevertheless, the FFC Cambridge process has been recently commercialized and is licensed through Metalysis in South Yorkshire, UK. They claim to have adapted the process for the production of over 60 different types of metal powders, including transition metals, actinides, and lanthanides [17]. It remains to be seen how competitive this production technology will be with the Kroll method of Ti manufacture.

6.3.4 Metallothermic Reduction of $TiCl_4$

The Armstrong/ITP process [18] is a semicontinuous improvement of the Hunter process. It involves the injection of $TiCl_4$ vapor through a nozzle into a stream of liquid Na within a cylindrical chamber, with reduced Ti powder being carried in the excess Na stream. Ti powder, unreacted Na, and NaCl are separated through distillation, filtration, and washing. A 1,000 TPA pilot plant is in operation and has produced Grade 1 Ti powder. Despite the promised benefits, a number of challenges remain, including controlling particle size and morphology as well as the costly and energy intensive handling of molten sodium.

The Idaho Research Foundation has patented a process for the mechanochemical reduction of liquid $TiCl_4$ with Mg or CaH_2 powder via high energy milling in a SPEX mill [19]. The energy for the solid state chemical reaction is provided by the mechanical impingement by milling media as well as the highly exothermic decomposition of $TiCl_4$.

The reduction of $TiCl_4$ with Mg required 50 hours of milling time, although this was reduced to 6 hours when the Mg was premilled with NaCl and 15 minutes when CaH_2 was used. The process also requires a leaching stage to remove the reducing agent. The use of $TiCl_4$ and extensive high energy milling indicate that the process would have difficulty improving upon the economics of the Kroll process.

6.3.5 Metallothermic Reduction of TiO_2

The Okabe Preform Reduction Process [20] involves combining TiO_2 with CaO or $CaCl_2$ into a preform that is suspended just above a bath of molten Ca metal. The vapor reacts with the preform to produce a porous Ti and CaO powder compact. The compact is leached and washed to remove the CaO. The powder size and morphology is affected by the temperature, choice of flux, and flux/TiO_2 ratio. Zhang et al. reported a self-propagating high temperature synthesis (SHS) method of producing Ti powder from Mg and purified TiO_2 [21]. The reactants were mixed in a 3.0:1 ratio, compressed at different pressures into a green compact, and ignited with a tungsten filament inside a vacuum furnace. The calculated adiabatic temperature was between 2060 and 2140 K, although DTA measured a solid-state reduction reaction occurring at 767 K. Won reported a similar Ti powder making process involving the ignition of various mixtures of TiO_2 and Mg by a nichrome wire in an inert atmosphere [22]. The reaction reached temperatures of 1200 to 1750 ºC, depending on Mg/TiO_2 ratio, gas pressure, and sample diameter. Titanium powders with 2–8% oxygen content were produced. No plans for scale-up have been reported for either combustion process.

None of the aforementioned methods of titanium production appear to sufficiently improve the ease of processing or affordability of titanium metal. Figure 6.3 illustrates

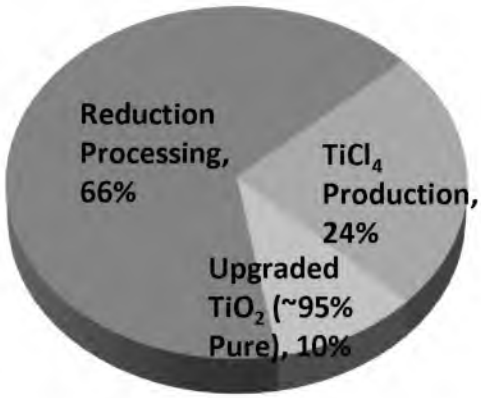

Figure 6.3. A comparison of the relative cost for each step of making Ti sponge.

the relative costs associated with conventional production of titanium [23]. Magnesium reduction processing (e.g., Kroll process) represents approximately 66% of total production costs. Chlorination to form $TiCl_4$ represents about 25% of the total production costs, with the remaining 10% attributable to production of synthetic rutile. While the impetus of research by reduction of TiO_2 has largely been to avoid high-temperature chlorination, most processes still require extensive processing to obtain synthetic rutile as feed. There remains a need for a simplified, more energy efficient, and lower cost method for the production of titanium metal powders.

6.4 Metal Hydride Reduction

One promising method for producing lower cost titanium powders is known as metal hydride reduction (MHR). A patent using the MHR reaction to created titanium hydride powders was filed in 1945 by Peter Alexander [24]. The described process involves mixing pigment grade titanium oxide with excess alkaline earth metal hydride (most favorably CaH_2) and heating it in an argon shielded reduction zone to a temperature sufficient to decompose the hydride and reduce the titanium oxide to metallic

titanium. The temperature is then lowered and hydrogen gas is flowed into the reaction zone to convert the elemental Ti to TiH_2 powder, which is subsequently leached with a solvent to remove CaO formed in the reduction reaction. No information is available as to why this process was not further developed commercially.

A similar process was developed commercially nearly 50 years ago by Borok and Teplenko in 1965 in the former Soviet Union [25]. The process involves reacting CaH_2 with purified rutile at 1100 °C to form Ti and CaO powders according to (6.1).

$$TiO_2 + 2\ CaH_2 = Ti + 2\ CaO + 2\ H_2 \qquad (6.1)$$

The CaO is leached away, leaving behind Ti powder. Alloyed powders have also been produced by using a mixture of oxides in the feed. The Polema Tulachermet plant in Tula, Russia is currently producing low chloride Ti powders via the MHR process [26]. This process has several advantages over traditional Ti production methods, including the elimination of the carbo-chlorination step. The powder product could be used to make near-net–shape (NNS) parts directly, which eliminates most of the postsponge processing cost of titanium parts. A major concern with this process is whether or not a sufficient amount of cost-affordable rutile could be obtained and thus maintain the savings from the elimination of $TiCl_4$. Therefore, the use of a low-cost TiO_2 feedstock is imperative to make such a process cost effective.

This reaction was also investigated and reported by Froes [27]. The goal was to reduce the temperature necessary to complete the reaction through mechanical activation and subsequent low temperature heat treatment. Purified TiO_2 and CaH_2 were milled in a SPEX mill from 1–72 hours at room temperature. The first set of experiments showed very limited conversion, so $TiCl_4$ was added with the hope that the enthalpy of reaction

between $TiCl_4$ and CaH_2 would enhance the conversion of the oxide, although this also resulted in limited conversion. After 4 hours of SPEX milling and heat treatment to 450 ºC, Ti and TiH_2 peaks began to appear, and at 600 ºC, the hydride peaks began to diminish as the Ti peaks increased in intensity, indicative of hydride decomposition. The author indicated the need to develop an effective leaching treatment for the powder to completely remove the CaO while not dissolving the hydrided powder, which is relatively more passive to oxidation than elemental Ti.

To date, it does not appear that any investigators have attempted to directly reduce slag to Ti or TiH_2 powders using MHR techniques.

6.5 A New Ti Powder Making Process

6.5.1 Description of the New Process

A new process was proposed to produce titanium hydride or Ti by direct reduction of Ti slag (DRTS) using metal hydrides such as MgH_2 followed by separation of the reaction product from MgO and remaining impurities. A schematic illustration of the new process is shown in Figure 6.4. Ti-slag usually contains ~80% TiO_2. The remainder is comprised of metal oxide impurities such as FeO, MgO, CaO, Al_2O_3, and SiO_2 [28]. The primary reactions during the direct reduction of Ti-slag are shown in (6.2)–(6.5).

$$TiO_2 + 2MgH_2 = TiH_2 + 2MgO + H_2 \quad (6.2)$$

$$Ti_3O_5 + 5MgH_2 = 3TiH_2 + 5MgO + 2H_2 \quad (6.3)$$

$$FeTi_2O_5 + 5MgH_2 = 2TiH_2 + 5MgO + 3H_2 + Fe \quad (6.4)$$

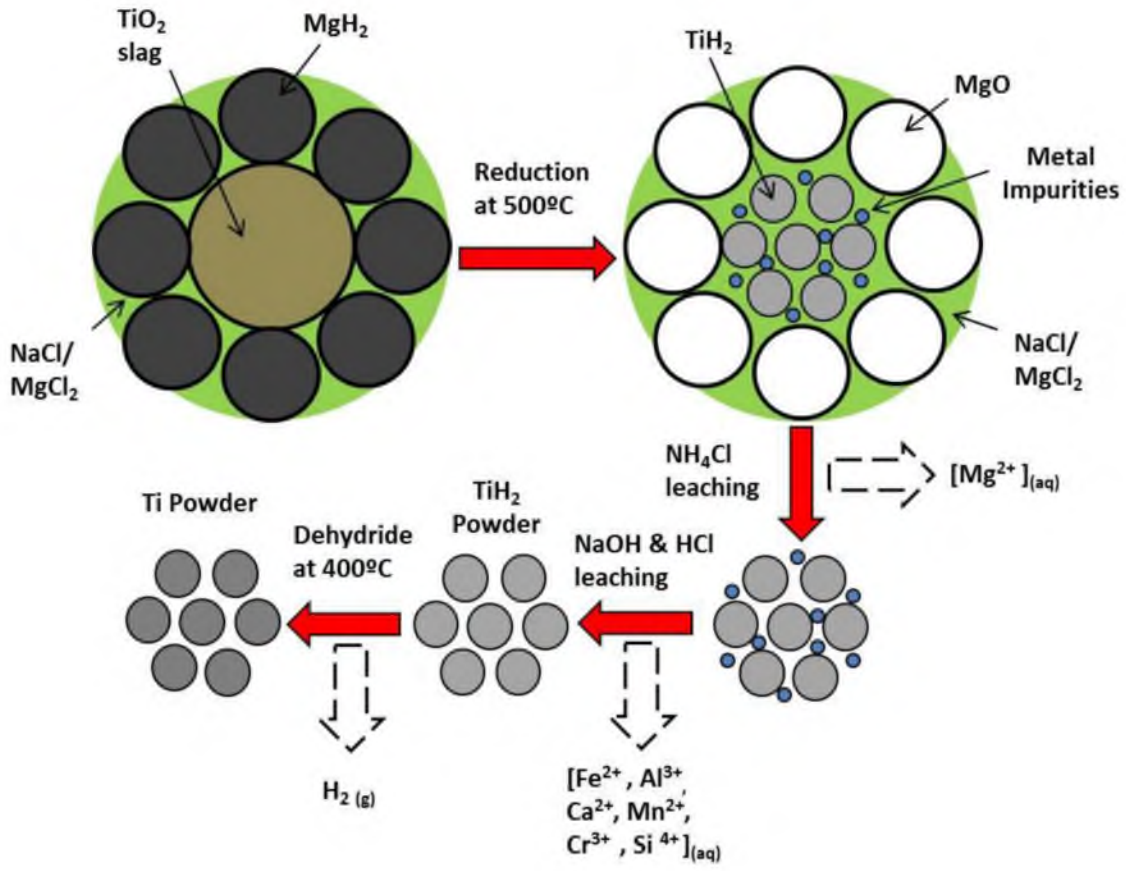

Figure 6.4. Schematic illustration of the three-step process for extracting Ti from upgraded Ti mineral (Ti slag) that consist of 1) the direction reduction of Ti slag using MgH_2, 2) the leaching processes to purify TiH_2, and 3) the dehydrogenation of TiH_2 to form Ti.

$$MgTi_2O_5 + 4MgH_2 = 2TiH_2 + 5MgO + 2H_2 \quad (6.5)$$

The reaction products of the above reactions will be TiH_2 mixed with MgO and other impurities. After the reduction reaction, the atmosphere can be changed to an inert argon atmosphere while still at high temperature, which allows for the dehydriding of titanium hydride to form titanium powder. Because TiH_2 is less prone to form alloys with other elements than Ti, TiH_2 is the preferred product of the reactions. In low partial pressures of hydrogen, TiH_2 decomposes into Ti and H_2 gas above 400 °C.

6.5.2 Process Flow Sheet

A flow sheet for the new process is shown in Figure 6.5. First, slag is milled to the proper size and blended with MgH_2 and salts and then charged into the reduction furnace. The reduced powder is then sequentially leached to remove different impurities. To remove MgO, ammonium chloride (NH_4Cl) solutions can be used [29], which reacts according to (6.6).

$$MgO_{(s)} + 2NH_4^{+}{}_{(aq)} \rightarrow Mg^{2+}{}_{(aq)} + 2NH_{3(aq)} + H_2O \quad (6.6)$$

It has been found that adding a chelating agent, such as sodium dihydrogen citrate ($NaC_6H_7O_7$), to the NH_4Cl solution can also significantly improve the solubility of MgO [30]. Second, leaching with NaOH solution can potentially remove any remaining silicates from the reduced powder that would otherwise be insoluble in mineral acids other than HF and will also remove Al_2O_3 and any other remaining acidic oxides. Finally, any remaining metal or metal oxide compounds such as Fe can be dissolved using a relatively dilute mineral acid [29], such as HCl, as shown in (6.7).

$$FeO_{(s)} + 2HCl_{(aq)} = FeCl_{2(aq)} + H_2O \quad (6.7)$$

Further, residual MgO in the mixture can also be dissolved by the dilute HCl solution. The purified TiH_2 is then filtered, dried, and dehydrogenated in an inert atmosphere by heating it above 400 °C, resulting in Ti powder.

6.5.3 Regeneration of Mg and HCl

As explained above, MgO will be leached using ammonium chloride (NH_4Cl) solutions. The products of the $NH_4Cl/NaC_6H_7O_7$ leaching of the powder are $MgCl_2$, NH_3,

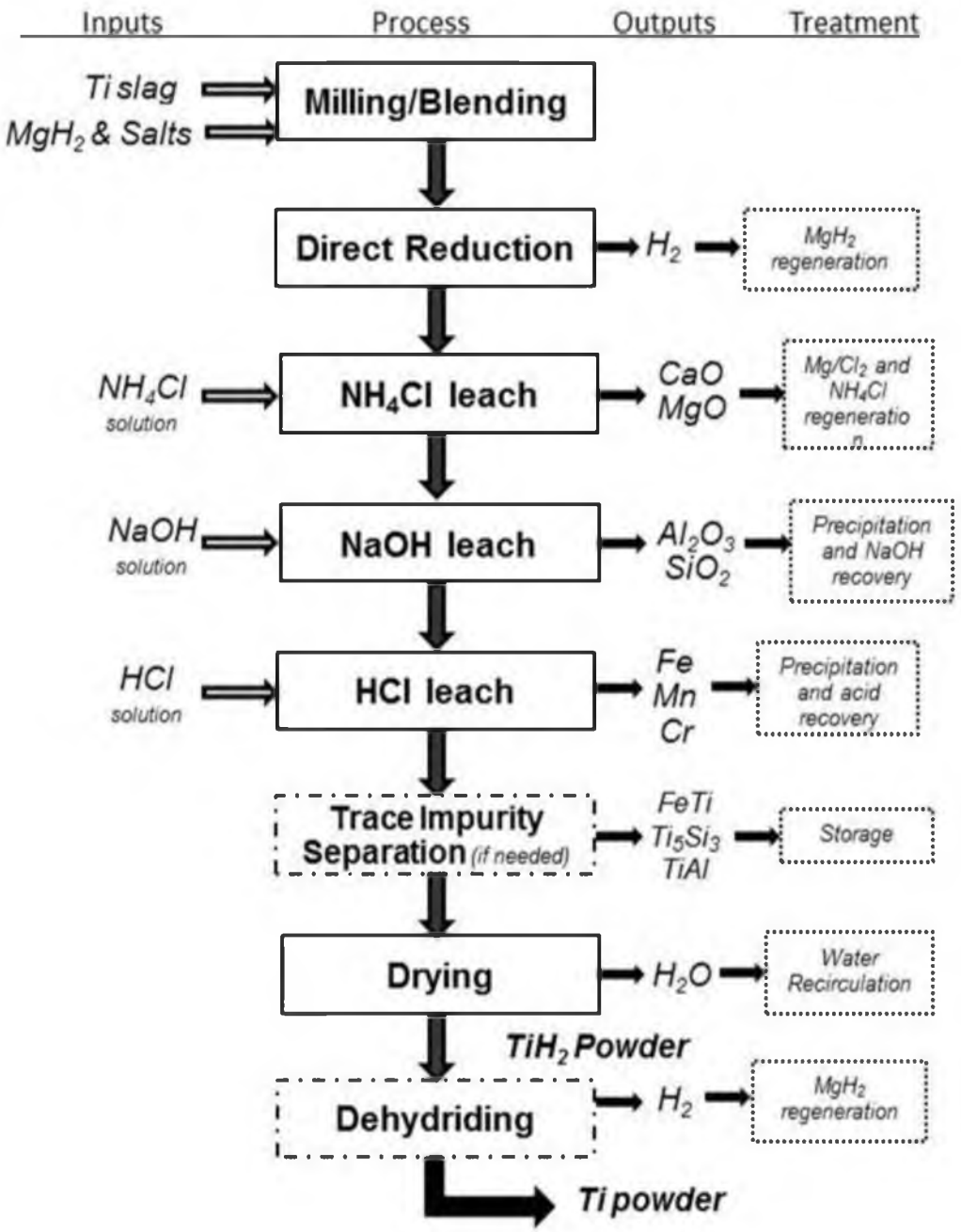

Figure 6.5. Flow sheet of the new Ti making process.

and H_2O. Fortunately, the solubility of sodium citrate rapidly decreases with decreasing temperature, so it can be precipitated by lowering the temperature of the solution and then recovered by filtration. The NH_3 is a gas, which can be collected, condensed and mixed with the HCl stream to generate more NH_4Cl. This would leave mainly $MgCl_2$, which can be converted by conventional electrolysis to form Mg and Cl_2. The chlorine could be used to generate more HCl. The chlorine will be combined with hydrogen gas in a burner to produce HCl according to (6.8). The resulting hydrochloric acid will be reused in the leaching process as needed.

$$H_{2(g)} + Cl_{2(g)} \rightarrow 2HCl_{(g)} \tag{6.8}$$

6.6 Potential Benefits of the New Process

Figure 6.2 illustrates the main steps of the new process as compared to the traditional and developing processes. The direct reduction of slag facilitates the elimination of three stages that substantially contribute to the high cost and inefficiency of current Ti production, namely synthetic rutile production, chlorination, and reduction of $TiCl_4$. Even if the proposed method cost more than that for producing TiO_2, the overall potential for cost reduction is still quite substantial. Furthermore, the proposed process is based on low temperature and ambient pressure processes that eliminate the need for high temperature carbo-chlorination, molten Mg reduction, and vacuum distillation processes. The potential for reducing energy consumption as compared to that for producing Ti sponge is also considerable. Also, as discussed in the TiO_2 production section, the carbo-chlorination process directly emits CO_2 as a byproduct. The proposed process would reduce the CO_2 footprint of Ti powder production by eliminating the use of $TiCl_4$ as a

feedstock. A cradle-to-gate analysis of the energy and emissions of the new process will be made and compared to the Kroll process.

6.7 References

[1] F.H. Froes, "Lowering the cost of titanium," *AMPTIAC Q.*, vol. 6, no. 2, p. 3, 2002.

[2] P.W. Merlin, "Design and development of the Blackbird:
challenges and lessons learned," in *7th AIAA Aerospace Sciences Meeting*, Orlando, FL, January 5–8, 2009, p. 16.

[3] Granta Design, *CES 2010 Edupak*, M. Ashby, Ed. Cambridge, UK: 2010.

[4] W. Kroll, "Method of manufacturing titanium and alloys thereof," US Patent No. 2 205 854A, June 25, 1940.

[5] W. Kroll, "The production of ductile titanium," *Trans. Met. Soc. AIME*, vol. 1215, pp. 546–553, 1959.

[6] J. Barksdale, *Titanium: Its Occurrence, Chemistry, and Technology.* New York: Ronald Press Co., 1966, pp. 54.

[7] G. Chen, D. Fray, and T. Farthing, "Direction electrochemical reduction of titanium dioxide to titanium in molten calcium chloride," *Nature*, vol. 407, pp. 361–364, 2000.

[8] K. Ono and R.O. Suzuki, "A new concept for producing Ti sponge by calciothermic reduction," *JOM*, vol. 54, no. 2, pp. 59–61, 2002.

[9] T. Abiko, I. Park, and T.H. Okabe, "Reduction of titanium oxide in molten salt medium," in *10th World Conf. Titanium,* F.H. Froes, Ed., Hamburg, Germany, 2003.

[10] J.C. Withers and R.O. Loutfy, "A novel electrolytic process to produce titanium," in *19th Annu. Titanium Conf. Int. Titanium Assoc.,* Monterey, CA, 2003.

[11] F. Cardarelli, "A method for electrowinning of titanium metal or alloy from titanium oxide containing compound in the liquid state," US Patent No. 7 504 017 B2, June 5, 2003.

[12] J. Mohanty, "Electrolytic reduction of titania slag in molten calcium chloride bath," *JOM*, vol. 64, no 5, pp. 582–584, 2012.

[13] A.M. Martinez, K.S. Osen, E. Skybakmoen, O.S. Kjos, G.M. Haarberg, and K. Dring, "New method for low-cost titanium production," *Key Eng. Mater.*, vol. 436, pp. 41–54, 2010.

[14] M.V. Ginatta, G. Orsello, and R. Berruti, "Method and cell for the electrolytic production of a polyvalent metal," US Patent No. 5 015 342, May 14, 1991.

[15] M.V. Ginatta and G. Orsello, "Plant for the electrolytic production of reactive metals in molten salt baths," US Patent No. 4 670 121, Jun 2, 1987.

[16] M.V. Ginatta, "Titanium electrowinning," *10th World Conf. Titanium,* F.H. Froes, Ed., Hamburg, Germany, 2003.

[17] Metalysis Ltd. (Jan. 10, 2013) *Metalysis Products* [Online]. Available: http:// http://www.metalysis.com/pure-metals.

[18] D.R. Armstrong, S.S. Borys, and R.P. Anderson, "Method of making metals and other elements," US Patent No. 6 409 797, June 25, 2002.

[19] F.H. Froes, B.G. Eranezhuth, and K. Prisbey, "Mechanochemical processing for metals and metal alloys," US Patent No. 6231636, May 15, 2001.

[20] T.H. Okabe, T. Oda, and Y. Mitsuda, "Titanium powder production by preform reduction process (PRP)," *J. Alloys Compd.*, vol. 364, no. 1–2, pp. 156–63, 2004.

[21] P. Zhang, T. Xia, G. Zhang, and L. Yan, "Study on preparation of Ti powder by self-propagating high-temperature synthesis with magnesiothermit reductive process," *Mater. Sci. Forum*, vol. 575–578, no. 2, pp. 1086–1092, 2008.

[22] C.W. Won, H.H. Nersisyan, and H.I. Won, "Titanium powder prepared by a rapid exothermic reaction," *Chem. Eng. J.*, vol. 157, pp. 270–275, 2010.

[23] A.D. Hartman, S.J. Gerdemann, and J.S. Hansen, "Producing lower-cost titanium for automotive applications," *JOM*, vol. 50, no. 9, pp. 16–19, 1998.

[24] P.P. Alexander, "Production of titanium hydride," US Patent No. 2 427 338, Sept. 16, 1947.

[25] B.A. Borok and V.G. Teplenko, "Obtaining powders of alloys and steels by a complex reduction of oxide mixtures by CaH_2," *Trans. Cent. Res. Inst. Ferrous Metall.*, vol. 43, pp. 69–80, 1965.

[26] V.S. Moxson, O.N. Senkov, and F.H. Froes, "Innovations in titanium powder processing," *JOM*, vol. 52, no. 5, pp. 24–26, 2000.

[27] F.H. Froes, "The production of low-cost titanium powders," *JOM*, vol. 50, no. 9, pp. 41–43, 1998.

[28] M. Gueguin and F. Cardarelli, "Chemistry and mineralogy of titania-rich slags–Part 1–Hemo-ilmenite, sulphate, and upgraded titania slags. *Min. Proc. Extract. Metall. Rev.*,

vol. 28, no. 1, pp. 1–58, 2007.

[29] D.R. Lide, *CRC Handbook of Chemistry and Physics,* 67th ed. Abingdon, UK: CRC Press; 1987.

[30] J. Fink, *Petroleum Engineer's Guide to Oil Field Chemicals and Fluids,* 1st ed. Oxford, UK: Gulf Professional Publishing, 2012.

CHAPTER 7

DIRECT REDUCTION OF TITANIUM SLAG

7.1 Introduction

7.1.1 Thermodynamic Analysis

The proper conditions for the reduction of Ti slag were initially determined through conducting a thermodynamic analysis using the commercial thermodynamics software HSC Chemistry 5.11. The reactants for the calculation are 100 g of Ti slag broken down into individual oxide components and 125% the stoichiometric amount of MgH_2 needed to reduce these oxides to metal or metal hydride compounds. The $H_2(g)$ shown in the plot includes the hydrogen gas injected into the tube furnace to create a flowing hydrogen atmosphere of 1 bar pressure within the tube furnace. The equilibrium amounts (in log(mole)) of all possible product compounds were calculated for temperatures between 100 and 700 °C. The results are shown in Figure 7.1. Clearly, the main reaction products are TiH_2 (slightly less than 1 mole) and MgO. Considering that the maximum level for each impurity element in Commercially Pure Ti is 0.1 wt% [1], any element or compound with an equilibrium amount larger than 10^{-4} (i.e., log(mole) > -4) has been plotted and is considered as a significant impurity species; based on the figure, there are 25 solid elements and compounds mixed with TiH_2. It appears that the equilibrium amount of TiH_2 decreases as the amount of Ti intermetallics increases with an increase in temperature; therefore, a suitable intermediate reaction temperature of

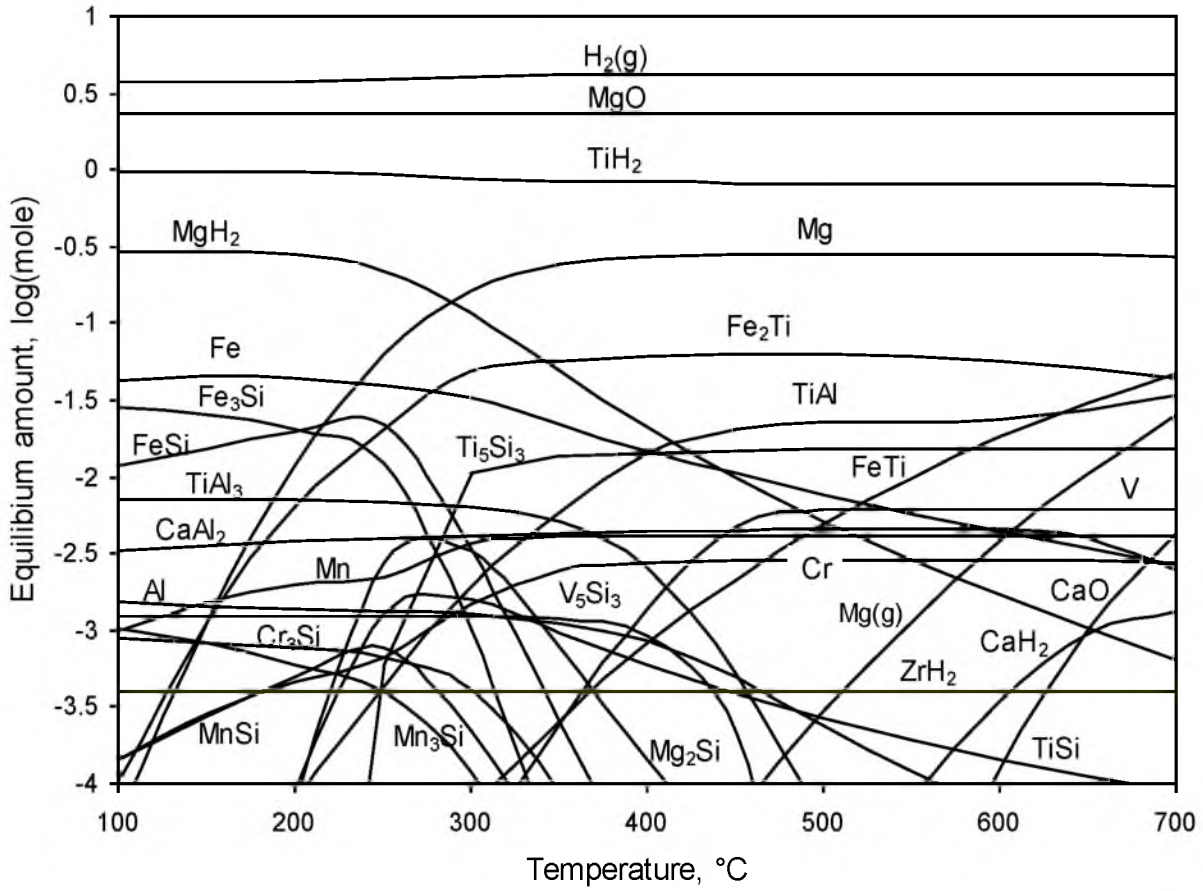

Figure 7.1. Equilibrium amounts of reaction products of 100 g of Ti slag reacted with 125% stoichiometric amount MgH_2 in 1 bar H_2 atmosphere at different temperatures. Data calculated using HSC Chemistry 5.11.

650 °C was chosen for initial experiments. Note that the relative differences between the equilibrium pressure of hydrogen with MgH_2 and TiH_2 and the vapor pressure of Mg at the reaction temperature all play a role in determining the feasibility of the reduction reaction.

It is indicated that MgO and CaO are the only oxides in the reaction products if the reduction process is complete. In reality, it is possible that there will be some residual oxides such as Al_2O_3, SiO_2, TiO_2, and FeO in the product due to incomplete reduction. Although the fractions of these secondary phase particles are very small, they will need to

be removed through leaching.

7.2 Experimental Methods

7.2.1 Materials and Equipment

Sorelslag® provided by Rio Tinto Iron and Titanium was also used in this investigation. Hydrogen storage grade MgH_2 and CaH_2 were purchased from Alfa Aesar, and the magnesium powder and chloride salts were also analytical grade. The unmilled slag used was -400 mesh unless otherwise stated. Unmilled slag/reductant mixtures were ground by hand with a porcelain mortar and pestle, while other mixtures were milled in a stainless steel cylinder in either a SPEX mill or a high-energy planetary ball mill (HEM). The milling media was a 50/50 by weight mixture of 1/8" and 1/4" 304 stainless steel balls. Powder compacts were formed by pressing with a Leco Press in a stainless steel die. The reduction took place in an MTI GSL-1300-40X model tube furnace with a 1.25"D x 30"L mullite tube. Initially, 10 mL MgO crucibles were used for the reduction experiments, but would frequently crack during the reaction, even at slow heating and cooling rates. It was determined that the pressure of the hydrogen being released during the dehydrogenation of MgH_2 as well as the high vapor pressure of Mg were responsible for the cracking. Inconel crucibles lined with molybdenum foil proved to be suitably strong and unreactive for the reduction reaction. A few larger runs were performed in a 250 mL MgO crucible lined with Mo foil and heated inside an MTI tube furnace with a 4" diameter mullite tube.

Dissolved metal concentrations were determined using an ICP Agilent 7500ce quadrupole mass-spectrometer. X-ray diffraction was performed with a Philips 1140 diffractometer (Cu Kα), and the patterns were analyzed using X'Pert High Score Plus

software. SEM microscopy was performed with a Leo 440 Scanning Electron Microscope or a Topcon SM100 model.

7.2.2 Procedure for Reduction Experiments

The reducing agent and slag mixtures were prepared in an inert glove box environment to prevent oxidation. A 125% stoichiometric amount of reductant was used to ensure complete reaction. Slag and/or reductant mixtures were milled for 2–8 hours at a ball to powder ratio of 50:1 by weight. Heptane was added to the milling jars to minimize oxidation. After milling, the powder was vacuum dried for at least 24 hours and further dried in an inert atmosphere at 200 ºC for 4 hours to remove residual heptane. If only slag was milled, it was dried in air overnight in a drying furnace.

The prepared reaction mixture was then placed inside a crucible and covered with a molybdenum cap. The loaded crucible was weighed and placed inside a tube furnace and flushed with ultra-high purity Ar for at least 30 minutes and ultra-high purity H_2 gas for 30 minutes prior to the start of the heating program. Regular purity gases were used initially but were not sufficient to prevent oxidation inside the furnace. While still under a constant H_2 gas flow at 1 bar pressure, the furnace was heated to the desired temperature at a rate of 20 ºC per minute and held for 4–48 hours. The crucible was kept in the hydrogen atmosphere as it cooled. The crucible was removed from the furnace and weighed, and the powder was analyzed.

7.2.3 Composition Analysis

In order to properly assess the effectiveness of different reduction treatments, the composition of the reduction product need to be quantitatively determined. Dissolution of the powder in acids and solution analysis can be used to accurately measure the

composition. To determine the amount of TiH_2 in the reduced samples, an appropriate HCl acid concentration was needed that would dissolve all of the converted TiH_2 in the sample but not any Ti compounds remaining in any unreacted slag. This was determined experimentally by comparing the acid solubility of Ti in slag samples heated with and without reducing agent, all other conditions being equal. As-received slag was milled for 2 hours in the planetary mill and heated to 500 °C for 48 hours in a H_2 atmosphere with 25% excess reducing agent, as described before. To simulate unreacted slag in the reduction mixture, this procedure was repeated but without a reducing agent. 0.5 g samples of slag heated both with and without reducing agent were leached for 30 minutes at 85 °C in 50 mL of various concentrations of HCl acid solution. The solutions were filtered, diluted, and analyzed using ICP-OES. The concentrations of Ti and Fe for each sample were plotted versus acid concentration and are shown in Figure 7.2.

The concentration of Ti and Fe appears to be unchanged for each HCl

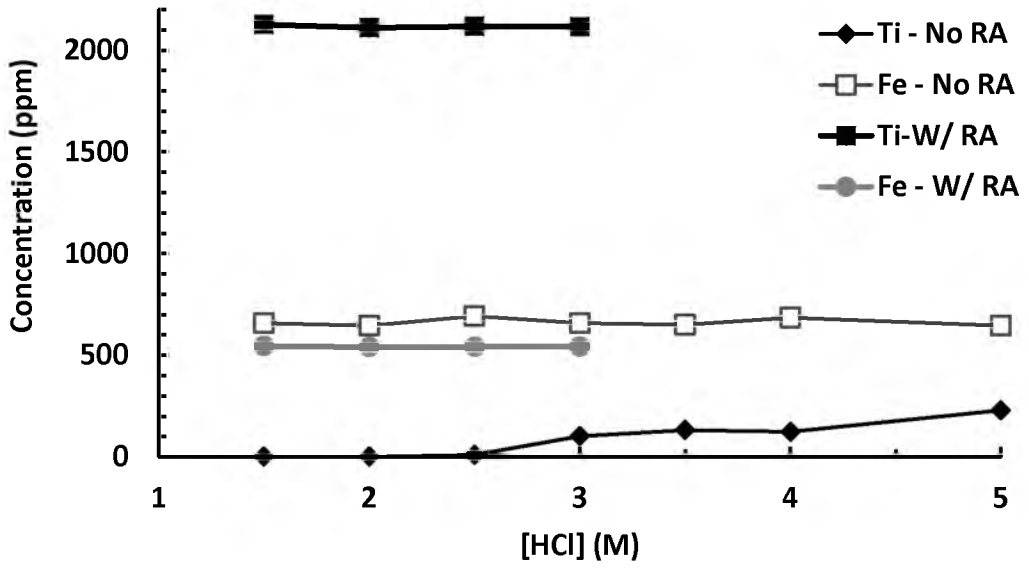

Figure 7.2. Concentrations of Ti and Fe after leaching slag heated with and without reducing agent (RA) (48 hours at 500 °C, H_2 atmosphere) in various concentrations of HCl acid. Leach time: 30 minutes; leach temperature: 85 °C.

concentration tested for the samples with reducing agent, whereas the Ti in the slag without reducing agent did not begin to leach out until 2.5 M HCl. XRD analysis of the reduced samples indicated that TiH_2 and slag were the only Ti containing compounds; therefore, at an acid concentration of 2.5 M HCl or less, any Ti measured in the leach solution is from TiH_2 only and not from unreacted slag.

The measured Ti concentration in the dissolved reduced slag product can be divided by the total Ti content in the slag (as determined in the original assay from RTIT) to obtain the degree of conversion X_{Ti}, which is the percentage of Ti in the slag converted to TiH_2, as shown in (7.1).

$$X_{Ti} = 100 \times \frac{C_{Ti} \times V}{m_{rps} \times F_{Ti} \times \frac{m_s}{m_{tot}}} \tag{7.1}$$

C_{Ti} is the measured concentration adjusted for dilution (g/L), V is the volume of acid solution (L), and m_{rps}, m_s, and m_{tot} are the mass of the reduction product sample being dissolved, original mass of slag put into the crucible, and total mass of slag and reducing agent, respectively. F_{Ti} is the fraction of Ti per gram of slag as determined in the original slag assay. The factor of 100 is to convert the value to a percent.

Alternatively, the elemental composition of the reduced powder was determined by total digestion using concentrated HNO_3/HF acid solution and ICP-MS analysis. This method was used to determine the degree of Ti conversion where noted in results and discussion.

7.3 Initial Reduction Experiments

7.3.1 Effect of Reducing Agent on TiH_2 Formation

Based on the literature search discussed previously, three reducing agents were selected for initial experiments for the reduction of slag: Mg, MgH_2, and CaH_2. The X-ray diffraction patterns of unmilled slag reduced with each reductant for 48 hours, as well as MgH_2 with TiO_2 as a reference, is shown in Figure 7.3. It appears that each of the reductants led to the formation of TiH_2 peak; however, the use of CaH_2 resulted in only very weak TiH_2 peaks, even after 48 hours of reaction time; therefore, only MgH_2 and Mg were considered for subsequent experiments. Although thermodynamically both CaH_2 and MgH_2 should work, CaH_2 has a much lower vapor pressure at the temperatures of interest. Also, the equilibrium decomposition temperature of CaH_2 at 1 atm is 1018 ºC (as calculated by HSC), suggesting that the equilibration of CaH_2 at this temperature is between the liquid and gas phases. These factors likely contribute to the lower reduction capability of CaH_2 at the studied temperature.

7.3.2 Effect of Time and Temperature on TiH_2 Formation

The reduction of slag with MgH_2 or Mg was further studied by conducting the reaction for 4, 15, 24, and 48 hours. The effect of time was qualitatively observed by X-ray diffraction analysis of each sample, and the patterns are shown in Figure 7.4. Generally, the intensity of TiH_2 and MgO peaks increased relative to the intensity of the slags peaks with longer reduction times, indicating a greater extent of reaction. Not much change is observed in the intensity of the TiH_2 peaks after 24 hours, indicating that further time did not increase the extent of reaction. Although TiH_2 and MgO have the most intense peaks, a considerable amount of slag remains unreacted. For the next

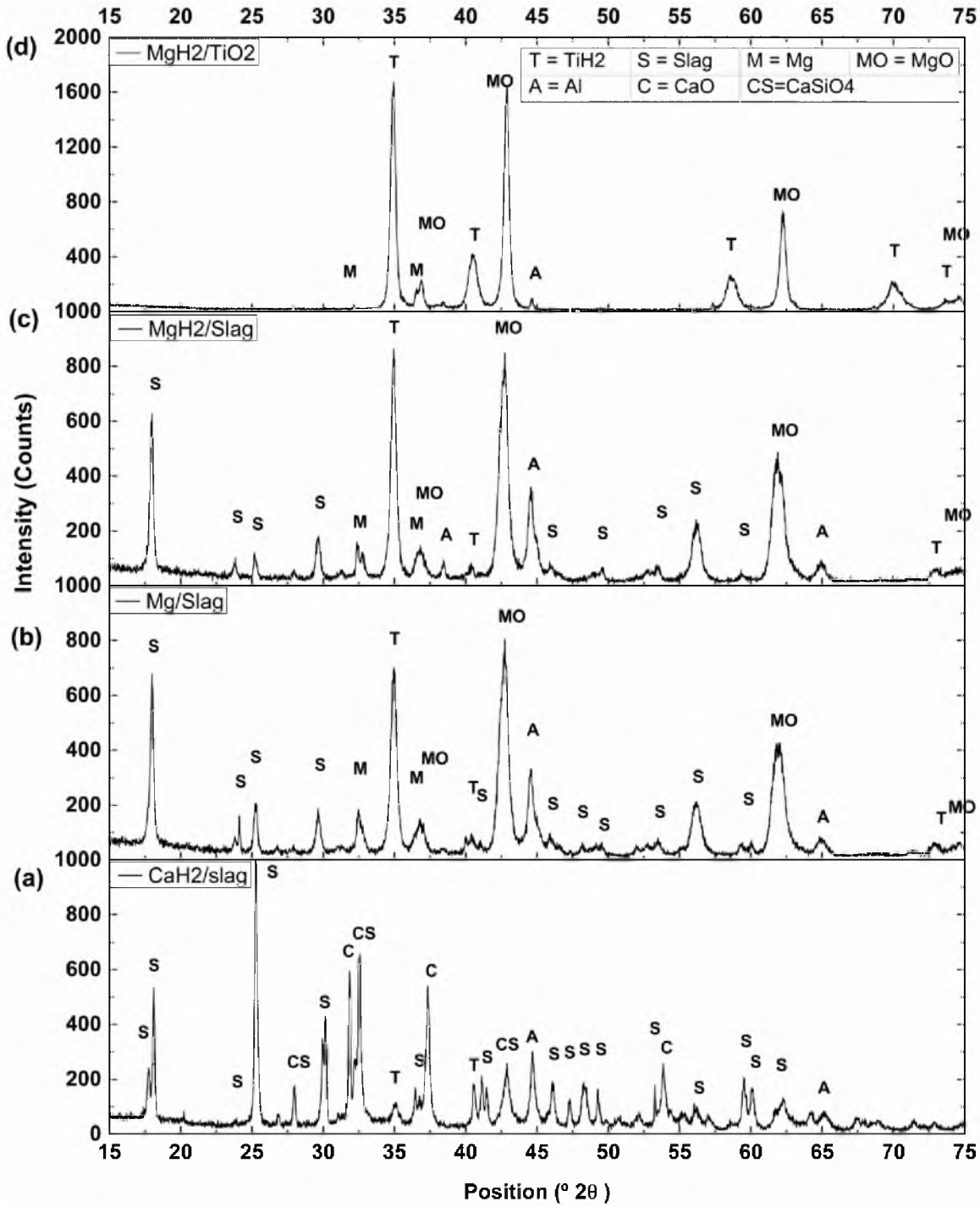

Figure 7.3. X-ray diffraction pattern of a) slag reduced with CaH_2, b) slag reduced with Mg, c) slag reduced with MgH_2, and d) TiO_2 reduced with MgH_2. The reaction time for each sample was 48 hours at 650 ºC.

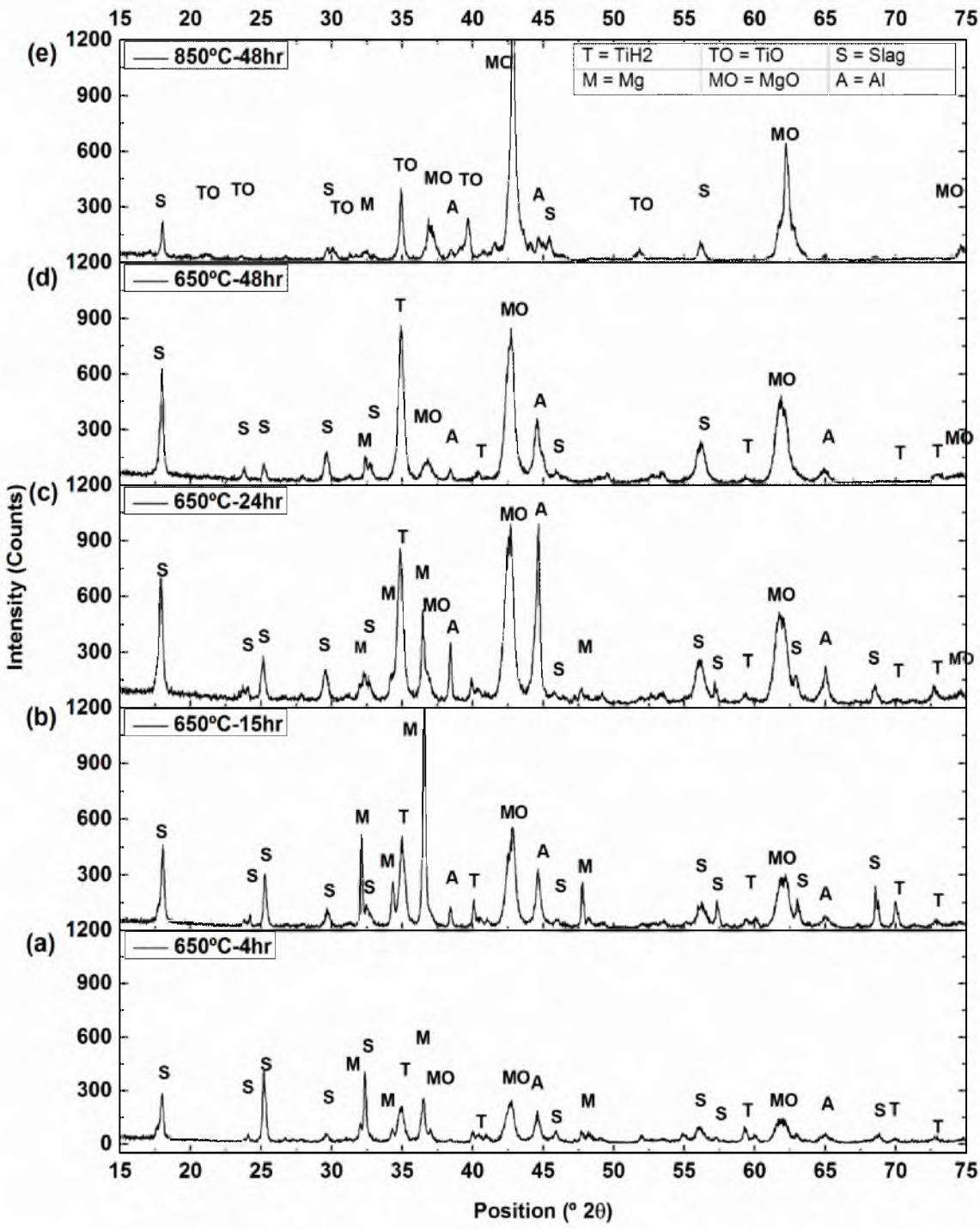

Figure 7.4. X-ray diffraction patterns of unmilled TiO_2 slag reduced with MgH_2 for a) 4 hours at 650 °C, b) 15 hours at 650 °C, c) 24 hours at 650 °C, d) 48 hours at 650 °C, and e) 48 hours at 850 °C.

experiment, the reduction temperature was increased to 850 ºC, and the diffraction pattern of the reduced sample is also shown in Figure 7.4. An increase in temperature led to significant evaporation of Mg and did not increase the formation of TiH_2, and instead led to the formation of Ti monoxide.

7.3.3 Effect of Particle Size on TiH_2 Formation

It was hypothesized that ball milling the slag and reductant prior to heat treatment would increase the kinetics and overall conversion of slag to TiH_2. Due to the difficulty of milling Mg, only MgH_2, which is considerably more brittle, was milled with slag. Slag and MgH_2 were mixed in the same proportion as before but were SPEX milled for 4 and 8 hours and heated for 48 hours at 650 ºC. The XRD graphs of these samples are shown in Figure 7.5. It is apparent that SPEX milling prior to the heat treatment led to a significant decrease in the intensities of the slag phase, indicating a greater degree of slag conversion to TiH_2. The decrease in intensity and broadening of TiH_2 peaks is likely due to the significant reduction in particle size resulting from the high energy milling and is characteristic of nanosized powders. SEM images of the reduced powder confirm that the product size is considerably less than 1 micron. Increasing milling time past 4 hours appeared to have a minimal effect on the extent of the reaction. The extremely fine product size makes the separation of TiH_2 from others impurities difficult and warranted further investigation to resolve.

A series of experiments was performed to investigate the effect of using various sizes of MgH_2 reductant on different sizes of Ti slag. It hypothesized that finer MgH_2 would allow for better contact with the slag particles and would allow for higher conversion at coarser particle sizes and would lead to a coarser product. The different

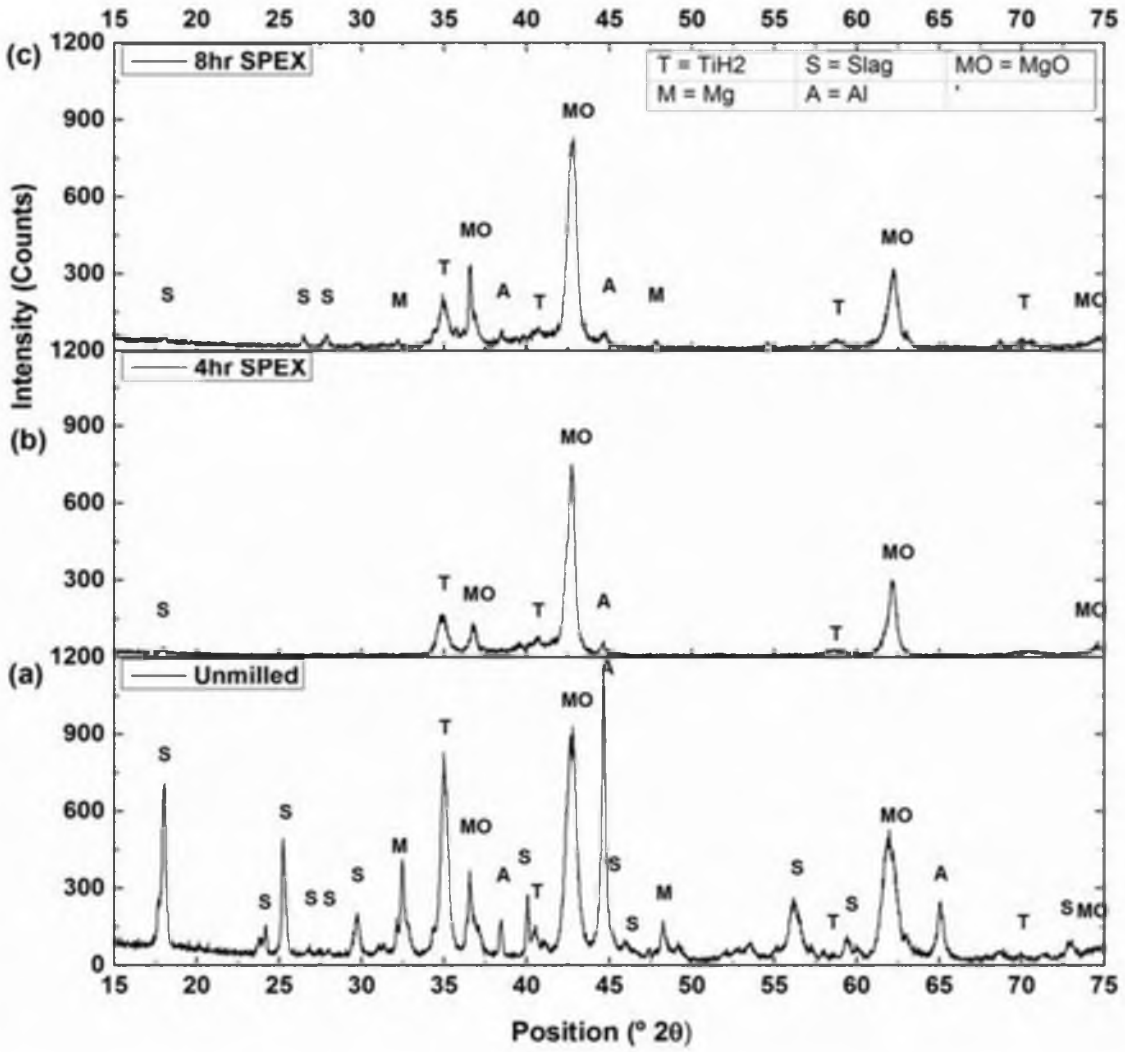

Figure 7.5. X-ray diffraction patterns of TiO_2 slag reduced with MgH_2 for 48 hours after a) no milling, b) 4 hours SPEX milling, and c) 8 hours SPEX milling.

size fractions of MgH_2 used were as-received/unmilled (about 100 μm), 2 hour SPEX milled (~200–500 nm), and 2 hour planetary ball milled (< 200 nm). The slag was sized with screens of different mesh and had size classes of 32–45 μm, 45–62 μm, 62–75 μm, 75–90 μm, and 90–105 μm. Each size class of slag was mixed each size class of MgH_2 reductant (15 samples in all). The samples were heat treated at 650 °C for 48 hours and dissolved according to the procedure previously described.

The percent conversion versus slag particle size is shown in Figure 7.6. The unmilled MgH_2 resulted in more conversion than milled MgH_2, indicating that the reduction reaction is either relatively insensitive to the size of the MgH_2 and/or that milling decreased the extent of conversion by the introduction of more impurities. A comparison of the XRD patterns of 62–75 μm slag reduced with unmilled, SPEX milled, and planetary milled MgH_2 showed no significant difference in structure or proportion of phases in the reduced product.

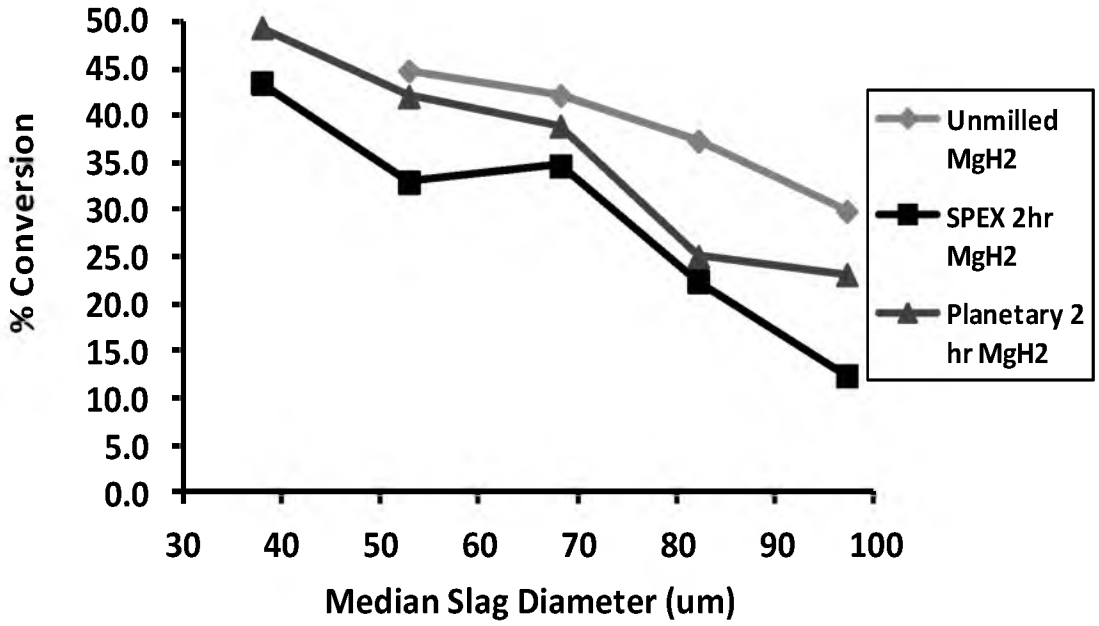

Figure 7.6. Percent conversion vs. median slag diameter for the reduction of slag with unmilled, 2 hour SPEX milled, and 2 hour planetary milled MgH_2.

It is readily apparent that the degree of conversion is highly sensitive to the slag particle size and a marked decrease in conversion is observed with an increase in slag particle size. Based on SEM analysis of the reduced powder samples, it appears that the size of the TiH_2 product particles is similar in both coarser and finer slag particle fractions and is generally less than 200 nm in diameter. It appears that once the magnesium has reacted with the slag, the resulting product becomes very brittle and easily breaks into very fine particles. Using EDAX, the magnesium, titanium, and iron rich phases in the product appeared well interspersed, and no phase segregation was observed.

7.4 Effect of Chloride Salts

The relatively low conversion rates and very fine product sizes indicated a need for a different experimental approach in order to increase the reaction kinetics and particle size. Bredthauer et al. [2] were able to successfully reduce tungsten and molybdenum oxide powders with hydrogen in the presence of alkali salts. The use of low melting alkali salts facilitated crystal growth by promoting material transport through liquid phase diffusion as opposed to only solid and gas phase diffusion and resulted in an average particle size >50 μm. Alkali salts have also catalyzed the reduction of nickel oxide and magnetite concentrates [3, 4]. It was hypothesized that mixing the MgH_2 and slag with a eutectic mixture of highly conductive alkali salts could also potentially facilitate faster mass transport and result in a coarser product size. After the reduction, the salts can easily be removed during the leaching treatments.

7.4.1 Choice of Salt Mixtures

By examining the phase diagrams of various binary and ternary chloride systems [5], three salt systems were chosen: KCl–$MgCl_2$ (60/40 mol%), NaCl–$MgCl_2$ (62/38 mol%), and NaCl–$CaCl_2$ (50/50 mol%). These mixtures have a eutectic melting temperature of 435, 450, and 500 °C, respectively, with each being well below 650 °C. Using HSC Chemistry 5.11, it was determined that none of these salt mixtures form compounds with Ti at this temperature.

Unmilled slag and MgH_2 were mixed in the same proportion as previous experiments; however, 20% by weight of eutectic salt mixture was added. The samples were heated to 650 °C for 48 hours, also in a flowing H_2 atmosphere. The XRD pattern of each sample is shown in Figure 7.7. The KCl–$MgCl_2$ and the NaCl–$MgCl_2$ systems seem to show slightly greater conversion as indicated by a decrease in the intensity of the slag peaks, although there is some ambiguity from the similar heights of the TiH_2. However, the degree of conversion calculated from ICP data indicates that KCl–$MgCl_2$ and the NaCl–$MgCl_2$ samples had 98% and 95% conversion, respectively, compared to 81% for the NaCl–$CaCl_2$. It is likely that the lower melting eutectic systems were less viscous and facilitated greater mass transport during the reduction. Hence, only the KCl–$MgCl_2$ and the NaCl–$MgCl_2$ systems were used for subsequent experiments.

7.4.2 Effect of Salts on Particle Size

The addition of salts also affects the morphology of the reduced powder. SEM images of the reduced powder after 48 hour reduction at 650 °C and 500 °C with and without salts are shown in Figure 7.8. The 500 °C sample was also washed with water to remove the soluble salt. Despite the coarseness of the unmilled slag particles, the

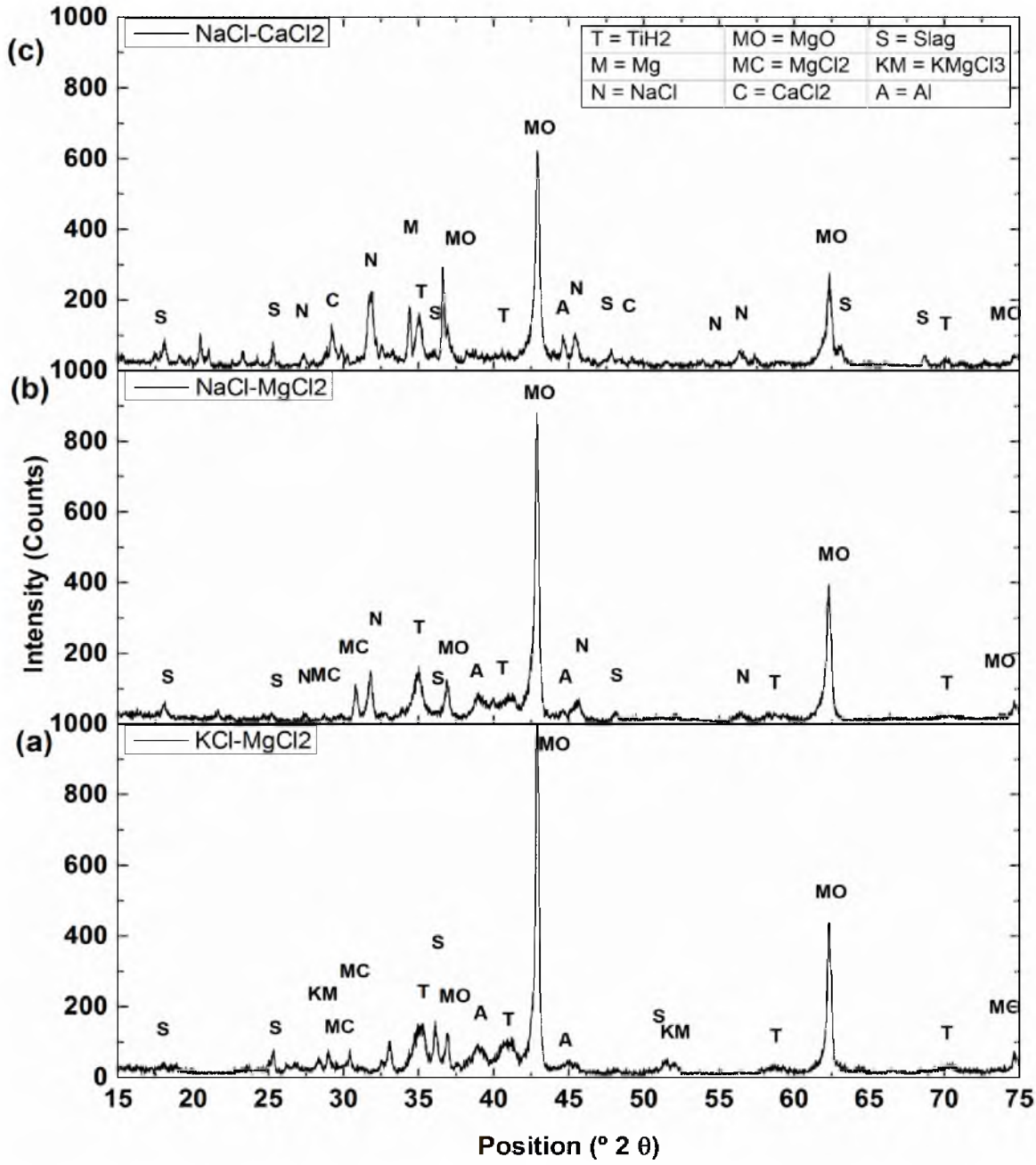

Figure 7.7. X-ray diffraction patterns of TiO_2 slag reduced with MgH_2 for 48 hours at 650 °C with 20 wt. % addition of eutectic mixture of a) KCl–$MgCl_2$, b) NaCl–$MgCl_2$, and c) NaCl–$CaCl_2$.

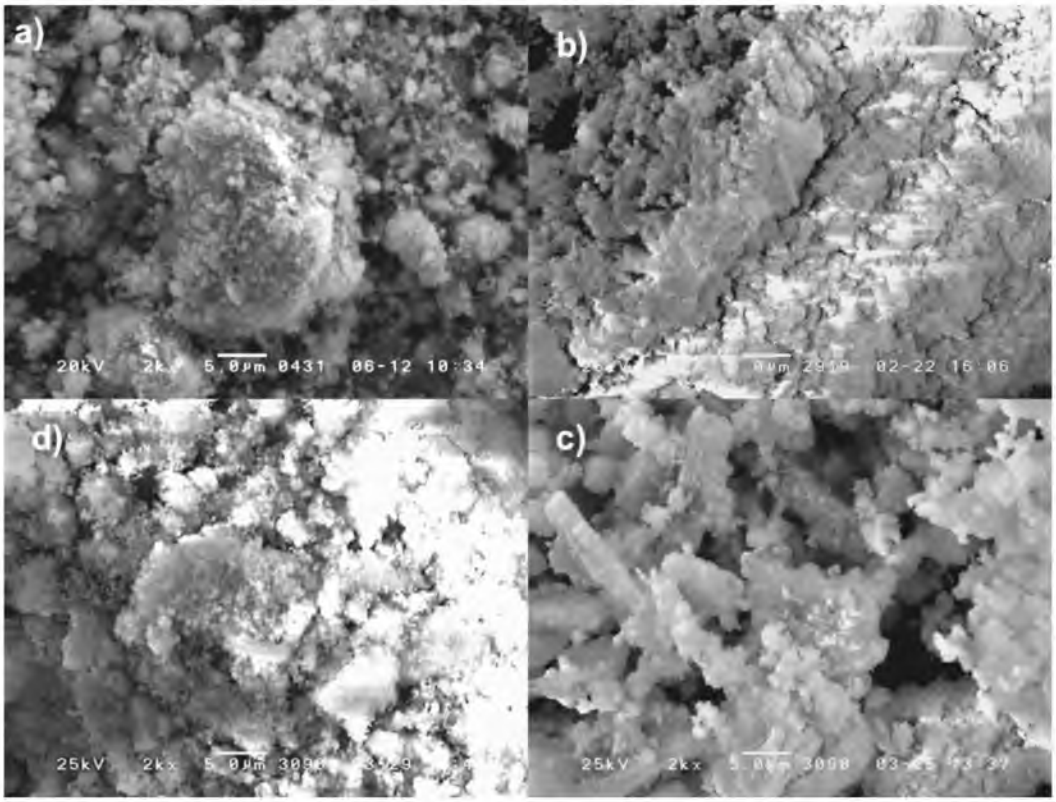

Figure 7.8. SEM images (2000x) of slag reduced with MgH_2 for 48 hours with a) unmilled slag at 650 ºC without added salts, b) 2 hour SPEX milled slag at 650 ºC with 20 wt. % KCl–$MgCl_2$, c) 2 hour planetary milled slag at 500 ºC with 20 wt. % KCl–$MgCl_2$, and d) same treatment as c but rinsed with distilled water and dried.

resulting product particles are quite loose and less than 1 μm in diameter. The particles in the 650 ºC sample with salts are "cemented" together with the chloride salt mixture. The particles in the 500 ºC sample with salt are also cemented together, but are looser and do not have the sintered texture of the 650 ºC sample. The washed particles have a similar texture as the particles without salts but appear too similar in size to conclude that the addition of chloride salts leads to a coarser product.

7.4.3 Effects of Temperature and Powder Compaction

Compaction of the slag and MgH_2 powders into pellets prior to reduction was another technique considered to increase the extent of conversion. It was hypothesized

that compaction would increase the contact area between the powders and decrease Mg evaporation, which had been quite substantial in some experiments. 3 grams of slag/MgH_2/KCl–$MgCl_2$ salt mixture were HEM milled for 2 hours and pressed into a 0.8"D x 0.5"H pellet with a stainless steel die under inert conditions. The compaction force was 7000 lbs. Unpressed samples were also prepared and were heat treated at 500 °C. The XRD graph for the resulting powder of each sample is shown in Figure 7.9. By comparing the uncompacted and compacted samples at each temperature, it does not appear that compaction made any significant difference. It also appears that TiH_2 only formed at 500 °C and that Ti monoxide and/or suboxide formed in the samples heated to 650 °C. ICP data indicated that the degree of conversion for the 500 and 650 °C unpressed samples (88 and 99%, respectively) was greater than for the pressed samples (85 and 90%) and that the samples heated at 650 °C showed a greater reduction conversion than at 500 °C, although the dissolved Ti in the 650 °C samples was from TiO and not TiH_2. The amount of Mg evaporation was lower in the 500 °C samples.

Another test was run using the same milled slag/MgH_2/salt system but at a slightly lower temperature of 470 °C for 48 hours. Although TiH_2 formed at this temperature, the amount of unreacted slag was greater than at 500 °C. Thus, it was concluded that 500 °C was the most suitable temperature for subsequent reduction experiments.

7.4.4 Effect of Reaction Time

The effect of reaction time while holding temperature and composition constant was also examined. Slag was planetary milled for 2 hours with either the KCl–$MgCl_2$ or NaCl–$MgCl_2$ eutectic salt mixture and then blended with as-received MgH_2 and heated to

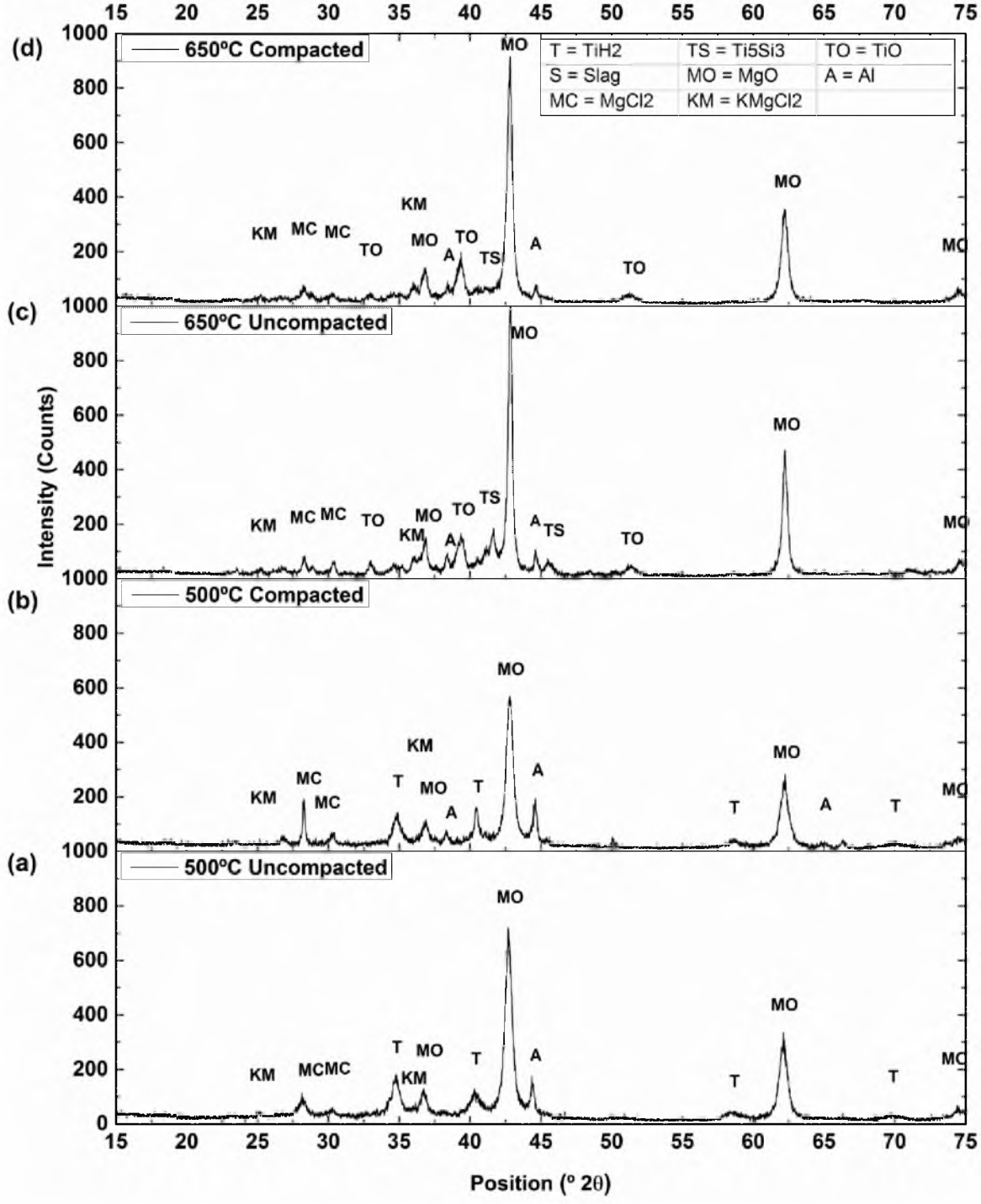

Figure 7.9. X-ray diffraction patterns of TiO_2 slag reduced with MgH_2 and 20 wt. % addition of KCl–$MgCl_2$ for 48 hours at a) 500 °C, uncompacted; b) 500 °C, compacted; c) 650 °C, uncompacted; and d) 650 °C, compacted.

500 °C for various amounts of time. The XRD patterns for the NaCl–$MgCl_2$ mixtures heated for 6, 12, and 24 hours as well as for KCl–$MgCl_2$ at 24 and 48 hours are shown in Figure 7.10. A comparison of the NaCl–$MgCl_2$ patterns show that the intensity of slag peaks decreased slightly from 12 hours to 24 hours while the MgO peaks slightly intensified. The shape and intensity of the TiH_2 peaks does not appear to change significantly after 12 hours, indicating that the reduction reaction was nearly complete at this time. Similarly, few differences in peak intensity are observed for the KCl–$MgCl_2$ samples from 24 to 48 hours. SEM images of the 12 and 24 hour reduced powder indicated a slight increase in the particle size after 24 hours, indicating that after the primary reaction has completed, further heating results in particle growth.

The degrees of conversion for the NaCl–$MgCl_2$ samples were determined using the total digestion method. The degrees of Ti conversion in the 12 and 24 hours samples were 105 and 98%. Conversion values greater than 100% indicate that the measured Ti concentration in the HCl leached solution was slightly higher than the expected amount calculated from complete digestion of the reduced powder samples. The leaching/digestion procedures are still being refined for greater reproducibility. However, it still appears that the reaction had reached its completion after 12 hours and did not increase further with time. The conversion value for a 2 hour milled sampled heated at 500 °C for 48 hours without salts was only 49%. This is further evidence that the addition of chloride salts significantly improves the rate and extent of the reduction of Ti slag with MgH_2.

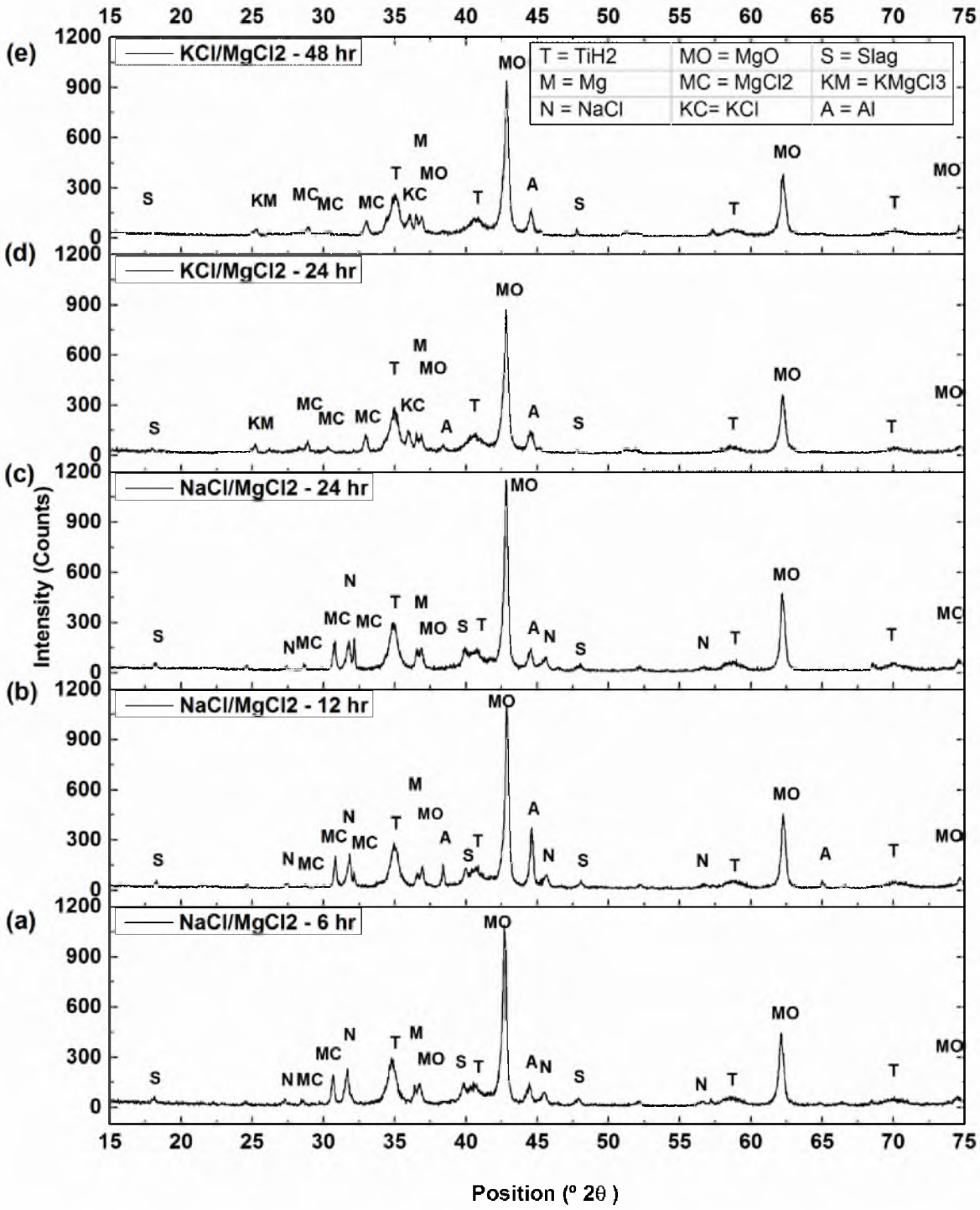

Figure 7.10. X-ray diffraction patterns of TiO_2 slag reduced at 500 ºC with as-received MgH_2 and 20 wt % addition of NaCl–$MgCl_2$ for a) 6 hours, b) 12 hours, and c) 24 hours. Reduction was also performed at the same temperature but adding 20 wt. % KCl–$MgCl_2$ for d) 24 hours, and e) 48 hours.

7.5 Conclusion

The feasibility of reducing Ti slag with MgH_2 to form TiH_2 has been investigated. Characterization by X-ray diffraction has indeed confirmed that TiH_2 forms when reduction is performed in a reducing H_2 atmosphere. The best reduction conditions were found to be 24 hours at 500 ºC using 25% excess MgH_2, adding 20% KCl–$MgCl_2$ or NaCl–$MgCl_2$ eutectic mixtures, and high energy ball milling for 2 hours. The addition of eutectic salts appeared to enhance the extent of the reaction but did not appear to have a significant effect on the product size. The compaction of reactant powders did not appear to have much effect on the extent of the reduction of slag.

7.6 References

[1] "Standard specification for powder metallurgy (P/M) titanium alloy structural components," in *ASTM Handbook*, ASM International, West Conshohocken, PA, 2008, p. 3.

[2] J. Bredthauer, B. Gries, and B. Szesny, "Ultra-coarse monocrystalline tungsten carbide and a process for the preparation thereof and hardmetal produced therefrom," US Patent No. 6 749 663, June 15, 2004.

[3] C.I. Lin, "The effect of alkali salt catalyst on the carbothermic reduction of nickel oxide," *Met. Trans. B,* vol. 19B, pp. 685–686, 1987.

[4] Y.K. Rao and H.G. Han, "Catalysis by alkali carbonates of carbothermic reduction of magnetite concentrates," *Ironmaking Steelmaking*, vol. 11, no. 6, pp. 308–318, 1984.

[5] E.M. Levin, C.R. Robbins, and H.F. McMurdie, *Phase Diagrams for Ceramists*. Westerville, OH: American Ceramic Society, 1964.

CHAPTER 8

LEACHING AND DEHYDROGENATION OF REDUCED SLAG

8.1 Introduction

In the previous chapter it was demonstrated that titanium oxide compounds in slag could indeed be reduced to TiH_2 using MgH_2 as a reducing agent. To be of further technological use, the resulting TiH_2 powder must be separated from impurities in the reduction product by a series of targeted leaching steps. After purification, the hydride powder can be dehydrogenated to Ti by heating in vacuum or an inert atmosphere. The feasibility of separating TiH_2 from impurities was investigated through a series of preliminary leaching experiments using common industrial chemical reagents such as NH_4Cl, NaOH, and HCl. Key reaction parameters such as reagent concentration, leaching temperature, and time were varied in order to determine the best conditions for impurity removal and recovery of the TiH_2 product. Additionally, the energy and emissions of the reduction, leaching, and dehydrogenation processes on an industrially significant scale will be estimated in a similar manner as the new TiO_2 making process in Chapter 5.

8.2 Experimental Methods

Leaching of the reduced powder and other powder reagents were performed in 125 mL Nalgene bottles placed inside a water bath placed on a Corning stirring hot plate equipped with an automatic temperature probe with a +/- 1 ºC accuracy. Solution was

stirred with a 1 inch magnetic stir bar at 200 rpm unless otherwise noted. For timed leaching tests, 2–3 mL aliquots of solution were taken at the appropriate time intervals and filtered using a Becton-Dickinson 0.2 μm syringe filter, diluted with 2.5% nitric acid, and analyzed using ICP-OES as previously described. MgO–TiH_2 and FeO standards were ball milled for 2 hours with stainless steel balls in a stainless steel jar using a laboratory SPEX mill. For maximum solubility experiments, an arbitrary amount of powder was added to a weigh boat and weighed. The powder was added step wise from this boat to the solution, and the final weight of the boat and powder were measured. After each addition, the powder/solution was allowed to stir for at least 30 minutes in order to determine if more powder should be added. The leaching chemicals and standard powders used were all reagent grade. XRD was performed using the same equipment as previously described, and SEM/EDS microscopy was performed with a Leo 440 Scanning Electron Microscope equipped with an EDAX detector.

8.3 Targeted Leaching Stages

8.3.1 NH_4Cl Leaching

Due to the use of MgH_2 as a reducing agent, the bulk removal of MgO from the reduction product is required. As mentioned in the previous chapter. Although MgO is highly soluble in mineral acid, its dissolution would significantly increase acid consumption. Additionally, initial leaching tests showed that fine reduced TiH_2 powder is very sensitive to the concentration of HCl in solution and will readily dissolve in concentrations greater than 1.0 M. MgO can also be dissolved with NH_4Cl solutions [1] according to the following reaction:

$$MgO_{(s)} + 2NH_4Cl_{(aq)} \rightarrow MgCl_{2(aq)} + 2NH_{3(aq)} + H_2O \quad (8.1)$$

The dissolution of MgO with NH_4Cl solutions allows more dilute HCl solutions to be used in the process, leading to greater recovery of TiH_2 powder.

8.3.1.1 Determining Maximum Solubility of MgO

The addition of chelating agents like sodium dihydrogen citrate ($NaC_6H_7O_7$) to NH_4Cl solution have been found to significantly improve the solubility of MgO [2]. Finding solubility data for specific concentrations of $NH_4Cl/NaC_6H_7O_7$ for MgO proved difficult; therefore, solubility was experimentally determined. The effect of $NaC_6H_7O_7$ addition on the solubility of MgO was investigated by starting with a NH_4Cl or $NH_4Cl/NaC_6H_7O_7$ solution of a certain concentration and adding MgO stepwise (10–20 mg increments) until the solution saturated. 100 mL solutions of 0.1, 0.5, 1.0, 1.3, 2, and 3 M NH_4Cl were prepared as well as solutions with 0.077, 0.035, 0.77, 1.0, 1.5, and 2.3 M $NaC_6H_7O_7$ added, which kept the $NH_4Cl/NaC_6H_7O_7$ ratio of each solution fixed at 1.3:1. The MgO solubility is plotted versus NH_4Cl concentration in Figure 8.1.

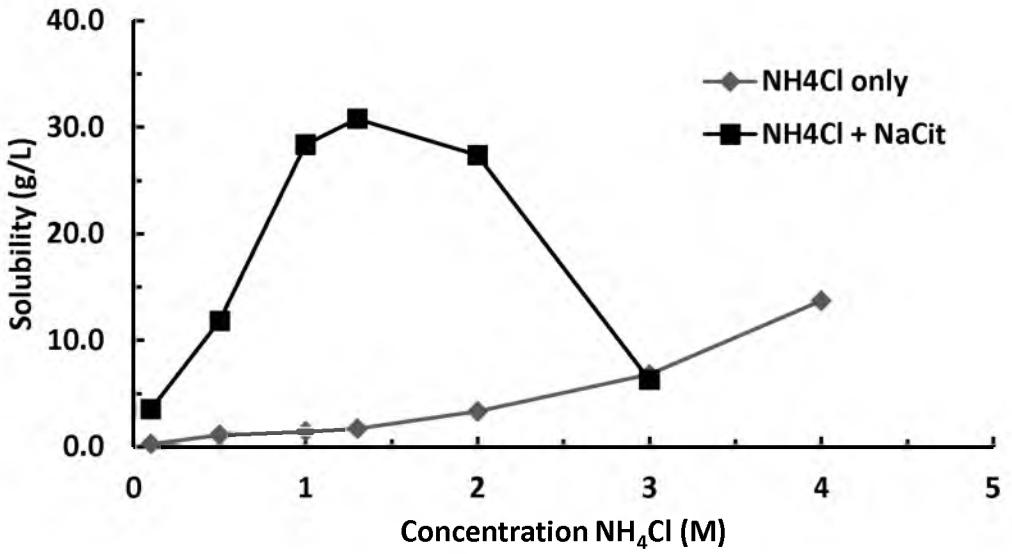

Figure 8.1. Maximum solubility of MgO at different concentrations of NH_4Cl with and without sodium dihydrogen citrate (NaCit). Temperature: 30 °C; NH_4Cl /$NaC_6H_7O_7$ ratio: 1.3; Stirring speed: 300 rpm.

For the NH_4Cl solutions, the solubility of MgO increases only gradually with an increase in concentration and reaches a maximum of 13.7 g/L at 4 M concentration. Even at 0.1 and 0.5 M concentrations, the addition of $NaC_6H_7O_7$ increases the solubility by more than a factor of 10 and increases to a factor of 20 at 1 M concentration. The NH_4Cl /$NaC_6H_7O_7$ solution reaches a maximum solubility of 30.8 g/L at a 1.3 M /1 M concentration, respectively. This is in good agreement with Fink [2] who reported a maximum solubility of 28 g/L at this same concentration, although the temperature is unknown. The solubility of the solution for $NaC_6H_7O_7$ becomes a limiting factor, and the solutions above 1 M $NaC_6H_7O_7$ had to be heated to 70–80 ℃ to dissolve the powder and then cooled to 30 ℃ for use in the experiment. The decreasing solubility of MgO is attributed to the limited $NaC_6H_7O_7$ solubility, which is 0.25 M at 20 ℃ [3].

8.3.1.2 Effect of Time on MgO Removal

Determining the required leaching time for the removal of MgO from the reduced powders is critical as the residence times affect the size of reactors and equipment in a scaled-up process. The change in Mg concentration in the leaching solutions was investigated by leaching 4 grams of reduced powder in 400 mL of 1.0 NH_4Cl/ 0.77 M $NaC_6H_7O_7$ solution for 6 hours at 70 ℃. 3 mL solution samples were taken at 0.5, 1, 2, 4, and 6 hours. This experiment was repeated 3 times, and the average concentration at each time was determined and is shown in Figure 8.2. The error shown is equal to one standard deviation. Within the margin of error, it appears that the concentration of Mg reach its maximum after 0.5 hours and does not change significantly with further time. Therefore, a leaching time of 0.5–1 hours was determined to be sufficient for subsequent experiments.

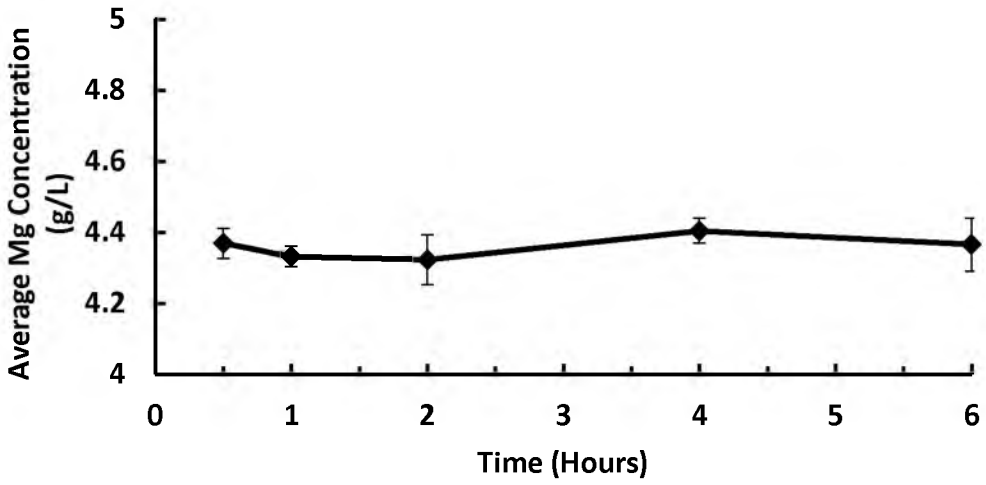

Figure 8.2. The change in Mg concentration with time for the leaching of reduced slag with 1.0 M NH_4Cl/ 0.77 M $NaC_6H_7O_7$ solution. Temperature: 70 °C; Stirring speed: 200 rpm; 1 g powder/100 mL solution.

8.3.1.3 Determining Solubility of MgO in Reduced Powders

The solubility of MgO from leach powders was investigated using a range of $NH_4Cl/NaC_6H_7O_7$ solutions. Additionally, the appropriate leaching temperature also needed to be determined. The goal was to maximize the removal of MgO from the powder and minimize the necessary temperature since the heating of solutions contributes a significant portion of the overall energy consumption of the process. A large batch of reduced powder was prepared by reducing Ti slag (2 hour high energy milled) with 1.25X the stoichiometric amount of MgH_2 and 20 wt. % of $MgCl_2$/NaCl eutectic salt. The reduction occurred for 24 hours at 500 °C. 1 g of reduced powder was added to 100 mL solutions containing 0.26, 0.5, 0.75, and 1.0 M NH_4Cl with $NaC_6H_7O_7$ added to bring the NH_4Cl/ $NaC_6H_7O_7$ ratio to 1.3:1. The reduced powders were leached for 1 hour at temperatures of 40, 50, 60, and 70 °C. The predicted concentration of the solutions was 5.25 g/L, assuming full dissolution of Mg. After each test, the solution was quenched in a cold water bath and allowed to stand for 30 minutes, after which the solution was

sampled and filtered through a syringe filter and then diluted and analyzed using ICP-OES.

To determine the maximum solubility, the recovered solution from the 50, 60, and 70 ºC tests were filtered and reused for a second and/or third leaching stage using fresh powder at the same pulp density as the initial test. Some of the 40 ºC test solutions had begun to form precipitates and were not reused. The percent of Mg recovered from each leach test versus the NH_4Cl concentration is shown for each temperature and leaching stage in Figure 8.3.

Several trends can be observed. For the leach solutions with a concentration of

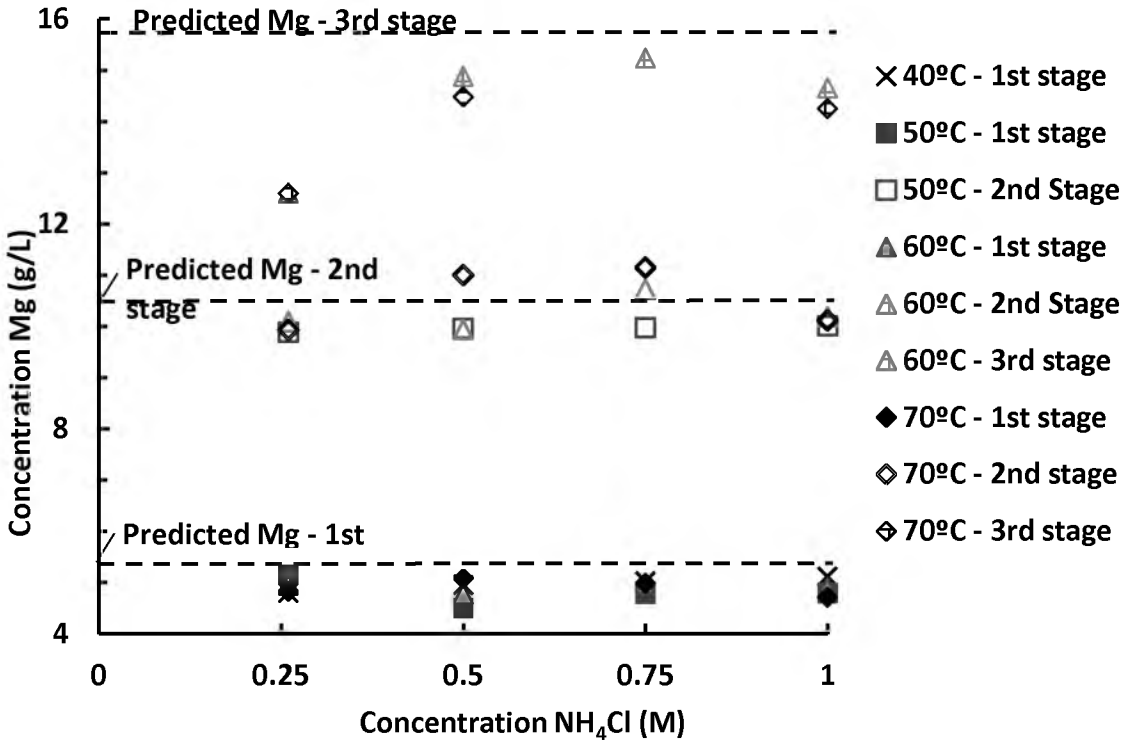

Figure 8.3. Maximum solubility of Mg from reduced slag in different concentrations of $NH_4Cl/NaC_6H_7O_7$ solutions and at different temperatures and leaching stages. NH_4Cl /$NaC_6H_7O_7$ ratio: 1.3; Stirring speed: 200 rpm; 1 g powder/100 mL solution. The predicted Mg is the concentration assuming full dissolution and is based on the Mg content of the reduced powder as determined by the ICP-OES measurements of the HCl dissolution of reduced powder.

0.26 M, the temperature of solution did not appear to affect the solubility at any stage. At the lowest leaching temperature of 40 °C, the change in concentration did not result in a significant increase in solubility. For each temperature and concentration, the 2nd stage of leaching appeared to be just as efficient as the 1st stage. Some values were observed above the predicted amount, likely due to the presence of small condensed Mg flakes that were interspersed in the reduced powder, raising the Mg content in some samples above the average composition. At the 3rd stage of leaching, a noticeable decrease in the relative solubility was observed, with the decrease in solubility more significant for the samples heated at 70 °C. It is possible that the higher temperature led to a greater decomposition of NH_4Cl to NH_3 gas. A maximum solubility of 15.2 g/L Mg (25.2 g/L MgO equivalent) was observed for the 0.75 M solution heated at 60 °C. It appears that for the reduced powders, leaching with 0.5–0.75 M NH_4Cl at 60 °C results in the best overall removal of Mg if multiple leaching stages are used.

The leached, rinsed, and dried powder was analyzing using XRD. The XRD pattern of reduced powder after leaching for 6 hours with 1 M NH_4Cl/0.77 M $NaC_6H_7O_7$ solution at 70 °C is shown in Figure 8.4. The bulk removal of MgO from the powder is confirmed by the significant reduction in the height of the MgO peaks.

8.3.2 NaOH Leaching

Although NH_4Cl removes the most abundant impurity, MgO, many other metal impurities must be removed. Leaching with hot NaOH solution has been shown to dissolve siliceous material from Ti minerals that would otherwise be insoluble in mineral acids other than HF [4, 5]. NaOH will also remove Al compounds with minimal dissolution of TiH_2 [6]. Initial NaOH leaching experiments on milled TiH_2 and Ti

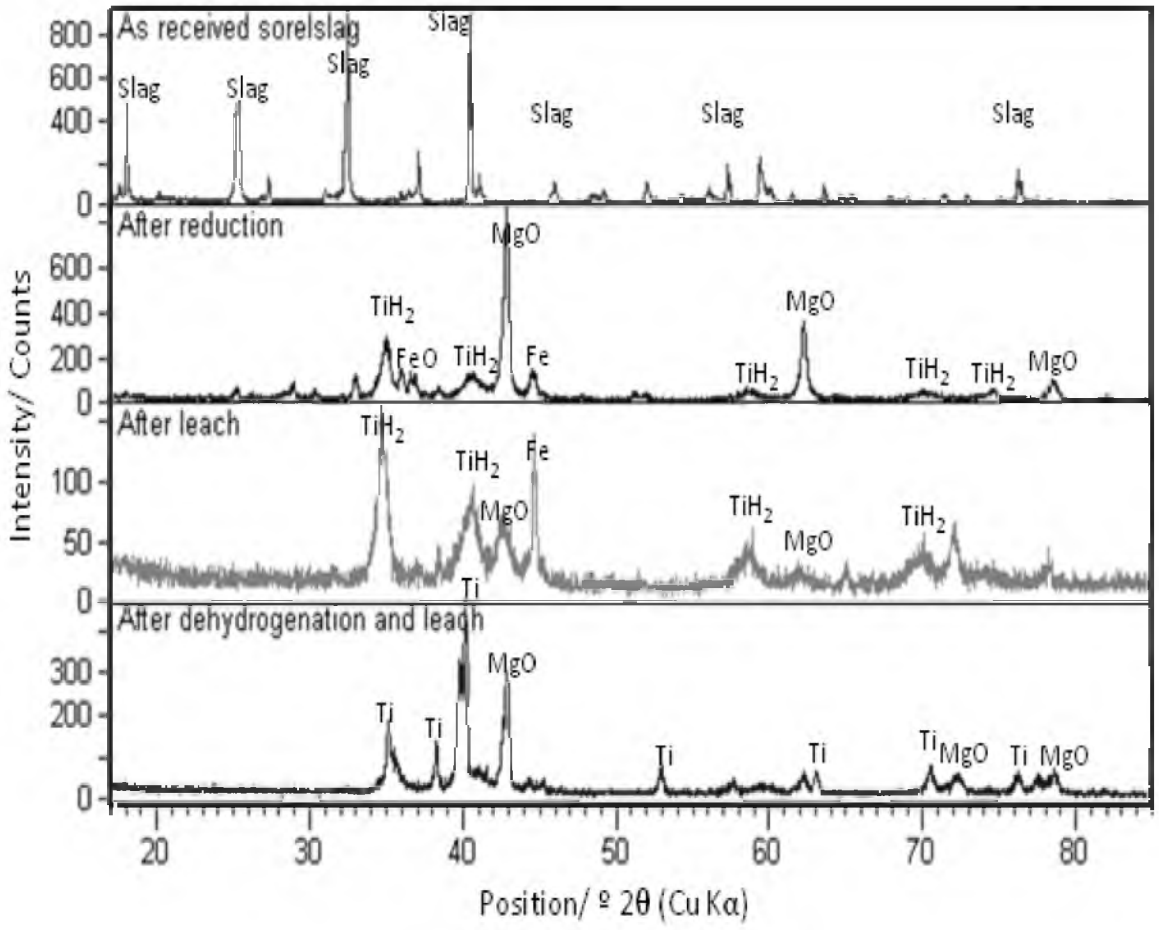

Figure 8.4. X-ray diffraction patterns of Ti slag a) as received, b) after 24 hour MgH_2 reduction at 500 ºC, c) after leaching with 1 M NH_4Cl/0.77 M $NaC_6H_7O_7$ solution, and d) dehydrogenation at 400 ºC for 6 hours.

standard powders showed minimal dissolution. When 1 g of 50% MgO/50% TiH_2 and 50% MgO/50% Ti powders were leached for 30 minutes for 50 ºC, only 0.1% of the Ti in the powder was measured in the leach solution. It should be emphasized that the majority of the oxides including FeO, Al_2O_3, and SiO_2 are reduced along with TiO_2 during the direct reduction process, forming minor amounts of intermetallic compounds such as Fe_2Ti, TiAl, and Ti_5Si_3 (based on the thermodynamic analysis); therefore, only residual oxides in any unreacted slag are of concern.

8.3.2.1 Removal of Si and Al Compounds With NaOH Solution

The leaching behavior of SiO_2 in various concentrations of NaOH was determined experimentally. 1.00 g of reagent SiO_2 was added to 100 mL of NaOH solution prepared at different concentrations, including 0.33, 0.42, 0.50, 0.58, 1.0, 1.5, 2.0, and 2.5 M NaOH, with 0.33 M being the stoichiometric amount needed for full dissolution. The leaching was performed for 2 hours at 70 ºC at a stirring speed of 200 rpm. The SiO_2 fully dissolved at every concentration.

Additionally, 1 g of untreated +400/-325 sized slag particles were leached for 1 hour with 100 mL of 2 M NaOH at a temperature of 80 ºC. The solution was filtered, diluted, and analyzed using ICP-OES. This leaching procedure resulted in the removal of 77% of the Si and 55% of Al, confirming that NaOH solutions could indeed remove these impurities from slag particles.

NaOH leaching was performed on reduced slag that had been previously leached with a 1.0 M NH_4Cl/0.77 M $NaC_6H_7O_7$ solution. The powder was leached for 4 hours using the same conditions as the SiO_2 standard test; however, solutions with 0.011, 0.016, 0.022, 0.027, 0.05, 0.1, 0.5, and 1.0 M NaOH were used. At the end of the test, the solution was filtered and analyzed using ICP-MS. The amount of Si in the solution was below the detectable limit of 7 ppm for that particular calibration. The change in the concentration of Al with the change in NaOH concentration is shown in Figure 8.5. The removal of Al increased with an increase in the NaOH concentration. No Ti was detected in the solutions; however, the weight of the filtered, rinsed, and dried powder increased for the 0.05 M concentrations and above, ranging from a 6% increase for the 0.05 M sample to 42% for the 1.0 M sample, indicating that perhaps some reaction had taken

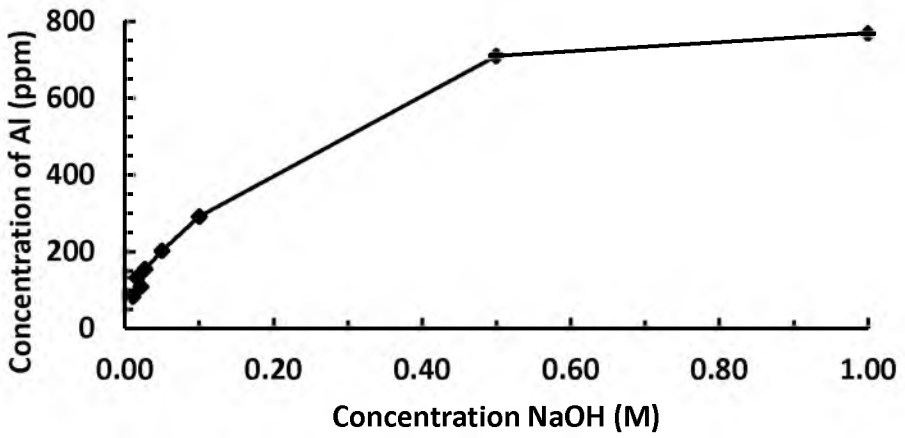

Figure 8.5. The concentration of Al in different concentrations of NaOH solution after leaching reduced powder for 2 hours at 70 °C. Stirring speed: 200 rpm; 1 g powder/ 100 mL solution.

place. The powders were analyzed using XRD, and the resulting patterns of 0.025–1.0 M NaOH leaching are shown in Figure 8.6. It is apparent that a sodium titanate compound, $NaTiO_4$, formed at the expense of the TiH_2 and increases in amount with greater NaOH concentrations. Sodium titanate is soluble in HCl which results in even greater Ti dissolution upon leaching of the reduced powder. Once again, the Al peaks are an artefact and were caused by interference from the powder holder.

8.3.3 Leaching of the Reduction Product with HCl

Any remaining metal or metal oxide compounds such as Fe can be dissolved using a relatively dilute mineral acid [1], such as HCl, as shown in (8.2).

$$FeO_{(s)} + 2HCl_{(aq)} = FeCl_{2(aq)} + H_2O \quad (8.2)$$

TiH_2 has been found to have a lower dissolution rate in HCl acid than in H_2SO_4 [4], and FeO has been found to have a higher reactivity in HCl than in H_2SO_4 [5]; therefore, HCl was chosen as the preferred mineral acid. Further, residual MgO in the mixture can also

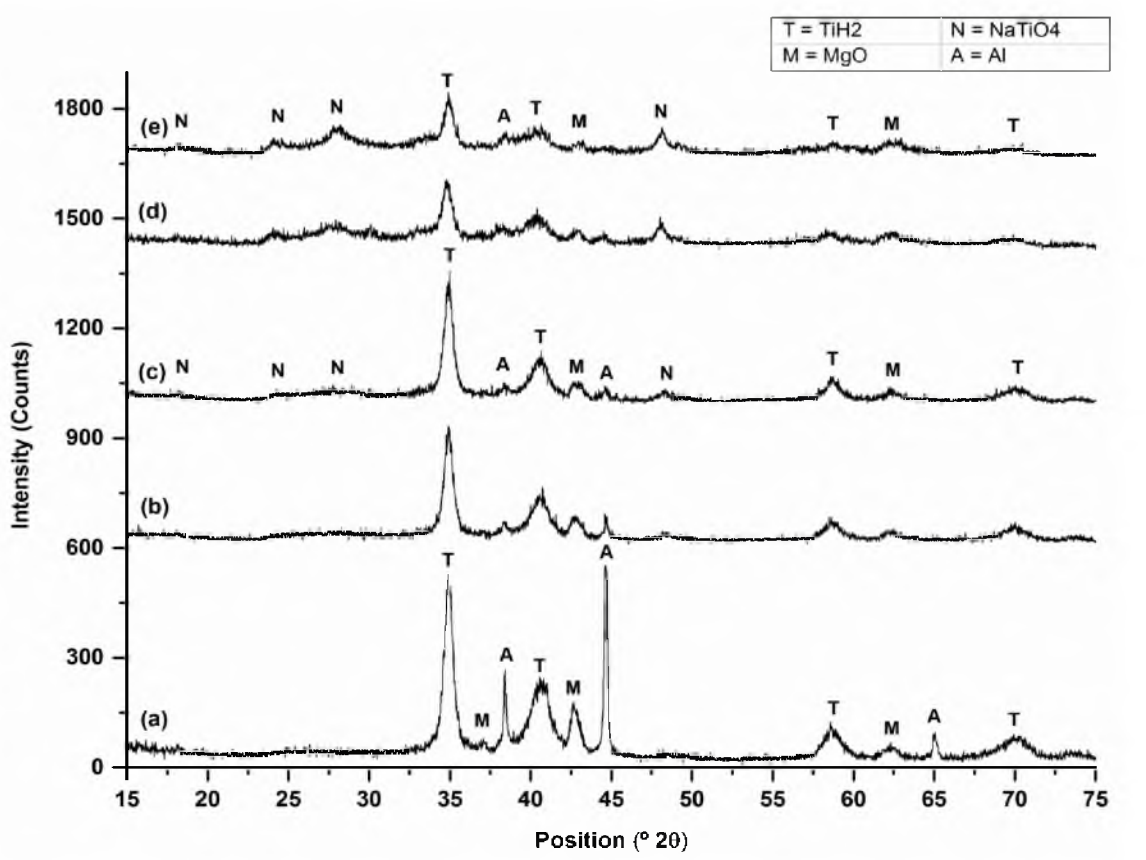

Figure 8.6. X-ray diffraction patterns of reduced slag after leaching with a) 0.025, b) 0.05, c) 0.1, d) 0.5, and e) 1.0 M NaOH for 4 hours at 70 °C. Stirring speed: 200 rpm; 1 g powder/100 mL solution. The Al peaks are an artefact and caused by interference from the Al powder holder.

be dissolved by the dilute HCl solution.

8.3.3.1 Effect of Particle Size

In order to determine the effect of particle size on the reactivity of reduced powders to HCl solutions, several powder mixtures were prepared that were similar in composition to that of reduced powders. These powders included a 50/50 wt. % mixture of MgO and TiH_2, MgO and Ti, and a 65/35/10 wt. % mixture of MgO, TiH_2, and slag. The as-received Ti and TiH_2 powder were -325 mesh. A portion of the powder mixtures was SPEX milled for 2 hours. The milled powders were on the order of 10 to several

hundred nanometers in size. 1 gram of mixed powder was added to 100 ml of 2 M HCl and mixed for 30 minutes at 50 °C. The solutions were then filtered and diluted for ICP analysis. The measured concentration of each element was compared to the predicted amount (assuming full dissolution) for both the milled and unmilled powders. The measured and predicted concentrations of Mg, Ti, and Fe of the standard powders are shown in Table 8.1.

MgO is readily dissolved in both milled and unmilled samples, and the measured amount of Mg is in fair agreement with the predicted amount. It also appears that both bulk TiH_2 and Ti powders are resistant to acid leaching; however, fine milled powders are readily dissolved. Some extra Fe was detected in the milled samples due to attrited contaminants from the milling media. Although Ti is inherently quite reactive, it is known to readily form an adherent passivating layer that inhibits further chemical attack. However, due to the high surface area of the milled powders, the passivating effect cannot be realized. This confirmed that efforts needed to be made to increase the product size of the TiH_2 in order to make an effective separation from other impurities.

8.3.3.2 Determining Effect of HCl Concentration

Due to the sensitivity of the fine reduced powder to the concentration of HCl acid, the appropriate concentration of HCl needs to be determined that will leach the chief remaining impurity, Fe (or FeO). A 4 g sample of 99.9% pure FeO was SPEX milled for 2 hours in order to simulate the size of the Fe in the reduced powder. 0.5 g of the milled FeO was added to 50 mL of HCl at concentrations corresponding to 100–300% the stoichiometric amount of acid (0.28–0.84 M HCl) needed to dissolve the FeO. A small amount of attrited Fe from the milling media was also in the samples. The concentration

Table 8.1. Measured and predicted concentration of Ti, Fe, and Mg from leaching unmilled and 2 hour SPEX milled standard powders with 2 M HCl. The % dissolved is determined by dividing the reported concentration by the predicted. Leach time: 2 hours; Temperature: 50 ℃; 10 g powder/L solution.

Unmilled Standards	Conc (ppm)	Ti	Fe	Mg
50MgO–50TiH_2	Measured	11	0	3029
	Predicted	4798	0	3015
	% Dissolved	0.2	0	100.5
65MgO–25TiH_2–10Slag	Measured	2	0	3636
	Predicted	2866	77	3920
	% Dissolved	0.1	-	92.8
50MgO–50Ti	Measured	1	0	2708
	Predicted	5000	0	3015
	% Dissolved	0.02	0	89.8

Milled Standards	Conc (ppm)	Ti	Fe	Mg
50MgO–50TiH_2	Measured	3837	127	2432
	Predicted	4798	0	3015
	% Dissolved	80.0	-	80.7
65MgO–25TiH_2–10Slag	Measured	2126	221	3084
	Predicted	2866	77	3920
	% Dissolved	74.2	286.4	78.7
50MgO–50Ti	Measured	2656	38	2604
	Predicted	5000	0	3015
	% Dissolved	53.11	-	86.4

of Fe in the solutions after leaching for 10 hours at 70 °C at each concentration of acid is shown in Figure 8.7. The concentration of Fe increased with an increase in acid concentration up to a maximum concentration of 10.1 g/L, which was reached at 0.56 M HCl (200% of the stoichiometric amount) and did not significantly increase afterwards. When leaching the reduced powder, other impurities such as CaO or remaining MgO will consume acid; therefore, a slightly higher concentration of 0.6 M HCl was chosen for subsequent leaching experiments.

8.3.3.3 HCl Leaching of Reduced Powder

Reduced powders that had previously been leached with 1.0 M NH_4Cl and 0.05, 0.1, 0.5, and 1 M NaOH solutions were rinsed thoroughly with DI water and dried at 90 °C. Leaching of 0.45 g of each of the powders was conducted with 50 mL of 0.6 M HCl for 2 hours at 70 °C. The filtered samples were diluted and analyzed using ICP-MS. The concentration of Ti, Fe, Mg, and Al of the solution is shown in Table 8.2. Significant dissolution of each of the powders occurred. It appears that the increase in $NaTiO_4$ formation with an increase in NaOH concentration (as shown in Figure 8.6) led to a

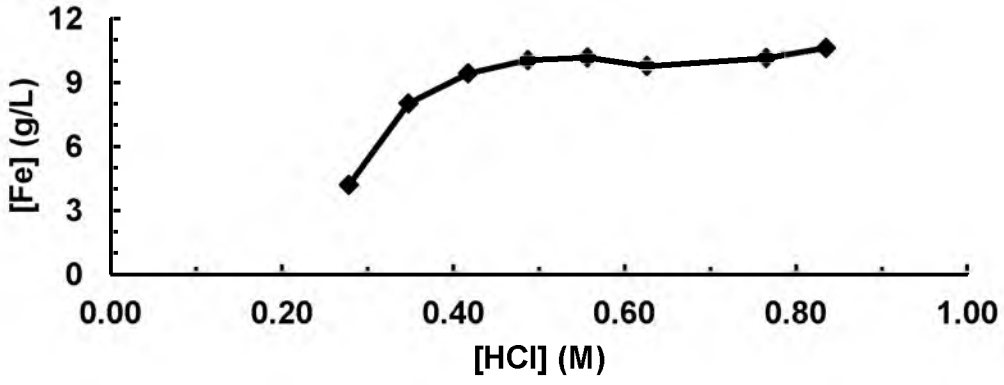

Figure 8.7. Concentration of Fe in HCl solutions of different concentration after leaching milled FeO reagent. Leach time: 8 hours; Temperature: 70 °C; 1 g powder/ 100 mL solution.

Table 8.2. Concentration of Ti, Fe, Mg, and Al in 0.6 M HCl leaching solutions of reduced powder that had previously been leached with various concentrations of NaOH. Leach time: 2 hours; Temperature: 70 ºC; 9 g powder/L solution.

	Concentration (ppm)			
[NaOH] (M)	Ti	Fe	Mg	Al
0.05	8360	1400	172	140
0.1	9330	1530	188	143
0.5	5120	1370	139	66
1	4760	1380	139	62

greater dissolution of Ti in the reduced powder. However, it is likely that the concentration of Ti, Fe, and other metals decreased at 0.5 M and 1.0 M leached samples as they comprised a smaller percentage of the composition of the powders than the other powders that had less $NaTiO_4$ formation. The high level of dissolution is also attributed to the fineness of the powder. Thus, the efficiency of the acid leaching stage is highly dependent on the previous leaching treatments.

8.3.4 Conversion of TiH_2 to Ti

The hydride powder can be dehydrogenated to produce Ti metal (if so desired) by heating it to 400 ºC or greater in an inert atmosphere. The XRD spectra of reduced powder after NH_4Cl leaching and dehydrogenation at 400 ºC for 6 hours in an argon flushed tube furnace is shown in Figure 8.4. The hydride peaks have clearly been replaced by α–Ti peaks, demonstrating the flexibility of the process to make either Ti metal or hydrided powders. The dehydrogenation process can occur immediately after the reduction process inside the same reactor simply by evacuating the hydrogen and flowing an inert gas such as argon. The X-ray diffraction patterns of reduced slag treated in this manner have confirmed the feasibility of this option. However, due to the increased alloying tendency of Ti versus TiH_2, it was determined that conducting the

dehydrogenation stage after purification was the best option.

8.3.5 SEM Analysis of Leach Products

Figure 8.8 shows SEM images of Ti slag reduced at 500 °C for 48 hours with salts after washing with water, leaching with 1 M NH_4Cl/0.77 M $NaC_6H_7O_7$ for 6 hours, leaching with 1 M NaOH for 2 hours, and leaching with 0.6 M HCl for 2 hours. In the water washed powder, it was difficult to differentiate between reduced slag and the MgO particles; however, after NH_4Cl leaching, the loose clusters reduced particles are more readily observed and appear to range in size from a few hundred nanometers to several microns. After NaOH leaching, the reduced particles appear to agglomerate into slightly

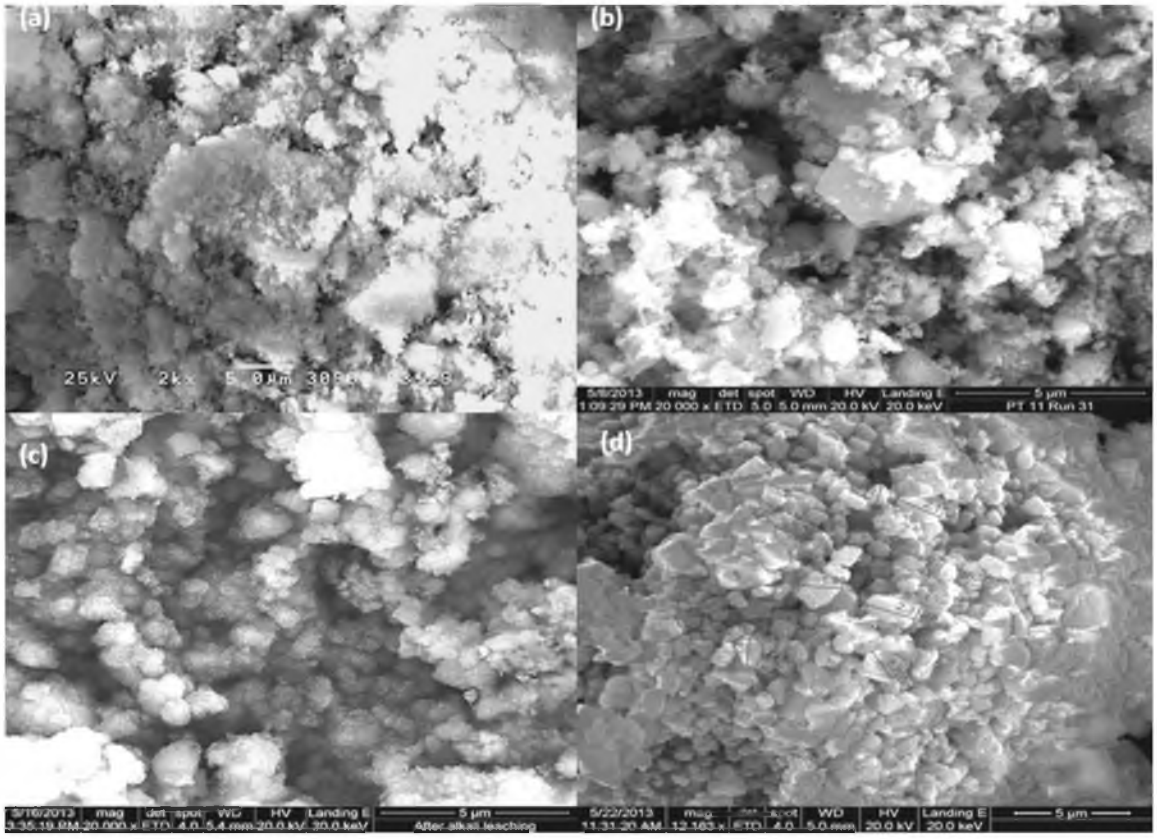

Figure 8.8. SEM images of Ti slag reduced at 500 °C for 48 hours with salts after a) washing with water, b) leaching with 1M NH_4Cl/0.77 M $NaC_6H_7O_7$ for 6 hours, c) leaching with 1 M NaOH for 4 hours, and d) leaching with 0.6 M HCl for 2 hours. Scale bars are equal to 5 µm.

larger clusters and are covered in very fine acicular particles, which are likely crystallized NaOH residue, but which are absent after acid leaching. The final product after acid leaching contains particles about 0.5–3.0 μm in diameter.

EDS analysis of the final TiH_2 product is shown in Figure 8.9. A scan of a large collection of the particles indicates that the product is predominantly Ti with only a small amount of oxygen content. The exact compositions of the impurity elements were not able to be determined with great accuracy using this technique. Further efforts are needed to accurately measure the level of impurities in the final product.

8.3.6 Recommendations for Future Research

Although the current embodiment of the process has successfully demonstrated the formation of TiH_2 and Ti powders, further refinements in the reduction and leaching process are needed to produce powder of commercially acceptable purity. The key challenges include removing silicides and other persistent intermetallic compounds that form during the reduction and reducing the dissolution of the TiH_2 product during the

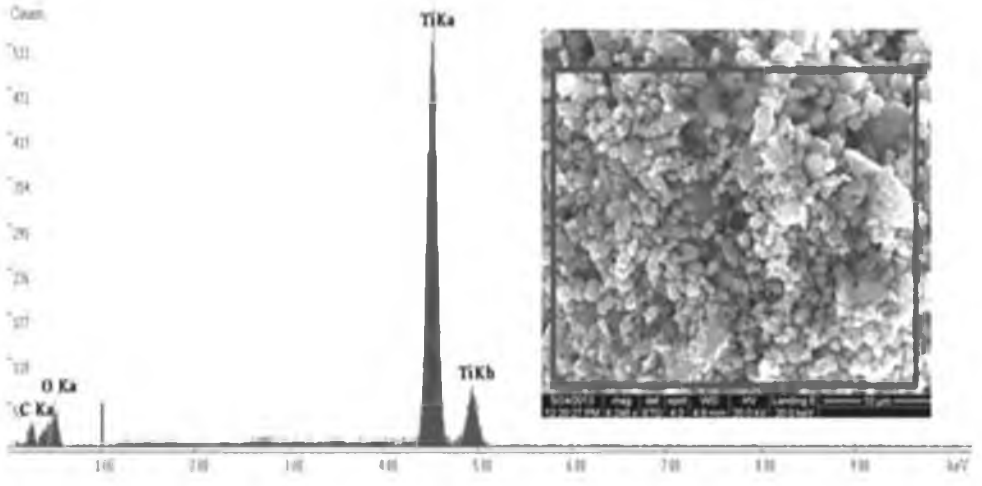

Figure 8.9. SEM/EDS analysis of titanium hydride powder product using the DRTS process as described.

leaching of Fe and other metals. One possible solution to the particle size issue would be to reduce the degree of milling and find an optimal slag particle size that will allow for acceptable degrees of conversion but form coarser TiH_2 product sizes than in the current process. Additionally, performing NaOH leaching of slag prior to the reduction process would allow the bulk of the Si and Al compounds to be removed before they can potentially form compounds with Ti in the reduced powder.

8.4 TiH_2 Energy and Emissions Analysis

8.4.1 Energy Analysis Approach

As discussed previously, the high cost of Ti products is largely due to the high energy consumption of producing raw Ti sponge via the Kroll process. The new process uses a significantly less energy intensive approach to produce Ti powder, which could potentially be used as a direct substitute for Ti sponge. The approximate energy consumption of the proposed DRTS process on an industrial scale can be calculated and compared with the Kroll process. A schematic diagram of the cradle-to-gate boundary comparison of the DRTS and the Kroll processes is shown in Figure 8.10. Based on a typical industrial production target of 10,000 metric tons per year, a model plant was designed that would employ the proposed process. The energy required for each step (in the form of electrical power or natural gas) in the process was calculated based on the process parameters from experimental results, although several assumptions also had to be made. The system boundary for the process calculation includes the milling and blending of slag with MgH_2 and salts, direct reduction, leaching, filtering, drying, and dehydrogenation of TiH_2 powder. The energy required to make slag as well as recover and regenerate MgH_2 is calculated separately. The emissions were also calculated in the

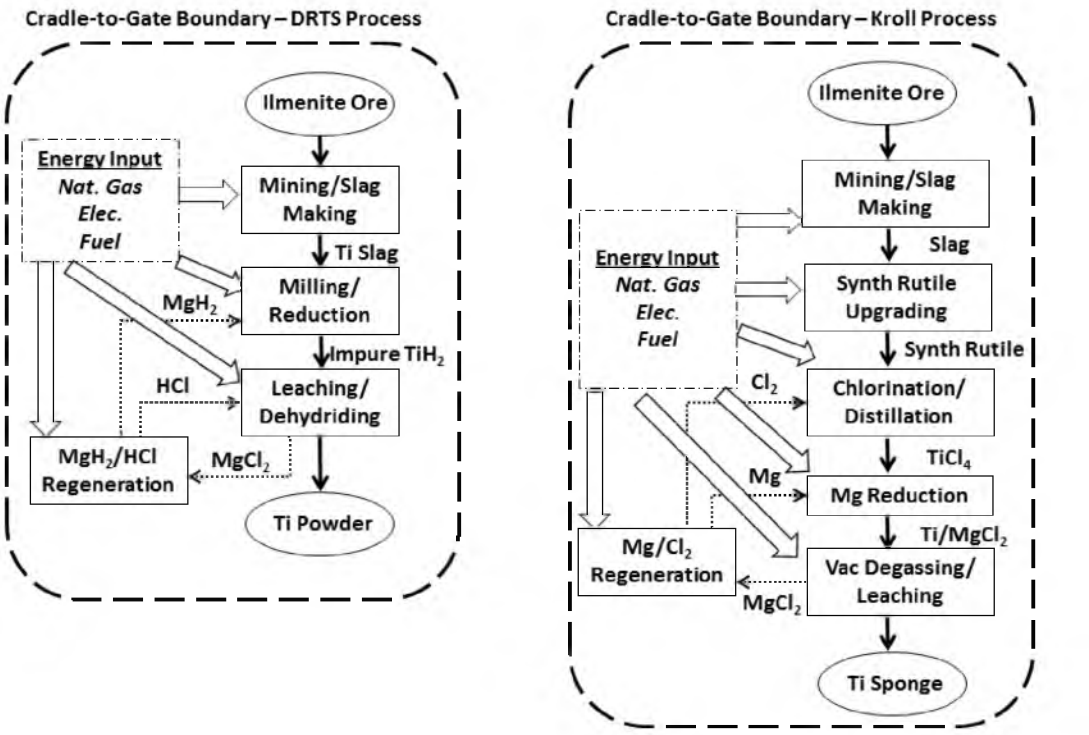

Figure 8.10. Cradle-to-Gate energy boundary comparison of the DRTS and Kroll processes.

same manner as previously discussed.

8.4.2 Unit Process Energy Calculations

8.4.2.1 Slag Milling and Blending

In order to reach the annual production goal, 1.19 tph of Ti must be produced, which, assuming a 97% Ti recovery, requires 2.56 tph of slag as feed. In order to prevent overgrinding, the as-received slag is sized using a 20 hp dual-fan air classifier, with only the oversized material being sent to the ball mill. The energy required to mill the slag to the desired particle size can be determined using Bond's Law as previously described. A value of 1 μm was chosen as the P_{80}. Grinding slag thus requires 220 kWh/ton, which will require a 10'D x 13'L ball mill driven by a 753 hp motor [6]. The blending of 2.56

tph slag with 1.10 tph salts and 1.46 tph MgH_2 requires 50 kWhr/ton [7], or a total of 256 kWhr.

8.4.2.2 Reduction and Dehydrogenation

The energy required for the reduction reaction was calculated using HSC Chemistry 5.11 software. The energy required to heat the reactants from 25 °C to 500 °C and the energy of the reaction at 500 °C was calculated separately and is shown in Table 8.3. It is evident that the net reaction is exothermic. However, since the reaction is performed in a batch reactor, energy must be supplied to heat the reactants. Assuming 10% conductive heat loss in the furnace, the reduction reaction will require 3,704 MJ/ton Ti. The energy required for dehydrogenation of 1.27 tph of the purified TiH_2 in Ar at 400 °C was also calculated using HSC Chemistry 5.11 and is shown in Table 8.4. Once, again, a 10% conductive heat loss in the furnace was assumed. It is evident that the reaction is endothermic and requires a total energy input of 3,943 MJ/ton Ti. It should be noted that the amount of heat released during the exothermic reduction reaction is approximately 10% greater than the heat required for the endothermic dehydrogenation reaction. The heat from the hot hydrogen gas that must be vented from the reduction furnace can be captured using a thermal storage refractory material and used for the dehydrogenation reaction.

8.4.2.3 Leaching Stages

After reduction, 5.14 tph of reduced powder will be leached for 1 hour at 60 °C with 46.3 tph 0.75 M NH_4Cl solution (assuming 10% solids) in a series of two closed 6400 gallon leaching tanks each agitated with a 5.5'D mixing blade driven by a 15 hp

Table 8.3. Energy required to heat reduction reactants from 25 ºC to 500 ºC and energy released by reduction reaction at 500 ºC.

Reduction Process Step	**Adjusted Energy (MJ)**	**Energy/ton Ti (MJ/ton)**
Heat Reactants	4408	3704
Hydride	-5137	-4316
Total	-729	-613

Table 8.4. Energy required to heat TiH_2 and Ar from 25 ºC to 400 ºC and dehydrogenate at 400 ºC.

Dehydrogenation Step	**Adjusted Energy (MJ)**	**Energy/ton Ti (MJ/ton)**
Heat TiH_2	486	408
Dehydride	4207	3535
Total	4692	3943

motor [8]. The energy required to heat the solution will be provided from boiler steam and will require 5.5 MBTU of natural gas or 5,440 MJ/ton, assuming 10% heat loss in the reactor. The leached powder is then thickened to 50% solids in a 75'D bridge thickener with a 5 hp motor, with the overflow being sent to the Mg recovery process. The underflow is sent to a three stage countercurrent washing circuit, with each stage occurring in a 50'D high capacity thickener driven by a 2 hp motor [6]. The rinsed powder is then filtered using an 8'D x 8'L drum filter driven by 10 hp motor. Each of the subsequent leaching stages follows a similar procedure with nearly identical equipment, although the leaching temperature will be 50 ºC for each stage. Pumps were sized for conveying the solution to and from each process and were also included in the energy tally. The pumping of solutions from each stage will require a total of 17 hp.

8.4.2.4 Drying

After the final rinsing and filtration of the TiH_2 powder, it still contains 10% by weight water (312 lbs) that must be removed prior to dehydrogenation. The moist powder is fed to a 3'D x 10'L rotary drying kiln driven by a 10 HP motor. Drying requires 1,800 BTU/lb of water [6]; therefore, the drying will require 562 kBTU per hour, or about 500 MJ/ton Ti.

8.4.3 Total Energy Consumption

The energy consumption for each step in the DRTS process as well as total energy is summarized in Table 8.5. The most power intensive step of the new process is the milling and blending of the slag, while leaching consumes the most natural gas due to the energy required to heat solutions. After further optimization of the process, it is likely that lower solution temperatures could be used and the process would require

Table 8.5. Energy consumption of each step in the proposed DRTS process.

Process	**Electricity**		**Natural Gas**		**Total**	
	(MJ/ton)	% Total	(MJ/ton)	% Total	(MJ/ton)	% Total
Milling/Blending	7751	84.0	-	-	7751	35.9
Redux/Dehyd	35	0.4	4240	34.3	4275	19.8
Leaching	957	10.4	7611	61.6	8568	39.7
Drying/Filtering	488	5.3	498	4.0	986	4.6
Total	**9230**		**12349**		**21580**	

significantly less energy. The total energy consumption for the process from slag to Ti powder was calculated to be 21,580 MJ/ton Ti. The energy to produce raw Ti sponge from raw ilmenite using a combination of the Becher and Kroll processes has been reported as 360 MJ/ton Ti (100 kW–hr/kg) [9], which includes the energy for upgrading to synthetic rutile, which has been reported to consume 35.0 MJ/ton TiO_2 [10]. The making of slag has been reported to consume at 35.5 MJ/ton TiO_2 [10]. Based on the TiO_2 content of the slag, the proposed process will require 2.15 tons of slag per ton Ti. The total amount of energy from slag production is calculated to be 60,900 GJ/ton Ti, as shown in (8.3).

$$35,500\ \frac{MJ}{ton\ TiO2} * 0.798\ \frac{ton\ TiO2}{ton\ slag} * 2.15\ \frac{ton\ slag}{ton\ Ti} = 60{,}900 \frac{MJ}{ton\ Ti} \qquad (8.3)$$

Adding this amount to the calculated energy consumption from slag to Ti powder, a total of 82,500 MJ/ton Ti (22.9 kWhr/kg) is obtained. The system boundary considered by Norgate et al. also included the energy to recover and regenerate Mg through electrolysis; therefore, it shall also be included in this analysis. The electrolysis of $MgCl_2$ to form Mg and Cl_2 gas has been reported to consume 13.0 kWhr of electrical energy per kg of Mg, much less than the energy required to produce Ca, which is 33–55 kWhr/kg

[11]. The energy for producing Mg can be calculated as shown in (8.4).

$$1.31\ \frac{kg\ MgH2}{kg\ Ti} * 0.924\ \frac{kg\ Mg}{kg\ MgH2} * 13.0\ \frac{kWhr}{kg\ Mg} = 15.7 \frac{kWhr}{kg\ Ti} \quad (8.4)$$

The addition of this value brings the total energy consumption for the DRTS process to 38.6 kWhr per kg Ti (139,200 MJ/ton Ti). Based on this preliminary assessment, the proposed process would consume ~60 % less energy than the Kroll process, which for an annual domestic Ti production rate of 18,000 tons is equivalent to 4,000 TJ.

8.4.4 Total Carbon Emissions

The carbon footprint of the new process was calculated by using the CO_2 emissions per kWhr of electricity (0.7 kg) and therm (10^5 BTU) of natural gas (5 kg) as reported in the EPA website [12]. The proposed process will consume 992 kWhr and 139 therms of natural gas resulting in 1.17 kg of CO_2 per kg Ti. Based on a report from Battelle laboratories [13], the carbon footprint of slag production was calculated to be 3.08 kg CO_2/ kg TiO_2. The CO_2 emissions from slag production can be calculated as shown in (8.5).

$$3.08\ \frac{kg\ CO2}{kg\ TiO2} * 0.798\ \frac{ton\ TiO2}{ton\ slag} * 2.15\ \frac{ton\ slag}{ton\ Ti} = 5.28 \frac{kg\ CO2}{kg\ Ti} \quad (8.5)$$

Thus, the total emission from slag production is 5.28 kg CO_2/ kg Ti, which when added to the process emissions gives a total of 6.45 kg CO_2/ kg Ti. The emissions from the Mg electrolysis are 11.0 kg of CO_2 per kg Ti, bringing the total emissions for the process to 17.5 kg CO_2/kg Ti, which is 51% less than the 36 kg CO_2/kg Ti of the Kroll process [9]. This is equivalent to an annual reduction of 333 ktons of CO_2 for domestic Ti

production. Additionally, the DRTS process avoids the carbo-chlorination step of the Kroll process that emits significant amounts of CO_2 as a direct byproduct; hence, the reduction in CO_2 emissions is even more substantial.

8.5 Conclusion

The targeted removal of various metal impurities from TiH_2 reduced from Ti slag has been investigated. MgO in the reduction product was effectively removed using NH_4Cl solutions, which showed a 10–20 fold increase in MgO solubility with the addition of $NaC_6H_7O_7$ at a $NH_4Cl/NaC_6H_7O_7$ ratio of 1.3:1. The best NH_4Cl leaching conditions were determined to be 0.5–1 hour at 60 °C with 0.5–0.75 M concentration and 10 g powder per liter. At these conditions, the solution removed 95% Mg after one stage and could be reused for multiple stages, removing 86% Mg after a 3rd stage. NaOH leaching was used to remove Si and Al from the powders and showed an increase in removal rate with increasing concentration; however, $NaTiO_4$ began to form and increased in abundance with higher concentrations of NaOH. Leaching with NaOH prior to reduction is recommended. The fineness of the reduction product led to significant Ti dissolution and oxidation even with dilute HCl leaching; therefore, efforts to increase the TiH_2 product size are also recommended.

Additionally, an analysis of the energy consumption of the new Ti-making process indicates that it would potentially consume 139.2 GJ/ton of Ti, which is 60% less than the traditional Kroll process. The largest portion of the energy is consumed in recycling and regeneration process reagents with the second largest being the preparation and milling of the slag feed. The calculated total CO_2 emission of the new process is 17.5 tons/ton TiO_2, which is 51% less than the Kroll process. Further development of the

processes on a larger scale would be necessary to refine and verify these conclusions.

8.6 References

[1] D.R. Lide, *CRC Handbook of Chemistry and Physics, 67th ed.* Abingdon, UK: CRC Press, 1987.

[2] J. Fink, *Petroleum Engineer's Guide to Oil Field Chemicals and Fluids. 1 ed.* Oxford, UK: Gulf Professional Publishing, 2012.

[3] Chemical Book. (June 12, 2010). *Sodium dihydrogen citrate chemical properties.* [Online]. Available: http://www.chemicalbook.com/ChemicalProductProperty_EN_CB2476982.htm

[4] I.M. Astrelin, G.N. Prokofyeva, V.I. Suprunchuk, Y.V. Knyazev, V.M. Panashenko, and I.A. Morozov, "Interaction of TiHx with solutions of acids and alkalies," *Hydrog. Mater. Sci. Chem. Metal Hydrides*, vol. 82, pp. 133–140, 2002.

[5] C.M. Cotell, F.A. Sprague, and J. Smidt, *ASM Handbook, Volume 5 : Surface Engineering*. Materials Park, OH: American Society for Metals, 1994, pp. 1039.

[6] *Mine and Mill Equipment Costs Estimators Guide: Capital and Operating Costs*, 2012 Ed., Infomine, Vancouver, BC, 2012.

[7] R. Kirchain and R. Roth, "The role of titanium in the automobile," Cambridge, MA, Camanoe Associates Reports, 2002.

[8] W.D. Baasel, *Preliminary Chemical Engineering Plant Design, 2nd ed.* New York City: Van Nostrand Reinhold, 1990.

[9] T.E. Norgate, S. Jahanshahi, and W.J. Rankin, "Assessing the environmental impact of metal production processes," *J. Clean. Prod.*, vol. 15, pp. 838–848, 2007.

[10] E. Reck and M. Richards, "Titanium dioxide - manufacture, environment and life cycle analysis: The tioxide experience," *Surface Coatings Int. Part B: Coatings Int.*, vol. 80, no. 12, pp. 568–572, 1997.

[11] European Commission, "Integrated Pollution Prevention and Control, Best Available Techniques for the Manufacture of Large Volume Inorganic Chemicals-Solids and Other Industries," Seville, Spain: Integrated Pollution Prevention and Control, 2001.

[12] U.S. Environmental Protection Agency. (May 10, 2013) *Greenhouse Gas Equivalencies Calculator* [Online]. Available: http://www.epa.gov/cleanenergy/energy resources/calculator.html.

[13] R.W. Hale, "Energy use patterns in metallurgical and nonmetallic mineral processing-Phase 5 – Energy data and flowsheets, intermediate priority commodities," Columbus, OH, Battelle Laboratories, US Bureau of Mines Report, 1975.

CHAPTER 9

CONCLUSION

The development of two new hydrometallurgical processes to reduce the energy consumption and CO_2 emission from the production of titanium dioxide (TiO_2) pigment and titanium (Ti) powders has been described. Both methods seek to obviate the high temperature carbo-chlorination of TiO_2 bearing raw materials that produce large quantities of CO_2.

The new process for producing TiO_2 pigment includes alkaline roasting, HCl leaching, solvent extraction, hydrolysis, and calcination stages. The critical parameters for leaching of the roasted product with HCl acid included pulp density, acid concentration, leaching temperature, and time, with the best Ti recovery obtained when leaching at 10% pulp density with 5 M HCl for 2 hours at 50 °C. Contacting this solution with 15 vol. % tertiary amine extractant diluted in kerosene resulted in complete Fe extraction in a single stage and reduced the concentration of discoloring impurities in the final pigment to commercially acceptable levels.

The effects of hydrolysis and calcination on the size, shape, phase, and surface area of metatitanic acid particles precipitated from titanium chloride leach solutions were also evaluated. Increasing the amount of diluting water to the leach solutions resulted in an increased rate of hydrolysis but had little effect on the final TiO_2 recovery from solution. Increased dilution also favored finer and more porous precipitates, higher

anatase content, and a greater sensitivity to particle coarsening with increases in calcination temperatures.

Initial experimental results confirm the concept of reducing titanium slag with MgH_2 to produce TiH_2 powders. The optimal conditions for the conversion of slag to TiH_2 included high energy milling the slag for 2 hours, heating for 24 hours at 500 ºC using 25% excess MgH_2, and adding 20 wt. % $NaCl–MgCl_2$. The addition of eutectic salts appeared to enhance the extent of the reaction but did not appear to have a significant effect on the product size. The compaction of reactant powders had minimal effect on the extent of slag to hydride conversion. The hydride powders were converted to Ti powders by heating to 400 ºC in an inert atmosphere.

The feasibility of separating TiH_2 from impurities through NH_4Cl, NaOH, and HCl leaching stages was also investigated. Key reaction parameters such as reagent concentration, leaching temperature, and time were varied in order to determine the best conditions for impurity removal and recovery of the TiH_2 product. $NH_4Cl/NaC_6H_7O_7$ solutions effectively removed over 95% of MgO in the reduction product; however, the fineness of the reduction product resulted in significant Ti dissolution with dilute HCl leaching; therefore, further efforts to increase the TiH_2 product size are recommended.

A model plant employing the new method of TiO_2 pigment manufacture was designed with an annual production of 100,000 tons TiO_2. A cradle-to-gate comparison of the new process and the chloride process indicated a 25% decrease in energy consumption and CO_2 emissions when using high-titania slag as the feedstock. A model plant with a production of 10,000 tons per year Ti powder using the metal hydride reduction method was designed and compared with the traditional Kroll process,

indicating a potential for over 60% less energy consumption and 50% less CO_2 emission. Further testing of the TiO_2 process at the pilot scale is required to refine and validate these findings. Further optimization of the Ti making process is also recommended.